

Dispersal and Connectivity in Physical, Seasonal, and Extreme Landscapes

Dissertation zur Erlangung der naturwissenschaftlichen Doktorwürde

(Dr. sc. nat.)

vorgelegt der

Mathematisch-naturwissenschaftlichen Fakultät

der

Universität Zurich

von

David Denis Hofmann

von

Schwerzenbach ZH

Promotionskommission

Prof. Dr. Arpat Ozgul (Vorsitz)

Prof. Dr. Lukas Keller

Prof. Dr. Juan M. Morales

Dr. Gabriele Cozzi

Dr. John W. McNutt

2024

Summary

Connectivity is a crucial prerequisite for animals to move and disperse, which in turn promotes genetic exchange, facilitates range-shifts, and enables the recolonization of vacant habitats. Preserving and establishing movement corridors that enhance connectivity and facilitate dispersal have therefore become tasks of utmost importance in conservation science. Nevertheless, many of the methods employed to study dispersal and connectivity suffer from important limitations that inhibit a more holistic understanding of landscape connectivity. In this doctoral thesis, I investigate various aspects of animal dispersal and landscape connectivity, focusing on several of these limitations. Specifically, I propose a novel method for quantifying landscape connectivity, examine the impact of changing environmental conditions due to climate change, and investigate the role of seasonal factors when modeling connectivity. I also present and compare multiple methods for dealing with temporally irregular data when estimating habitat and movement preferences of dispersers from GPS data. These aspects are researched primarily using dispersing African wild dogs from northern Botswana as a study system. Due to the study species' wide-ranging behavior and the study areas' highly seasonal habitats, the study system offers a unique opportunity to investigate patterns of dispersal and connectivity in light of the outlined considerations.

Chapter 1 introduces the general background and research topics of this thesis. In particular, I discuss the importance of dispersal and connectivity in the context of conservation science and highlight multiple limitations in current connectivity research. I also describe the study system and give a brief overview of the data collection and general research methods.

Chapter 2 introduces a novel and simple workflow for examining landscape connectivity using simulations from individual-based movement models. To date, connectivity is primarily investigated using least-cost path models or circuit theory. However, both approaches require highly subjective permeability surfaces as inputs and make unreasonable assumptions that are rarely met by dispersing individuals. The proposed simulation workflow overcomes these shortcomings and provides a powerful alternative for studying connectivity via simulated dispersal trajectories and a complementary set of connectivity metrics. I exemplify the application of the proposed workflow and assess connectivity for dispersing wild dogs in the Kavango-Zambezi Transfrontier Conservation Area, revealing major movement

corridors and highlighting dispersal hotspots. This chapter was published in *Landscape Ecology* in 2023 (<https://doi.org/10.1007/s10980-023-01602-4>).

Chapter 3 investigates how changing environmental conditions due to climate change affect on-the-ground conditions and, ultimately, species' ability to disperse. Specifically, I investigate how changes in the flooding regime of the Okavango Delta impact wild dogs' ability to disperse between adjacent regions. For this, I combine the simulation framework from Chapter 2 with long-term remote sensing data of the Delta's flood extent and simulate dispersal under an increased and a reduced flood scenario. Both scenarios represent conceivable outcomes under the impact of climate change. I show that an increased flood reduces connectivity and prolongs dispersal durations, yet that the opposite is true under a reduced flood. Importantly, I highlight that the likely hotspots for human-wildlife conflict shift depending on future flood conditions. This chapter was published in *Global Change Biology* in 2024 (<https://doi.org/10.1111/gcb.17299>).

Chapter 4 conceptually motivates that seasonality can enter connectivity analyses at three distinct modeling stages, resulting in multiple configurations that greatly differ in terms of the dynamism they encapsulate. To test whether the incorporation of seasonality into connectivity analyses improves their predictive ability, I fit the models associated with each configuration and employ a rigorous validation procedure that compares predicted with observed movement. I also demonstrate that the simulation workflow presented in previous chapters can accommodate for a previously unseen degree of seasonality by allowing the landscape to change as the simulated dispersers move. Surprisingly, I find that predictions from the fitted models only marginally improve upon increasing the degree of seasonality. Nevertheless, inferred patterns of connectivity differ, with connectivity being more evenly distributed when seasonality is accounted for.

Chapter 5 revisits the statistical framework of integrated step-selection functions, which are frequently employed in connectivity studies to assess habitat preferences from GPS data. Currently, step-selection functions require temporally regularly spaced GPS data, which implies that irregular data need to be removed. This can result in a substantial loss of data, especially in studies where data are already scarce. Hence, I propose and compare several methods for dealing with irregular data, thereby allowing to retain additional data for modeling. I compare different methods using simulated data with known parameters and show that retaining irregular data can aid to reduce model uncertainty if appropriate methods are employed. Finally, I exemplify the application of the best performing method using GPS data collected on a spotted hyena from northern Botswana. The use of hyena data instead of wild dog data was mainly due to the availability of an extensive dataset on a single spotted hyena. This chapter was published in *Movement Ecology* in 2024 (<https://doi.org/10.1186/s40462-024-00476-8>).

Finally, in Chapter 6, I summarize my findings and embed them in a broader context. I also provide an outlook for topics that require further research, and provide conservation insights for the African wild dog.

Overall, this thesis provides a detailed investigation of dispersal and connectivity for the endangered African wild dog and propose several novel methods and approaches. It thereby challenges established practices and suggests new avenues to model dispersal movements. By combining methodological novelty with conservation insights, this thesis not only advances our understanding of connectivity in general, but yields specific insights that facilitate the implementation of targeted conservation measures. The dispersal model refined throughout the chapters furthermore sets the foundation for a comprehensive population viability analysis that realistically captures how dispersers move across the landscape.

Contents

1 General Introduction	1
1.1 Ecological Networks in the Anthropocene	2
1.2 Dispersal	3
1.3 Connectivity	3
1.4 Modeling Connectivity	4
1.5 Limitations of Current Approaches	5
1.6 Thesis Goals	8
1.7 Study Species	8
1.8 Study Area	9
1.9 General Methods	11
1.10 Thesis Outline	13
2 A Three-Step Approach for Assessing Landscape Connectivity via Simulated Dispersal: African Wild Dog Case Study	17
2.1 Introduction	19
2.2 Materials and Methods	21
2.3 Results	28
2.4 Discussion	33
Appendices	40
3 Dispersal and Connectivity in Increasingly Extreme Climatic Conditions	57
3.1 Introduction	59
3.2 Materials and Methods	62
3.3 Results	69
3.4 Discussion	74
Appendices	79
4 The Effects of Increasing Seasonal Dynamism when Predicting Connectivity: Advantages or Unnecessary Complications?	92
4.1 Introduction	94
4.2 Methods	98
4.3 Results	107
4.4 Discussion	111
Appendices	116

5 Methods for Implementing Integrated Step-Selection Functions with Incomplete Data	136
5.1 Introduction	138
5.2 Materials and Methods	145
5.3 Results	151
5.4 Case Study	151
5.5 Discussion	155
Appendices	161
6 General Discussion	169
6.1 A Fresh Take on Connectivity	170
6.2 Conservation Insights	173
6.3 Methodological Considerations and Limitations	174
6.4 Ecological Considerations and Limitations	177
6.5 Conclusion	180
Acknowledgements	182
Appendix Additional Works	188
A.1 Cameratrap Survey	189
A.2 Supervised Theses	190
A.3 R-Packages	193
References	195



Chapter 1

General Introduction

1.1 Ecological Networks in the Anthropocene

Life on earth is in constant motion. Birds migrate seasonally between their summering and wintering grounds from the Northern to the Southern Hemisphere (Alerstam, 1993), humpback whales (*Megaptera novaeangliae*) traverse thousands of kilometers to gather at breeding sites (Rasmussen et al., 2007), monarch butterflies (*Danaus plexippus*) relocate from their summer habitats in North America to their winter roosts in Mexico in a multi-generational journey (Reppert & De Roode, 2018), and zebras (*Equus quagga*) and wildebeest (*Connochaetes taurinus*) participate in one of nature's most spectacular migrations, traversing from the southern Serengeti in Tanzania to the Masai Mara in Kenya (Serneels & Lambin, 2001). If there wasn't any movement, there wouldn't be any life. Life is movement, and movement is life.

Although life on Earth has thrived in motion for millennia, we have entered an era of decline (IPBES, 2019; Almond et al., 2022). The beginning of the Anthropocene (Crutzen, 2006) not only cemented the domination of humanity over nature (Kareiva et al., 2007; Johns et al., 2022), but also heralded a sixth mass extinction event (Barnosky et al., 2011; Ceballos et al., 2015). With the current extinction rate surpassing the background rate by several orders of magnitude (Ceballos et al., 2015; Ceballos et al., 2017), approximately 1 million species are at the brink of extinction (IPBES, 2019). This rapid decline in biodiversity can mainly be attributed to an ever-expanding human footprint and a continued exploitation of natural resources (Venter et al., 2016; Ceballos et al., 2017). To date, 18% of the Earth's land is heavily modified, 56% is less severely transformed, and only 26% remain unaffected and intact (Locke et al., 2019). The loss of formerly healthy habitats and their fragmentation into isolated patches not only reduces biodiversity directly but also entails a reduction in species ability to roam freely (Haddad et al., 2015), thus limiting their capacity to cope with altered climatic conditions via range shifts (Fahrig, 2003; Heller & Zavaleta, 2009; Chen et al., 2011; Tucker et al., 2018). The need for conservation action is evident and urgent.

In order to slow or even reverse the biodiversity loss, many countries have taken conservation measures and established or expanded protected areas (Bingham et al., 2021). Besides the direct protection of endangered ecosystems through protection zones, the identification and preservation of major movement corridors that provide connectivity and promote dispersal between remaining areas is a prominent conservation strategy (Fahrig, 2003; Doerr et al., 2011; Rudnick et al., 2012). By linking national parks, wildlife management areas, and other biodiversity hotspots, connectivity shifts conservation from small isolated "wildlife islands" to transboundary ecological networks (Hilty et al., 2020). Within these networks, animals can again roam freely, allowing them to overcome resource scarcity, re-colonize extinct patches, and track suitable habitat conditions. The ability to move and disperse thus crucially contributes to population viability, stressing the importance of preserving and enhancing dispersal and connectivity, especially in light of anticipated challenges due to climate change (Heller & Zavaleta, 2009).

1.2 Dispersal

Dispersal of individuals, i.e., the movement of individuals away from their natal range to the site of first reproduction, is an important process governing the dynamics of spatially distributed species (Howard, 1960; Clobert et al., 2012). By moving individuals from one area to another, dispersal constitutes the main mechanism by which connectivity among subpopulation arises and can be maintained (Fahrig, 2003). Dispersal differs from migration in that dispersing individuals do not seasonally move between known patches, but venture into areas they are unfamiliar with (Hundertmark, 2007). This promotes the colonization of vacant habitats (Gustafson & Gardner, 1996; Hanski, 1999b; MacArthur & Wilson, 2001) and facilitates the reinforcement of small and nonviable subpopulations (Brown & Kodric-Brown, 1977). Because dispersing individuals (hereafter referred to as dispersers) cross an inhospitable matrix more willingly than resident individuals (hereafter residents), they help to offset some of the negative consequences of habitat-fragmentation by moving between otherwise isolated habitats (Marsh et al., 2004; Elliot et al., 2014). At a macro-evolutionary scale, dispersal enhances range expansions and enables species to track suitable environmental conditions under climate change (Kokko, 2006; Hodgson et al., 2012; Hodgson et al., 2016). Finally, dispersal plays a central role in maintaining gene-flow, thus facilitating adaptation and promoting metapopulation viability and resilience (Brachet et al., 1999; Marsh et al., 2004; Heinz et al., 2006). Overall, dispersal reduces the risk of stochastic extinctions (Shaffer & Samson, 1985; Melbourne & Hastings, 2008), making it a key element of many conservation strategies (Baguette et al., 2013).

1.3 Connectivity

A species' ability to disperse hinges on a sufficient amount of landscape connectivity (Doerr et al., 2011). Connectivity is typically defined as the degree to which a landscape facilitates or impedes movement of organisms among resource patches (Taylor et al., 1993), and can be subdivided into *structural* and *functional* connectivity (Tischendorf & Fahrig, 2000). Structural connectivity is primarily focused on the size and configuration of habitat patches within the landscape. It is therefore considered an inherent property of the landscape that is independent of the focal species, thus overlooking many of the interesting but complex interactions between organisms and their environment. Under a *functional* connectivity perspective, conversely, the focal species' behavioral response to prevailing environmental conditions is taken into account (Tischendorf & Fahrig, 2000). A landscape with similar structural properties can thus result in vastly different patterns of functional connectivity depending on the species of interest. In functionally well-connected landscapes, species can effectively migrate, disperse, forage, and establish new populations. Together, these processes contribute to the resilience, functioning, and diversity of natural systems,

and, ultimately, sustain life on Earth. Preserving functionally connected landscapes has therefore become the gold-standard in conservation management (Heller & Zavaleta, 2009; Doerr et al., 2011; Rudnick et al., 2012).

1.4 Modeling Connectivity

Although dispersal and connectivity have fascinated and interested scientists for decades, they both remained notoriously difficult to study until recently. Dispersers only make up a small fraction of an entire population, and the proximate causes of dispersal are seldom known (but see Behr et al., 2020). This makes it challenging to select appropriate individuals and to predict the exact moment they will emigrate, thus resulting in modest sample sizes, even for large studies (Nathan, 2001; Rudnick et al., 2012; Fattebert et al., 2015). Following dispersers is also logistically challenging, due to animals leaving well-defined study areas and crossing national borders. This holds particularly true for species that disperse over vast distances (Elliot et al., 2014; Osipova et al., 2019; Cozzi et al., 2020). The choice of data and an appropriate connectivity model is therefore often driven by data availability (Baguette et al., 2013) and frequently lacks biological justification (Sawyer et al., 2011; Zeller et al., 2012). Furthermore, connectivity studies usually cover extensive spatial extents, requiring coherent environmental data at very large spatial and temporal scales. Thanks to the uprise and miniaturization of automated tracking devices, the task of monitoring dispersal has become less problematic, allowing to remotely follow the fate of dispersing individuals (Cagnacci et al., 2010; Kays et al., 2015; Jønsson et al., 2016; Williams et al., 2019; Nathan et al., 2022). Simultaneously, an increased availability of remote sensed satellite products allows obtaining environmental data at the necessary spatio-temporal scale to link observed dispersal movements to habitat characteristics (Toth & Józków, 2016; Rumiano et al., 2020).

Thanks to the rapid increase in data-availability on both species and landscapes, various modeling techniques to quantify connectivity have emerged (see e.g. Etherington, 2016 and Diniz et al., 2019 for reviews, Figure 1.1). Early approaches were limited to examining structural aspects of connectivity, focusing on the composition and configuration of habitat patches, while ignoring the focal species' response to environmental conditions (Doerr et al., 2011; Diniz et al., 2019). With the uprise of tracking data and novel methods to study species' habitat and movement preferences (Boyce et al., 2002; Fortin et al., 2005; Cushman and Lewis, 2010; Avgar et al., 2016; Fieberg et al., 2021), however, the focus has shifted towards a more functional view, taking into account how species react to prevailing habitat conditions (Diniz et al., 2019). Presently, the most prominent functional connectivity models are based on least-cost path analysis (LCPA; Adriaensen et al., 2003), circuit theory (CT; McRae, 2006; McRae et al., 2008) and individual-based movement models (IBMMs; Kanagaraj et al., 2013; Allen et al., 2016; Fletcher Jr. et al., 2019; Hauenstein et al., 2019; Zeller, Wattles, et al., 2020; Unnithan Kumar, Turnbull, et al., 2022; Fletcher Jr. et al., 2023).

LCPA and CT are graph-based methods that estimate conductance of the landscape, whereas IBMMs use simulations to quantify connectivity. LCPA attempts to identify least-costly routes between predefined start and endpoints, whereas CT assumes a random walk and uses laws from electrical circuit theory to calculate conductance through each area of the landscape. Notably, LCPA and CT are linked via a concept coined *randomized LCPA*, which allows deviations (the degree of which can be specified by the user) from the least-costly route, thus approximating a random walk (Panzacchi et al., 2016). Except for a few IBMMs, all functional connectivity models require a permeability surface as an input (Diniz et al., 2019). This surface is a spatial raster layer indicating the expected ease or difficulty at which the focal species can traverse a specific area given the area's environmental characteristics (Adriaensen et al., 2003; Zeller et al., 2012). Permeability can be gauged from expert opinion or using empirical data, yet the latter approach has proven more accurate (Clevenger et al., 2002; Zeller et al., 2012), especially when GPS data are available (Elliot et al., 2014; Graves et al., 2014; Gastón et al., 2016; Jackson et al., 2016; Keeley et al., 2017). Unfortunately, due to the limited availability of dispersal data, most studies utilize data collected on resident individuals (e.g., Brennan et al., 2020; Lines et al., 2021), despite the perception and motivation of dispersing and resident individuals to cross landscape features is arguably different (Elliot et al., 2014; Benz et al., 2016). Popular approaches to empirically parametrize permeability surfaces are resource-selection functions (Fortin et al., 2005; Manly et al., 2007; Cushman & Lewis, 2010; Thurfjell et al., 2014), which estimate habitat preferences of the focal species by comparing used habitat to available habitat (Zeller et al., 2012). For GPS data, the use of integrated step-selection functions (iSSFs) has proven particularly useful, as they readily account for the autocorrelation inherent to GPS data (Fortin et al., 2005; Avgar et al., 2016).

1.5 Limitations of Current Approaches

Despite significant advances in the realms of modeling dispersal and connectivity, important limitations remain. For my master's thesis, I applied iSSFs to parametrize a permeability surface and employed LCPA to identify major movement corridors for dispersing African wild dogs (Hofmann et al., 2021). This work exposed me to several of the existing limitations and sparked the motivation for some of the chapters of this PhD thesis.

1.5.1 Use of Traditional Connectivity Models

A first limitation concerns the use of traditional LCPA and CT (e.g., Elliot et al., 2014; Mallory and Boyce, 2019; Brennan et al., 2020), which both make assumptions that are rarely met by dispersers. LCPA, for instance, assumes that dispersers have perfect knowledge about their target location and associated move-

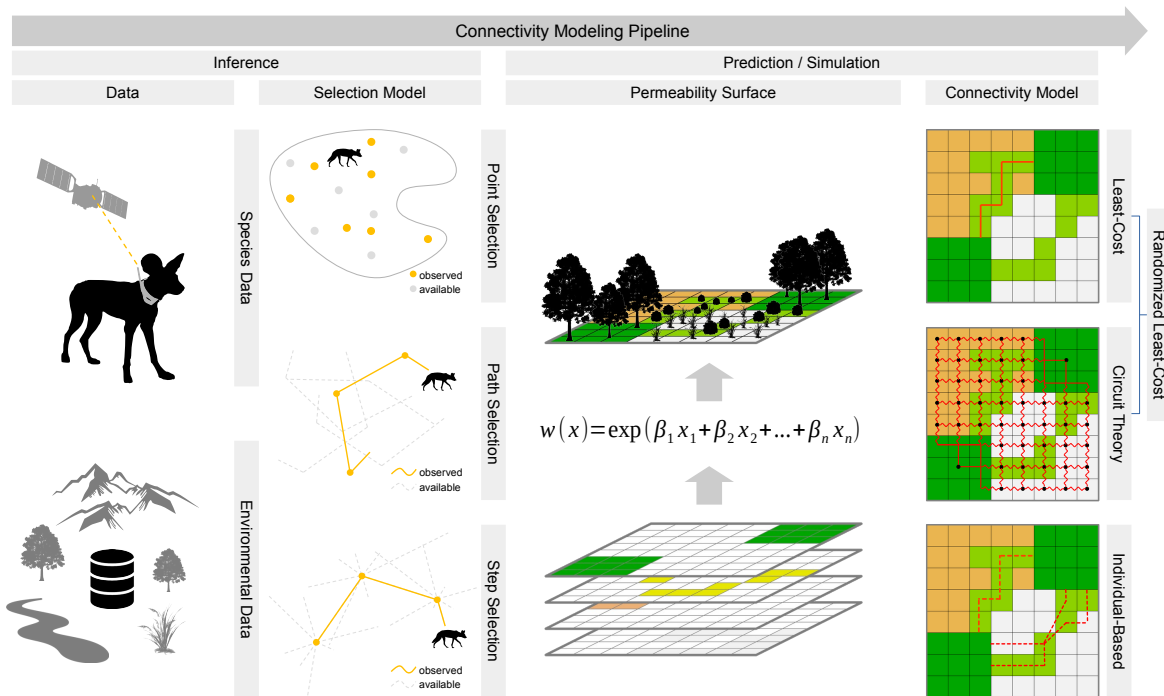


Figure 1.1: Conceptualized illustration of a typical connectivity modeling pipeline. The pipeline typically starts by collection information on the focal species, as well as on environmental features believed to influence the species' movement. In a next step, this data is paired and fed into a selection model, which empirically estimates selection or avoidance towards different landscape conditions. Most frequently, this is achieved via point- (or home-range) selection functions, path-selection functions, and step-selection functions (Zeller et al., 2012). Estimated preferences (here denoted β) are then used to predict a permeability surface, indicating the expected ease or difficulty at which the modeled species can traverse each grid-cell in the landscape, given that grid-cell's covariate values. Finally, the permeability surface is used as an input to a connectivity models. Currently, least-cost models and circuit theory are among the most prominent connectivity models, yet individual-based have been employed as well (Diniz et al., 2019). Figure adapted from Zeller et al. (2012) and Diniz et al. (2019).

ment costs, allowing them to find the least-costly route. CT, conversely, presumes that individuals follow a random walk and are ignorant of their target location. Furthermore, both methods hinge on a permeability surface, which is an *unconditional* prediction of permeability and cannot render that an animal's decision to disperse across a certain habitat is contingent on what else is available (Signer et al., 2017). IBMMs are a promising alternative that eliminate the need for a permeability surface (Signer et al., 2017; Diniz et al., 2019; Unnithan Kumar, Turnbull, et al., 2022) and enable more realistically rendering an animal's landscape perception (Zeller, Lewison, et al., 2020; Zeller, Wattles, et al., 2020). However, a unified framework for the parametrization and application of IBMMs to estimate connectivity is missing.

1.5.2 The Assumption of Static Landscapes

A second limitation in current connectivity analyses lies in their exclusive focus on present environmental conditions without consideration of how climate change could affect on-the-ground conditions and therefore species' ability to disperse (but see Ashrafzadeh et al., 2019 and Luo et al., 2021). Yet, an emphasis on present rather than future environmental conditions might lead to misguided conservation recommendations in light of ongoing climate change. The ability to model how climate change affects landscape connectivity would therefore be highly valuable. A similar limitation arises from the use of static environmental data, which provide only a snapshot in time and, consequently, overlook spatio-temporal variations in connectivity due to seasonality (Simpkins & Perry, 2017; Zeller, Lewison, et al., 2020). Since most ecosystems experience significant seasonal changes in environmental conditions, it can be anticipated that connectivity is not a static property and should be modeled dynamically. Since incorporating seasonality entails substantial complexity, the question then becomes to what degree seasonality should enter connectivity analyses to still distill meaningful conservation insights (Zeller, Lewison, et al., 2020).

1.5.3 Data Irregularity

Finally, a last and more technical limitation relates to the use of iSSFs. iSSFs are regularly used in connectivity modeling to obtain species-specific habitat preferences and movement capacities (or movement preferences) from GPS location data (Avgar et al., 2017; Fieberg et al., 2021). For the method to work, GPS data need to be collected at regular temporal intervals, which in reality is rare due to GPS devices occasionally failing to obtain a location. The current practice of removing irregular data can result in substantial losses of data, which can have negative consequences, especially in cases where data are already scarce. Alternatives that allow coping with slightly irregular data would therefore be desirable.

1.6 Thesis Goals

My goal with this thesis is to address the above outlined limitations and, where applicable, to provide methodological alternatives. I will do so using dispersing African wild dogs from the Okavango Delta area in northern Botswana as a study system. This system lends itself to examine the described limitations for several reasons. Firstly, the African wild dog is among the world's most wide-ranging species and a species of immediate conservation concern. The study population in Botswana is considered a stronghold population that likely acts as a source for the recolonization of surrounding areas (Cozzi, 2013; Cozzi et al., 2020). Furthermore, the African wild dog exemplifies a species that crucially depends on dispersal and transboundary connectivity for population viability (cfr. Section 1.7). Because the study area in Botswana undergoes significant seasonal changes (Mendelsohn et al., 2010) and is among the most vulnerable to climate change (Akinyemi & Abiodun, 2019; IPCC, 2022), it also offers a unique opportunity for studying the impacts of seasonality and climate change on connectivity (cfr. Section 1.8).

1.7 Study Species

The African wild dog (henceforth abbreviated as AWD, *Lycaon pictus*) is a medium-sized canid native to Sub-Saharan Africa and the only extant representative of its genus (Kingdon, 2015). It is recognized by its individually distinct, tricolored coat pattern and large ears (Figure 1.2). The AWD is a highly social animal, forming packs comprising 5 to 15 adult individuals that operate as cohesive units (Kühme, 1965; Frame et al., 1979). Established packs exhibit a well-defined social structure, with a dominant pair monopolizing the majority of reproduction and subordinates helping to rear pups (Frame et al., 1979).

Once widespread across Sub-Saharan Africa (Figure 1.3a), AWDs have disappeared from a vast majority of their historic range. This decline is mainly traced back to deadly diseases, human persecution, and habitat destruction (Fanshawe et al., 1991; Woodroffe & Sillero-Zubiri, 2020). With fewer than 6,000 individuals remaining in the wild, the IUCN categorizes the AWD as endangered (Woodroffe & Sillero-Zubiri, 2020). The biggest continuous population remains in northern Botswana, which is the main study area of this research project. AWDs occupy vast home-ranges, encompassing between 200 km² and 2,000 km² (Pomilia et al., 2015). Due to their need for vast, undisturbed spaces, AWDs are particularly vulnerable to habitat fragmentation and have become an umbrella species for conservation efforts across sub-Saharan Africa (Dalerum et al., 2008; Brennan et al., 2020). AWDs thus offer a unique opportunity for studying transboundary connectivity.

AWDs are crepuscular to diurnal hunters (Saleni et al., 2007), active primarily during the cooler morning and evening hours (Kühme, 1965; Creel, 2001), as well as during moonlit nights (Estes & Goddard, 1967;

Saleni et al., 2007; Cozzi et al., 2012). With a lean and athletic build, they are exceptionally well-adapted to endurance hunting (Estes & Goddard, 1967; Taylor et al., 1971; Koshy et al., 2020; Smith et al., 2020), allowing them to chase prey until exhaustion (Estes & Goddard, 1967; Creel & Creel, 1995; Rhodes & Rhodes, 2004). In the focal study area, packs mainly hunt by means of opportunistic and individual chases (Hubel et al., 2016). They predominantly predate on medium-sized antelopes, including impala (*Aepyceros melampus*) and kudu (*Tragelaphus strepsiceros*), but occasionally take smaller quarry, such as warthogs (*Phacochoerus africanus*) and steenbok (*Raphicerus campestris*, Creel and Creel, 1995; Mills and Gorman, 1997; Hayward et al., 2006; Tshimologo et al., 2021).

Across the majority of their range, AWDs coexist and compete with stronger competitors, especially with lions (*Panthera leo*) and spotted hyenas (*Crocuta crocuta* Creel, 2001; Cozzi et al., 2012; Vogel et al., 2019; Creel et al., 2023). To evade potentially fatal encounters, AWDs avoid both species temporally and spatially (Creel & Creel, 1996; Cozzi et al., 2012; Dröge et al., 2017), particularly during the denning season (Van Der Meer et al., 2013; Jackson et al., 2014; Mbizah et al., 2014; Davies et al., 2016; Alting et al., 2021). The displacement of AWDs by stronger competitors may explain why the species occurs predominantly in areas of intermediate prey density (Mills & Gorman, 1997; Creel & Creel, 2002; Mbizah et al., 2014; Creel et al., 2023).

Upon reaching sexual maturity (1.5 to 3 years of age), individuals disperse from their natal pack in an attempt to find potential mates and a suitable territory to settle (McNutt, 1996; Behr et al., 2020). Both sexes disperse, typically in same-sex sibling coalitions comprising two to five members (Frame et al., 1979; McNutt, 1996; Behr et al., 2020). On average, dispersing AWDs cover Euclidean distances between 5 and 500 km (Davies-Mostert et al., 2012; Masenga et al., 2016; Cozzi et al., 2020; Sandoval-Seres et al., 2022), yet cumulative distances up to 5,000 km have been reported (Masenga et al., 2016). Studies on habitat-selection suggest that dispersing AWDs avoid areas covered by water and dominated by humans, but prefer open shrubs and grassland (Cozzi et al., 2020; O'Neill et al., 2020; Hofmann et al., 2021). During dispersal, their movements are characterized by fast, directional bursts away from their natal location (Cozzi et al., 2020; Hofmann et al., 2021).

1.8 Study Area

Data on dispersing AWDs were collected in northern Botswana as part of a collaborative effort between the Botswana Predator Conservation Program (BPC) and the University of Zurich. BPC was founded in 1989, when John Weldon "Tico" McNutt commenced his pioneering work on AWDs in Botswana and established a research station (Fuller et al., 1992; McNutt, 1996; Osofsky et al., 1996). The program has continued ever-since, making it the longest running research program on AWDs and resulting in invaluable



Figure 1.2: (a) An adult African wild dog photographed in northern Botswana. The distinct fur markings are unique to each individual. (b) An anesthetized wild dog is being equipped with a GPS/Satellite collar, allowing to remotely follow its movements. (c) An African wild dog chasing prey at high speed.

long-term data (e.g., McNutt, 1996; Cozzi et al., 2012; Broekhuis et al., 2013; Abrahms et al., 2016; Behr et al., 2020; Jordan et al., 2022).

BPC's historic study area (approx. 3,000 km², centered at 19°31'S, 23°38'E, Figure 1.3b) is located at the Eastern fringes of the world-renowned Okavango Delta, a flood-pulse driven mosaic of patchy woodlands, permanent swamps, and seasonally flooded grasslands that lie within the otherwise dry and sandy Kalahari Basin (Wilson & Dincer, 1976; Ramberg et al., 2006; Mendelsohn et al., 2010). The Okavango Delta represents the world's largest inland delta and is classified as a Ramsar site, supporting a rich ecosystem with diverse flora and fauna. Precipitation in this area is highly seasonal and limited to the wet-season between October and April. Rainwater is collected in the Angolan highlands and only slowly descends through the Okavango Delta's tributaries into its alluvial fan, so the flood is out of sync with local rains and reaches its maximum extent during peak dry season in July-August (Wolski et al., 2017).

Human influence across the study area remains low, with large portions of land being gazetted national parks, wildlife management areas, or other protected areas. The study area is also part of the Kavango-Zambezi Transfrontier Conservation-Area (KAZA-TFCA, Figure 1.3a), the world's largest transboundary conservation initiative. The KAZA-TFCA was initially aimed towards restoring connectivity for migrating elephants (*Loxodonta africana*), but has gained momentum as an opportunity to establish connectivity for

several other wide-ranging species, including the African wild dog (Brennan et al., 2020; Hofmann et al., 2021; Sandoval-Seres et al., 2022).

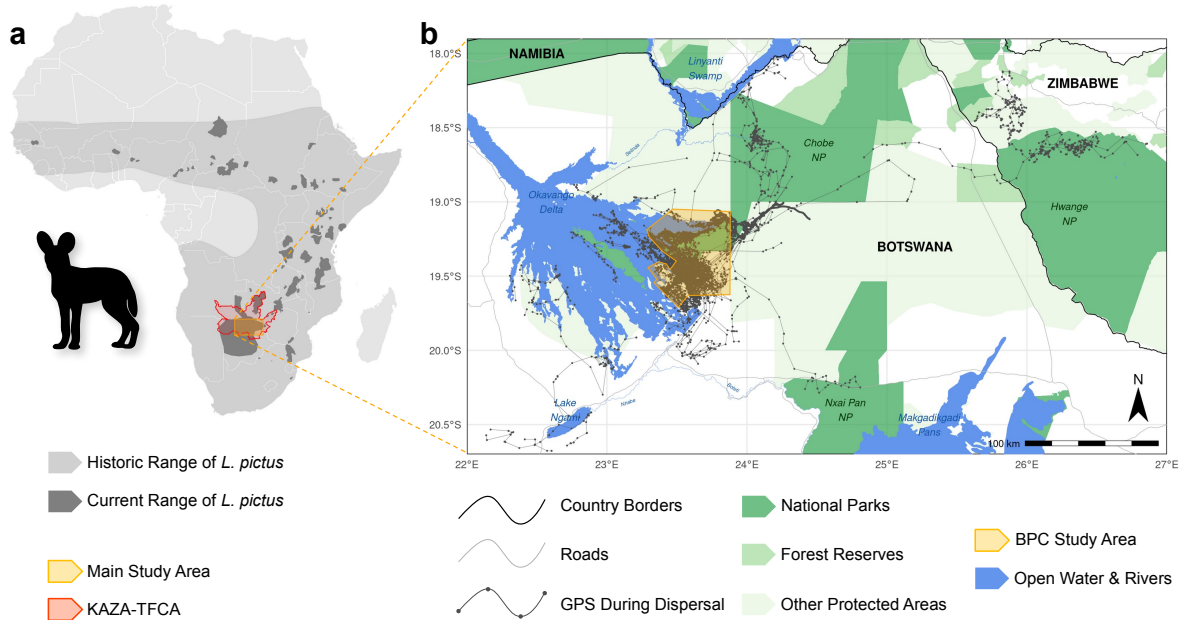


Figure 1.3: (a) The main study area of this thesis is located in northern Botswana and forms part of the world's largest transboundary conservation initiative, the Kavango-Zambezi Transfrontier Conservation Area (KAZA-TFCA). (b) Within this area, Botswana Predator Conservation (BPC) has continuously monitored a core area, spanning about 3,000 km². The dominant geographical feature of this ecosystem is the Okavango Delta, a flood pulse driven conglomerate of diverse habitats. Dispersers were collared within BPC's main study area and moved into various regions, including the Chobe National Park in Botswana and the Hwange National Park in Zimbabwe.

1.9 General Methods

1.9.1 Data Collection

GPS data on dispersing AWDs were collected between 2011 and 2023 using GPS/Satellite collars (Vertex Lite; Vectronic Aerospace GmbH, Germany). Candidate dispersing individuals were selected based on age, number of same-sex siblings, pack size and presence of unrelated individuals of the opposite sex in their pack (McNutt, 1996; Behr et al., 2020). Following the procedure described by Osofsky et al. (1996), selected individuals were immobilized using a mixture of ketamine and xylazine, which was subsequently reversed with yohimbine. Drugs were injected through a dart shot from a CO₂-pressurized dart-gun (DanInject, Denmark) at distances ranging from 10-12 m. During anesthesia, collars were attached, body measurements recorded, and blood samples collected. After 45 minutes, the anesthesia was reversed and the animal's recovery was monitored until it rejoined its pack. All required procedures were conducted by a Botswana-registered wildlife veterinarian, and all dispersers were collared while they were still with

their natal pack. Deployed collars weighed about 330 g ($\approx 1\%$ of the species' body weight) and contained a decomposable mechanism that ensured drop-off of the collar after 12–18 months. Collars were programmed to record a GPS location every 4 hours during dispersal, and to regularly transmit data via Iridium satellite system to a base station. To distinguish between residency and dispersal in the recorded data, I relied on a combination of data collected in the field and visual inspection of the net-squared displacement metric. Net-squared displacement measures the squared Euclidean distance of a location to a reference point (Börger & Fryxell, 2012), which I set at the center of the dispersing wild dog's natal range. Thus, I deemed dispersal to have started when an individual left its pack and natal range, and I defined settlement once the net-squared displacement metric flattened off. Besides GPS data on dispersers, I compiled an extensive collection of data on environmental conditions (e.g. water cover, human influence, temperature) sourced through publicly available services, or remote sensed from free satellite imagery. Specific details about additional data will be introduced in the relevant chapters.

I completed all processing steps and analyses using R (R Core Team, 2023) and performed computations exclusively on a desktop PC with AMD Ryzen 7 2700X octa-core processor (8 x 3.6 GHz, 16 threads) and 64 GB DDR4 RAM. All R-scripts and L^AT_EX files associated with this thesis are available through GitHub (<https://github.com/DavidDHofmann/PhD>).

1.9.2 Statistical Analyses

Throughout all chapters, I heavily rely on the framework of iSSFs. I therefore briefly summarize the method here. iSSFs are frequently applied in movement ecology to study an animal's habitat preferences and movement capacity (Fortin et al., 2005; Thurfjell et al., 2014; Avgar et al., 2016). They operate in discrete time and mathematically model the probability u of finding an individual at a location s at time $t + 1$, given the animal's past positions at time t and $t - 1$, s_t and s_{t-1} . Formally, this probability is given by:

$$u(s_{t+1}) = \frac{\phi(s_{t+1}, s_t, s_{t-1}; \gamma)w(x(s_{t+1}); \beta)}{\int_{s \in G} \phi(s_{t+1}, s_t, s_{t-1}; \gamma)w(x(s_{t+1}); \beta)ds} \quad (\text{Equation 1.1})$$

The function ϕ represents an animal's movement kernel which is usually expressed in terms of a step-length and turning-angle distribution, with γ representing parameters in these distributions (for simplicity, I will sometimes refer to the *movement kernel* as *movement preferences*). The function w defines the habitat-selection function and reflects an animal's preferences β towards environmental characteristics x at location s_{t+1} . In most applications, w is defined as the log-linear function $w = \exp(x^\top \beta)$. Finally, the integral in the denominator of Equation 1.1 ensures that u is a proper probability distribution and integrates to one.

To estimate parameters in Equation 1.1 using empirical data, one needs to convert observed GPS locations into sequences of temporally regularly-spaced steps. Here, a step is defined as the straight line

connecting two consecutive GPS locations (Turchin, 1998) and is characterized by a step length, absolute turning angle (a.k.a. heading), and relative turning angle. The likelihood in Equation 1.1 can then be maximized by comparing observed steps with random steps in a (mixed effects) conditional logistic regression model (Fortin et al., 2005; Muff et al., 2020, but see Michelot et al., 2016 for alternatives). The required random steps can be generated by sampling step lengths and turning angles from parametric distributions fitted to empirical data (Fortin et al., 2005; Thurfjell et al., 2014).

To jointly estimate parameters in ϕ and w , movement descriptors (e.g., step length (sl), its natural logarithm ($\log(sl)$)), and the cosine of the turning angle ($\cos(\text{ta})$)) can be included in the regression model, and their estimated coefficients serve to update the tentative parameters of the step-length and turning-angle distributions (Duchesne et al., 2015; Avgar et al., 2016; Fieberg et al., 2021). By including the relevant predictors, iSSFs allow modeling highly complex movement behaviors (e.g., Munden et al., 2021; Forrest et al., 2024). Notably, a model fitted using iSSFs constitutes a mechanistic movement model from which movement can be simulated (Avgar et al., 2016; Signer et al., 2017; Signer et al., 2024).

1.10 Thesis Outline

This thesis comprises six chapters; a general introduction, four data chapters, and a general discussion. All published chapters of this thesis are verbally reproduced as they appeared in the respective journals, including personal pronouns, jargon, and abbreviations. References cited in each chapter are listed at the end of the thesis.

In Chapter 2, I present a novel simulation approach to study landscape connectivity via simulated dispersal. Specifically, I introduce a simple three-step approach to quantify landscape connectivity using IBMMs, starting from empirical dispersal data and a set of landscape layers. The simulation approach relies on iSSFs, which enable a detailed representation of dispersers' habitat and movement preferences. In contrast to traditional connectivity modeling techniques, this approach bypasses the need for a permeability surface and overcomes several important limitations, such as the assumption that dispersers move towards a predefined endpoint. To translate simulated dispersal trajectories into meaningful measures of functional connectivity, I propose three complementary connectivity metrics, each focused on a different aspect of connectivity. This includes a heatmap, revealing frequently traversed areas, a betweenness map, highlighting critical movement corridors, and a map of inter-patch connectivity, summarizing dispersal frequencies and durations. I demonstrate the application of the approach using dispersing AWDs in the KAZA-TFCA as a case-study. I thereby show how landscape connectivity varies across the KAZA-TFCA landscape and reveal critical movement corridors. This chapter was published in *Landscape Ecology* in 2023 (<https://doi.org/10.1007/s10980-023-01602-4>).

In Chapter 3, I study functional connectivity for AWDs in light of increasingly extreme climatic conditions due to climate change. Specifically, I study how climate-induced changes to the Okavango Delta's flooding regime could influence AWDs' ability to move between remaining populations. For this, I compile over 20 years of remote sensed satellite data on flood conditions and derive two extreme scenarios that serve to approximate flood conditions under climate change. For both scenarios, I simulate AWD dispersal and investigate emerging connectivity patterns. I show that periods of increased flooding result in isolated subpopulations and reduced dispersal prospects. Conversely, I find that periods of reduced floods reveal vast dispersal habitats that can be used to transfer from one subpopulation to another. Overall, this work highlights the importance of accounting for anticipated on-the-ground conditions in light of climate change when assessing landscape connectivity. This chapter was published in *Global Change Biology* in 2024 (<https://doi.org/10.1111/gcb.17299>).

In Chapter 4, I investigate the importance of accounting for seasonal dynamism when investigating landscape connectivity. To do so, I first provide a conceptual framework to motivate that seasonality can enter connectivity analyses at multiple stages; when (1) extracting spatial covariates for model fitting, (2) when fitting the selection model, and (3) when making predictions from the fitted model. Via combination, this provides six distinct configurations that differ in their amount of dynamism. Using GPS data on dispersing AWDs, I parametrize the models associated with each configuration and employ a rigorous validation approach to assess at which stages rendering seasonality is critical. I also employ IBMMs to simulate dispersal under varying degrees of seasonal dynamism and examine the emerging patterns of connectivity. Notably, in the most dynamic configuration, I update seasonal covariates as the simulated dispersers move; a similar degree of seasonality cannot be achieved via traditional approaches. Even though the validation procedure reveals only a marginal benefit of increasing dynamism, I find that emerging patterns of connectivity differ markedly depending on the level of incorporated dynamism. Specifically, a static approach results in more clumped dispersal hotspots, whereas a dynamic take suggests more heterogeneously distributed dispersal movements. This chapter highlights that the predictive improvements reaped by incorporating seasonality into connectivity analyses may be moderate, despite marked differences in inferred patterns of connectivity.

In Chapter 5, I revisit the iSSF framework utilized throughout Chapters 2 to 4. A major drawback of iSSFs is that they presume that GPS data were collected at regular time intervals, whereas in reality GPS data are often incomplete and gappy, thus exhibiting slight irregularities between successive GPS locations. Usually, such irregular data need to be removed, implying a substantial reduction in effective sample size. To overcome this limitation, I introduce and compare several methods that account for irregularity, thereby allowing to retain additional GPS data for modeling. I use simulations with known parameters to compare the effectiveness of different methods and show that irregularity can be effectively accounted

for when appropriate methods are used. I also exemplify the application of the best performing method to a case study using GPS data on a spotted hyena. The divergence from using AWD dispersal data was primarily due to the availability of an extensive dataset on a single spotted hyena. This chapter was published in *Movement Ecology* in 2024 (<https://doi.org/10.1186/s40462-024-00476-8>).

Finally, in Chapter 6, I synthesize and reflect on the main insights of this thesis and discuss how this work integrates into the existing literature. I also elaborate on some of the methodological and biological implications of my work, with a particular focus on conservation insights for the African wild dog. Finally, I highlight potential limitations and give an outlook for future research.



Chapter 2

A Three-Step Approach for Assessing Landscape Connectivity via Simulated Dispersal: African Wild Dog Case Study

David D. Hofmann , Gabriele Cozzi , John W. McNutt, Arpat Ozgul , and Dominik M. Behr 

Abstract

Dispersal of individuals contributes to long-term population persistence, yet requires a sufficient degree of landscape connectivity. To date, connectivity has mainly been investigated using least-cost analysis and circuit theory, two methods that make assumptions that are hardly applicable to dispersal. While these assumptions can be relaxed by explicitly simulating dispersal trajectories across the landscape, a unified approach for such simulations is lacking. Here, we propose and apply a simple three-step approach to simulate dispersal and to assess connectivity using empirical GPS movement data and a set of habitat covariates. In step one of the proposed approach, we use integrated step-selection functions to fit a mechanistic movement model describing habitat and movement preferences of dispersing individuals. In step two, we apply the parameterized model to simulate dispersal across the study area. In step three, we derive three complementary connectivity maps; a heatmap highlighting frequently traversed areas, a betweenness map pinpointing dispersal corridors, and a map of inter-patch connectivity indicating the presence and intensity of functional links between habitat patches. We demonstrate the applicability of the proposed three-step approach in a case study in which we use GPS data collected on dispersing African wild dogs (*Lycaan pictus*) inhabiting northern Botswana. Using step-selection functions we successfully parametrized a detailed dispersal model that described dispersing individuals' habitat and movement preferences, as well as potential interactions among the two. The model substantially outperformed a model that omitted such interactions and enabled us to simulate 80,000 dispersal trajectories across the study area. By explicitly simulating dispersal trajectories, our approach not only requires fewer unrealistic assumptions about dispersal, but also permits the calculation of multiple connectivity metrics that together provide a comprehensive view of landscape connectivity. In our case study, the three derived connectivity maps revealed several wild dog dispersal hotspots and corridors across the extent of our study area. Each map highlighted a different aspect of landscape connectivity, thus emphasizing their complementary nature. Overall, our case study demonstrates that a simulation-based approach offers a simple yet powerful alternative to traditional connectivity modeling techniques. It is therefore useful for a variety of applications in ecological, evolutionary, and conservation research.

2.1 Introduction

Dispersal of individuals is a vital process that allows species to maintain genetic diversity (Perrin & Mazalov, 2000; Frankham et al., 2002; Leigh et al., 2012; Baguette et al., 2013; LaPoint et al., 2013), rescue non-viable populations (Brown & Kodric-Brown, 1977), and to colonize unoccupied habitats (Hanski, 1999a; MacArthur & Wilson, 2001). However, the ability to disperse depends on a sufficient degree of landscape connectivity (Fahrig, 2003; Clobert et al., 2012), making the identification and protection of dispersal corridors that promote connectivity a task of fundamental importance (Doerr et al., 2011; Rudnick et al., 2012). Identifying dispersal corridors not only necessitates a comprehensive understanding of the factors that limit dispersal, but also an appropriate model to estimate connectivity (Baguette et al., 2013; Vasudev et al., 2015; Hofmann et al., 2021). To date, the most commonly used connectivity models are least-cost path analysis (LCPA; Adriaensen et al., 2003) and circuit theory (CT; McRae, 2006; McRae et al., 2008). Unfortunately, both models rest on assumptions that appear unsuitable for dispersers, thus calling for the development of alternative approaches. One promising alternative is to assess landscape connectivity via simulated dispersal trajectories generated from individual-based movement models (IBMMs, Diniz et al., 2019). However, IBMMs require a large number of subjective modeling decisions, thus making among-system comparisons difficult.

Traditional connectivity models make assumptions that are rarely met for dispersers. LCPA, for instance, assumes that individuals move towards a preconceived endpoint and choose a cost-minimizing route accordingly (Sawyer et al., 2011; Abrahms et al., 2017). While this assumption may be justifiable for migrating animals, it is unlikely to hold for dispersers, as dispersers typically move across unfamiliar territory towards an unknown endpoint (Koen et al., 2014; Cozzi et al., 2020). CT, on the contrary, posits that animals move according to a random walk, entailing that autocorrelation between subsequent movements cannot be rendered (Diniz et al., 2019). For dispersers, however, autocorrelated movements are regularly observed (Cozzi et al., 2020; Hofmann et al., 2021), meaning that dispersal trajectories are usually strongly directional. An interesting generalization that bridges the continuum between LCPA and CT has been proposed by Panzacchi et al. (2016) and enables to capitalize on the merits of both approaches. Despite these and several other generalizations of LCPA and CT (e.g. Pinto and Keitt, 2009; Landguth et al., 2012; Panzacchi et al., 2016; Brennan et al., 2020), some shortcomings remain. Most notably, all of these methods rely on static permeability or resistance surfaces that can't reflect the temporal dimension of dispersal. This permits statements about the expected duration for moving between habitat patches (Martensen et al., 2017; Diniz et al., 2019).

The shortcomings inherent to LCPA and CT can be overcome by simulating dispersal using IBMMs and by converting simulated trajectories into meaningful measures of connectivity (Diniz et al., 2019). In

contrast to LCPA and CT, IBMMs allow to explicitly simulate how individuals move across and interact with the encountered landscape (Kanagaraj et al., 2013; Clark et al., 2015; Allen et al., 2016; Hauenstein et al., 2019; Zeller, Wattles, et al., 2020), as well as to render potential interactions between movement behavior and habitat conditions (Avgar et al., 2016). This shifts the focus towards a more functional view on connectivity (Tischendorf & Fahrig, 2000). Furthermore, IBMMs generate movement sequentially, i.e. they generate a series of steps, so that the temporal dimension of dispersal becomes explicit and allows modeling autocorrelation between successive steps (Diniz et al., 2019). Finally, simulations from IBMMs do not enforce movement or connections towards preconceived endpoints but allow individuals to adjust their route “on the go”, thereby preventing biases arising from misplaced endpoints. Despite these advantages, a unifying approach to simulate dispersal and assess connectivity using IBMMs is lacking. Considering the large number of subjective decisions entailed by IBMMs, an approach that streamlines and standardizes the application of dispersal simulations to assess connectivity will, however, be critical to safeguard comparability among studies.

Here, we propose and exemplify a simple three-step approach for simulating dispersal and assessing landscape connectivity (Figure 2.1). In step one, we combine GPS movement data of dispersing individuals with habitat covariates to fit a mechanistic movement model via integrated step-selection functions (iSSFs, Avgar et al., 2016). We chose to use iSSFs because the framework not only allows inference on the study species’ habitat kernel (i.e. its habitat preferences), but also its movement kernel (i.e. its movement preferences/capabilities) and potential interactions among the two (Avgar et al., 2016; Fieberg et al., 2021). In step two, we use the parametrized movement model to simulate dispersal across the study area. Comparable simulations have already been applied to estimate steady-state utilization distributions of resident individuals (Potts et al., 2013; Signer et al., 2017) and to model landscape connectivity, yet disregarding interdependencies between habitat and movement kernels (Clark et al., 2015; Zeller, Wattles, et al., 2020). Finally, in step three, we convert the simulated trajectories into three complementary connectivity maps; (i) a heatmap revealing frequently traversed areas (e.g. Hauenstein et al., 2019; Zeller, Wattles, et al., 2020), (ii) a betweenness-map delineating dispersal corridors and bottlenecks (e.g. Bastille-Rousseau et al., 2018), (iii) and a map of inter-patch connectivity, depicting the presence and intensity of functional links between habitat patches, as well as the average dispersal duration required to realize those connections (e.g. Gustafson and Gardner, 1996; Kanagaraj et al., 2013).

We showcase the application of the proposed approach using GPS movement data collected on dispersing African wild dogs (*Lycaon pictus*). The African wild dog is a highly mobile species whose population persistence heavily relies on the availability of large, natural or semi-natural landscapes and a sufficient degree of connectivity among remaining subpopulations. Once common throughout sub-Saharan Africa, this species has disappeared from much of its historic range, largely due to human persecution, habitat

fragmentation, and disease outbreaks (Woodroffe & Sillero-Zubiri, 2012). Wild dogs typically disperse in single-sex coalitions (McNutt, 1996; Behr et al., 2020) and are capable of dispersing several hundred kilometers (Davies-Mostert et al., 2012; Masenga et al., 2016; Cozzi et al., 2020). Although previous studies have investigated connectivity for this species using LCPA (Hofmann et al., 2021) and CT (Brennan et al., 2020), a more comprehensive and mechanistic understanding of dispersal and connectivity is missing (but see Creel et al., 2020). Nevertheless, with about 6,000 free-ranging wild dogs remaining in fragmented subpopulations (Woodroffe & Sillero-Zubiri, 2012), reliable information on dispersal behavior and landscape connectivity is essential for the conservation of this endangered carnivore. We anticipated that a connectivity assessment based upon our three-step approach would overcome several of the conceptual shortcomings of traditional connectivity models, while providing a more detailed view on movement behavior during dispersal its implications for landscape connectivity.

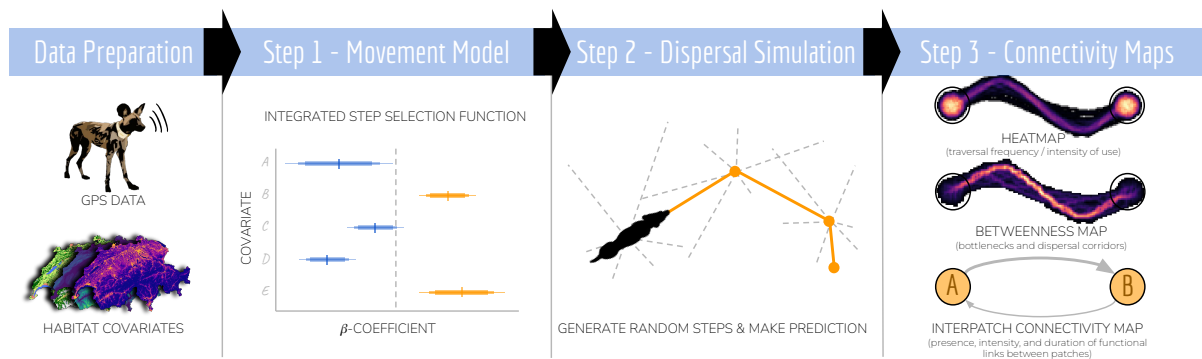


Figure 2.1: Flowchart of the simulation-based connectivity analysis. First, GPS data and habitat covariates must be collected. The combined data is then analyzed using an integrated step selection model (step 1). The parametrized model is then treated as an individual-based movement model and used to simulate dispersal trajectories (step 2). Ultimately, simulated trajectories are translated into a set of maps that are pertinent to landscape connectivity (step 3). This includes a heatmap, indicating the traversal frequency across each spatial unit of the study area, a betweenness map, highlighting movement corridors and bottlenecks, and, finally, an inter-patch connectivity map, where the frequency of connections and their average duration can be depicted.

2.2 Materials and Methods

2.2.1 Case Study

GPS Data

We applied the three step approach presented in Figure 2.1 to GPS movement data from 16 dispersing African wild dog coalitions (7 female and 9 male coalitions). This data has been collected between 2011 and 2019 from a free-ranging wild dog population in northern Botswana. During dispersal, GPS collars recorded a fix every 4 hours and regularly transmitted data over the Iridium satellite system. To ensure

comparable time intervals between GPS fixes, we removed any fixes that were not successfully obtained at the desired 4-hour schedule (allowing for a tolerance of \pm 15 minutes). To prepare the data for step-selection analysis, we converted the fixes ($n = 4'169$) into steps, where each step represented the straight-line movement between two consecutive GPS fixes (Turchin, 1998). We only considered steps with equal step-durations (i.e. 4 hours) for further analysis. We will refer to these steps as “realized steps”. We did not differentiate between sexes, for previous research found little differences between sexes during dispersal (Cozzi et al., 2020; Woodroffe & Sillero-Zubiri, 2020). Additional details on the data collection and preparation can be found in Cozzi et al. (2020) and Hofmann et al. (2021).

Study Area

Our simulation of dispersal trajectories and assessment of connectivity spanned across the entire Kavango-Zambezi Transfrontier Conservation Area (KAZA-TFCA, Figure 2.2a and b) and encompassed a rectangular extent of roughly 1.3 Mio. km². With an area of 520,000 km², the KAZA-TFCA is the world’s largest trans-boundary conservation area and comprises parts of Angola, Botswana, Namibia, Zimbabwe, and Zambia, thus hosting a rich diversity of landscapes, ranging from savannah to grassland and from dry to moist woodland habitats. In its center lies the Okavango Delta, a dominant hydro-geographical feature and the world’s largest flood-pulsing inland delta. Large portions of the KAZA-TFCA are formally protected in the form of national parks (NPs) or other protected areas, yet a considerable portion of the landscape remains human-dominated (e.g. roads, agricultural sites, and settlements).

Habitat Covariates

We represented the physical landscape in our study area by the habitat covariates water-cover, distance-to-water, woodland-cover, shrub/grassland-cover, and human-influence. To render the seasonal dynamics of water-cover for the extent of the Okavango Delta, we applied an algorithm that enabled us to obtain weekly updated raster-layers for water-cover and distance-to-water from MODIS satellite imagery (Wolski et al., 2017; Hofmann et al., 2021). This algorithm is now implemented in the `floodmapr` package (available on GitHub; <https://github.com/DavidDHofmann/floodmapr>). To ensure a consistent resolution across habitat covariates, we coarsened or interpolated all layers to a resolution of 250 m x 250 m. A detailed description of how we prepared each habitat covariate is provided by Hofmann et al. (2021).

We performed all data preparations, spatial computations, and statistical analysis in R, version 4.2.2 (R Core Team, 2023). Some helper functions were written in C++ and imported into R using the `Rcpp` package (Eddelbuettel & François, 2011; Eddelbuettel, 2013; Eddelbuettel & Balamuta, 2018).

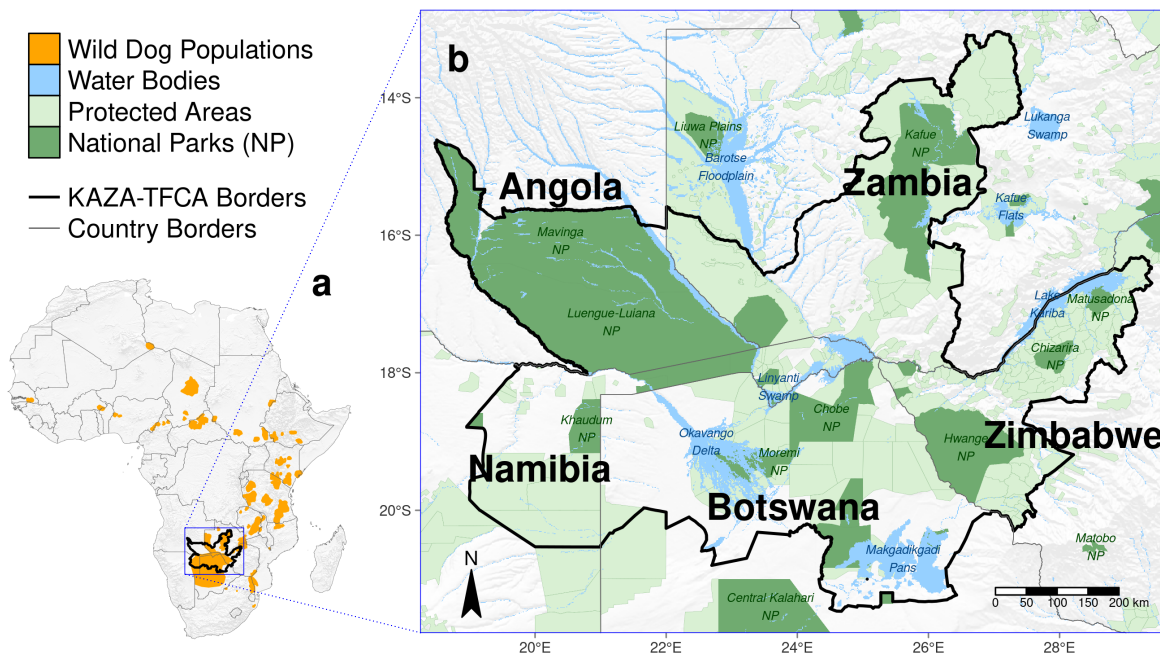


Figure 2.2: Illustration of the study area in southern Africa. (a) The study area was confined by a bounding box spanning the entire KAZA-TFCA which comprises parts of Angola, Namibia, Botswana, Zimbabwe, and Zambia. Data on remaining wild dog populations (orange) has been sourced from Woodroffe and Sillero-Zubiri (2012). (b) The KAZA-TFCA represents the world's largest terrestrial transfrontier conservation area and covers a total area of 520,000 km². Its main purpose is to re-establish connectivity between already-existing NPs (dark green) and other protected areas (light green).

2.2.2 Step 1 - Movement Model

We combined the collected GPS data with habitat covariates and used iSSFs (Avgar et al., 2016) to parametrize a mechanistic movement model. More specifically, we paired each realized step with a set of 24 randomly generated alternative steps. A realized and its 24 random steps together formed a stratum that received a unique identifier. As suggested by Avgar et al. (2016), we generated random steps by sampling random turning angles from a uniform distribution ($-\pi, +\pi$) and step lengths from a gamma distribution that was fitted to realized steps (scale $\theta = 6,308$ and shape $k = 0.37$). Note that our approach of sampling turning angles from a uniform distribution does not imply that we assume uniform turning angles, as we will account for directionality later in the model (Avgar et al., 2016; Fieberg et al., 2021).

Along each realized and random step, we extracted values from underlying habitat covariate layers and we computed averages of each covariate along the steps. Besides extracting *habitat covariates*, we also computed movement metrics that we used as *movement covariates* in the iSSF models (Avgar et al., 2016; Fieberg et al., 2021). Specifically, we computed the step length (sl), its natural logarithm ($\log(sl)$), and the cosine of the relative turning angle ($\cos(ta)$), which is a measure of directionality (Turchin, 1998), for each step. Because wild dog activity is low during the hot midday hours (Cozzi et al., 2012), we additionally created the variable LowActivity, indicating whether a step was realized during periods of low wild dog activity (09:00 to 17:00 local time) or high wild dog activity (17:00 to 09:00 local time). To facilitate model convergence, we standardized all continuous covariates to a mean of zero and a standard deviation of one. Correlations among covariates were low ($|r| < 0.6$; Latham et al., 2011), so we retained all of them for modeling.

To contrast realized steps (scored 1) and random steps (scored 0), we assumed that animals assigned a selection score $w(x)$ to each step (Equation 2.1; Fortin et al., 2005), where $w(x)$ depended on the step's associated covariates (x_1, x_2, \dots, x_n) and on the animal's relative selection strengths (Avgar et al., 2017) towards these covariates ($\beta_1, \beta_2, \dots, \beta_n$):

$$w(x) = \exp(\beta_1 x_1 + \beta_2 x_2 + \dots + \beta_n x_n) \quad (\text{Equation 2.1})$$

The probability of a step i being realized was then contingent on the step's selection score, as well as on the selection scores of all other steps in the same stratum:

$$P(Y_i = 1 | Y_1 + Y_2 + \dots + Y_i = 1) = \frac{w(x_i)}{w(x_1) + w(x_2) + \dots + w(x_i)} \quad (\text{Equation 2.2})$$

To estimate relative selection strengths (i.e. the β -coefficients), we used mixed effects conditional logistic regression analysis, implemented through the R-package `glmmTMB` (Brooks et al., 2017). The implementation of conditional logistic regression has been proposed by Muff et al. (2020) and allows to model

random slopes. The method requires to fix the variance of the stratum specific intercept to a large value, so we fixed it to an arbitrary high value of 10^6 and used disperser identity to model random slopes for all covariates.

Our movement model was based on a habitat selection model that was previously developed for dispersing wild dogs (hereafter referred to as *base model*, Hofmann et al., 2021). In the base model, no interactions among habitat covariates and movement covariates were considered, so we here expanded the model and allowed for such interactions, acknowledging that movement preferences during dispersal could depend on habitat conditions (details in Section 2.A). To determine the most parsimonious movement model among model candidates, we ran stepwise forward model selection based on Akaike's Information Criterion (AIC, Burnham and Anderson, 2002). More specifically, we started with the base model and iteratively increased model complexity by adding all possible interactions between movement and habitat covariates. Given that the focus of our analysis lied on predicting dispersal patterns and all model candidates were biologically intuitive, we deemed the use of model selection appropriate. However, caution should be employed if causal relationships are of interest, as model selection may lead to biased parameter estimate (Whittingham et al., 2006). We validated the predictive power of the most parsimonious model using k-fold cross-validation for case-control studies as described in Fortin et al. (2009). This validation attests significant prediction ability to the movement model if the model outperforms a random guess and systematically assigns low ranks (high selection scores) to observed steps (details in Section 2.B).

2.2.3 Step 2 - Dispersal Simulation

We used the most parsimonious movement model to simulate individual dispersal trajectories across the study area. The simulation of a dispersal trajectory resembled an “inverted” iSSF and was set up as follows. (1) We defined a source point and assumed a random initial orientation of the simulated animal. (2) Starting from the source point, we generated 25 random steps by sampling turning angles from a uniform distribution $(-\pi, +\pi)$ and step lengths from our fitted gamma distribution. (3) Along each random step, we extracted and averaged values from the habitat covariate layers and we computed the movement metrics sl , $\log(sl)$, and $\cos(ta)$. To ensure compatible scales with the fitted movement model, we standardized covariate values using means and standard deviations from the empirical data. (4) We applied the parametrized movement model to predict the selection score $w(x)$ for each step using Equation 2.1 and we converted predicted scores into probabilities using Equation 2.2. (5) We randomly sampled one of the generated random steps based on assigned probabilities and determined the animal's new position. We repeated steps (2) to (5) until 2,000 steps were realized and we repeated the simulation until a total of 80,000 dispersal trajectories was reached.

As source points for the simulations, we distributed 50,000 points at random locations inside protected areas that were large enough to host an average size wild dog home range (i.e. $> 700 \text{ km}^2$; Pomilia et al., 2015). We placed another 30,000 points randomly inside the buffer zone, mimicking potential immigration into the study area (Figure 2.C.1).

To mitigate edge effects and to deal with random steps leaving the study area, we followed Koen et al. (2010) and artificially expanded all covariate layers by a 100 km wide buffer zone. Within the buffer zone, we randomized covariate values by resampling values from the original covariate layers. Through this buffer zone, simulated dispersers were able to leave and re-enter the main study area. In cases where random steps crossed the outer border of this buffer zone, we resampled steps until they fully lied within the buffer zone, essentially forcing simulated individuals to remain within the expanded study area.

To ensure reliable connectivity estimates, we determined the number of simulated dispersal trajectories required to reach a “steady state”. For this purpose, we distributed 1,000 rectangular “checkpoints”, each with an arbitrary extent of 5 km \times 5 km, at random coordinates within the study area (excluding the buffer). We then determined the relative frequency at which each checkpoint was traversed by simulated dispersal trajectories (hereafter referred to as relative traversal frequency) as we gradually increased the number of simulated trajectories from 1 to 50,000. To assess variability in the relative traversal frequency, we repeatedly subsampled 100 times from all 50,000 trajectories and computed the mean traversal frequency across replicates, as well as its 95% prediction-interval for each checkpoint. We considered connectivity to have reached a steady state once the width of the prediction-interval dropped below a value of 0.01 for all checkpoints.

2.2.4 Step 3 - Connectivity Maps

Heatmap

To identify dispersal hotspots within the study area, we created a heatmap indicating the absolute frequency at which different areas were traversed by simulated dispersal trajectories (e.g. Hauenstein et al., 2019; Zeller, Wattles, et al., 2020). Specifically, we rasterized all simulated trajectories onto a raster with 1 km \times 1 km resolution and tallied resulting layers into a single map. This procedure ensured that every trajectory was only counted once, even if it traversed the same raster-cell multiple times, thus reducing potential biases caused by individuals that were surrounded by unfavorable habitat and “moved in circles”. To achieve high performance rasterization, we used the R-package *terra* (Hijmans et al., 2024). For a subset of the study area, we also generated heatmaps at 250 m \times 250 m, yet found little qualitative differences to the coarser resolution, thus suggesting the choice of 1 km \times 1 km to be appropriate.

Betweenness Map

To pinpoint movement corridors and bottlenecks, we converted simulated trajectories into a network and calculated betweenness scores for all raster-cells in the study area (Bastille-Rousseau et al., 2018). Betweenness is a pertinent metric for connectivity as it measures how often a specific network-node (in our case a raster-cell) lies on a shortest path between any other pair of nodes (Bastille-Rousseau et al., 2018). To convert simulated trajectories into a network, we followed Bastille-Rousseau et al. (2018) and overlaid the study area (including the buffer) with a raster containing 2.5 km x 2.5 km raster-cells, where the center of each raster-cell served as node in the final network. To identify edges (i.e. connections) between the nodes, we used the simulated trajectories and determined all transitions occurring from one cell to another, as well as the frequency at which those transitions occurred (see also Section 2.D). This resulted in an edge-list that we translated into a weighted network using the r-package `igraph` (Csardi & Nepusz, 2006). The final weight of each edge was determined by the frequency of transitions, yet because `igraph` handles edge weights (ω) as costs, we inverted the traversal-frequency through each raster-cell by applying $\omega = \frac{\text{mean}(\text{TraversalFrequency})}{\text{TraversalFrequency}_i}$. Consequently, regularly used edges received small weights (i.e. low costs) and vice versa. We used the weighted network to calculate betweenness scores for all network nodes.

Inter-Patch Connectivity Map

To examine the presence and intensity of functional links (i.e. connections) between patches within the study area, we calculated inter-patch connectivity (e.g. Gustafson and Gardner, 1996, Kanagaraj et al., 2013). For this, we computed the relative frequency at which dispersers originating from one patch successfully moved into another patch. We considered movements between patches as successful if an individual's dispersal trajectory originating from the source patch intersected with the target patch at least once. For each trajectory we also recorded the number of steps required to reach the first intersection with the respective patch, allowing us to compute the average dispersal durations from one patch to another. In summary, we determined *if* and *how often* dispersers moved between certain patches, as well as *how long* individuals had to move to make these connections. In our case study, we used NPs as patches to determine inter-patch connectivity, hence we'll use the terms interchangeably from here on. The decision to focus on NPs was purely out of simplicity and should not imply that dispersal between other areas is impossible.

Validation

To validate our predictions of connectivity, we utilized additional dispersal data that was collected on eight dispersing coalitions between 2019 and 2022 (totalling to 2,668 GPS locations). We used a path selection

function (PSF, Cushman and Lewis, 2010) to assess if observed dispersal trajectories followed areas of high predicted connectivity. Similar to SSF, PSF enables to detect selection for certain features by comparing observed paths to randomly generated paths. Here, we paired each observed path with 50 random paths that we generated by randomly rotating and shifting observed paths by a random angle $\alpha \sim U(-\pi, +\pi)$ and a random distance $d \sim U(0 \text{ km}, 50 \text{ km})$. Along each path, we then extracted connectivity values from the heatmap (see above) generated after 68, 125, 250, 500, and 2,000 simulated steps, respectively. Finally, we ran conditional logistic regression to contrast observed and random paths. In case of systematic selection for high-connectivity areas, the regression coefficients from the corresponding conditional logistic regression model should be positive.

2.3 Results

The most parsimonious movement model consisted of movement covariates, habitat covariates, as well as several of their interactions, thus suggesting that movement behavior during dispersal depended on habitat conditions (Figure 2.3a, Table 2.E.1 and table 2.F.1). Although multiple models received an AIC weight > 0 (Table 2.E.1), we only considered results from the most parsimonious model for simplicity. This decision only marginally influenced subsequent steps as all models with positive AIC weights retained similar covariates (Table 2.E.1). The k-fold cross-validation showed that the final model substantially outperformed a random guess and provided reliable predictions (i.e. confidence intervals of $\bar{r}_{s,realized}$ and $\bar{r}_{s,random}$ did not overlap). Moreover, the model correctly assigned high selection scores to realized steps (Figure 2.3b), indicating a good fit between predictions and observations. As can be taken from the Spearman rank correlation coefficient, the inclusion of several interactions between movement and habitat covariates significantly improved model performance ($\bar{r}_{s,realized} = -0.65; 95\% - CI = [-0.67, -0.64]$), compared to the base model ($\bar{r}_{s,realized} = -0.55; 95\% - CI = [-0.57, -0.52]$; Hofmann et al., 2021). Our validation of the resulting connectivity maps using independent dispersal data showed that dispersers preferentially followed areas of high predicted connectivity, as coefficients from the PSF models were all significantly greater than zero (Figure 2.3c). The movement model thus successfully predicted functional connectivity.

Plots that aid with the interpretation of the most parsimonious movement model are provided in Figure 2.G.1 and suggest that, under average conditions, dispersing wild dogs avoided moving through water, woodlands, and areas dominated by humans, but preferred moving across shrublands or grasslands (Figure 2.3a). Dispersers realized shorter steps (indicating slower movements) in areas covered by water or woodland, while realizing larger steps in areas dominated by shrubs or grass (Figure 2.3a). We found a particularly large effect for the variable LowActivity, suggesting that dispersing wild dogs moved substantially faster during twilight and at night (i.e. between 17:00 and 09:00 o'clock; Figure 2.3a). Although dispersers revealed a preference for directional movements (i.e. low turning angles), especially when moving quickly,

they did less so in proximity to humans or water, resulting in more tortuous movements in such areas (Figure 2.3a).

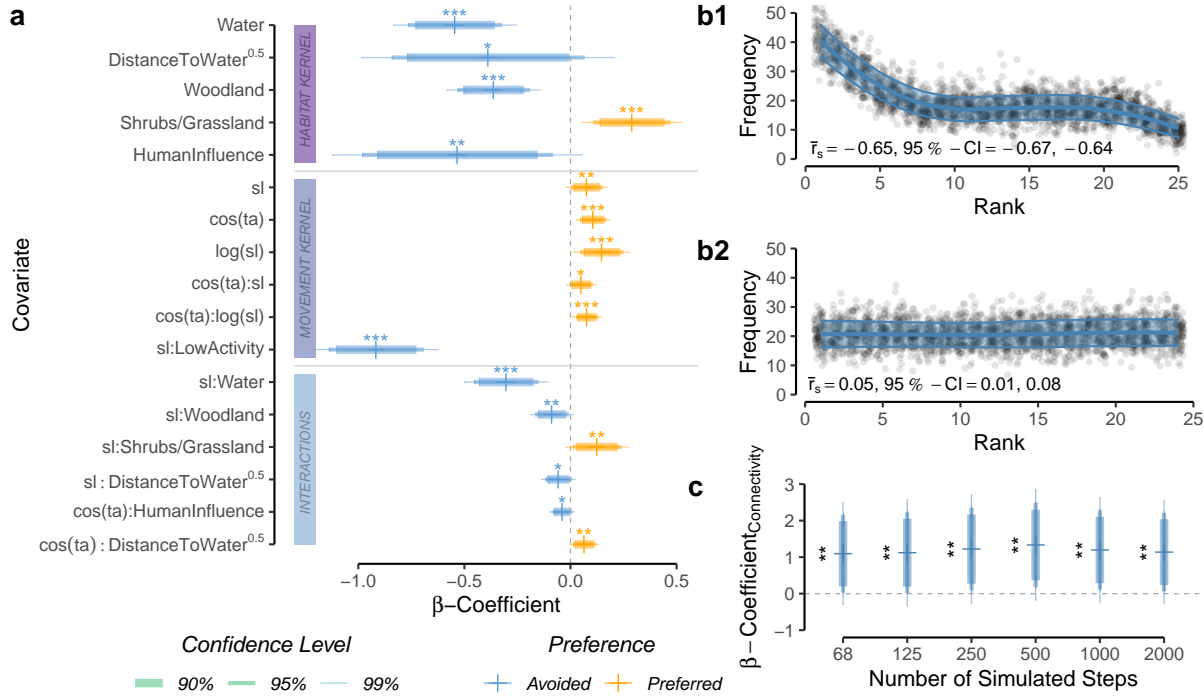


Figure 2.3: (a) Most parsimonious movement model for dispersing wild dogs. The model comprises a habitat kernel, a movement kernel, as well as their interactions. The horizontal line segments delineate the 90%, 95%, and 99% confidence-intervals for the respective β -coefficients. Significance codes: * $p < 0.10$, ** $p < 0.05$, *** $p < 0.01$. (b) Results from the k-fold cross-validation procedure. Subfigure b1 shows rank frequencies of realized steps according to model predictions with known preferences, whereas subfigure b2 shows rank frequencies of realized steps when assuming random preferences. The blue ribbon shows the prediction interval around a loess smoothing regression that we fitted to ease the interpretation of the plots. The significant correlation between rank and associated frequency in b1 highlights that the most parsimonious model successfully outperformed a random guess b2 and frequently assigned low ranks (i.e. high selection scores) to realized steps but only rarely high ranks (i.e. low selection scores). (c) Results from the PSF analysis using independent dispersal data show that dispersers preferably moved through areas where our heatmaps predicted high connectivity. Results are shown for heatmaps realized after 68, 125, 250, 500, and 2,000 simulated steps, respectively.

2.3.1 Dispersal Simulation

Dispersal simulations based on the most parsimonious movement model proved useful for assessing landscape connectivity. Of the 50,000 simulated dispersal trajectories that originated from the main study area, only 4.5% reached a map boundary, suggesting that we successfully mitigated biases from boundary effects. Moreover, our examination of the relative traversal frequency across all checkpoints showed that the relative traversal frequency reached a steady state after 10,500 simulated dispersal trajectories (Figure 2.H.1). Although variability in the relative traversal frequency kept decreasing as we increased the number of simulated dispersers, the marginal benefit of simulating additional trajectories diminished quickly (Figure 2.H.1).

2.3.2 Heatmap

The heatmap (Figure 2.4), which resulted from the summation of all simulated dispersal trajectories, allowed us to pinpoint areas that were frequently visited and enabled us to compare areas inside and outside the KAZA-TFCA borders with respect to the intensity at which they were used for dispersal. For instance, we could deduct that areas inside the KAZA-TFCA were frequently traversed by dispersers (median traversal frequency inside KAZA-TFCA = 166, IQR = 274, Figure 2.K.1a), whereas areas beyond the KAZA-TFCA boundary were comparatively rarely visited (median traversal frequency outside KAZA-TFCA = 61, IQR = 133, Figure 2.K.1a). Most notably, the region in northern Botswana south of the Linyanti swamp appeared to serve as highly frequented dispersal hotspot (median traversal frequency = 987, IQR = 558). Aside from revealing movement hotspots, the heatmap also provided information on areas that appeared to hinder movement. For example, extensive water bodies, such as the Okavango Delta, the Makgadikgadi Pan, and the Linyanti swamp, substantially restricted dispersal movements and limited realized connectivity inside the KAZA-TFCA. Similarly, the landscapes of Zambia and Zimbabwe were only rarely used for dispersal, even within the KAZA-TFCA boundaries (Figure 2.K.2a). Despite the fact that the heatmap improved our understanding of the frequency at which areas were traversed by simulated dispersers, it seemed impractical to pinpoint dispersal corridors.

2.3.3 Betweenness

The betweenness map (Figure 2.5) revealed several distinct dispersal corridors that run across the study area. In comparison to the heatmap, the betweenness map was less biased towards areas with many dispersers and pronounced narrower, more linear routes that were used by simulated individuals to move between regions. Again, northern Botswana emerged as a wild dog dispersal corridor that connected more remote regions in the study area. Towards east, the extension of this corridor ran through Chobe NP into Hwange NP. From there, a further extension connected to Matusadona NP in Zimbabwe. Northwest of the Linyanti ecosystem, a major corridor expanded into Angola, where it split and finally traversed over a long stretch of unprotected area into Zambia's Kafue NP. Several additional corridors with lower betweenness scores emerged, yet most of them ran within the KAZA-TFCA boundaries (median betweenness inside KAZA-TFCA = 6.947×10^6 , IQR = 54.311×10^6 , Figure 2.K.1b). Consequently, only few corridors directly linked the peripheral regions of the KAZA-TFCA and passed through unprotected areas outside its borders (mean betweenness outside KAZA-TFCA = 2.685×10^6 , IQR = 9.891×10^6 , Figure 2.K.1b).

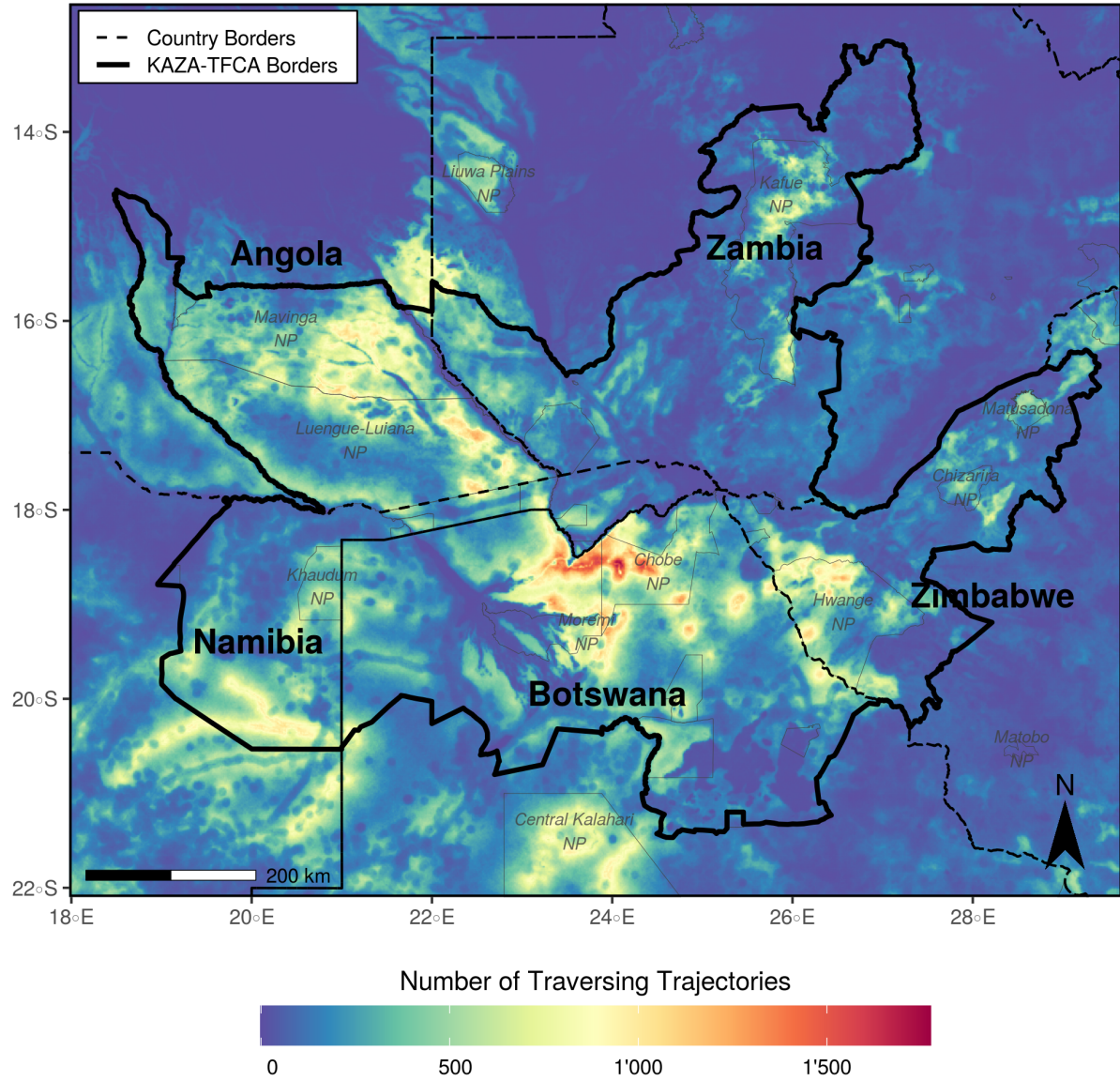


Figure 2.4: Heatmap showing traversal frequencies of 80,000 simulated dispersers moving 2,000 steps across the KAZA-TFCA. Simulations were based on an integrated step-selection model that we fitted to the movement data of dispersing African wild dogs. To generate the heatmap, we rasterized and tallied all simulated trajectories. Consequently, the map highlights areas that are frequently traversed. For spatial reference we plotted a few selected NPs (dark gray). Additional heatmaps showing the traversal frequency when individuals move fewer than 2,000 steps are provided in Figure 2.I.1.

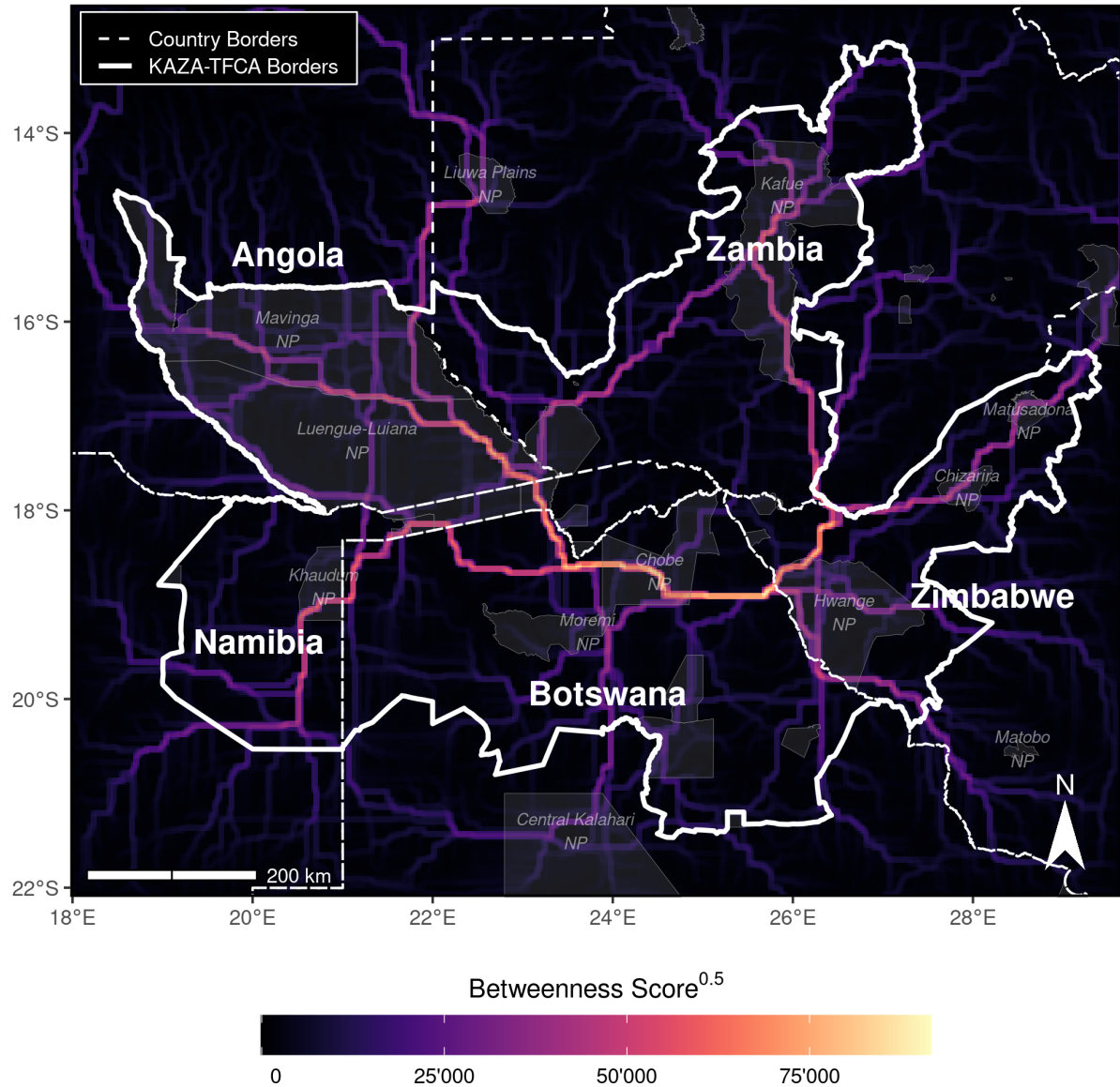


Figure 2.5: Map of betweenness scores, highlighting distinct dispersal corridors and potential bottlenecks across the extent of the KAZA-TFCA. Betweenness measures the number of shortest paths traversing through each node (raster-cell). Hence, a high betweenness score indicates that the respective area is exceptionally important for connecting different regions in the study area. The metric is therefore useful to pinpoint discrete movement corridors (Bastille-Rousseau et al., 2018). Note that we square-rooted betweenness scores to improve visibility of corridors with comparably low scores. Additional betweenness maps showing betweenness scores when individuals move fewer than 2'000 steps are provided in Figure 2.J.1.

2.3.4 Inter-Patch Connectivity

The inter-patch connectivity map showed that the relative frequency at which simulated dispersal trajectories moved from one patch to another varied, as did the average dispersal duration between patches (Figure 2.6). The map thereby completed the picture on connectivity and provided valuable insights into the frequency and duration of connections between patches. For some patches, we also detected imbalances between the number of incoming and outgoing links, hinting at possible source-sink dynamics. From Chobe NP, for instance, 510 individuals reached the Moremi NP, yet the opposite route was only realized by 340 individuals. Relative to the number of simulated individuals, however, these numbers correspond to fractions of 50% and 68%, respectively. Overall, inter-patch connectivity between patches in Angola, Namibia, Botswana, and Zimbabwe appeared to be high; between 54% and 87% of individuals originating from a patch in these countries successfully moved into at least one other patch (Figure 2.L.1a). Conversely, only 19% of the dispersers leaving from a patch in Zambia managed to find their way into some other patch (Figure 2.L.1b). Prior to reaching another patch, individuals from Angola, Namibia, Botswana, Zimbabwe, and Zambia had to move for an average of 630, 640, 940, 1,045, and 890 steps, respectively. Furthermore, it appeared that the corridor previously identified on Figure 2.6 between Angola's NPs and the Kafue NP in Zambia is only rarely realized.

2.4 Discussion

Here, we presented a simple three-step approach to assess landscape connectivity via simulated dispersal trajectories and we demonstrated its application using empirical data from a free-ranging population of African wild dogs. In step one, we used iSSFs to parametrize a fully mechanistic movement model describing how individuals move through the landscape. Aside from rendering habitat preferences, the model also encapsulated movement preferences and potential interactions between movement and habitat preferences. In step two, we employed the movement model and simulated dispersal trajectories across the landscape. In comparison to more traditional connectivity modeling techniques, such simulations require fewer unrealistic assumptions about dispersal and enable the derivation of multiple connectivity metrics. Hence, in step three, we translated the simulated trajectories into three complementary connectivity maps, each emphasizing a different aspect of landscape connectivity (e.g. frequently traversed areas, critical dispersal corridors and bottlenecks, and the presence and intensity of functional links between suitable patches).

Results on the habitat kernel from our model showed that dispersers avoided areas dominated by humans and covered by water, but selected for regions with open grassland in the vicinity to water bodies. This largely complied with previous studies that investigated habitat selection by dispersing wild dogs

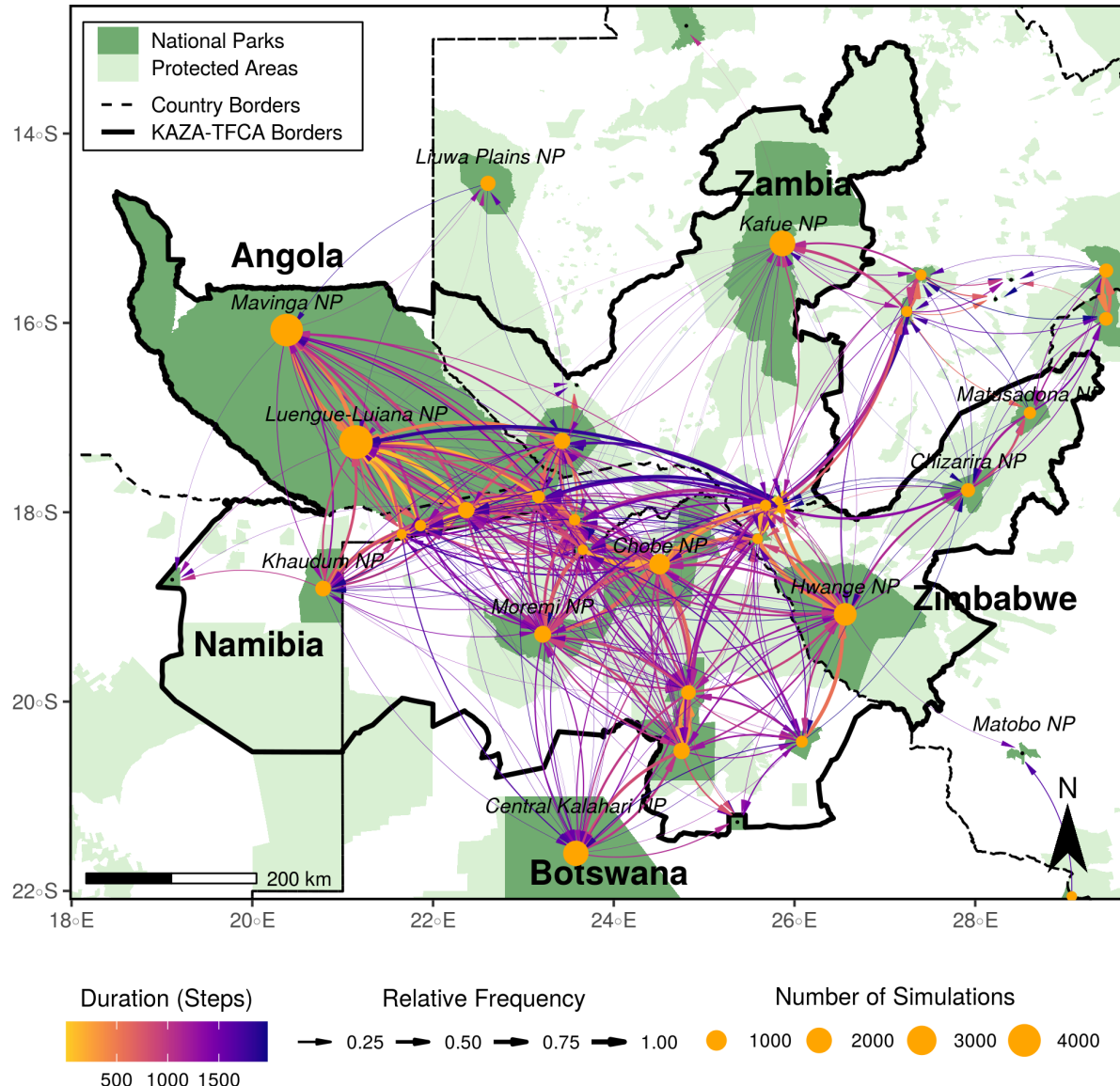


Figure 2.6: Map of inter-patch connectivity in relation to dispersal duration, highlighting connections between NPs (dark green). Yellow bubbles represent the center of the different NPs and are sized in relation to the number of simulated dispersers originating from each park. Black dots represent NPs that were smaller than 700 km² and therefore were not used as source areas. Arrows between NPs illustrate between which NPs the simulated dispersers successfully moved and the color of each arrow shows the average number of steps (i.e. 4-hourly movements) that were necessary to realize those connections. Additionally, the line thickness indicates the relative number of dispersers originating from a NP that realized those connections.

(Davies-Mostert et al., 2012; Masenga et al., 2016; O'Neill et al., 2020; Woodroffe & Sillero-Zubiri, 2020; Hofmann et al., 2021). However, instead of merely generating insights on dispersers' habitat preferences, the iSSF framework also permitted us to model several additional complexities common to dispersal. For instance, by including the interactions $\cos(\text{ta}):sl$ and $\cos(\text{ta}):\log(sl)$, we could accommodate that dispersers exhibit turning angles that are correlated with step lengths, meaning that turning angles tend to be smaller when individuals move fast. Although similar autocorrelations could be incorporated by sampling step lengths and turning angles from copula probability distributions (Hodel & Fieberg, 2022), the iSSF framework allowed us to conveniently model such peculiarities directly in the movement model. While we only considered first order autocorrelation, i.e. correlation between two consecutive steps, higher order autocorrelation is conceivable and may be desirable to model (Dray et al., 2010; McClintock et al., 2012). However, this will require vast amounts of GPS data that are not interrupted by missing fixes; something that is rarely achieved in reality (Graves & Waller, 2006). The power and flexibility of iSSFs to model additive effects between habitat and movement covariates (Avgar et al., 2016; Signer et al., 2017) furthermore allowed us to formally capture that dispersing wild dogs move slower and more tortuous in areas covered by water. Such effects may be of limited interest and novelty from a biological perspective, yet they are important to be considered when simulating dispersal, in particular if one is interested in estimating dispersal durations between habitat patches. Overall, the inclusion of interactions between habitat and movement covariates in our movement model lead to a significant improvement in predictive performance compared to an earlier model that omitted such interactions (Hofmann et al., 2021).

Each of the three connectivity maps derived from simulated dispersal trajectories highlighted a different aspect of landscape connectivity. The heatmap was most suitable for pinpointing frequently traversed areas and showed that an exceptionally large number of dispersers moved through the regions of the Moremi NP and the Chobe NP in northern Botswana. Hofmann et al. (2021) previously identified the same area as potential dispersal hotspot using LCPA, however, following their analysis it was not clear whether this was the consequence of the central location of the region and connections being enforced between predefined start and endpoints. Contrary to LCPA, a simulation-based approach as presented here does not require predefined endpoints, as endpoints emerge naturally from the simulated dispersal trajectories. This is especially useful for dispersal studies, where known endpoints are usually an unrealistic assumption (Elliot et al., 2014; Abrahms et al., 2017; Cozzi et al., 2020). The fact that the same region was emphasized using vastly different methods to model connectivity thus reinforces our notion that the area is of exceptional importance to dispersing wild dogs. Because simulated individuals are not forced to move towards certain endpoints, a simulation-based approach not only lends itself to study landscape connectivity, but also to uncover potential dispersal traps (Van Der Meer et al., 2014) or areas with a high susceptibility for human-wildlife conflicts (Cushman et al., 2018). Using independent dispersal data

we showed that dispersers indeed followed areas of high predicted connectivity. Importantly, however, these predictions were based on a scenario of a relatively extended flood, which may not have accurately represented environmental conditions for dispersers moving through areas affected by the flood. Accounting for such differences would have improved the predictive performance of our model.

In contrast to the heatmap, the betweenness map emphasized relatively narrow and linear movement routes. It thus facilitated the identification of discrete movement corridors. While in some cases both the heatmap and the betweenness map attributed a high importance to the same areas (e.g. northern Botswana), little consensus was found for other regions. For instance, the stretch of unprotected land between Luengue-Luiana NP in Angola and the Kafue NP in Zambia was characterized by a high betweenness-scores, yet it only received low scores on the heatmap. This is due to the differential way in which the maps view connectivity. While the heatmap attributes a high connectivity to areas that are frequently traversed, it does not distinguish between areas that truly bring individuals into other regions of the study area and regions that lead into ecological traps. The converse is true on the betweenness map, as it strictly highlights regions that promote movement into other areas of the landscape and thus promote gene-flow. However, neither of the two maps provides insights into functional links between distinct habitat patches or how connections depend on the dispersal duration. For this reason, we also produced a map of inter-patch connectivity. This map depicted the frequency at which simulated individuals moved between patches as well as the average dispersal duration (in steps) required to realize them. Calculating dispersal durations was only possible because trajectories were simulated spatially and temporally explicitly, something that is currently unfeasible with LCPA or CT. An explicit representation of time enables answering questions such as: *“How long will it take a disperser to move from A to B?”* or *“Is it possible for a disperser to move from A to B within X days?”*. Moreover, it yields opportunities to incorporate seasonality and to investigate whether dispersal corridors exist seasonally or all-year round (*dynamic connectivity*; Zeller, Wattles, et al., 2020). With LCPA or CT, seasonality can currently only be incorporated through the preparation of multiple permeability surfaces on which the same connectivity model is repeatedly applied (e.g. Osipova et al., 2019). With simulations from iSSFs, in contrast, the environment could change “as the dispersers move”, so that simulated trajectories would dynamically respond to seasonal fluctuations in the environment.

Our approach enabled us to translate a simple set of small-scale behavioral rules into large scale patterns of connectivity, something previously deemed computationally unfeasible, yet critical for linking structural and functional connectivity (Doerr et al., 2011). Structural connectivity focuses purely on the spatial arrangement of suitable habitat in the landscape, whereas functional connectivity also takes into account a species dispersal ability and behavioral response to the landscape (Tischendorf & Fahrig, 2000). Functional connectivity is of greater interest to conservation scientists, yet is difficult to quantify (Baguette

et al., 2013), which is why structural connectivity often serves as surrogate (Doerr et al., 2011; Fattebert et al., 2015). LCPA and CT incorporate functional aspects of connectivity through the permeability surface, which reflects a species habitat preferences and thus renders behavioral impacts of the landscape on the focal species. Aside from rendering habitat preferences, our model also integrates peculiarities of the focal species movement behavior, thus adding further insights on functional connectivity. In addition, we successfully used independent dispersal data to prove that our predictions of connectivity aligned with observed functional connectivity patterns.

Despite the many benefits and great flexibility offered by simulations from iSSFs, one must also be aware of the associated limitations. For example, while our approach of simulating dispersal proved useful to assess landscape connectivity, it was computationally costly. Simulating 80,000 dispersal trajectories for 2,000 steps across the KAZA-TFCA required five days of computation on a regular desktop machine (AMD Ryzen 7 2700X octa-core processor with 3.6 GHz, 64 GB of RAM). The long simulation time was primarily caused by the massive extent of the study area considered (ca. 1.3 Mio km²), the large number of simulated trajectories, and the fact that we extracted covariates along each step, rather than just at their start or endpoints. Most connectivity studies focus on smaller study areas (e.g. Kanagaraj et al., 2013; Clark et al., 2015; McClure et al., 2016; Abrahms et al., 2017; Zeller, Wattles, et al., 2020) and will therefore require fewer simulations and achieve faster simulation times (given the same spatial resolution). We also believe that fewer simulated trajectories will often suffice, as the relative traversal frequency by simulated trajectories through randomly placed checkpoints across our study area converged already after 10,500 runs. The exact number of required simulations to achieve reliable estimates of connectivity will, of course, vary depending on the structure of the landscape and the dispersal capabilities of the focal species (Gustafson & Gardner, 1996). For species that disperse short distances through homogeneous environments, few simulations may suffice to gauge connectivity, whereas for species that disperse over long distances through heterogeneous habitats, a large number of simulations will be required to sufficiently explore the spectrum of possible routes. Finally, it may often suffice to extract covariates at each step's start or endpoints, thus considerably speeding up simulation times (Signer et al., 2017).

Aside from the computational requirements, simulations further entail several non-trivial but important modeling decisions. On four such decisions we would like to further elaborate: (1) the number of simulated individuals, (2) the location of source points, (3) the simulated dispersal duration, and (4) the behavior at map boundaries.

(1) When simulating dispersal trajectories, the modeler needs to decide on the number of simulated individuals. A higher number is always desirable, as each additional trajectory provides information about landscape connectivity. However, each additional simulation imposes computational costs, so a trade-off needs to be managed. Signer et al. (2017) proposed to handle the trade-off by simulating additional in-

dividuals only until the metrics of interest converge towards a steady state. Here, we used the relative traversal frequency as target metric and found that it converged already after 10,500 simulated individuals. The exact number of required individuals might, however, vary depending on the employed target metric and the anticipated connectivity map. More sophisticated target metrics than the relative traversal frequency, preferably tailored to different connectivity maps, need to be developed in the future.

(2) To initiate dispersers, a modeler needs to provide a set of source points at which the virtual dispersers are released. We placed source points within protected areas large enough to sustain viable wild dog populations, implicitly assuming that wild dogs primarily survive in large, formally protected areas (Davies-Mostert et al., 2012; Woodroffe & Sillero-Zubiri, 2012; Van Der Meer et al., 2014). Moreover, we lacked precise knowledge about the distribution and abundance of wild dogs across protected areas, so we placed source points randomly within them. In cases where more detailed data about the distribution and abundance of the focal species are available, source points could be distributed accordingly. Alternatively, source points could be distributed homogeneously but later be weighted when computing connectivity metrics. In any case, the challenge of selecting meaningful source points is not unique to individual-based simulations but also applies to LCPA and CT.

(3) The use of iSSFs to simulate dispersers requires deciding on the number of simulated steps (i.e. the simulated dispersal durations). If sufficient dispersal data of the focal species has been collected, dispersal durations could be sampled from observed dispersal events or from parametric distributions fit to observed data. Due to the low number of observed dispersal events, we opted against this solution and instead simulated all individuals for 2,000 steps, which was at the upper end of observed dispersal durations in African wild dogs (Davies-Mostert et al., 2012; Masenga et al., 2016; Cozzi et al., 2020; Hofmann et al., 2021). This approach had the advantage that it allowed us to systematically shorten the simulated trajectories after their simulation and thereby to investigate the sensitivity of our results with respect to exact dispersal durations (Figure 2.I.1 and Figure 2.J.1).

(4) Unless simulated dispersal trajectories are strongly drawn towards a point of attraction inside the study area(e.g. Signer et al., 2017), some trajectories will inevitably approach one of the map boundaries. In this case, one or more of the generated random steps might leave the study area, making it impossible to compute a selection score. A possible solution is to simply terminate the simulation of the affected trajectory, assuming that the simulated individual has left the study area. However, this approach might produce ambiguous results in cases where many individuals are released near map borders, especially because already a single random step leaving the study area will break the simulation, thus resulting in biased connectivity estimates along map borders. Rather than breaking the simulation, we created a buffer zone (Koen et al., 2010) and resampled random steps until they fully lied within the study area. This proved to be an effective solution to overcome problems with boundary effects.

In summary, we proposed and applied a simple three-step approach that relies on iSSF-analysis and enables the simulation of dispersal trajectories and the assessment of landscape connectivity. The proposed approach overcomes several of the conceptual shortcomings inherent to LCPA and CT, such as the assumption of known endpoints, and provides a highly flexible tool for investigating connectivity. Moreover, the simulation of dispersal opens up new avenues for incorporating interactions between habitat and movement covariates and provides the foundation for a rich suite of complementary connectivity measures. With this work, we hope to have sparked interest in the application, optimization, or creation of methods to investigate dispersal and connectivity via individual-based simulations, while at the same time stressing some of the non-trivial modeling decisions involved. We also hope to provide a useful framework that helps unifying and streamlining the application of individual-based simulations for assessing landscape connectivity.

Appendices

2.A Candidate Interactions

We started with the base model developed by Hofmann et al. (2021) and incrementally increased model complexity by adding all possible two-way interactions between habitat covariates and movement covariates. For instance, for the covariate Water, we proposed the interactions Water:sl, Water:log(sl), and Water:cos(ta). Besides these interactions, we also allowed for correlations between turning angles and step lengths by proposing the interactions sl:cos(ta) and log(sl):cos(ta). Furthermore, we formed the interactions sl:LowActivity and log(sl):LowActivity to render that step lengths are likely to be shorter during periods of inactivity.

2.B K-Fold Cross Validation Procedure

We validated the predictive power of the most parsimonious movement model using k-fold cross-validation for case-control studies (Fortin et al., 2009). Specifically, we randomly assigned 80% of the strata to a training set and the remaining 20% to a testing set. Using the training set, we parametrized a movement model and predicted selection scores $w(x)$ for all steps in the testing set. Within each stratum, we then assigned ranks 1-25 to each step based on predicted selection scores, so that rank 1 was given to the step with the highest score $w(x)$. Within each strata, we determined the realized step's rank and calculated rank frequencies of realized steps across all strata. Finally, we computed Spearman's rank correlation between ranks and associated frequencies $r_{s,realized}$. We replicated this procedure 100 times and computed the mean correlation coefficient ($\bar{r}_{s,realized}$), as well as its 95% confidence interval across all replicates. For comparison, we repeated the same procedure 100 times assuming random preferences. Random preferences were implemented by discarding the realized step from all strata and identifying the rank of a random step in each stratum. Again, we calculated Spearman's rank correlation coefficient ($r_{s,random}$), its mean across repetitions ($\bar{r}_{s,random}$), and its 95% confidence interval. Ultimately, this validation proves a significant prediction in case the confidence intervals of $\bar{r}_{s,realized}$ and $\bar{r}_{s,random}$ do not overlap (Fortin et al., 2009).

2.C Source Areas & Points

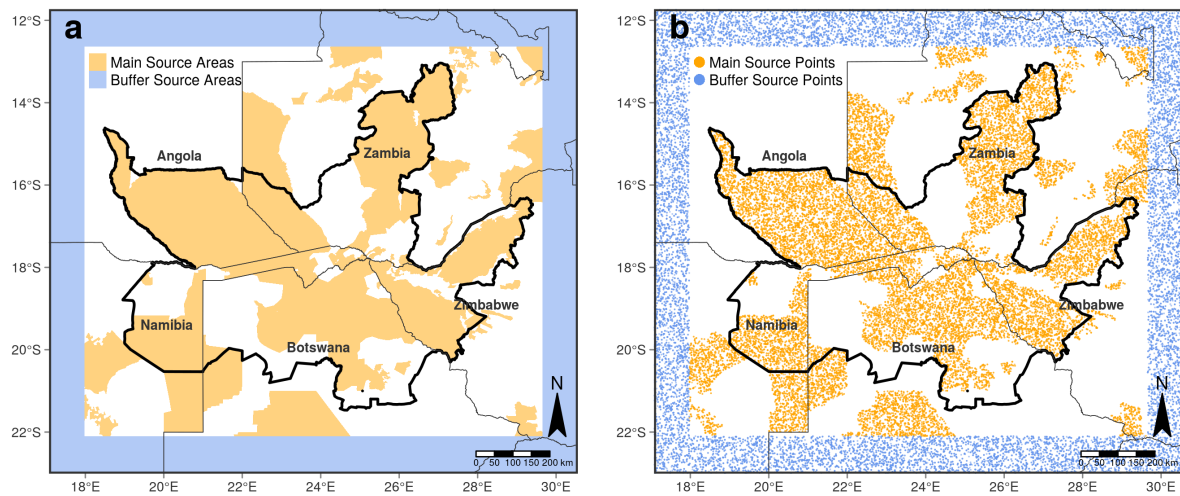


Figure 2.C.1: (a) Different source areas from which we released virtual dispersers. We only considered contiguous protected areas (national parks, game reserves, and forest reserves) that were larger than 700 km^2 . This size corresponds to the average home range requirement for viable wild dog populations (Pomilia et al., 2015). To render potential immigrants into the study system, we also initiated dispersers within a buffer zone (blue) surrounding the main study area. (b) Source points from which dispersers were released. 50,000 dispersers were released within the main study area (green dots) and another 30,000 dispersers within the virtual buffer (blue dots).

2.D Betweenness Maps

To generate betweenness maps, we first overlaid the study area with a regular grid with a resolution of 2.5 km x 2.5 km per grid cell. The grid cells were labeled with unique numbers, which allowed us to then generate a “visitation history” for each simulated trajectory, showing through which grid cells each simulated individual moved. Based on this history, we tallied the number of transitions that occurred from one cell to another. Ultimately, the so generated list of transitions served to generate a network and to compute betweenness scores. The resolution of the overlaid grid thus dictates the resolution at which betweenness can be mapped and has important implications for the way in which cell-transitions need to be determined. In the simplest case, cell-transitions can be determined by only looking at the start and endpoint of each step. If it ends in a different grid-cell than it started, a transition has occurred. This approach is computationally simple as it only requires a point extraction (at the start and endpoint of each step). However, relying on a point extraction has the disadvantage that transitions between non-adjacent cells can occur if a single step stretches across multiple grid-cells. Especially when the resolution of the grid is high, this problem becomes more pertinent. As an alternative, one could not only consider the start and endpoint of each step, but the entire line along the step, i.e. conduct a line extraction. However, this requires that extracted values (i.e. grid-cell labels) are ordered in accordance to the direction of movement. In R, such an extraction can be achieved e.g. using `raster::extract(raster, line, along = T)`, which is computationally very demanding and therefore often an nonviable solution. Here, we employed yet another approach and generated interpolated coordinates along each simulated step. We then determined cell transition using those interpolated coordinates. Since this approach still uses a point extraction, it is considerably faster while still enabling to detect cell-transitions at greater resolution. In Section 2.D, we use simulated movement paths to compare betweenness maps that are based on a (1) point extraction, a (2) line extraction, and a (3) point extraction with interpolated coordinates. As you can see, the approach using interpolated coordinates approximates the results from the line extraction very closely, even at higher resolutions. A detailed discussion about this is can also be found in (Bastille-Rousseau et al., 2018).

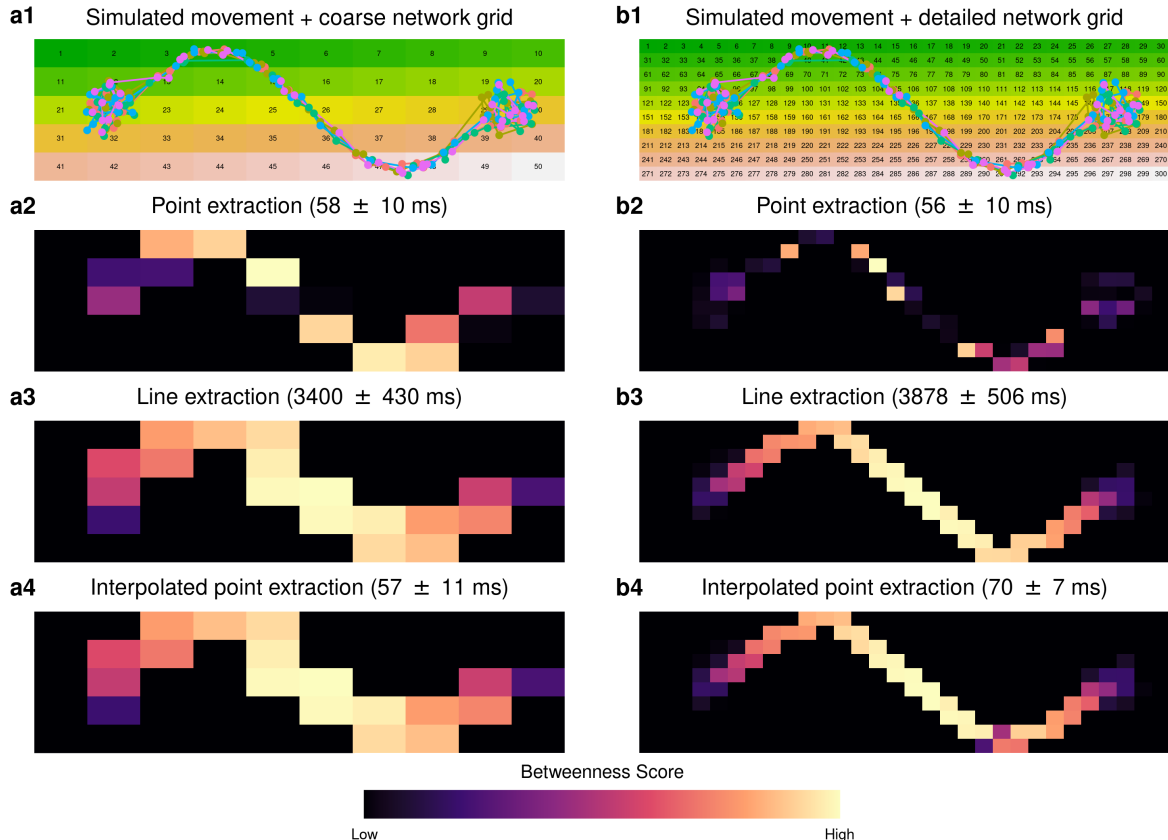


Figure 2.D.1: We simulated five trajectories where individuals moved through a narrow corridor. We then overlaid those simulations with a coarse (a1) and detailed (b1) grid that was used to compute betweenness scores. This required us to determine cell-transitions, which we did using three competing approaches. Once using a point extraction (a2 and b2), once using a line extraction (a3 and b3), and once using a point extraction with interpolated coordinates (a4 and b4). In brackets are the average computation times \pm SD as computed from 10 repetitions.

2.E Model Selection Results

Table 2.E.1: Results from the forward model selection procedure based on Akaike's Information Criterion (AIC; Burnham and Anderson, 2002). The model in the top row was the model that we used to simulate movement of dispersers. The base model upon which we based our movement model is depicted in the last row and was originally presented in Hofmann et al. (2021). We omitted all models with an AIC weight of zero from the table.

Covariates	AIC	ΔAIC	Weight	LogLik
Base Model + sl:LA + VWA:sl + log(sl):cos(ta) + DTV:cost(a) + WO:sl + Hl:cost(a) + DTV:sl + s:cost(a)	89392.88	0.00	0.15	-44670.44
Base Model + sl:LA + VWA:sl + log(sl):cos(ta) + DTV:cost(a) + WO:sl + Hl:cost(a) + SH:sl + DTV:sl + s:cost(a)	89393.92	1.04	0.09	-44669.96
Base Model + sl:LA + VWA:sl + log(sl):cost(a) + DTV:cost(a) + WO:sl + Hl:cost(a) + DTW:log(sl)	89394.13	1.25	0.08	-44670.06
Base Model + sl:LA + VWA:sl + log(sl):cost(a) + DTV:cost(a) + WO:sl + Hl:cost(a) + DTW:sl + s:cost(a) + DTW:log(sl)	89394.25	1.37	0.08	-44670.13
Base Model + sl:LA + VWA:sl + log(sl):cost(a) + DTV:cost(a) + WO:sl + Hl:cost(a) + DTW:sl + s:cost(a) + WO:log(sl)	89394.36	1.48	0.07	-44672.18
Base Model + sl:LA + VWA:sl + log(sl):cost(a) + DTV:cost(a) + WO:sl + Hl:cost(a) + DTW:sl + s:cost(a) + log(sl):LA	89394.44	1.56	0.07	-44670.22
Base Model + sl:LA + VWA:sl + log(sl):cost(a) + DTV:cost(a) + WO:sl + Hl:cost(a) + DTW:sl + s:cost(a) + Hl:sl	89394.56	1.68	0.07	-44670.28
Base Model + sl:LA + VWA:sl + log(sl):cost(a) + DTV:cost(a) + WO:sl + Hl:cost(a) + DTW:sl + s:cost(a) + WA:log(sl)	89394.57	1.69	0.07	-44670.29
Base Model + sl:LA + VWA:sl + log(sl):cost(a) + DTV:cost(a) + WO:sl + Hl:cost(a) + DTW:sl + s:cost(a) + WO:cost(a)	89394.59	1.71	0.07	-44670.30
Base Model + sl:LA + VWA:sl + log(sl):cost(a) + DTV:cost(a) + WO:sl + Hl:cost(a) + DTW:sl + s:cost(a) + WA:cost(a)	89394.63	1.75	0.06	-44670.31
Base Model + sl:LA + VWA:sl + log(sl):cost(a) + DTV:cost(a) + WO:sl + Hl:cost(a) + SH:sl + s:cost(a)	89394.68	1.80	0.06	-44672.34
Base Model + sl:LA + VWA:sl + log(sl):cost(a) + DTV:cost(a) + WO:sl + Hl:cost(a) + SH:sl + s:cost(a) + Hl:log(sl)	89394.69	1.81	0.06	-44670.35
Base Model + sl:LA + VWA:sl + log(sl):cost(a) + DTV:cost(a) + WO:sl + Hl:cost(a) + SH:sl + s:cost(a) + SH:cost(a)	89394.84	1.96	0.06	-44670.42
:	:	:	:	:
Base Model: cos(ta) + sl + log(sl) + WA + s:cost(a) + DTW + HI + SH	90091.40	787.67	0.00	-45030.70

Note: ta = Turning Angle, sl = Step Length, LA = Low Activity, WA = Water, DTW = Distance To Water, SH = Shrubs/Grassland, WO = Woodland, HI = Human Influence.

2.F Movement Model

Table 2.F.1: Most parsimonious movement model for dispersing wild dogs. The model consists of a movement kernel, a habitat kernel, and their interactions. The movement kernel describes preferences with regards to movement behavior, whereas the habitat kernel describes preferences with respect to habitat conditions. Interactions between the two kernels indicate that movement preferences are contingent on habitat conditions. Note that all covariates were standardized to a mean of zero and standard deviation of 1. Plots to aid with the interpretation of this model are given in Section 2.G.

Kernel	Covariate	Coefficient	SE	p-value	Sign.
Habitat Kernel	Water	-0.546	0.112	< 0.001	***
	DistanceToWater ^{0.5}	-0.390	0.231	0.092	*
	Woodland	-0.364	0.086	< 0.001	***
	Shrubs/Grassland	0.288	0.092	0.002	***
	HumanInfluence	-0.535	0.229	0.019	**
Movement Kernel	sl	0.075	0.037	0.042	**
	cos(ta)	0.105	0.031	0.001	***
	log(sl)	0.146	0.051	0.004	***
	cos(ta) : sl	0.049	0.026	0.064	*
	cos(ta) : log(sl)	0.076	0.026	0.003	***
	sl : LowActivity	-0.917	0.113	< 0.001	***
Interactions	sl : Water	-0.305	0.076	< 0.001	***
	sl : Woodland	-0.089	0.039	0.023	**
	sl : Shrubs/Grassland	0.124	0.058	0.032	**
	sl : DistanceToWater ^{0.5}	-0.058	0.031	0.056	*
	cos(ta) : HumanInfluence	-0.040	0.022	0.070	*
	cos(ta) : DistanceToWater ^{0.5}	0.063	0.026	0.017	**

Significance codes: * $p < 0.10$ ** $p < 0.05$ *** $p < 0.01$

2.G Movement Model Interpretation

To ease with the interpretation of the most parsimonious movement model, we followed recommendations published in Fieberg et al. (2021) and produced a series of plots highlighting how the habitat and movement kernel depended on covariate values (Figure 2.G.1). To visualize the movement kernel and its interactions with other covariates, we used model estimates and updated our tentative distribution parameters for turning angles (von Mises distribution with concentration $\kappa = 0$) and step lengths (gamma distribution with scale $\theta = 6'308$ and shape $k = 0.37$) by applying the function `update_vonmises()` from the R-package `amt` (Signer et al., 2019). This allowed us to compute probability densities of turning angles and step lengths under varying values of the associated covariates, while holding all other covariates constant (Figure 2.G.1, a1-a8). Moreover, we investigated the habitat kernel by computing relative selection strengths (RSS) between a set of steps where values of the covariate of interest was varied to a reference step where the covariate value was fixed to its centered value. To illustrate model uncertainty, we also generated large-sample confidence intervals using standard errors associated with each model estimate (Figure 2.G.1, b1-b5).

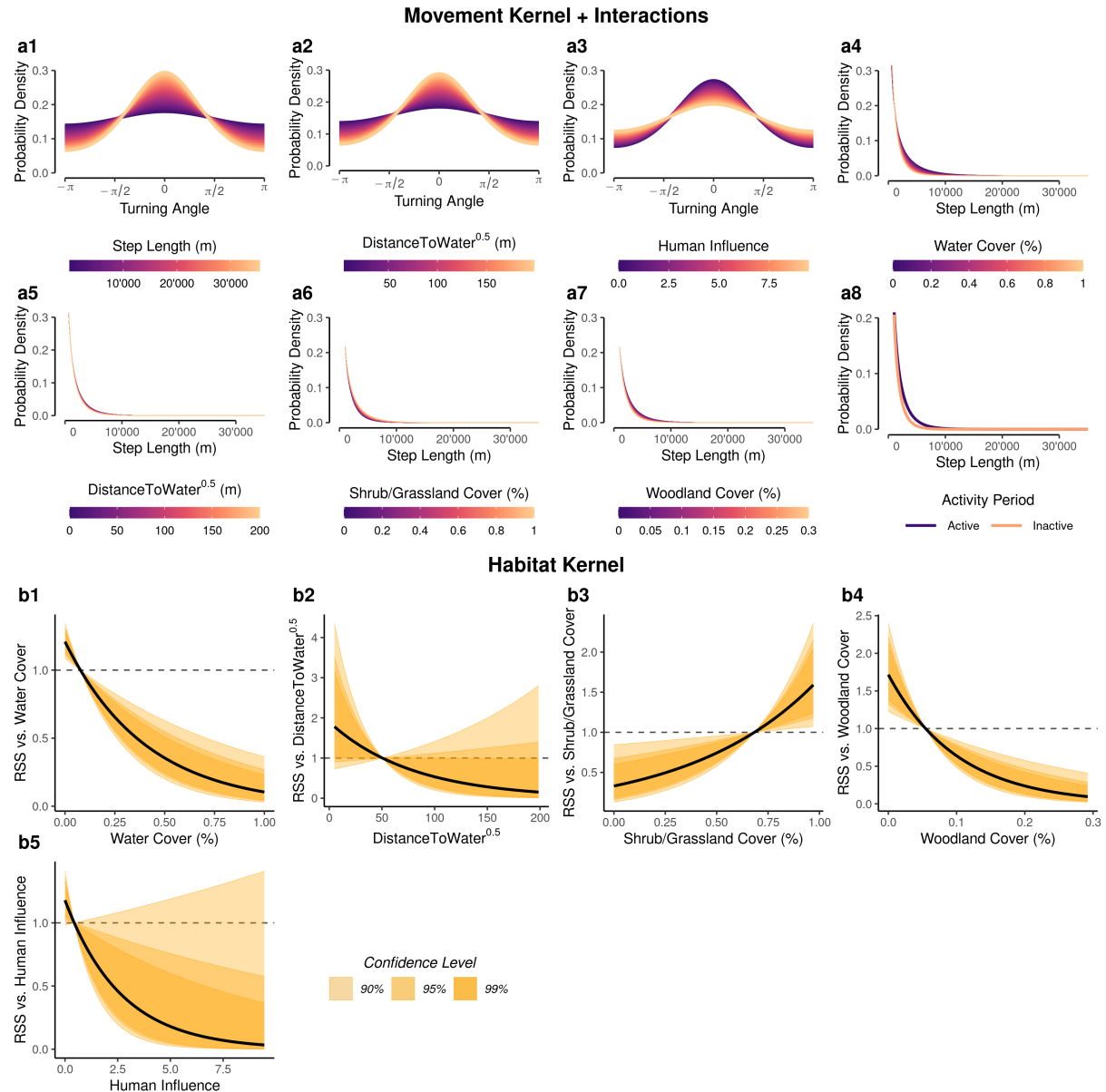


Figure 2.G.1: Auxiliary plots that help with the interpretation of the most parsimonious movement model. The plots were generated following recommendations reported in Fieberg et al. (2021). Subplots a1 to a8 highlight dispersing wild dogs' movement kernel and indicate how the kernel is influenced by interactions with other covariates. Subplots b1 to b5 depict results from dispersing wild dogs' habitat kernel and highlight differences in predicted relative selection scores (RSS) when varying values of the covariate of interest. For each covariate, predictions were made on the range of values that was observed in the real data, assuming that all other covariates were centered and that steps were realized during periods of "high" wild dog activity. Plot a1, for example, can be interpreted as follows: the probability of realizing a step with a low turning angle is much higher when the corresponding step is large. Moreover, b1 can be interpreted as follows: relative probability of using a step decreases as the amount of water cover along the step increases.

2.H Convergence

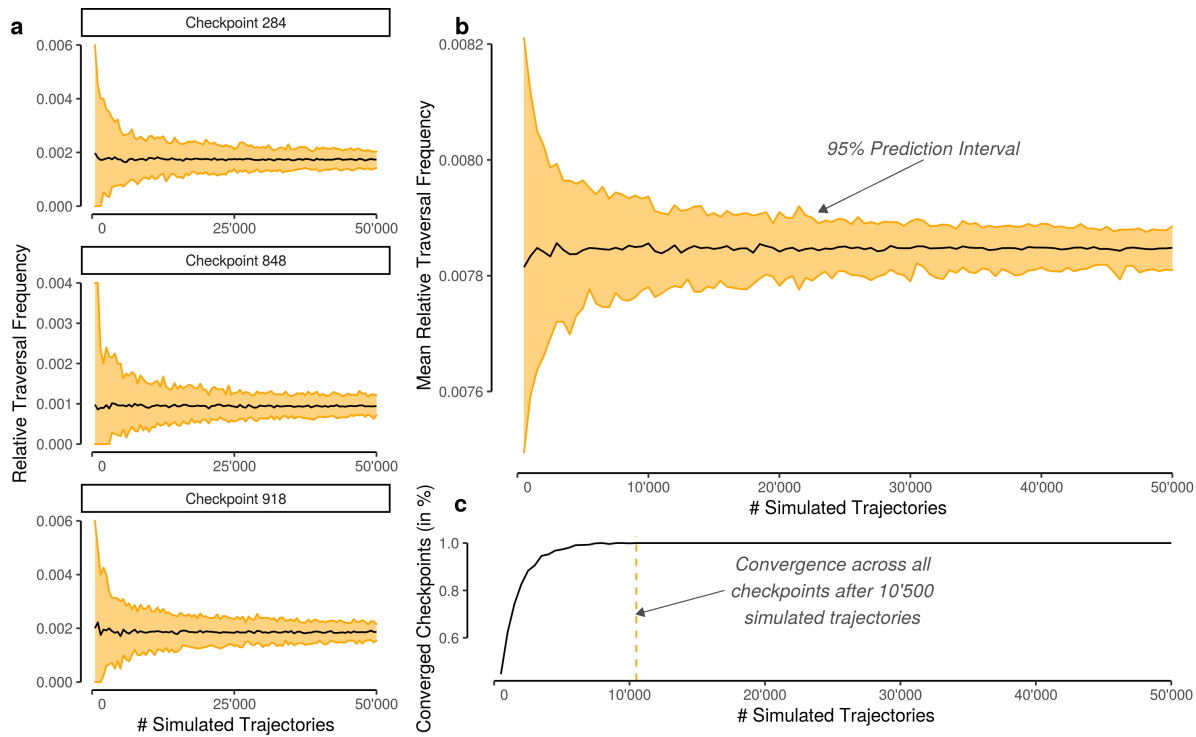


Figure 2.H.1: Relative traversal frequency through 1,000 checkpoints (5 km x 5 km) distributed randomly across the study area. The relative traversal frequency is plotted against the number of simulated individuals to visualize how quickly the metric converges to a steady state. (a) Replicated (100 times) relative traversal frequencies across three randomly chosen checkpoints as well as the corresponding 95% prediction interval (PI). (b) Averaged relative traversal frequency across all checkpoints and replicates including a 95% PI. (c) Width of the PI in relation to the number of simulated dispersers.

2.I Heatmaps in Relation to the Number of Simulated Steps

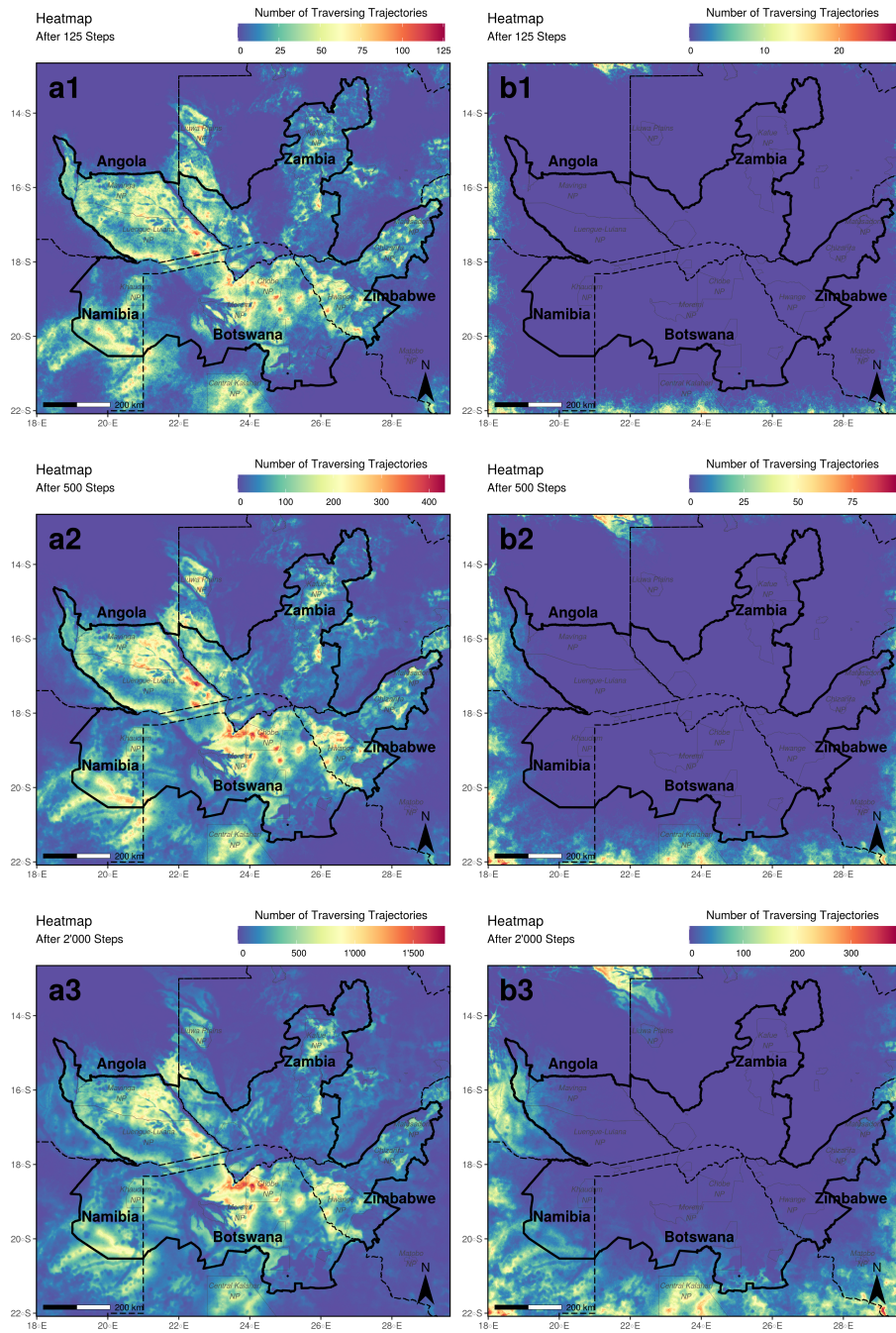


Figure 2.I.1: Heatmaps produced when considering 125, 500, and 2,000 simulated steps, respectively. The left panel (a1, a2, a3) was generated based on simulations initiated within the main study area, the right panel (b1, b2, b3) was generated based on simulations initiated within the buffer area. To produce the heatmap presented in the main manuscript Figure 2.4, we tallied the values from maps a3 and b3.

2.J Betweenness Maps in Relation to the Number of Simulated Steps

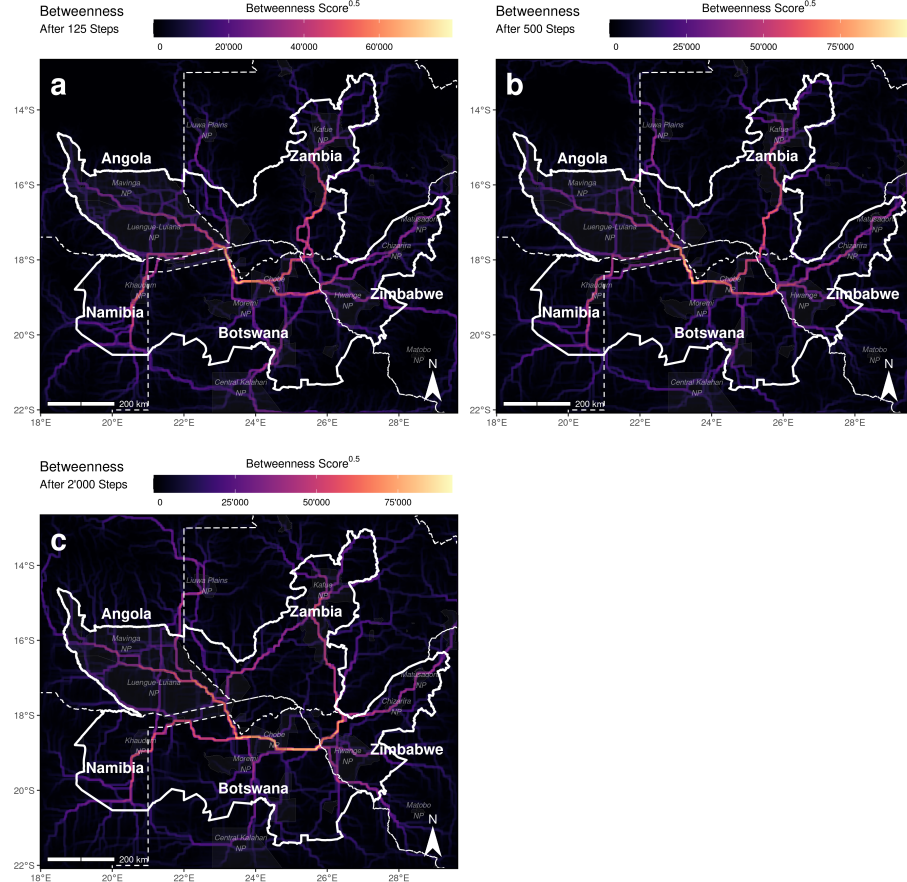


Figure 2.J.1: Maps of betweenness scores produced when considering (a) 125, (b) 500, (c) and 2,000 simulated steps, respectively. A high betweenness score indicates that the respective area has a high importance for linking other regions in the study area.

2.K Comparison of Traversal Frequencies and Betweenness Scores Inside and Outside KAZA-TFCA

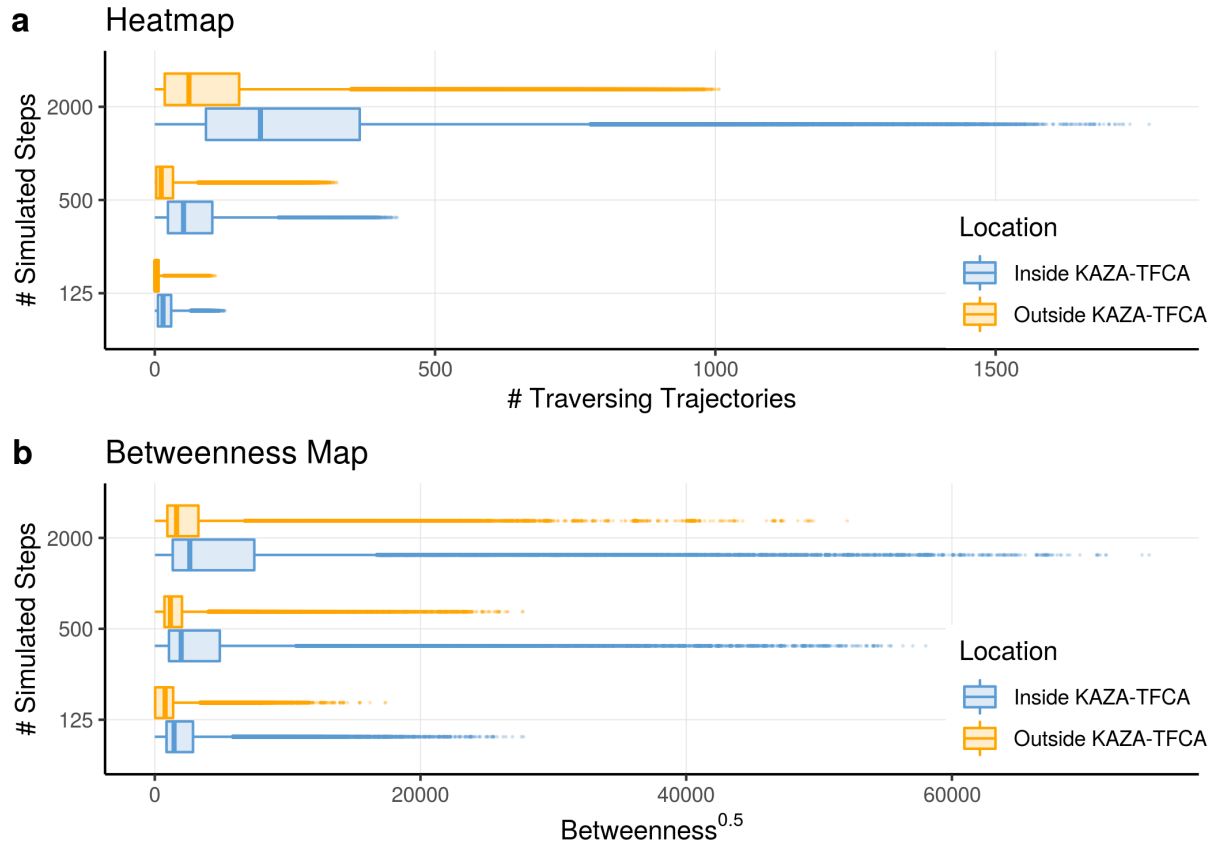


Figure 2.K.1: Comparison of values from the heatmap and betweenness map inside (blue) and outside (orange) the KAZA-TFCA borders.

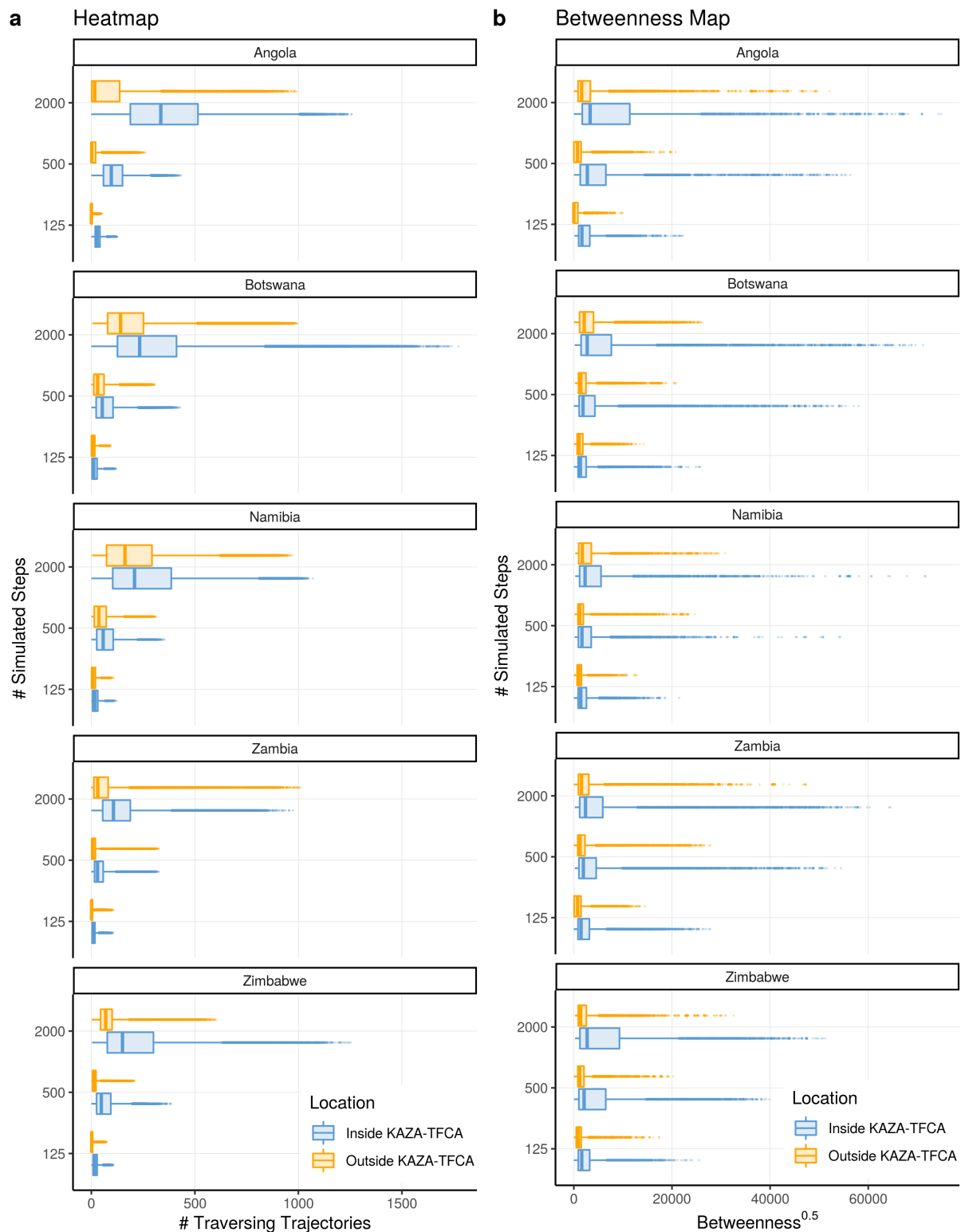


Figure 2.K.2: Comparison of values from the heatmap and betweenness map inside (blue) and outside (orange) the KAZA-TFCA borders within different countries.

2.L Dispersal into other National Parks

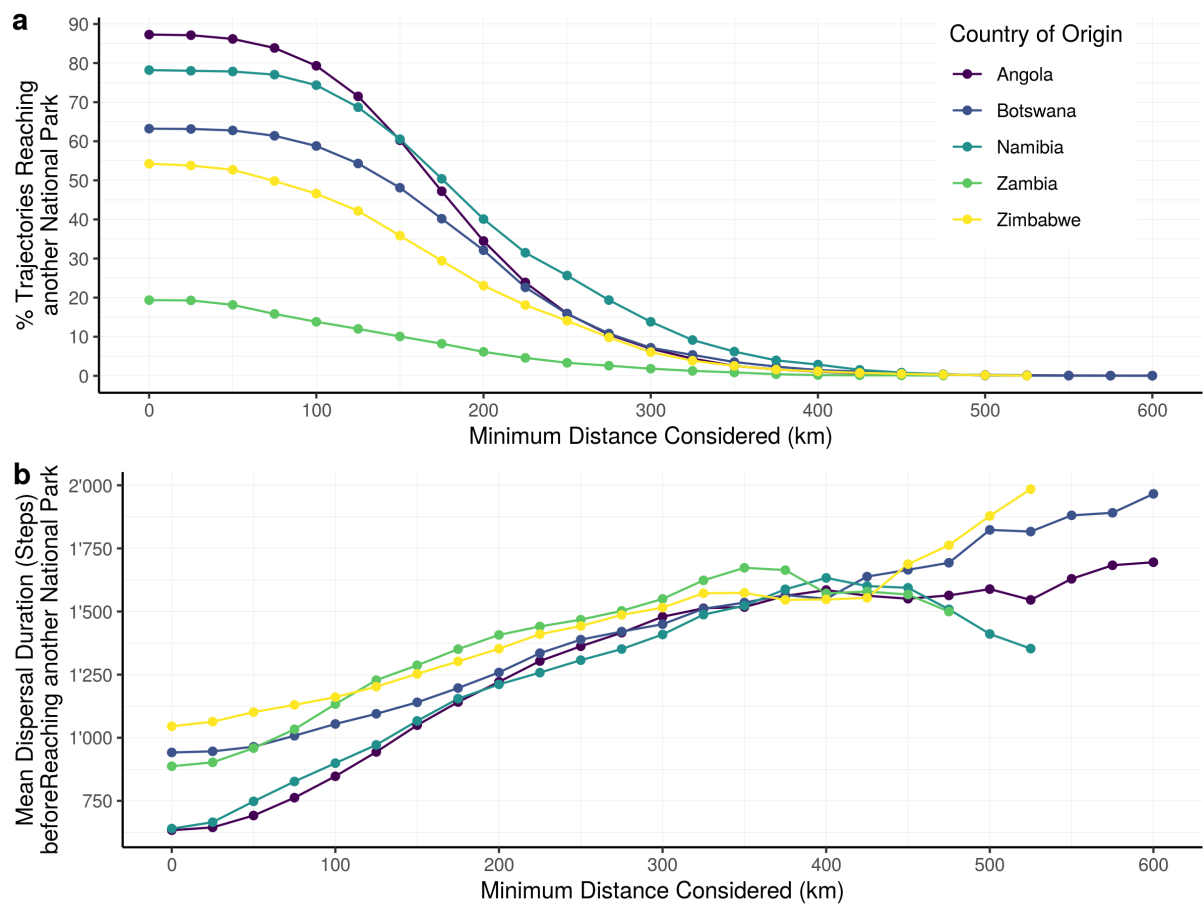


Figure 2.L.1: Relative number of simulated dispersal trajectories that successfully moved from one national park into another that is at least as far away as indicated on the x-axis. Percentages are given in relation to the number of simulated individuals from the national parks in the respective countries. For example, over 85% of all individuals originating from a national park in Angola moved from their natal national park into another one. However, the percentage gradually decreases as only national parks at higher euclidean distances are considered.



Chapter 3

Dispersal and Connectivity in Increasingly Extreme Climatic Conditions

David D. Hofmann , Dominik M. Behr , John W. McNutt, Arpat Ozgul , and Gabriele Cozzi 

Abstract

While climate change has been shown to impact several life-history traits of wild-living animal populations, little is known about its effects on dispersal and connectivity.

Here, we capitalize on the highly variable flooding regime of the Okavango Delta to investigate impacts of changing environmental conditions on dispersal and connectivity of the endangered African wild dog (*Lycaon pictus*). Based on remote sensed flood extents observed over 20 years, we derive two extreme flood scenarios: a minimum and a maximum flood extent; representative of very dry and very wet environmental periods. These conditions are akin to those anticipated under increased climatic variability, as it is expected under climate change. Using a movement model parametrized with GPS data from dispersing individuals, we simulate 12,000 individual dispersal trajectories across the ecosystem under both scenarios and investigate patterns of connectivity.

Across the entire ecosystem, surface water coverage during maximum flood extent reduces dispersal success (i.e., the propensity of individuals to disperse between adjacent subpopulations) by 12% and increases dispersal durations by 17%. Locally, however, dispersal success diminishes by as much as 78%. Depending on the flood extent, alternative dispersal corridors emerge, some of which in the immediate vicinity of human-dominated landscapes. Notably, under maximum flood extent, the number of dispersing trajectories moving into human-dominated landscapes decreases by 41% at the Okavango Delta's inflow, but increases by 126% at the Delta's distal end. This may drive the amplification of human-wildlife conflict.

Whilst predicting the impacts of climate change on environmental conditions on-the-ground remains challenging, our results highlight that environmental change may have significant consequences for dispersal patterns and connectivity, and ultimately, population viability. Acknowledging and anticipating such impacts will be key to effective conservation strategies and to preserve vital dispersal corridors in light of climate change and other human-related landscape alterations.

3.1 Introduction

Climate change is expected to impact ecosystems across the globe with far-reaching consequences for the species living therein (Paniw et al., 2019; Radchuk et al., 2019; IPCC, 2022; Ozgul et al., 2023). By altering environmental conditions, climate change has been shown to affect animal behavior (Fuller et al., 2016), resource availability (Durant et al., 2007), demographic rates of local populations (Paniw et al., 2021), range distribution of wild-living animals (Thomas et al., 2004; Thuiller et al., 2006), and the potential for human-wildlife conflict (hereafter referred to as HWC; Abrahms et al., 2023), thus threatening the viability of most wildlife species. An important life-history trait known to influence the persistence of wild living populations across large spatial scales is dispersal (Hanski, 1999b; Bowler & Benton, 2005; Kokko, 2006), which is defined as the movement of individuals away from their natal location to the site of first reproduction (Clobert et al., 2012). Despite the crucial role of dispersal in maintaining population viability, little is known about the impacts of climate change on long-distance dispersal and landscape connectivity. Nevertheless, assessing the consequences of climate change for dispersal is essential to anticipate potential shifts in range distributions and population dynamics.

Predicting how dispersal and connectivity respond to environmental change remains challenging (Littlefield et al., 2019). This is mainly due to insufficient data on dispersing animals at the appropriate spatial and temporal scales (Graves et al., 2014; Vasudev et al., 2015), coupled with limited insights into potential differences in environmental conditions under climate change (Scheiter & Higgins, 2009; IPCC, 2022). To address these shortcomings, one approach has been to combine climate projections and species distribution models with the aim of predicting future species ranges and investigating the impacts of such range shifts on structural connectivity (Wasserman et al., 2012; Ashrafzadeh et al., 2019; Luo et al., 2021). However, this approach fails to translate predicted atmospheric conditions into ground-level landscape characteristics (e.g., vegetation cover, surface-water). An alternative approach, albeit not primarily focusing on climate change, is to investigate how seasonality affects functional connectivity (e.g., Mui et al., 2017; Osipova et al., 2019; Zeller, Wattles, et al., 2020; Kaszta et al., 2021). This is usually achieved using seasonally updated resistance surfaces that depict the ease or difficulty at which the focal species can traverse a particular environment in a specific season (Zeller et al., 2012). Despite its biological relevance for understanding seasonal variability, this approach suffers from the short time-span at which processes are investigated and hinders drawing inferences on the long-term effects of climate change on dispersal and connectivity. Recently, alternative approaches for investigating landscape connectivity that combine empirical GPS movement data with a modeling framework to reconstruct and predict movement trajectories at the level of the individual have been suggested (Signer et al., 2017; Hofmann, Cozzi, McNutt, et al., 2023; Signer et al., 2024). Such predicted trajectories are uncoupled from any temporal constraint and

therefore suitable to investigate the effects of changing landscapes, as observed or predicted under the influence of climate change, on dispersal and connectivity. Given that climate change will shift systems towards conditions that currently represent extremes (Stott, 2016; Ummenhofer & Meehl, 2017; IPCC, 2022), we argue that a focus on extreme, rather than seasonal, variations could serve as a robust way to learn about the impacts of climate change on patterns of dispersal and connectivity. Such an approach appears particularly useful in cases where data on future environmental conditions are difficult to obtain or plagued by uncertainty (Collins et al., 2012).

One ecosystem that offers a unique opportunity to study the impacts of extreme environmental conditions on dispersal and connectivity in a large-scale natural experiment is the Okavango Delta in Botswana. The Okavango Delta (henceforth “Delta”) is the world’s largest inland delta and characterized by striking variability in its flood extent within and between years (Gumbrecht et al., 2004; Wolski et al., 2017). The area covered by the Delta’s floodwaters can fluctuate between 3,500 km² during particularly dry and 14,000 km² during particularly wet periods (McCarthy et al., 2003; Gumbrecht et al., 2004). The region is among the most vulnerable to climate change, as temperature increases of 4 to 6°C above pre-industrial levels are expected within the 21st century (Engelbrecht et al., 2015; Akinyemi & Abiodun, 2019); a prediction that goes far beyond the global average (IPCC, 2022). The rise in ambient temperature is likely to elevate evapotranspiration rates across the Delta’s alluvial fan, yet it is unclear whether water-losses to the atmosphere will be offset or exceeded by an increase in precipitation across the Delta’s catchment areas in Angola (Wolski & Murray-Hudson, 2008; IPCC, 2022). Despite the importance of the Delta as a driver of ecosystem functioning (Wolski & Murray-Hudson, 2008), species distribution (Bonyongo, 2005; Bennett et al., 2014), and dispersal corridors (Hofmann et al., 2021; Hofmann, Cozzi, McNutt, et al., 2023), forecasting its flooding regime under climate change has proven notoriously difficult. Predictions of the flood extent under climate change range from “much drier” to “much wetter” depending on the employed model and climate scenario (Murray-Hudson et al., 2006; Wolski & Murray-Hudson, 2008).

Within this ecosystem a keystone predator and an umbrella species for conservation efforts is the African wild dog (*Lycaon pictus*), a large carnivore that is characterized by a remarkable dispersal ability (McNutt, 1996; Davies-Mostert et al., 2012; Masenga et al., 2016; Cozzi et al., 2020; Sandoval-Seres et al., 2022). Under favorable conditions, young individuals that leave their natal pack can cover up to several hundred kilometers within a few days, crossing a vast diversity of habitat-conditions (e.g., Cozzi et al., 2020). While historically observed Euclidean dispersal distances are limited to 5-500 km (Davies-Mostert et al., 2012; Cozzi et al., 2020; Sandoval-Seres et al., 2022), cumulative dispersal distances of over 5,000 km have been recorded (Masenga et al., 2016). Previous research on dispersing individuals revealed that the Delta’s floodwater represents a major barrier to dispersal (Hofmann et al., 2021; Hofmann, Cozzi,

McNutt, et al., 2023) and it can be hypothesized that wild dog dispersal and connectivity will be profoundly influenced by future changes in the flood regime, as expected under the influence of climate change.

Utilizing a previously validated individual-based movement model parametrized with empirical GPS data collected on dispersing wild dogs, we simulated 12,000 individual dispersal trajectories under two extreme environmental scenarios: one assuming a maximum flood extent, representing above-average wet climatic conditions, and one assuming a minimum flood extent, representing acute dry conditions. Both scenarios reflect possible outcomes under the effect of climate change. For each scenario, we assessed dispersal success and dispersal durations of simulated trajectories between distinct regions, mapped the emergence of alternative dispersal corridors and bottlenecks, and investigated how differing corridor arrangements influenced the potential for HWC (Figure 3.1.1). We anticipated lower dispersal success and connectivity, as well as an increased propensity to disperse outside the main study area during maximum flood. Furthermore, we anticipated major dispersal corridors to differ between minimum and maximum flood, thus resulting in alternative hotspots for HWC. Ultimately, our goal was to highlight that altered climatic conditions and associated changes in landscape characteristics can substantially affect the spatial arrangement of movement corridors and, subsequently, the potential for HWC.

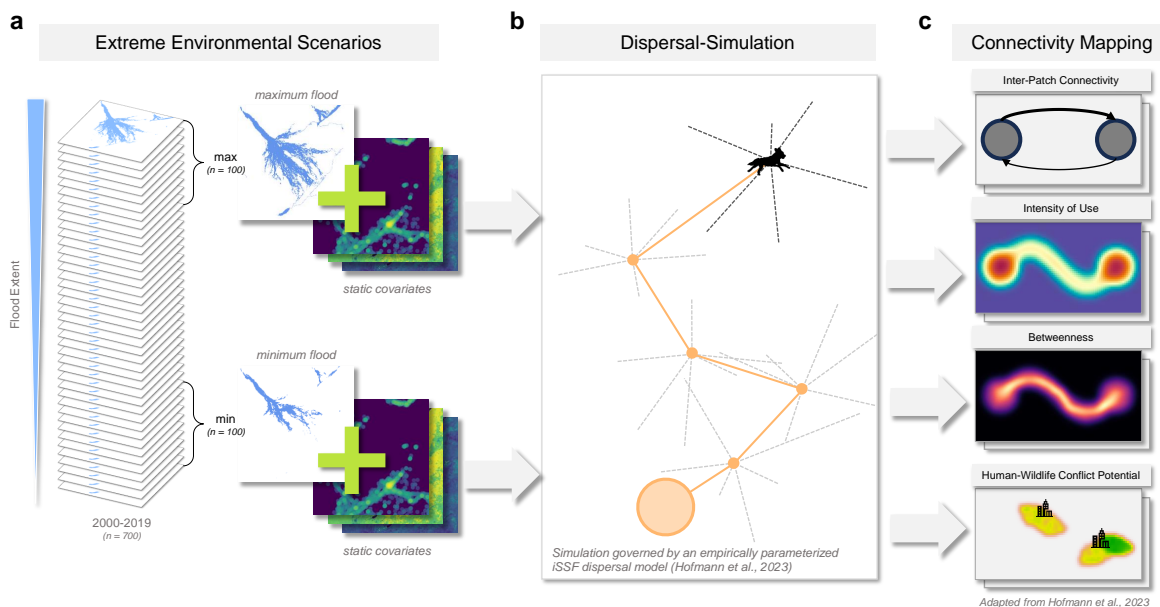


Figure 3.1.1: Conceptual illustration of the employed analytical framework to investigate connectivity for dispersing African wild dogs under a minimum and maximum flood extent in the Okavango Delta. (a) Based on a series of 700 floodmaps, obtained between the years 2000 and 2019, we derived extreme scenarios for a minimum and maximum flood, using the minimum 100 and maximum 100 historically observed flood extremes. These layers were then joined with a static set of covariates and fed into a dispersal simulation. (b) The dispersal simulation was based on a previously parametrized integrated step-selection function for dispersing wild dogs and allowed simulating dispersal trajectories in the two extreme scenarios. (c) From simulated dispersal trajectories we generated four summary maps, highlighting connectivity patterns and areas potentially prone to human-wildlife conflict.

3.2 Materials and Methods

3.2.1 Study Area

To investigate the effects of flood extremes on dispersal and connectivity, we focused on a *core study area* of 70,000 km² that comprised the Delta and its surroundings (Figure 3.2.1b; purple circle). To accommodate for the long-distance dispersal events observed in this ecosystem (Cozzi et al., 2020; Hofmann et al., 2021; Cozzi et al., 2023), we also considered an *extended study area* of 300,000 km² spanning from 21°30' S to 17°30' S to and 20°30' E to 26°E and comprising the Delta and parts of Angola, Namibia, Botswana, Zimbabwe, and Zambia (Figure 3.2.1a). Rainfall in this area averages at 450 mm and is mainly concentrated to the wet season between November and April (Mendelsohn & El Obeid, 2004). Even though local rains and ground table levels resulting from floods of previous years may impact annual flood levels (McCarthy, 2006), the Delta's flood extent is primarily driven by precipitation patterns in its catchment areas in the Angolan highlands, from where water is channeled into the Cubango and Cuito rivers and subsequently discharged into the Okavango Delta (McCarthy et al., 1997; McCarthy et al., 2003). Since water only slowly descends from the catchment areas into the Delta and across its shallow alluvial fan (gradient ~ 1/3,400, McCarthy et al., 1997), the flood usually reaches its maximum extent long after the local rains have ceased, during the peak dry season in July or August. Once the floodwater reaches the Delta's distal ends, it percolates at the Thamalakane and Kunyere Faults, two natural fault lines at which the water-flow is hindered (Figure 3.2.1b). After reaching its maximum extent, water evaporates or percolates and the flood steadily retracts over subsequent months. Such inner-annual dynamics are further amplified or buffered by multi-annual cycles in precipitation patterns across Angola (Wolski et al., 2012). Due to the intricate interplay between precipitation patterns in Angola, local ground-table levels, evapotranspiration, and anthropogenic water abstractions, predictions of the flood extent under climate change have proven challenging and range from "much drier" to "much wetter" depending on employed climate scenarios (Kgathi et al., 2006; Wolski & Murray-Hudson, 2008; Hughes et al., 2011; Wolski et al., 2012; Moses & Hambira, 2018). In the core study area, the vegetation is dominated by mopane forest (*Colophospermum mopane*), mixed woodland acacia-dominated (*Acacia spp.*), and grassland (Mendelsohn et al., 2010). Human influence is relatively low and mainly concentrated around small villages at the western and southern periphery of the Delta. The largest urban center is Maun, a spread-out settlement at the south-eastern tip of the Delta. Large portions of the core study area are designated as national parks, game reserves, or wildlife management areas. Some remaining sections of land are used for cattle farming and suffer from moderate levels livestock depredation and associated human-wildlife conflict (Gusset et al., 2009; McNutt et al., 2017). The core study area and its extended surroundings are part of the world's largest transboundary conservation initiative, the Kavango-Zambezi Transfrontier Conser-

vation Area (KAZA-TFCA, Figure 3.2.1a), which attempts to re-establish connectivity among several core habitats. Previous studies have indicated that this initiative has high potential for improving connectivity among subpopulations of various species (Brennan et al., 2020; Lines et al., 2021), including African wild dogs (Hofmann et al., 2021). However, a better understanding of connectivity within this ecosystem under climate change is lacking.

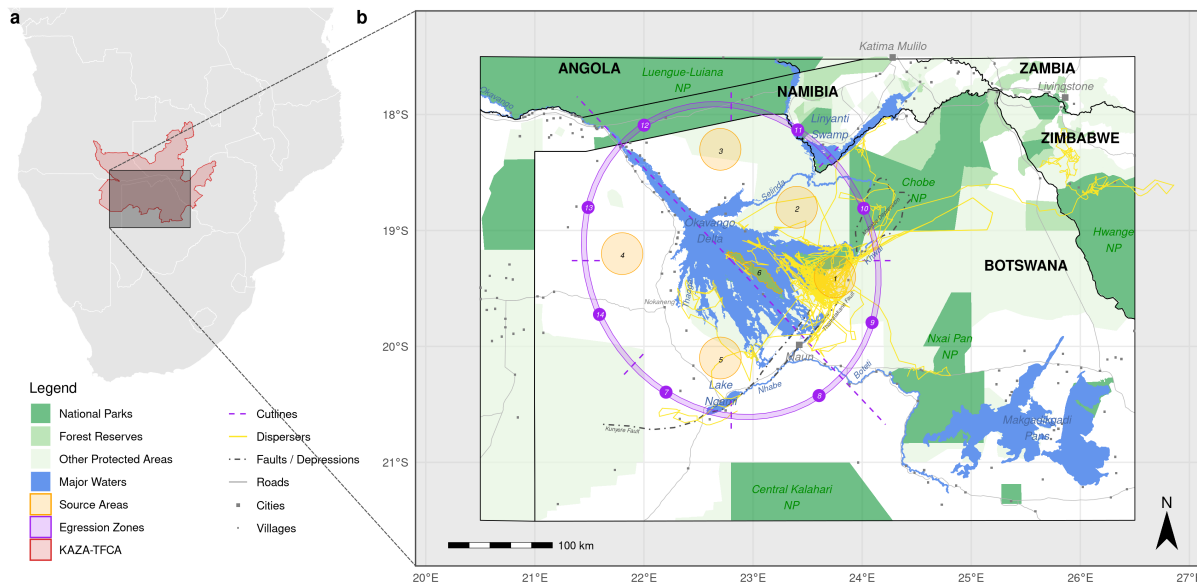


Figure 3.2.1: (a) Location of the study area, which forms part of the Kavango-Zambezi Transfrontier Conservation Area (KAZA-TFCA, red polygon) in Southern Africa. (b) The division of the core study area (enclosed by the purple ellipse) into sub-areas (1 to 6) was based on the hydrographic structure of the Okavango Delta and its tributaries. We simulated dispersal trajectories starting at random locations within each of the six source areas (orange circles). Purple zones (7 to 14) represent zones that we used to identify if and where simulated dispersers left the close surroundings of the Okavango Delta (thus called egression zones). These zones were generated using a set of cutlines (purple dotted lines) originating from the center of the Delta that dissected an elliptical buffer surrounding the Delta into sections of equal size and in accordance with cardinal directions. The yellow lines represent GPS trajectories of dispersing wild dogs that were observed using GPS collars. While not all of these individuals were used to parametrize the dispersal model presented by Hofmann, Cozzi, McNutt, et al. (2023), they serve to highlight the spatial scale at which the species disperses.

3.2.2 Spatial Habitat Layers

We represented the physical landscape through which dispersers could move by a set of spatially referenced habitat layers, each with a resolution of 250 m × 250 m. The set of layers included water-cover, distance-to-water, tree-cover, shrub/grassland-cover, and a composite human influence layer representing settlements, roads, and agricultural areas. A detailed description of these layers is provided by Hofmann et al. (2021). However, unlike Hofmann and colleagues, who used a single, static flood map, we employed composite flood maps to study connectivity. Specifically, we generated water-cover layers using MODIS Terra MCD43A4 satellite imagery that we classified into binary water-cover maps using an algorithm developed by Wolski et al. (2017) and implemented in R (<https://github.com/DavidDHofmann/floodmapr>).

This algorithm allowed us to generate weekly updated “flood extent maps”, thus providing detailed information about the flood at any given point in time. In total, we generated 700 flood extent maps, covering the years 2000 to 2019. We used these maps to produce minimum and maximum flood scenarios, representative of dry and wet climatic conditions, assuming that climate change will shift the system towards one of these extremes in the long run. To create the baseline minimum (and respectively, maximum) flood scenario, we averaged the 100 flood extent maps with the smallest (highest) flood extent and generated a binary layer by masking all pixels that were inundated in less than 50% of the maps (see also Figure 3.1.1). By averaging across 100 flood extent maps, we followed a conservative approach and mitigated chances of misrepresenting minimum and maximum flood extent due to inaccuracies or artifacts in single remote sensed flood extent maps. The final minimum and maximum flood extent maps (Figure 3.2.2) show that the flood in the two scenarios covers 3'500 km² and 9'500 km², respectively. Finally, we combined the two flood extent maps with the set of above-mentioned habitat layers into two spatial stacks, each representative of one scenario (Figure 3.1.1). To prevent edge effects during the dispersal simulation, we followed Koen et al. (2010) and expanded the stacks to an extent that was 20% wider and taller than the original, filling the so created buffer zone (gray buffer in Figure 3.2.1b) with randomized values from the respective layers. This would allow simulated dispersers to leave and re-enter the main study area via randomized buffer zones.

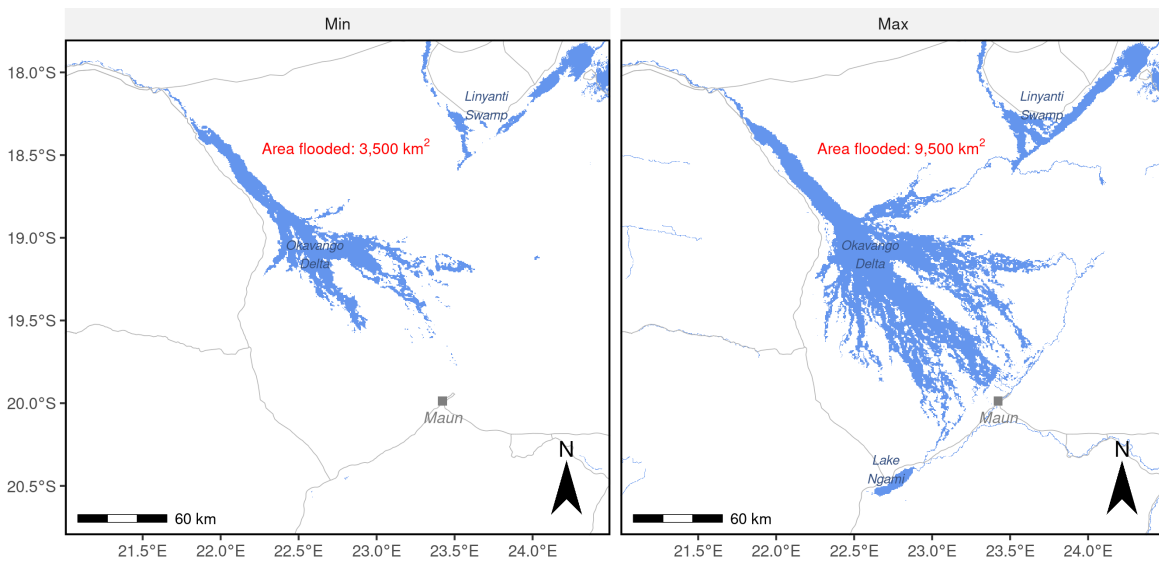


Figure 3.2.2: (a) Minimum and (b) maximum flood extent. The two maps were generated based on 100 minimum and 100 maximum flood extent maps from a series of 700 almost weekly updated remote sensed MODIS MCD43A4 satellite images spanning the years 2000 to 2019.

3.2.3 Source Areas and Egression Zones

We simulated dispersing wild dogs originating from six distinct *source areas* located within the main study area (Figure 3.2.1b). Defining these source areas was necessary to enable identification and quantification of the number of successful dispersal events between different regions of the core study area across the two flood scenarios. We selected source areas in regions that remained dry during both scenarios and are known to host viable African wild dog subpopulations. Nevertheless, these areas are not exhaustive and viable wild dog populations are known to reside outside of them. The study area comprises mostly of continuous habitat, yet natural and anthropogenic landscape features allow the subdivision of the core study area into several sub-regions. The Delta's hydrography and human settlements at its southern fringes result in a natural latitudinal split between the eastern (areas 1, 2, and 3) and western (areas 4 and 5) Delta (Figure 3.2.1b). Areas 1 and 2 are separated longitudinally by the Selinda Spillway, a waterway that connects the Delta with the Linyanti Swamp, while areas 2 and 3 are separated by the Khwai River, which inundates the Mababe Depression east of the Delta (Figure 3.2.1b). On the western side of the Delta, areas 4 and 5 are longitudinally separated by the Thaoga River drainage at Nokaneng (Figure 3.2.1b). Finally, the Delta hosts a central island, known as Chief's Island, which we defined as source area 6 (Figure 3.2.1b). The shape of this area was determined by its borders towards water during the maximum flood scenario, whereas all other source areas were defined using circular polygons with radii of 20 km at somewhat equal distances to each other. We deliberately selected equally sized areas to facilitate comparability between them and to minimize variability in simulated connectivity due to target-effects. We also avoided source areas that directly bordered each other, as simulated individuals initiated close to a shared border would immediately result in connectivity and obscure differences between the two scenarios. Besides source areas 1 to 6, we also generated *egression zones* (Figure 3.2.1b). These zones enabled us to determine through which regions simulated individuals left the core study area, as well as to identify after how many simulated steps they did so. We generated these zones by overlaying the Delta with an ellipse that we dissected into equally sized polygons in accordance with cardinal directions (Figure 3.2.1b). Overall, the selection of source areas and egression zones was based on a mixture between biological and computational considerations.

3.2.4 Dispersal Simulation

We used a previously parameterized and validated dispersal model to simulate dispersal of African wild dogs. This dispersal model was trained using GPS data obtained from 16 wild dog coalitions dispersing across northern Botswana (Hofmann, Cozzi, McNutt, et al., 2023). These data were collected at a sampling rate of four hours, with the exception of one GPS location in the afternoon being skipped in order to ac-

commodate the species tendency to be less active during this period (details in Cozzi et al., 2020; Hofmann et al., 2021). As such, a total of five GPS locations were collected per day. The collected data were then fed into an integrated step-selection function (iSSF, Avgar et al., 2016), where consecutive GPS locations were converted into *observed steps* (the straight-line connecting two consecutive GPS recordings; Turchin, 1998) and compared to a set of *random steps* using (mixed effects) conditional logistic regression (Fortin et al., 2005; Thurfjell et al., 2014; Muff et al., 2020; Fieberg et al., 2021; but see Michelot et al., 2024 for alternative approaches). iSSFs provide less biased estimates of habitat-selection than traditional resource-selection functions (Forester et al., 2009; Zeller et al., 2016) and bear the benefit that random steps are drawn from parametric step-length and turning-angle distributions, such that a model parametrized using iSSFs resembles a fully mechanistic model from which movement can be simulated (Signer et al., 2017; Potts & Börger, 2023; Signer et al., 2024). In contrast to graph-based connectivity models (e.g., least-cost path analysis or circuit-theory), simulations from iSSFs alleviate the need for resistance surfaces, which are often subjective (Simpkins et al., 2017; Marrec et al., 2020) and overestimate conductance in difficult to reach habitat (Signer et al., 2017; Hofmann, Cozzi, McNutt, et al., 2023). The dispersal model presented by Hofmann, Cozzi, McNutt, et al. (2023) comprised a habitat-selection function (describing habitat selection), a movement kernel (describing dispersers' movement capacities), and potential interactions between the two. According to the parametrized model, the main characteristics of wild dog dispersal movements are avoidance of water, avoidance of areas influenced by humans, and a preference for directional and fast movements. The associated model parameters (provided in Figure 3.B.1) can be used to predict probabilities of a step being chosen among a set of random steps (details in Section 3.A), which allows to simulate movements in discrete time.

Originating from each of the six source areas (Figure 3.2.1b), we simulated 2,000 individual dispersing trajectories, each composed of 2,000 steps. Two thousand steps corresponded to a dispersal duration of ~ 400 days, which marks the longest dispersal duration recorded in the study area (Cozzi et al., 2020; Hofmann et al., 2021). By simulating 2,000 steps, we generated the maximum amount of information possible and did not limit connectivity by defining a dispersal cap. Note that we assumed that individuals would not disperse for longer than 2,000 steps, but did not model settlement explicitly. This is because only little is known about how dispersing wild dogs locate potential mates and a suitable territory to settle. Olfactory cues at shared scent-marking sites appear to play a crucial role, yet these are extremely difficult to find and monitor (Apps et al., 2022; Claase et al., 2022). We simulated 1,000 trajectories under the minimum flood extent, the remaining 1,000 under the maximum flood extent. Across the six source areas, this resulted in the simulation of a total of 12,000 individual dispersal trajectories, which sufficed to achieve convergence in relevant connectivity metrics (Hofmann, Cozzi, McNutt, et al., 2023). The simulation procedure was based on the algorithm described by (Signer et al., 2017) and Hofmann,

Cozzi, McNutt, et al. (2023) and works as follows. A random location within the source area is defined as the starting point. Originating from the starting point, a set of 25 random steps is generated by sampling step lengths (sl) from a gamma distribution fitted to observed steps (shape = 0.37, scale = 6,316) and turning angles (ta) from a uniform distribution ($-\pi, +\pi$). Along each random step, the underlying spatial covariates are extracted, and relevant movement metrics computed ($\log(sl)$ and $\cos(ta)$). β -estimates from the fitted dispersal model are then used to predict the probability of each step being chosen, given the step's associated covariates and movement metrics, as well as characteristics of all other proposed steps. Among the 25 proposed steps, one is chosen at random based on assigned probabilities. The procedure is then repeated until a total of 2,000 steps is simulated.

3.2.5 Derived Metrics

Based on simulated dispersal trajectories, we quantified connectivity, identified the emergence of alternative dispersal corridors, and highlighted areas with elevated potential for HWC. Our approach drew upon the set of complementary connectivity metrics for individual-based movement models discussed by Hofmann, Cozzi, McNutt, et al. (2023), and was expanded to include a map highlighting areas with elevated HWC potential. The set of connectivity metrics comprised *inter-patch connectivity* metrics, summarizing dispersal success and duration into distinct habitat patches, *heatmaps*, depicting areas of intense use by dispersers, and *betweenness maps*, highlighting dispersal corridors and bottlenecks. Finally, the *HWC maps* served to reveal areas where simulated dispersers moved into the vicinity of human-dominated landscapes. To illustrate differences between metrics during maximum and minimum flooding, we computed difference maps for the heatmaps, betweenness maps, and HWC maps.

Inter-Patch Connectivity

To measure inter-patch connectivity, we tallied the number of trajectories successfully moving from one source-area to another and computed the average minimum dispersal duration (in number of steps) required to make those connections. Dispersal between two areas was said to be successful whenever a trajectory originating from one area intersected with the polygon of another area. If a trajectory moved through multiple areas, a connection into each of them from the original source was recorded. We also estimated the number of individual trajectories that left the core study area and moved into one of the egression zones. To quantify variability in our estimates, we generated bootstrap samples by randomly drawing 1,000 simulated trajectories per source area 1,000 times with replacement and computing 95%-percentile intervals.

Intensity of Use

To quantify intensity of use of different areas, we generated heatmaps (also known as *utilization distributions* or *flow-maps*) by superimposing the study area with a grid with a spatial resolution of 1 km x 1 km and determining the number of simulated trajectories traversing each grid cell. Such maps are essentially movement-restricted permeability surfaces, thus highlighting areas of intense use (Signer et al., 2017; Hofmann, Cozzi, McNutt, et al., 2023; Potts & Börger, 2023). Heatmaps are relatively insensitive towards the chosen resolution and a 1 km x 1 km grid appeared to provide a good balance between detail and computational feasibility.

Betweenness

To compute spatially mapped betweenness scores, we overlaid the study area with a grid that had a resolution of 2.5 km x 2.5 km and computed the frequency at which simulated individuals transitioned from one grid-cell to another. A cell-transition was said to occur whenever a simulated step crossed from one grid-cell across or into another. In case the same individual repeatedly realized the same cell-transition, we only counted a single transition to avoid overemphasizing regions where individuals moved in circles. This procedure resulted in a weighted edge-list that we used to compute weighted betweenness scores for each grid-cell, i.e. the importance of the respective grid-cell in facilitating movement into adjacent areas (Bastille-Rousseau et al., 2018; Bastille-Rousseau & Wittemyer, 2020). We computed betweenness using the `igraph` R-package (Csardi & Nepusz, 2006). Calculations of betweenness scores are computationally demanding and result in discrete and narrow dispersal corridors (Hofmann, Cozzi, McNutt, et al., 2023). A higher map resolution thus results in increased computation time and narrower corridors. In our case, a grid size of 2.5 km x 2.5 km provided a sensible compromise between computational efficiency and biological relevance of emerging corridors (see also the appendix of Hofmann, Cozzi, McNutt, et al., 2023).

Human-Wildlife Conflict

To pinpoint potential hotspots for HWC, we identified regions where simulated trajectories moved into the vicinity of human-dominated landscapes. For this, we isolated locations along simulated trajectories that ranged \leq 500 meters to the nearest grid-cell with human influence > 0 . Based on the so isolated coordinates, we generated density maps highlighting likely hotspots for HWC. While this approach of mapping potential HWC ignores human population density, we also generated a compound metric by multiplying the generated heatmaps with a continuous human-influence map (Section 3.J). Notably, not every animal in the vicinity of human-dominated landscapes implies conflict, hence we chose to use the term *potential* hotspots for HWC. We prepared these maps at a resolution of 1 km x 1 km.

3.2.6 Software

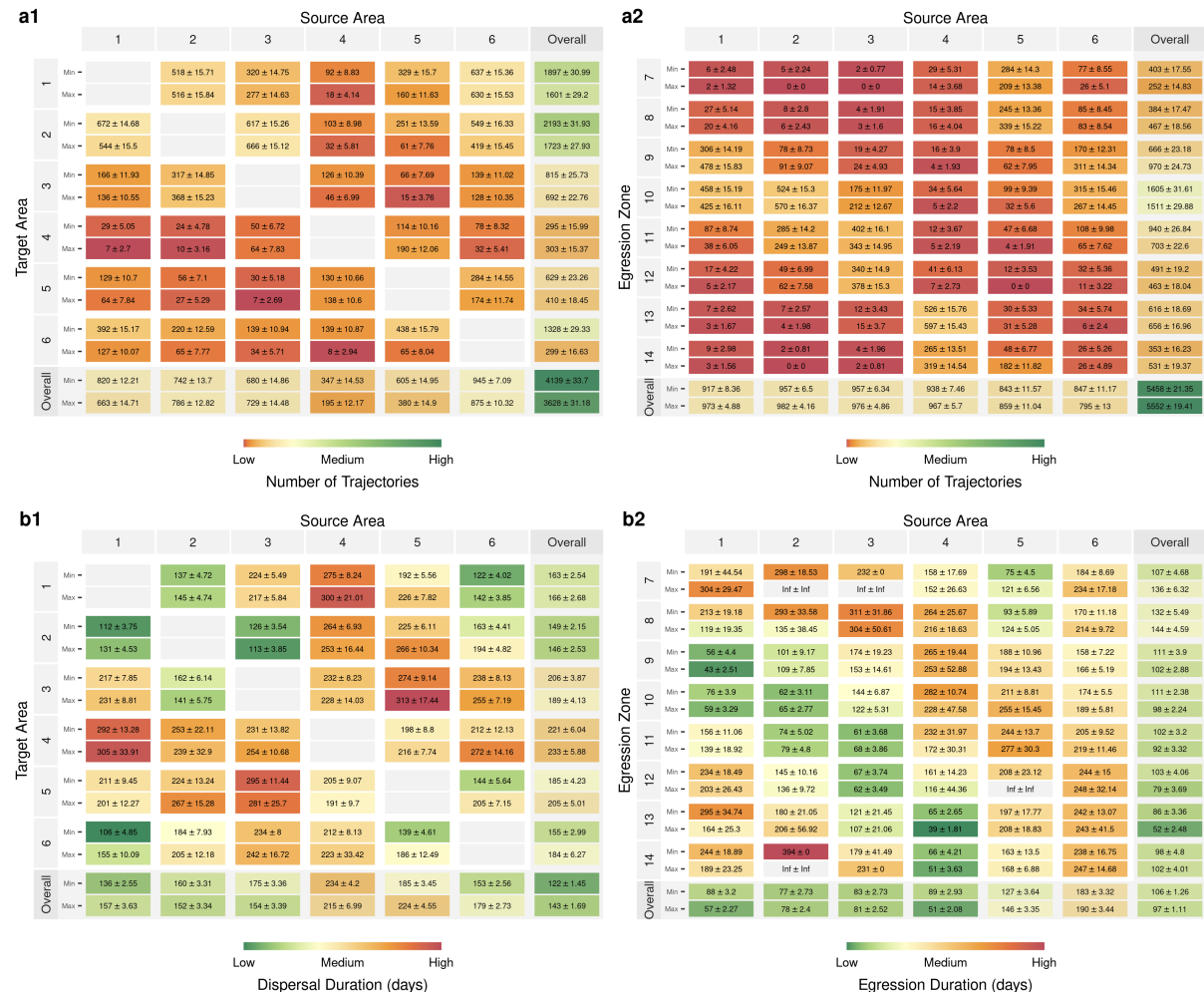
We conducted all data preparation and analyses using the programming language R (R Core Team, 2023). For any spatial data manipulation, we used the R-packages `terra` (Hijmans et al., 2024) and `spatstat` (Baddeley et al., 2015). Several helper functions for the dispersal simulation algorithm were written in C++ and imported into R using the `Rcpp` package (Eddelbuettel & François, 2011). Network analysis was achieved in `igraph` (Csardi & Nepusz, 2006) and figures were generated using `ggplot2` (Wickham et al., 2024) and `ggnetwork` (Briatte et al., 2024). All R-scripts required to replicate our analyses are provided through an online repository. Notably, a similar simulation procedure as employed in our analysis has recently been added to the `amt` R-package (Signer et al., 2024).

3.3 Results

3.3.1 Inter-Patch Connectivity

Our analysis of inter-patch connectivity revealed significant differences in dispersal success and duration depending on the flood scenario (Table 3.3.1, Figure 3.3.1, Figure 3.C.1). Of the 6,000 simulated dispersal trajectories for each flood scenario, $4,137 \pm 35$ trajectories reached another source area during minimum flood, whereas $3,625 \pm 32$ trajectories did so during maximum flood, indicating a 12% lower dispersal success during maximum flood (Table 3.3.1a1). Concurrently, the average dispersal duration of trajectories moving from one source area to another was 17% lower during maximum flood, with 122 ± 1 days compared to 143 ± 2 days (Table 3.3.1b1) during minimum flood. The disparities were most pronounced for trajectories dispersing into source area 6 (the Delta's center), with $1,327 \pm 30$ simulated trajectories reaching area 6 during minimum flood compared to 297 ± 17 trajectories (i.e., 78% lower) during maximum flood (Table 3.3.1a1). Source area 6 therefore appeared to be particularly vulnerable to isolation in the maximum flood scenario. Interestingly, connectivity between some source areas was higher during maximum flood. For instance, the number of trajectories running from area 5 into area 4 was 67% higher, with 114 ± 10 trajectories during minimum flood compared to 190 ± 12 trajectories during maximum flood (Table 3.3.1a1). Simulated individuals therefore responded to unfavorable habitat conditions by dispersing into another region of the landscape. Contrary to our expectations, movement into egression zones (areas 7 - 14) was only marginally higher during maximum flood, with the number of trajectories rising by 2%, from $5,457 \pm 22$ to $5,553 \pm 20$ (Table 3.3.1a2 and Figure 3.E.1).

Table 3.3.1: (a) Dispersal frequency (measured as the number of dispersal trajectories) and (b) dispersal duration (in days) between (a1, b1) source areas (labeled 1 to 6) and (a2, b2) egression zones (labeled 7 to 14) during minimum and maximum flood. Final rows and columns of each subplot represent summary statistics across all areas. For instance, the bottom row in a1 highlights for each source area the total number of trajectories successfully dispersing into a target area. The last column, in contrast, indicates the total number of trajectories immigrating into each target area. Values indicate mean \pm SD. The colors are mapped in a non-linear fashion to avoid over-emphasis on final rows and columns.



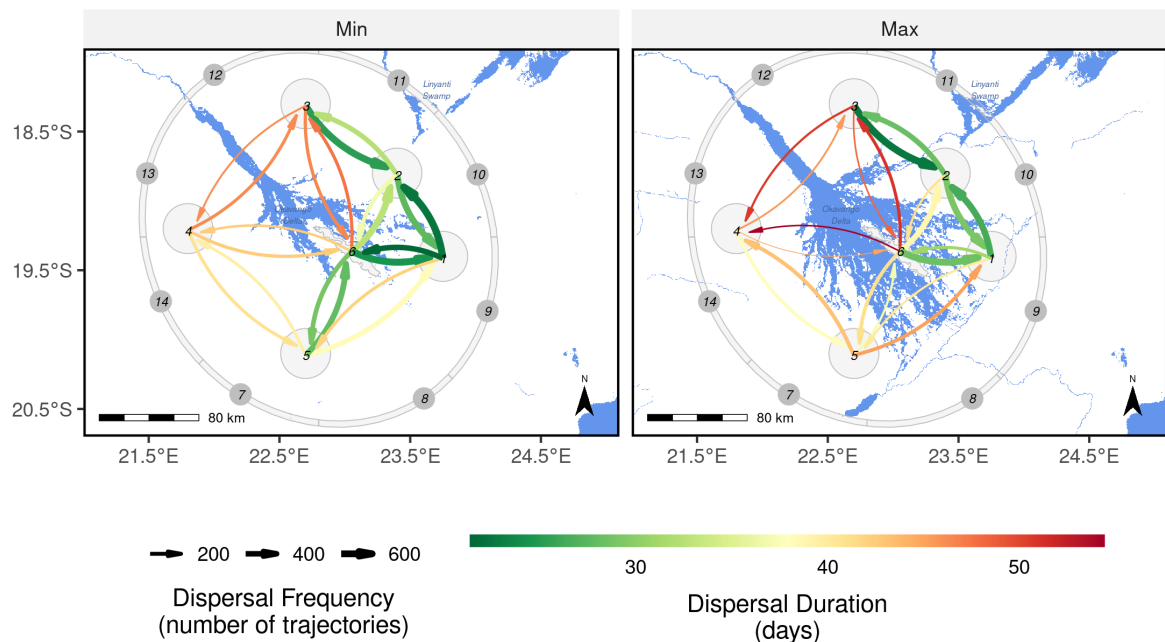


Figure 3.3.1: Dispersal frequency and duration between source areas 1 to 6 in the core study area during the minimum (left panel) and maximum (right panel) flood scenario. The dispersal frequency shows the number of trajectories that emigrated from a specific source area and successfully immigrated into another one. The dispersal duration indicates the mean dispersal duration (in days) required before trajectories arrived at the respective area. Although links between non-neighboring source areas occurred in the simulation, we here only present links between adjacent source areas for brevity. Detailed plots about source-specific inter-patch connectivity are provided in Figure 3.D.1 and Figure 3.D.2.

3.3.2 Intensity of Use

Heatmaps revealed that the Delta acted as a major dispersal barrier during maximum flood, but became permeable during minimum flood (Figure 3.3.2a). During maximum flood, the floodwater extended from the Delta's inflow until the densely inhabited regions at its southern fringes (the town of Maun and its surroundings), such that the negative impacts of water on dispersal were further aggravated by the negative effects of anthropogenic presence. Consequently, there was a substantial decrease in the dispersal frequency across the southern fringes of the Delta during maximum flood (Figure 3.3.2a). During minimum flood, however, the retracting flood revealed vast dispersal areas that individuals used to move across the otherwise inundated regions (Figure 3.3.2a).

3.3.3 Betweenness

Findings from the betweenness maps, which display corridors and pinch-points between neighboring areas, reinforced patterns observed on the heatmaps (Figure 3.3.2b). Multiple corridors linking source area 6 to the surrounding source areas existed during minimum flood, but many of them vanished during maximum flood (Figure 3.3.2b). Instead, a single corridor at the south-eastern tip of the Delta emerged (Figure 3.3.2b). Despite the corridor's high betweenness score, its apparent ability to link the eastern and western sections of the Delta was limited, as evidenced by a low traversal frequency on the heatmap (Figure 3.3.2a).

3.3.4 Human-Wildlife Conflict

The HWC maps highlighted two potential hotspots for HWC that depended on climatic extremes (Figure 3.3.2c). The first hotspot was located at the Delta's inflow between source areas 3 and 4 and was most prominent during minimum flood. During maximum flood, by contrast, the density of simulated locations in the vicinity of humans decreased by 41% in this area (Figure 3.3.2c and Figure 3.I.1). Another hotspot, albeit visually less distinct, covered the region at the distal end of the Delta, extending across the town of Maun (Figure 3.3.2c). This area was particularly relevant during maximum flood, with a density that was 126% higher than during minimum flood (Figure 3.3.2c and Figure S9). The diversion of individuals from one area to another depending on flood conditions therefore drives the emergence of potential hotspots for HWC.

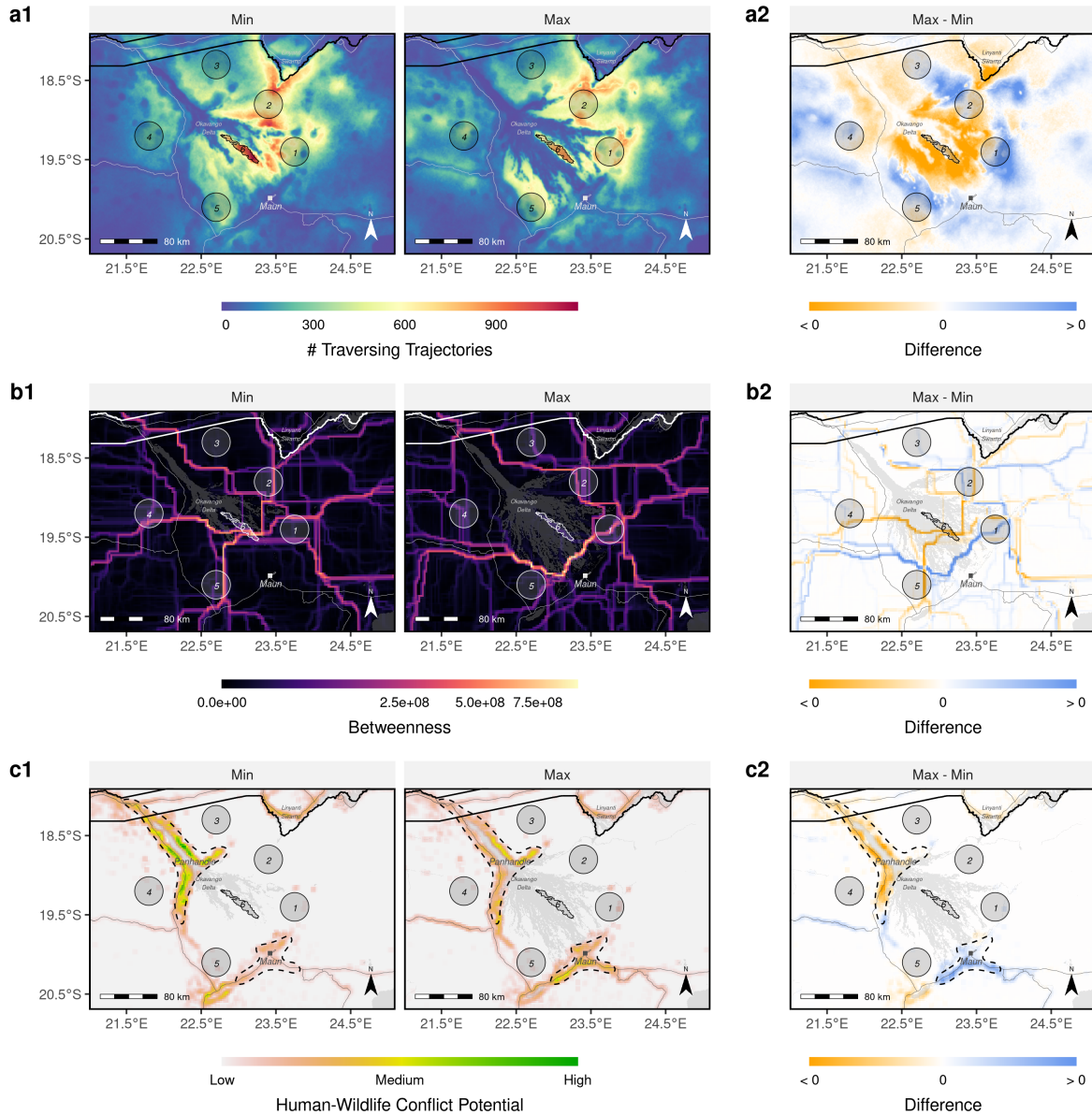


Figure 3.3.2: (a) Heatmaps, (b) betweenness maps, and (c) maps of potential for HWC derived from simulated dispersal trajectories. Left panels were derived from the minimum flood scenario, right panels from the maximum flood scenario. Source areas from which dispersers were released are numbered 1-6. The color scale for betweenness scores in subfigure b was square-rooted to improve visibility of corridors with lower values. Source-specific heatmaps, betweenness maps, and HWC maps are provided in Figures Figure 3.F.1, Figure 3.G.1, and Figure 3.H.1.

3.4 Discussion

We investigated the impacts of extreme environmental conditions, as anticipated under the influence of climate change, on dispersal and connectivity. For this, we employed a previously parameterized and validated movement model and simulated dispersal trajectories of African wild dogs in the Okavango Delta under extreme conditions. Our findings indicate that an amplified flood can significantly reduce dispersal success, prolong dispersal durations, and alter the spatial structure of major dispersal corridors, thereby creating or shifting hotspots of potential human-wildlife conflict (HWC).

Wetter-than-usual climatic conditions, a likely scenario for this study area (Wolski & Murray-Hudson, 2008; IPCC, 2022), resulted in significant barriers to dispersal and connectivity, and in an overall increase in dispersal durations. This was largely a result of simulated individuals avoiding large water bodies, thus detouring through more suitable habitats (Cozzi et al., 2013; Cozzi et al., 2020; Hofmann et al., 2021; Hofmann, Cozzi, McNutt, et al., 2023). Movement constraints due to changes in environmental conditions can thus lead to subpopulation isolation (up to > 75% in our case), thereby jeopardizing recolonization efforts following local extinctions, and impacting population dynamics, gene flow, and genetic diversity (Hanski, 1999b; Frankham et al., 2002; Leigh et al., 2012; Baguette et al., 2013).

The African wild dog exhibits a remarkable dispersal ability, sometimes dispersing several hundred kilometers across international borders (McNutt, 1996; Davies-Mostert et al., 2012; Masenga et al., 2016; Cozzi et al., 2020; Sandoval-Seres et al., 2022; Cozzi et al., 2023). This ability likely evolved as an adaptation to the relatively low density at which the species occurs (Creel & Creel, 2002; Masenga et al., 2016) and may have been sustained by a historically well-connected landscape that imposed low mortality (*sensu* Fahrig, 2007). Today, however, the need for vast dispersal habitats makes this species vulnerable to habitat loss and fragmentation (Woodroffe & Sillero-Zubiri, 2012; 2020). When dispersing animals are forced to alter their dispersal routes due to changing environmental conditions, this could result in non-optimal dispersal behavior in human-altered landscapes (Fahrig, 2007). This is particularly problematic when dispersers are channeled through areas with high anthropogenic resistance and elevated risk of mortality (Fahrig, 2007; Van Der Meer et al., 2014; Ghoddousi et al., 2021). For a population of African wild dogs in Zambia, Leigh et al. (2012) revealed that dispersal and the associated mortality indeed led to a decline in genetic diversity and, subsequently, to a net-loss of individuals. At present, our own study population appears to benefit from moderate levels of dispersal, as an analysis across Southern Africa revealed a genetically healthy cluster in the Kavango-Zambezi Transfrontier Conservation Area (Tensen et al., 2022). This cluster may, however, be at risk depending on future flood conditions.

As dispersal is a key process influencing population dynamics (Hanski, 1999b; Clobert et al., 2012), any climatic-induced alteration will have cascading effects that amplify or buffer the effect of climatic changes

on population persistence and viability. Lower connectivity and prolonged dispersal durations due to adverse environmental conditions will inevitably result in increased energetic expenditures and exposure to various threats such as predation, competition, human encounters, and diseases (Alberts & Altmann, 1995; Yoder, 2004; Stamps et al., 2005; Bonte et al., 2012), thus further jeopardizing dispersal success and its effect on population dynamics. Higher ambient temperatures have previously been associated with negative effects on wild dog reproductive success (Woodroffe et al., 2017; Abrahms et al., 2022), survival (Rabaiotti et al., 2021), and, consequently, population persistence (Rabaiotti et al., 2023). The negative effect of hotter climatic conditions on local population survival and recruitment may be further exacerbated by reduced dispersal success and connectivity in case of amplified flooding regimes.

Even though our finding that an increased flood extent reduces connectivity seems unsurprising, it is non-trivial to quantify such impacts and to predict the spatial rearrangements of movement corridors they entail. Wild dogs avoid crossing water bodies, yet are capable of doing so if they really need to, especially during dispersal (McNutt, 1996; Cozzi et al., 2013; Cozzi et al., 2020; Hofmann, Cozzi, McNutt, et al., 2023). By simply assuming such obstacles to be impenetrable, one may miss important corridors that lead across narrow sections of unsuitable habitat (Marrec et al., 2020). Using simulations from integrated step-selection functions (iSSFs), however, one can realistically render that an animals' decision to disperse across a specific habitat is conditional on what's available at alternative steps. A disperser surrounded by a hostile matrix may readily cross water, whereas an individual dispersing through favorable habitat can choose to avoid water entirely. Another challenge when predicting the impacts of climate change on connectivity is that future on-the-ground conditions are rarely known (e.g., Wolski and Murray-Hudson, 2008). To overcome this, we leveraged historic data on seasonal variation of the flood extent and assumed that climate change would shift the ecosystem towards conditions that currently mark extremes. A similar approach can be applied in systems where the relationships between changing conditions and functional connectivity are less evident.

While wet extremes appear to hinder dispersal and connectivity, the opposite applies for amplified dry conditions, because areas that are inundated under normal circumstances become free of water and therefore passable. Predictions suggest that climate change will result in elevated precipitation across the Delta's catchment areas in Angola (Wolski & Murray-Hudson, 2008; IPCC, 2022), thus resulting in above-average flooded regions. Concomitantly, however, hotter temperatures and increased levels of evapotranspiration are anticipated for the Delta's basin in Botswana, suggesting that dry periods may be experienced too (Wolski & Murray-Hudson, 2008; Moses & Hambira, 2018; Akinyemi & Abiodun, 2019; IPCC, 2022). The Delta's expanse is also affected by multi-decadal oscillations in precipitation patterns, which may periodically offset or amplify long-term trends (Wolski et al., 2012). The overall impact of climate change on flood patterns therefore remains unknown (Wolski & Murray-Hudson, 2008; Wolski et

al., 2012) and this lack of knowledge is aggravated by uncertainties regarding future anthropogenic water abstractions along the Okavango River (Kgathi et al., 2006; Murray-Hudson et al., 2006; Hughes et al., 2011). It is nonetheless worth noting that our maximum flood extent map, which was prepared based on 100 maximum flood extents observed on over 700 weekly-updated floodmaps, is conservative compared to historically observed flood extents in the Delta. While the flood in our map encompasses an area of 9'500 km², the Delta may inundate an area of up to 14,000 km² in exceptional cases (McCarthy et al., 2003; Gumbrecht et al., 2004). Changes in dispersal behavior and connectivity due to climate change may therefore be more pronounced than reported here.

Our analysis revealed that dispersers utilize different movement corridors depending on flood conditions, leading to the emergence and shifting of potential hotspots for HWC. An increased proximity between humans and carnivores is typically associated with a higher potential for conflict (e.g., Michalski et al., 2006; Chapman and McPhee, 2016). Especially dispersers, which often venture outside protected areas, expose themselves to anthropogenic hostility (Elliot et al., 2014; Cozzi et al., 2020; Vasudev et al., 2023). In our case, the funneling of individuals through alternative dispersal corridors resulted in the shift of potential HWC hotspots, potentially increasing HWC and retaliatory killing. One example is the area surrounding Maun, where HWC is expected to rise during wet periods, exacerbating existing human-wildlife conflict (Gusset et al., 2009; McNutt et al., 2017; Cozzi et al., 2020). Identifying and mapping the conflict-connectivity interface (i.e., areas prone to HWC) in light of climate change can improve our understanding of connectivity (Vasudev et al., 2023) and could aid in prioritizing mitigation and prevention measures that have the highest impact (Treves et al., 2011; Buchholtz et al., 2020) or to develop appropriate compensation schemes (McNutt et al., 2017). However, it is important to note that encounters between animals and humans do not imperatively imply HWC, and that the severity of conflict and its impact on connectivity likely depends on humans' perception and attitude towards wildlife (Ghodousi et al., 2021). Besides the risks associated with direct mortality through human persecution, a higher proximity to humans also increases the risk of indirect mortality through disease transmissions from domestic animals (Cleaveland et al., 2000; Van De Bildt, 2002). Previous outbreaks of distemper and rabies have caused the local extermination of African wild dogs in several African countries (Woodroffe et al., 2004). As infected dispersing individuals may further spread diseases within protected areas, a better understanding of points of interaction between humans and wildlife will facilitate the implementation of targeted vaccination programs in the face of climatic change (Vial et al., 2006).

In the present study, we ignored mortality during dispersal and assumed all simulated dispersers to survive for 2,000 steps (~ 400 days). This likely resulted in an overestimation of connectivity, especially between distant source areas (Kramer-Schadt et al., 2004; Diniz et al., 2019; Fletcher Jr. et al., 2019; Day et al., 2020). The inclusion of mortality in individual-based simulations is relatively straight forward

(Fletcher Jr. et al., 2019; Fletcher Jr. et al., 2023), yet its estimation for dispersing individuals has proven difficult (Behr et al., 2023). During the course of our study, we recorded and confirmed only two mortality events during dispersal, thus precluding a detailed investigation. Notably, unless the risk of mortality is included in simulations in a spatially explicit manner, its inclusion will merely shorten the length of simulated trajectories and its impact on inferred connectivity patterns will be relative in nature.

Even though we assumed vegetation to remain unchanged in both extreme scenarios, we acknowledge that vegetation cover and phenology may shift in response to climate change, potentially influencing dispersal indirectly through prey availability (Bonyongo, 2005). While flooding represents the primary barrier to dispersing individuals (Cozzi et al., 2020; Hofmann et al., 2021; Hofmann, Cozzi, McNutt, et al., 2023), refining and capturing the role of vegetation dynamics on prey distribution and dispersal will therefore be crucial. However, predicting the impacts of climate change on vegetation cover and its effect on the distribution of prey will be challenging and is an area for continued research.

Our dispersal model was validated using independent dispersal data (see Hofmann, Cozzi, McNutt, et al., 2023), yet validating predictions of connectivity and HWC under the two presented scenarios remains challenging. This is mainly owed to the difficulty of monitoring dispersing individuals *per se*, coupled with the low likelihood of observing dispersal during periods of extreme flooding. Genetic data could serve to validate predictions of historical connectivity patterns (Cushman & Lewis, 2010; Spear et al., 2010), yet is equally difficult to collect and does not provide a means of validating predicted connectivity patterns in the short run. Observational data, including photographic evidence from citizen scientists, however, could serve to fill this gap (Marnewick et al., 2014; Cozzi et al., 2023). Most carnivores are individually identifiable, either by their coat pattern or other unique morphological features (e.g., Pennycuick and Rudnai, 1970 and Kelly, 2001). Automatic recognition of individuals from photographic evidence using artificial intelligence will therefore open up new avenues to track individuals through space and time (Cozzi et al., 2023). The so collected data provides a means to monitor dispersal across unprecedented temporal and validate predicted patterns of landscape connectivity.

In conclusion, our dispersal simulation across two extreme environmental scenarios revealed striking differences in dispersal prospects and landscape connectivity for dispersing animals. We thereby showed that extreme environmental conditions, akin to those projected under climate change, will have important impacts on functional connectivity and may alter areas susceptible to human-wildlife conflict. Gaining insights into the dispersal patterns of various wide-ranging species under changing conditions will be critical for designing and preserving movement corridors (Vasudev et al., 2015). Wildlife managers and conservation bodies would also benefit from moving beyond a static assessment of connectivity and considering multiple, potentially extreme, projections of environmental conditions to help gauge the impacts of climate change on dispersal and connectivity. Successful conservation strategies will be of particular

relevance for wide-ranging and dispersal-dependent species that are already threatened with extinction, such as the African wild dog. Ultimately, our study provides valuable insights into the potential effects of climate change on dispersal, connectivity, and human-wildlife-conflict dynamics, emphasizing the relevance of proactive conservation measures and targeted mitigation strategies that incorporate predictions of environmental change.

Appendices

3.A Dispersal Model

The model employed to simulate dispersal was based on an integrated step selection function (iSSF). In (integrated) step selection functions (iSSFs, Fortin et al., 2005; Avgar et al., 2016), observed GPS locations are converted into steps (the straight-line traveled between two GPS recordings (Turchin, 1998)) and compared to a set of *random* steps in a conditional logistic regression framework (Fortin et al., 2005; Thurfjell et al., 2014; Muff et al., 2020; Fieberg et al., 2021). The model presented in (Hofmann, Cozzi, McNutt, et al., 2023) used dispersal data collected on 16 dispersing AWDs from a free-ranging wild dog population in northern Botswana. GPS data during dispersal was collected at 4-hourly intervals and translated into steps of similar duration. Observed steps were then paired step with 24 random steps that were generated using a uniform distribution for turning angles ($-\pi, +\pi$) and step lengths from a gamma distribution fitted to observed steps (scale $\theta = 6,308$ and shape $k = 0.37$). It was then assumed that animals assigned to each observed and random step a selection score of the form (Fortin et al., 2005):

$$w(x) = \exp(\beta_1 x_1 + \beta_2 x_2 + \dots + \beta_n x_n) \quad (\text{Equation 3.1})$$

Where (x_1, x_2, \dots, x_n) represent the covariate values along each of the steps and the $(\beta_1, \beta_2, \dots, \beta_n)$ are the animal's relative selection strengths (Avgar et al., 2017) towards these covariates. The benefit of *integrated* SSFs over regular SSFs is that they provide a means to render two complementary "kernels". A *movement kernel* that describes general movement behavior of dispersing AWDs and a *habitat kernel* that describes preferences of AWDs with regards to environmental conditions (Fieberg et al., 2021). iSSFs also allow interactions among the two kernels and are thus suitable to render that movement behavior may change depending on habitat conditions. A fitted iSSF model can be used as an individual-based movement model to simulate dispersal (Signer et al., 2017; Hofmann, Cozzi, McNutt, et al., 2023).

3.B Dispersal Model Estimates

Figure 3.B.1 depicts estimates from the model developed by Hofmann, Cozzi, McNutt, et al. (2023) that we used to simulate dispersal trajectories in the present.

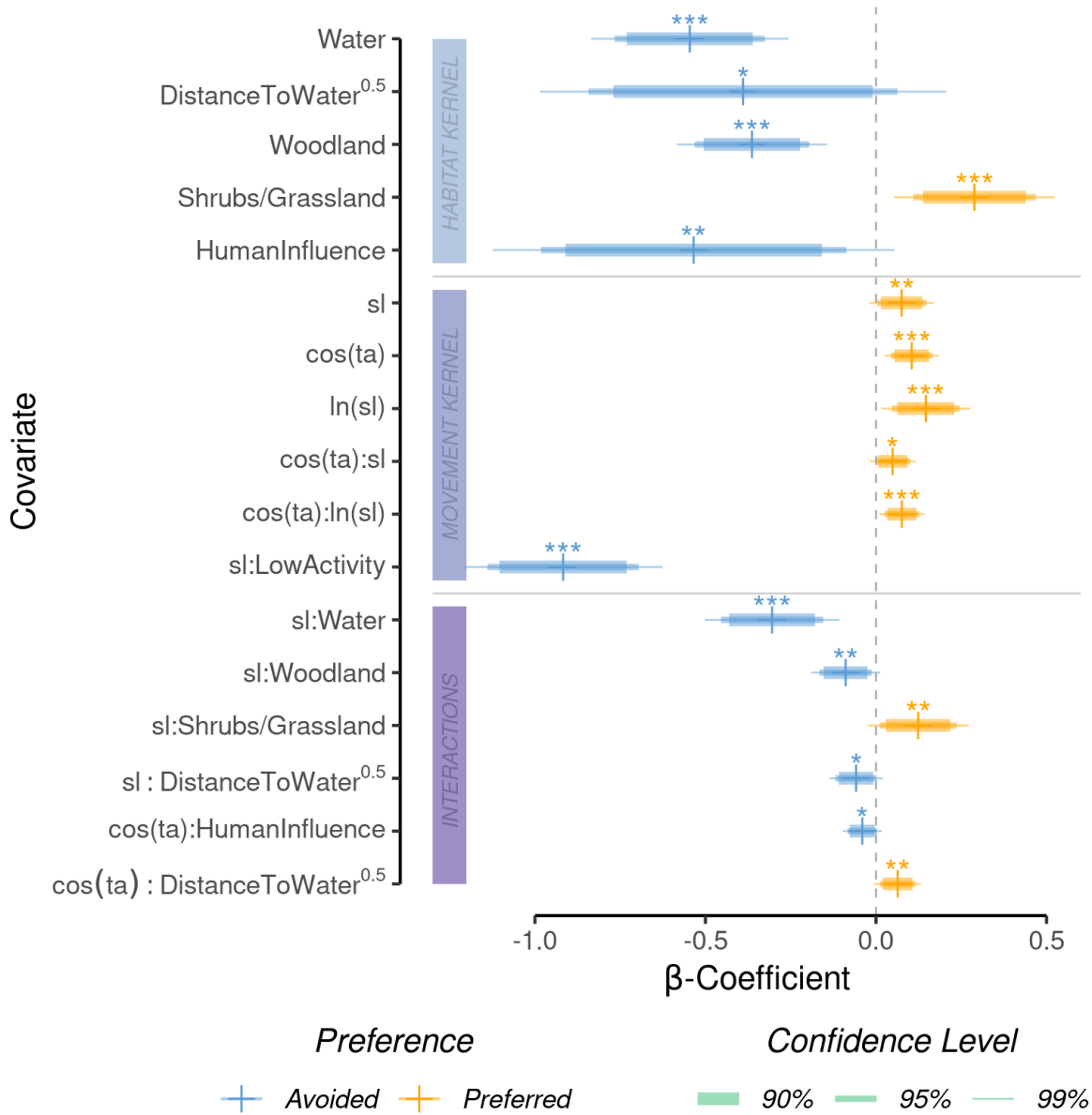


Figure 3.B.1: Model parameters from the step-selection model implemented by Hofmann, Cozzi, McNutt, et al. (2023). The model was fit to GPS data of dispersing African wild dogs and comprises of a habitat kernel (light blue band), a movement kernel (dark blue band), and their interactions (purple band). Abbreviations are as follows: sl = step-length, ln(sl) = natural logarithm of the step-length, cos(ta) = cosine of the relative turning angle.

3.C Immigration & Emigration by Source Area

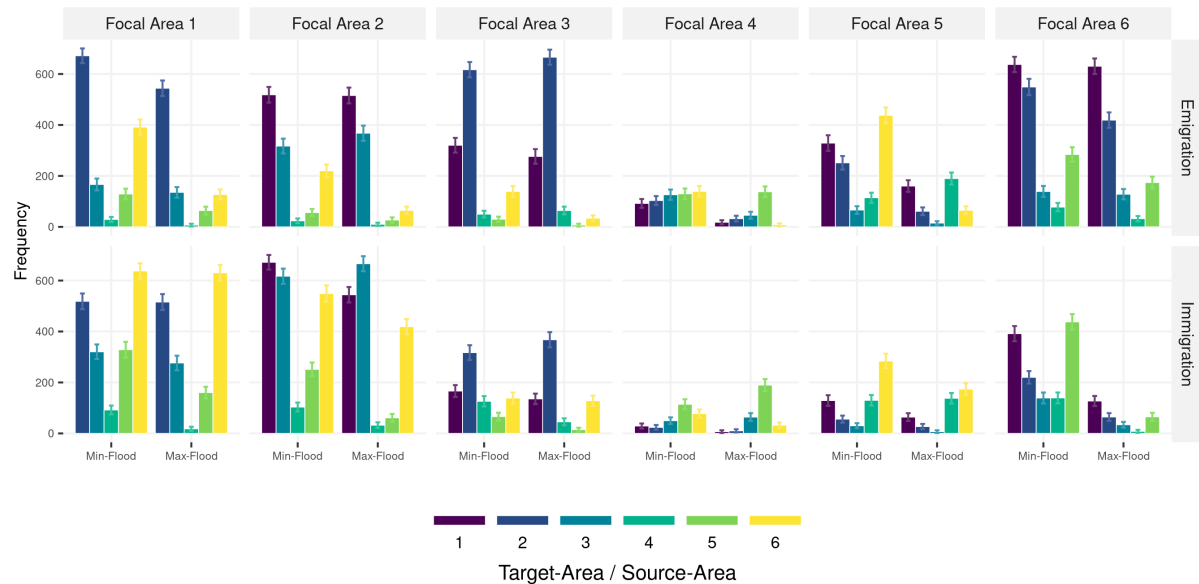


Figure 3.C.1: Number of individuals emigrating from, or immigrating into a specific source area (focal area). Colors indicate into which other areas emigrants moved or from which other areas immigrants originate. For instance, the most left plot in the upper panel shows the number of individuals moving from source area 1 into the six other source areas during minimum and maximum flood, respectively.

3.D Source-Specific Inter-Patch Connectivity

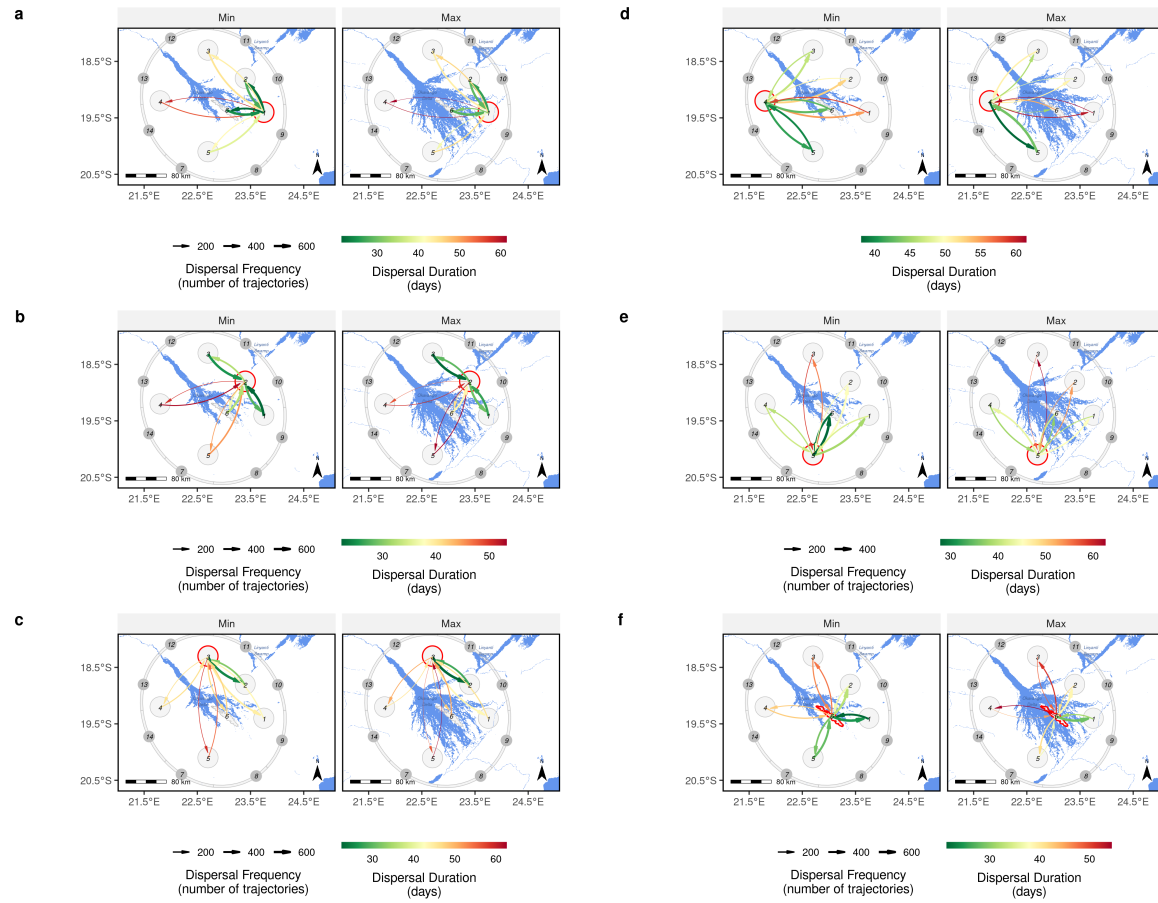


Figure 3.D.1: Spatial representation of inter-patch connectivity derived for each source area separately across the two extreme flood-scenarios. The focal source area of each subfigure is highlighted by a red circle. Subfigure a, for instance, depicts inter-patch connectivity for source area 1.

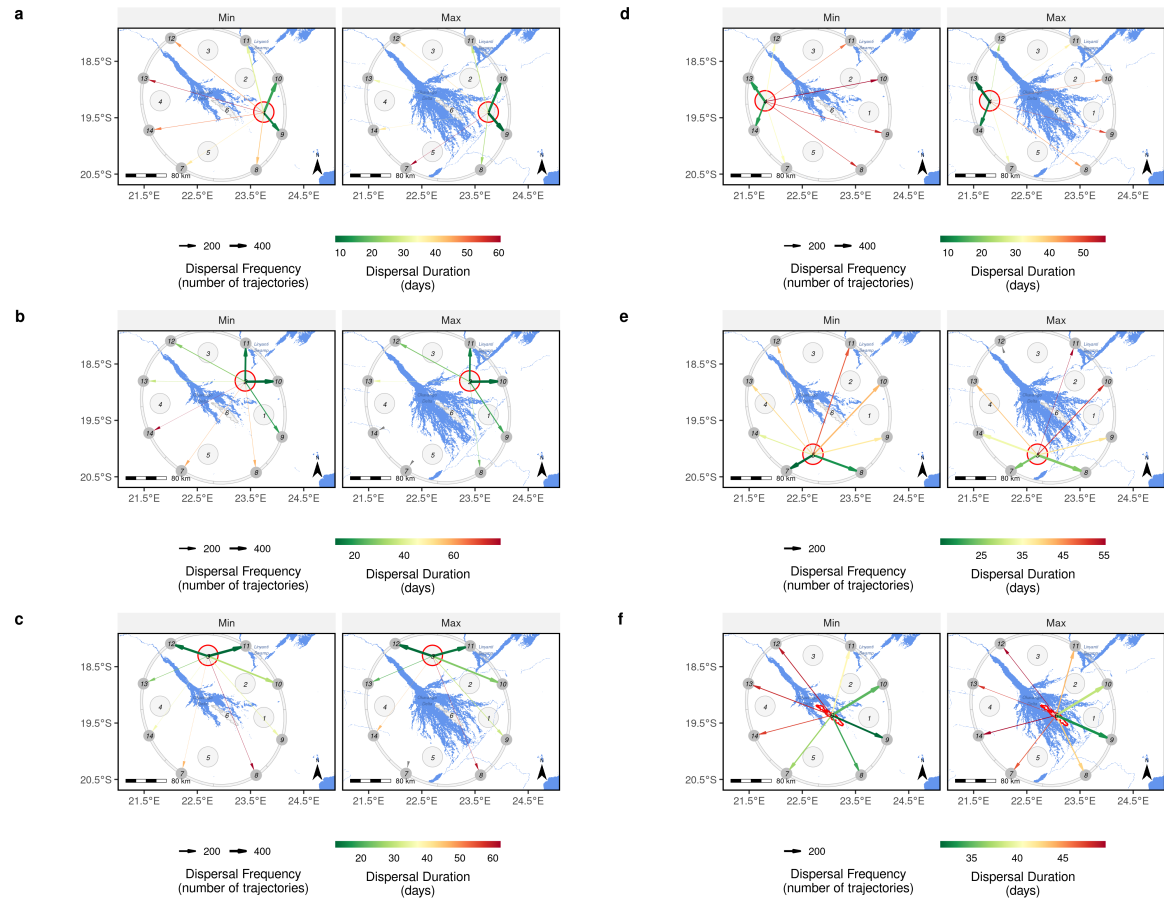


Figure 3.D.2: Spatial representation of egression patterns derived for each source area separately across the two extreme flood-scenarios. The focal source area of each subfigure is highlighted by a red circle. Subfigure a, for instance, depicts the number of individuals egressing from source area 1.

3.E Dispersal into Egression Zones

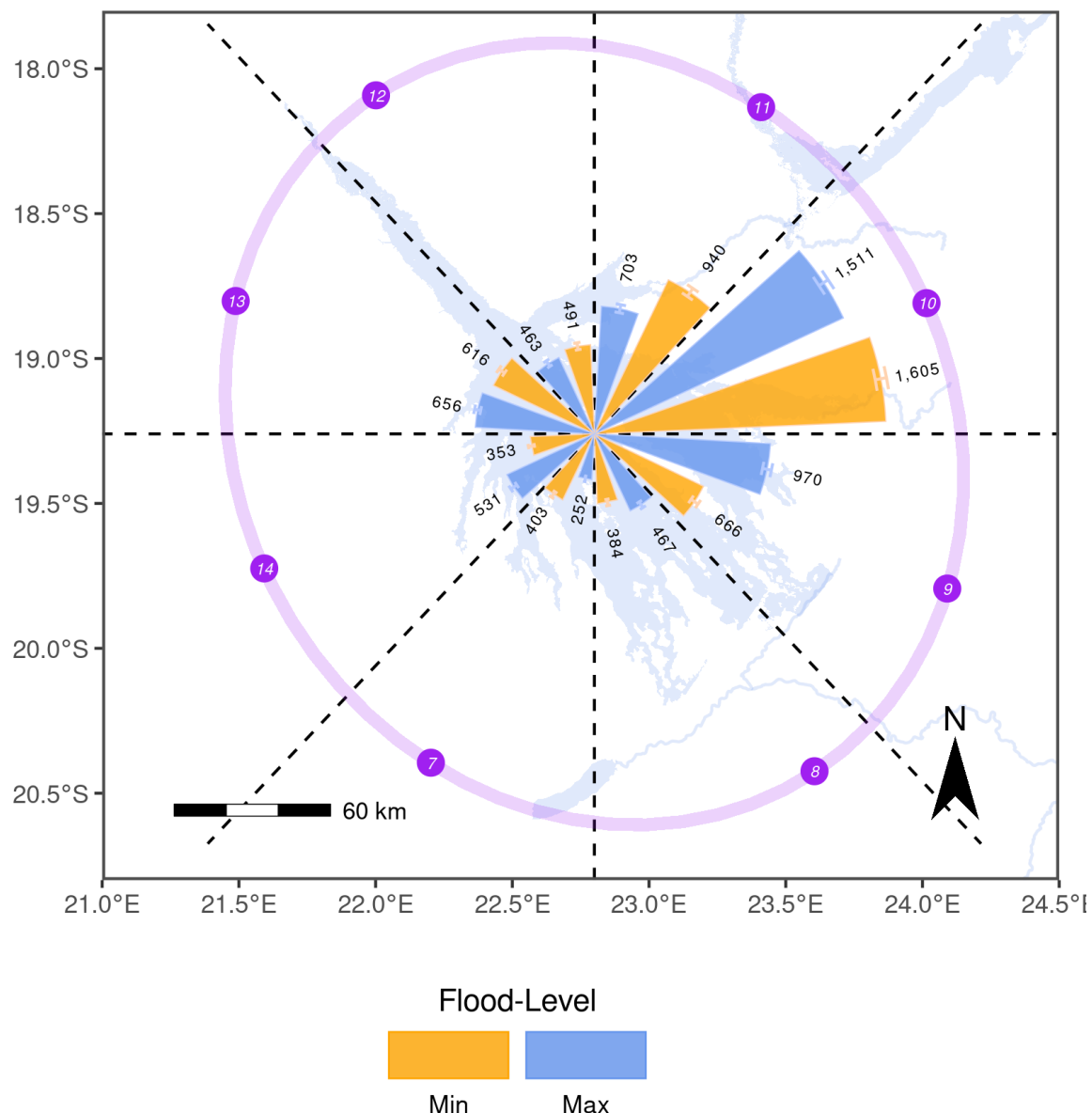


Figure 3.E.1: Absolute number of simulated trajectories running into each of the designated egression zones (purple) during minimum and maximum flood.

3.F Source-Specific Intensity of Use

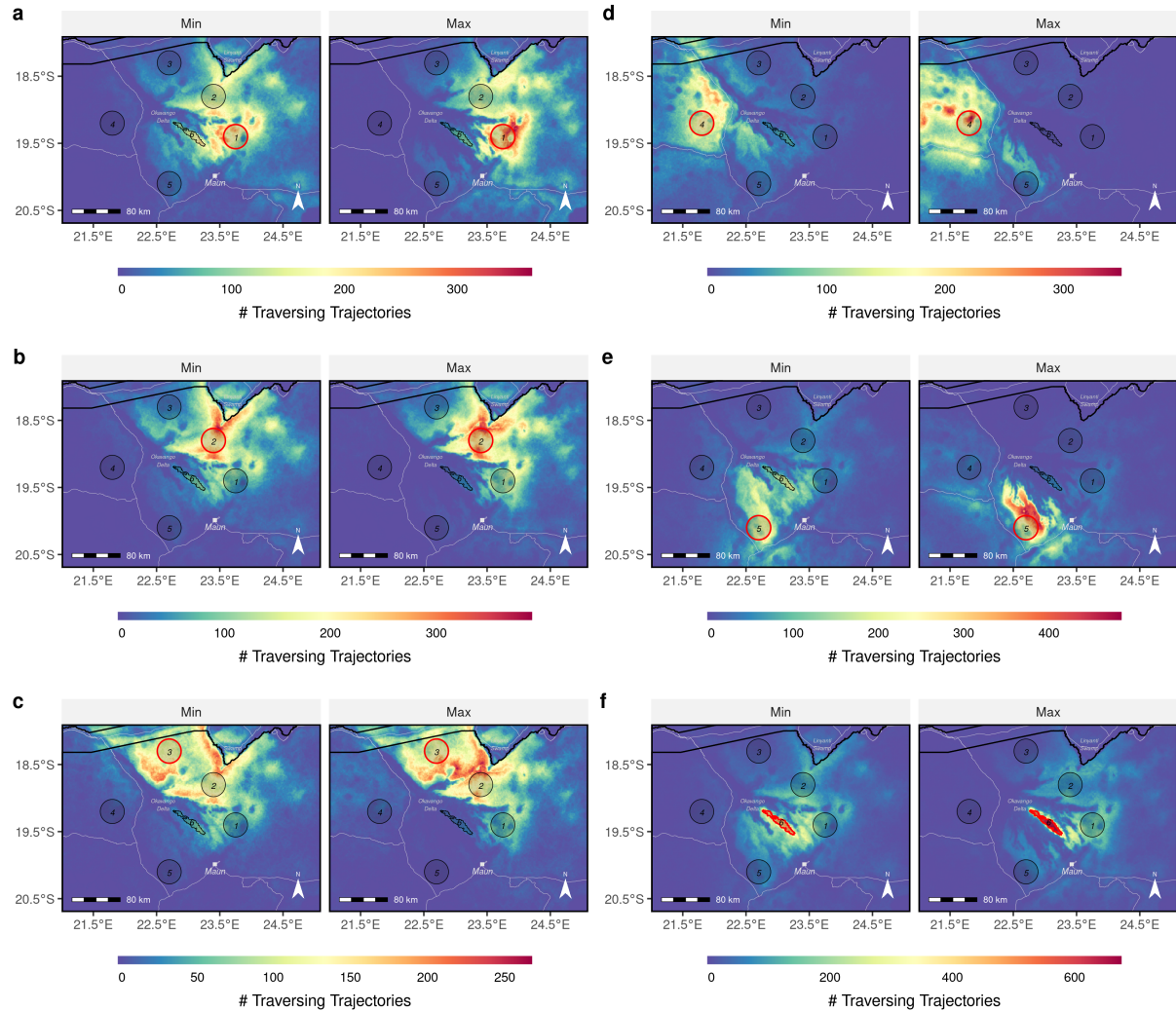


Figure 3.F.1: Heatmaps showing the intensity of use for each source area separately across the two extreme flood-scenarios. The focal source area of each subfigure is highlighted by a red circle. Subfigure a, for instance, depicts the heatmaps for source area 1.

3.G Source-Specific Betweenness

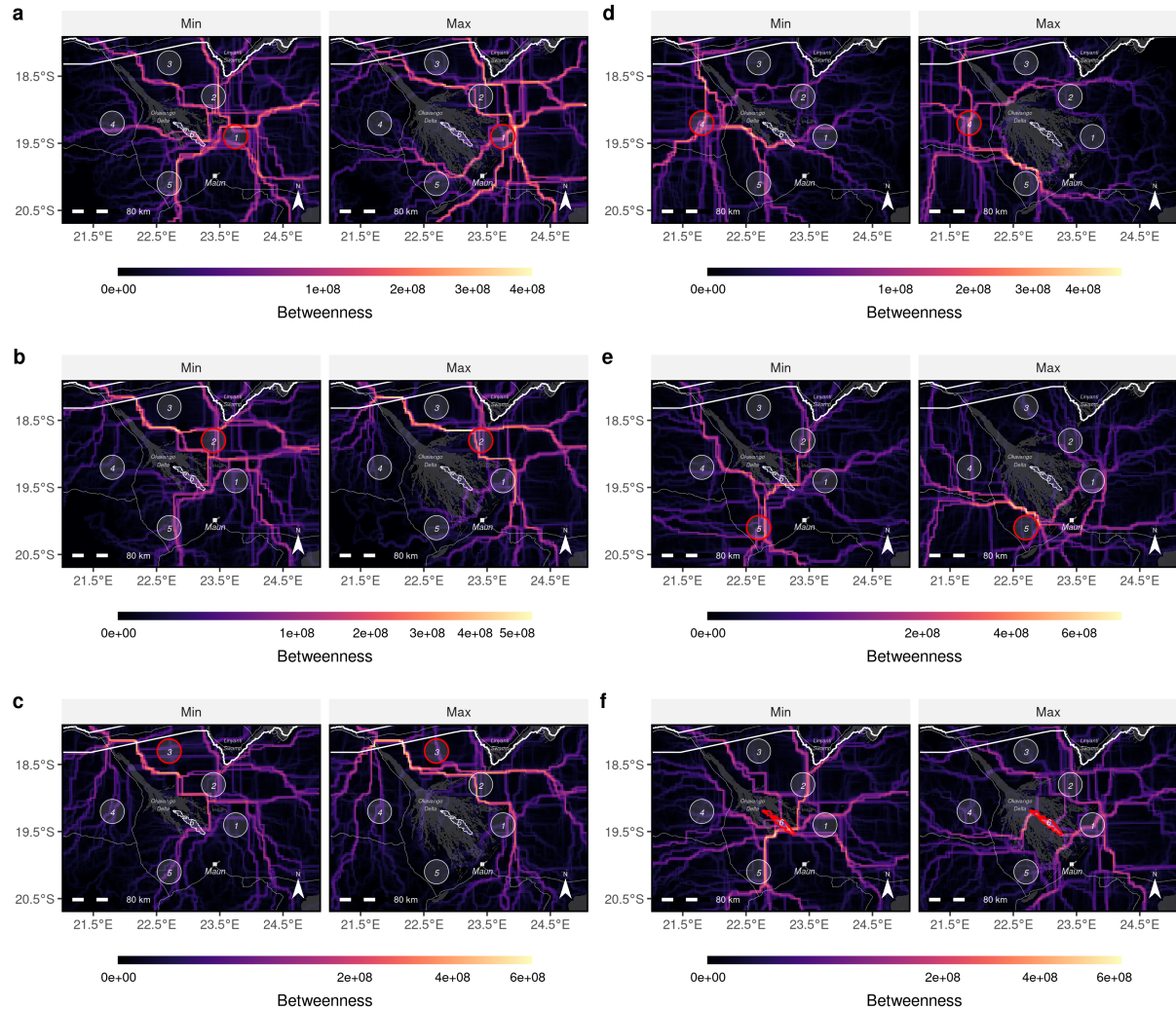


Figure 3.G.1: Betweenness maps prepared for each source area separately across the two extreme flood-scenarios. The focal source area of each subfigure is highlighted by a red circle. Subfigure a, for instance, depicts the betweenness maps for source area 1.

3.H Source-Specific Human-Wildlife Conflict

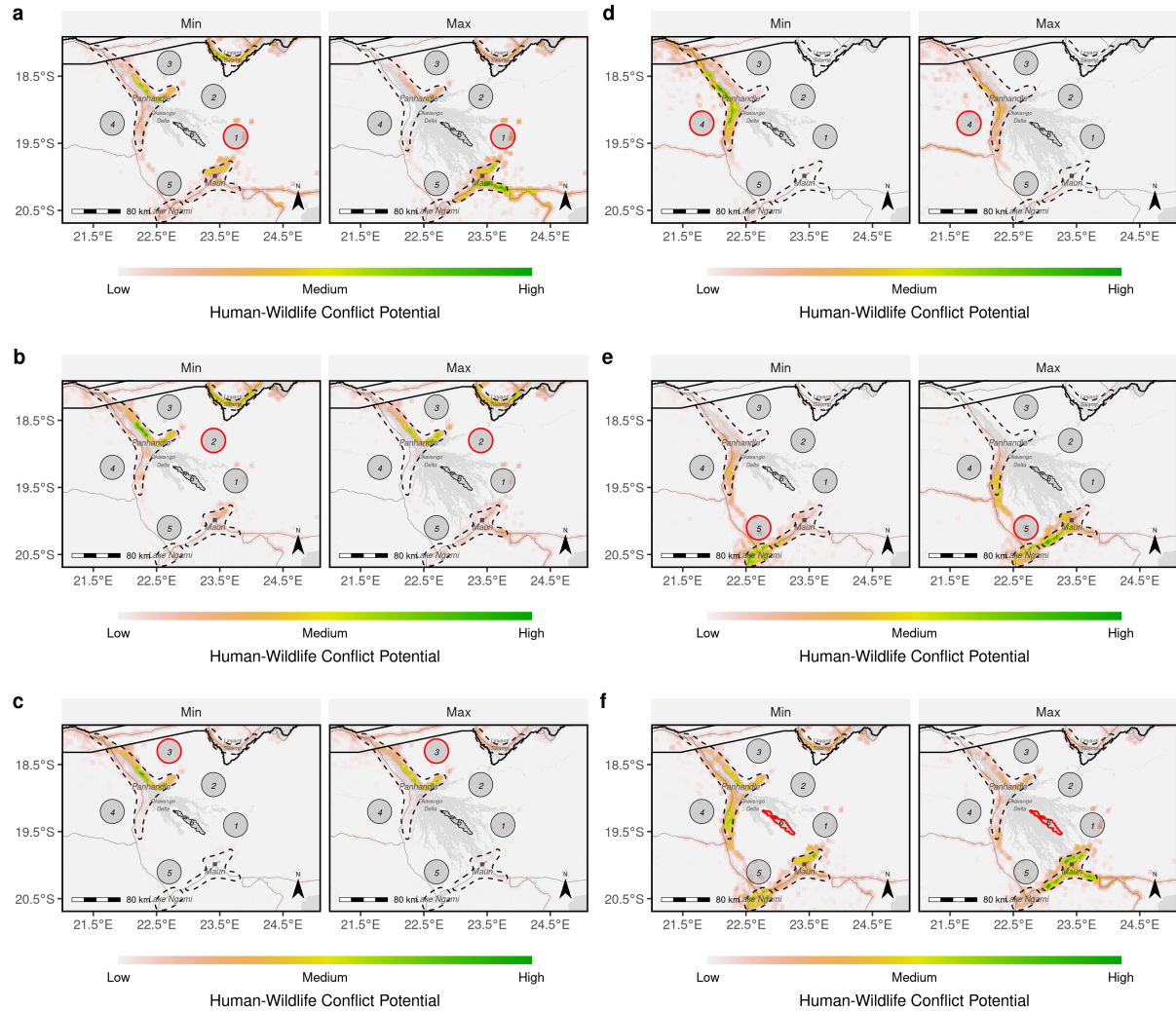


Figure 3.H.1: Human wildlife conflict maps prepared for each source area separately across the two extreme flood-scenarios. The focal source area of each subfigure is highlighted by a red circle. Subfigure a, for instance, depicts the human wildlife-conflict maps for source area 1. Dotted shapes were used to compare human-wildlife conflict within specific areas (see also Section 3.J.).

3.I Changes in Potential for Human-Wildlife Interactions

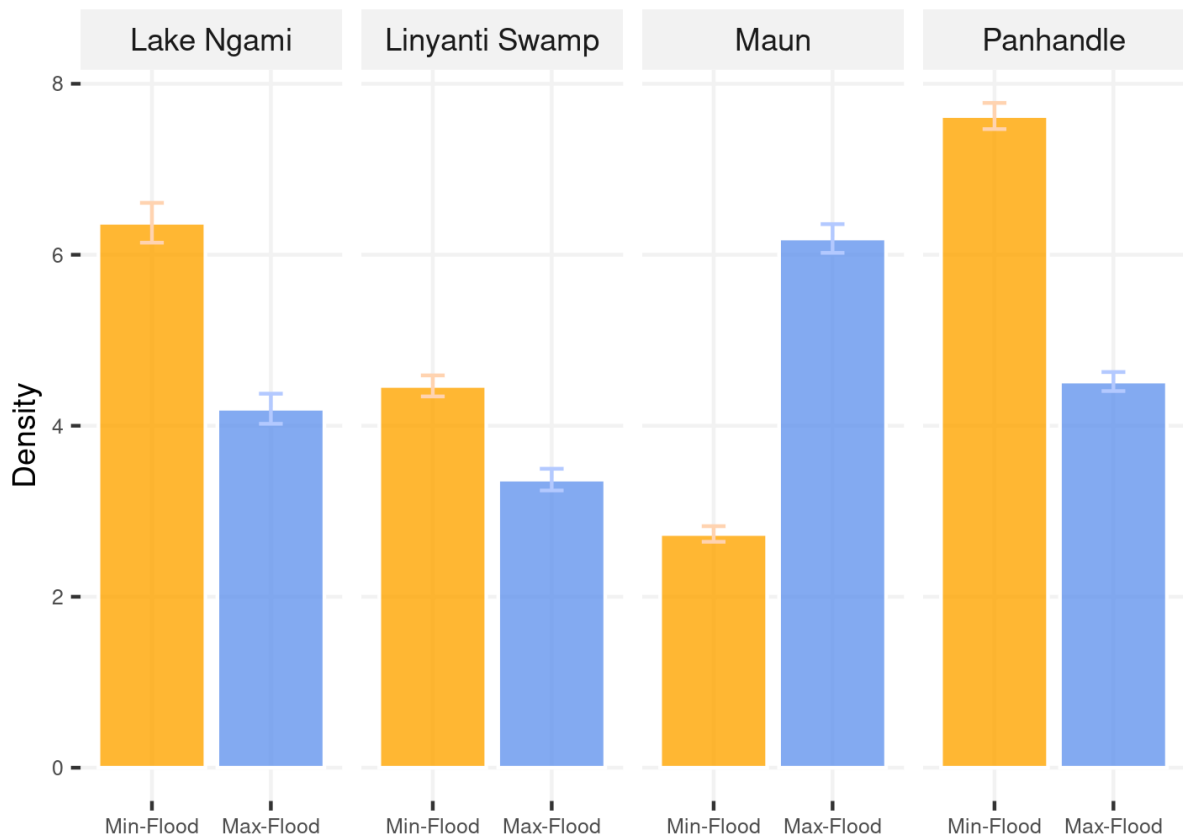


Figure 3.I.1: Number of simulated trajectories within the vicinity of human-dominated landscapes in different areas of interest across the minimum and maximum flood scenarios. The areas are represented by the black dotted shapes in Figure 3.H.1

To identify potential hotspots for human-wildlife conflict and generate Figure 3.3.2c, we isolated all simulated animal locations within 500 meters to a human-influenced grid-cell (Figure 3.3.2c in the main manuscript). To compute the needed distances, we assumed human-influence to be binary (influence = 1, no influence = 0), thus ignoring potential impacts of human density. We argue that the severity of human-wildlife conflict is not necessarily related to human density, yet humans' attitude towards wildlife. Attitude often correlates negatively with habitat suitability for the species of interest (Behr et al., 2017), and so conflict is often pronounced in peripheral areas (McNutt et al., 2017). Since we lacked detailed information of anthropogenic resistance (Ghoddousi et al., 2021) across the study area, we deemed a binary representation of human impacts as appropriate. Alternatively, one can also compute a compound score by multiplying the human-influence layer with the heatmaps derived from simulated dispersal. This is presented in Figure 3.J.1, where we multiplied the heatmaps (Figure 3.J.1a) with the human-influence layer (Figure 3.J.1b) and produced maps showing potential for human-wildlife conflict. Qualitatively, the maps in Figure 3.J.1 are very similar to the ones presented in Figure 5c.

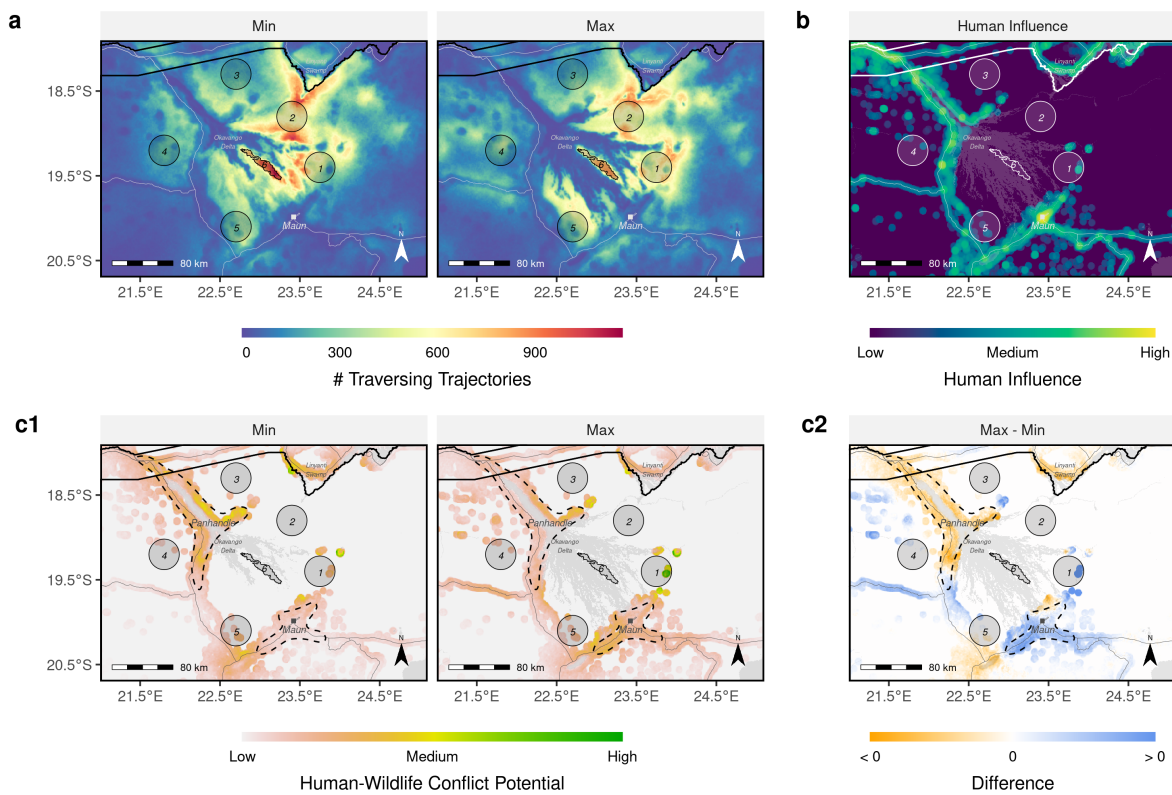


Figure 3.J.1: Alternative approach to quantifying the potential for human-wildlife conflict. Here, we multiplied the heatmaps (a) with the human-influence layer (b) to obtain human-wildlife conflict maps (c1). We also computed a difference map (c2) for the layers shown in c1.



Chapter 4

The Effects of Increasing Seasonal Dynamism when Predicting Connectivity: Advantages or Unnecessary Complications?

David D. Hofmann , Dominik M. Behr , John W. McNutt, Arpat Ozgul , and Gabriele Cozzi 

Abstract

Seasonally changing conditions can drastically alter landscape connectivity. Nevertheless, most connectivity studies ignore seasonal dynamism and instead employ a static set of spatial covariates and assume their focal species to exhibit a static set of preferences. Ignoring seasonality may, however, mask important ecological features and processes, thus resulting in poor agreement between predicted and observed movements and therefore a misrepresentation of connectivity.

We present a simple framework highlighting that seasonality may enter a connectivity analysis at three distinct stages, namely when (1) extracting spatial covariates for model fitting, (2) when fitting the selection model, and (3) when making predictions from the fitted model. In combination, this provides six possible configurations that differ in terms of the seasonal dynamism they encapsulate.

Capitalizing on natural seasonal fluctuations of the Okavango Delta in northern Botswana and on GPS data collected on dispersing African wild dogs (*Lycaon pictus*) across different seasons, we investigate the degree to which a better representation of seasonal dynamism improves our ability to predict dispersal and connectivity. For this, we fit integrated step-selection functions and predict connectivity using an individual-based dispersal simulation while explicitly considering seasonal dynamism in both environmental covariates and the species' preferences. Using a rigorous cross-validation procedure, we compare predictive model performances under each of the six proposed configurations. While we expected that an increasing degree of seasonal dynamism would lead to improved predictions, we were particularly interested in identifying at which stage the inclusion of seasonality would provide the biggest benefits.

We show that, for our study system, improvements in predictive performances achieved by incorporating seasonal dynamism were moderate. In fact, accounting for seasonality only improved predictions when an overly simplistic model formula assumed. Upon using a more complex model formula, the benefits of accounting for seasonality vanished, resulting in imperceptible performance differences. Despite this, patterns of connectivity as obtained from dispersal simulations revealed marked differences between the most static and most dynamic configurations. Most notably, connectivity was more homogeneously distributed throughout the study area when seasonality was taken into account, suggesting the existence of seasonal stepping stones that facilitate dispersal into otherwise inaccessible areas.

Besides a better understanding of the importance of dynamic connectivity, our results also provide insights into the conservation needs of the endangered African wild dog.

4.1 Introduction

Landscape connectivity is defined as the degree to which the landscape facilitates or impedes movement among habitat patches (Taylor et al., 1993) and is a central prerequisite for maintaining biodiversity (Fahrig, 2003). Improved connectivity facilitates dispersal (Doerr et al., 2011; Baguette et al., 2013), which in turn promotes genetic diversity (Perrin & Mazalov, 2000; Frankham et al., 2002) and the colonization of vacant habitats (Hanski, 1999b; MacArthur & Wilson, 2001). Due to its beneficial impacts on metapopulation dynamics, restoring connectivity is among the most frequently recommended strategies to conserve biodiversity and to promote resilience against climate change (Heller & Zavaleta, 2009; Rudnick et al., 2012). Quantifying connectivity and identifying critical dispersal corridors have therefore become crucial tasks in conservation science (Heller & Zavaleta, 2009; Rudnick et al., 2012; Keeley et al., 2019; Hofmann et al., 2021). One aspect that has received limited attention in the study of connectivity is the role of seasonality. Yet, seasonal changes in the environment and an animal's willingness to traverse a particular habitat type can profoundly impact landscape connectivity (Zeller, Lewison, et al., 2020).

Seasonality can impact functional connectivity through spatio-temporal variation in the landscape itself, or through temporal variation in species' preferences towards prevailing conditions (Mui et al., 2017; Simpkins & Perry, 2017; Zeller, Lewison, et al., 2020). In ecosystems that experience alternations between wet and dry seasons, for example, the onset of the rainy season initiates distinct "green-up" waves, which affect the availability of food resources for herbivores and, subsequently, shape their movements (Merkle et al., 2016). In its most remarkable form, the variation in environmental conditions drives herbivore migrations across massive spatial scales, resulting in short-lived movement corridors between otherwise disconnected habitats (Serneels & Lambin, 2001; Naidoo et al., 2016). Alternatively, seasonality can affect functional connectivity via temporal changes in a species' habitat preferences. Amphibians, for instance, require both aquatic and terrestrial habitats, but their preference for one habitat over the other heavily depends on the season (Baldwin et al., 2006). Although such seasonal intricacies are likely to play a fundamental role in many ecosystems, they only rarely enter connectivity studies in an explicit manner. In fact, most connectivity studies represent their study system by a static set of environmental layers and assume that their focal species to exhibit a fixed set of preferences (e.g., Elliot et al., 2014; Abrahms et al., 2017; Brennan et al., 2020). However, this may result in biased connectivity estimates and a misallocation of scarce conservation funds (Osipova et al., 2019; Zeller, Wattles, et al., 2020). Therefore, a more dynamic approach to connectivity that acknowledges and renders seasonal variation has been recommended (Zeller, Lewison, et al., 2020).

Functional connectivity can be estimated using a variety of modeling techniques (Diniz et al., 2019), which all comprise four main steps. First, presence data of the focal species, preferably collected dur-

ing dispersal (Elliot et al., 2014; Vasudev et al., 2015; Benz et al., 2016, but see Fattebert et al., 2015), and a set of spatial covariate layers that are believed or known to be critical determinants of connectivity are compiled. Second, these data are combined and fed into a selection model that enables estimating the focal species' preferences towards environmental features. Popular frameworks for estimating preferences are case-control designs, where covariate values extracted at observed locations are contrasted with those extracted at available locations (Beyer et al., 2010; Fieberg et al., 2010). This can be achieved using point-selection functions (Boyce et al., 2002; Manly et al., 2007), path-selection functions (Cushman & Lewis, 2010), and step-selection functions (Fortin et al., 2005; Thurfjell et al., 2014). A particularly powerful approach is that of *integrated step-selection functions* (iSSFs), which provides an effective means to jointly model an animal's movement kernel (i.e., movement capacity or movement preferences) and habitat-selection (Avgar et al., 2016; Fieberg et al., 2021). Third, inferred preferences are used to predict a permeability surface, which is a spatial layer that indicates the expected ease or difficulty at which the focal species can traverse a certain area given the area's environmental characteristics (Zeller et al., 2012). Finally, in a fourth step, the permeability surface serves as an input to a connectivity model that reveals crucial movement corridors. At present, the most popular connectivity models are least-cost path analysis (Adriaensen et al., 2003) and circuit theory (McRae et al., 2008), although individual-based movement models (IBMMs) have recently gained some momentum too (Kanagaraj et al., 2013; Allen et al., 2016; Hauenstein et al., 2019; Zeller, Wattles, et al., 2020; Unnithan Kumar, Kaszta, et al., 2022; Unnithan Kumar, Turnbull, et al., 2022; Hofmann, Cozzi, McNutt, et al., 2023). A major benefit of using IBMMs is that they allow estimating connectivity directly via simulated dispersal trajectories, thus bypassing the generation of a permeability surface (Unnithan Kumar, Kaszta, et al., 2022; Hofmann, Cozzi, McNutt, et al., 2023).

Seasonality can enter the connectivity modeling workflow described above at three distinct stages (Figure 4.1.1). At the first stage, one can either extract covariate values on environmental features, such as water and vegetation, from static layers (i.e., a single snapshot per covariate) or from stacks of layers (i.e., a sequence of snapshots per covariate) that capture seasonal variation across the landscape (Figure 4.1.1, Stage 1). The former approach has historically been the norm (e.g., Elliot et al., 2014; Brennan et al., 2020), yet advances in remote sensing technologies and a facilitated access to petabytes of landscape data have opened up new avenues for obtaining spatial layers at unprecedented spatio-temporal resolutions (Toth & Józków, 2016; Rumiano et al., 2020), such that the representation of study systems via dynamic covariate layers has become more frequent (e.g., Osipova et al., 2019; Kaszta et al., 2021). At the second stage, one can assume their focal species to exhibit a fixed set of preferences across seasons by pooling all presence data, or can try to account for seasonal changes in preferences by splitting the data accordingly (Figure 4.1.1, Stage 2; e.g., Fortin et al., 2005; Manly et al., 2007; Cushman and Lewis,

2010; Zeller, Wattles, et al., 2020). Chetkiewicz and Boyce (2009), for instance, partitioned their data by season to derive seasonal habitat preferences for pumas (*Puma concolor*) and grizzlies (*Ursus arctos*). At a third stage, one can estimate connectivity for either “average” environmental conditions, or utilize seasonally updated layers to estimate connectivity for distinct seasons (Figure 4.1.1, Stage 3). For connectivity models that rely on permeability surfaces, the latter case implies repeatedly applying the connectivity model using seasonally updated permeability surfaces (e.g. Osipova et al., 2019; Zeller, Wattles, et al., 2020; Ciudad et al., 2021; Kaszta et al., 2021). This is demonstrated *ad extreamum* by Kaszta et al. (2021), who prepared monthly updated permeability surfaces and repeatedly employed circuit theory to estimate dynamic connectivity for African elephants (*Loxodonta africana*). IBMMs, by contrast, allow for a more elegant solution, as seasonality can be modeled as the simulated dispersers move. Such an approach has, however, not yet been followed. Irrespective of the method used, including seasonality into connectivity analyses is analytically and computationally demanding (Bishop-Taylor et al., 2018), raising the question to what degree it should be considered.

To study the importance of seasonal dynamism for dispersal and connectivity, we use an African wild dog population (*Lycaon pictus*) inhabiting the seasonally highly variable Okavango Delta ecosystem in northern Botswana as a study system (McNutt, 1996; Wolski et al., 2017). While once present across the entire Sub-Saharan continent, the African wild dog has disappeared from a majority of its historic range due to human persecution, deadly diseases, and habitat destruction (Woodroffe et al., 2020). With about 6,000 adult individuals remaining in the wild, the species is considered as endangered on the IUCN red list. Wild dogs are pack-living carnivores, primarily active during the cooler morning and evening hours (Rasmussen & Macdonald, 2012) or during moonlit nights (Cozzi et al., 2012). Higher ambient temperature is associated with shorter activity periods, as the species usually rests during times of elevated heat (Rabaiotti & Woodroffe, 2019). Upon reaching sexual maturity, individuals born into a pack disperse in single-sex coalitions to find suitable mates and a territory to settle (McNutt, 1996). In Botswana, the timing of dispersal is seasonal, with female dispersal peaking prior to the mating season in March, and male dispersal peaking at the onset of the rainy season in December (Behr et al., 2020). Euclidean distances moved by dispersers range from 5 km to 500 km, with some coalitions covering several hundred kilometers within only a few days (Davies-Mostert et al., 2012; Masenga et al., 2016; Cozzi et al., 2020; Sandoval-Seres et al., 2022). Studies of habitat-selection during dispersal show that wild dogs avoid water, prefer moving along it, prefer moving across open grassland or shrubs, yet avoid areas dominated by humans and densely covered by forests (O’Neill et al., 2020; Hofmann et al., 2021). Given the species’ considerable mobility and the study area’s significant seasonal variability, we deemed the study-system well-suited to examine the importance of seasonal dynamism on dispersal and connectivity.

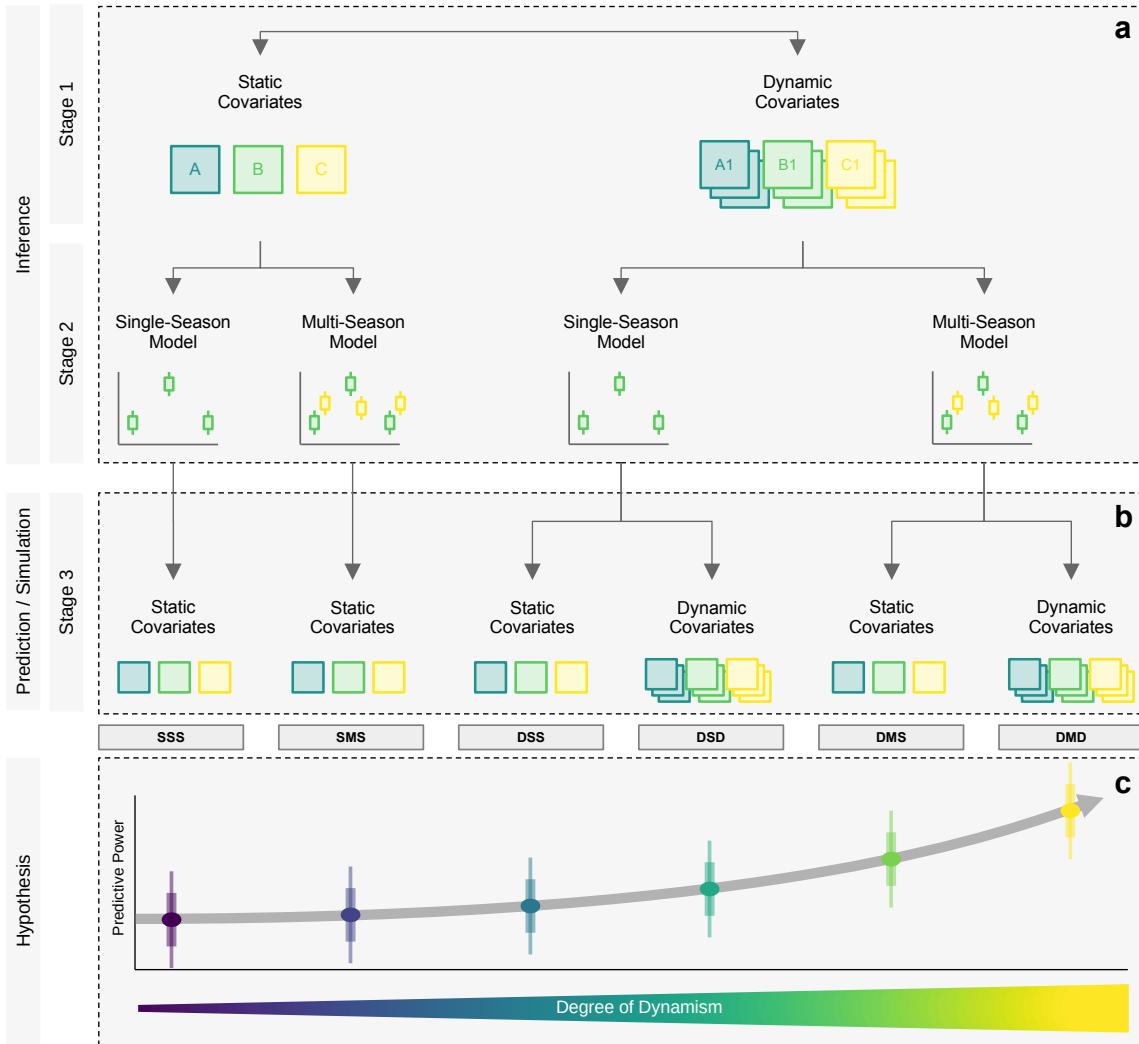


Figure 4.1.1: Overview of the different stages at which seasonality can be rendered in studies of dispersal and landscape connectivity. (a) During model fitting, one needs to decide whether to represent the environment by a static set of covariate layers, thus ignoring seasonality, or to obtain a dynamic set covariate layers that allow showing how the landscape changes over time. One also needs to decide whether to parameterize a single-season model, assuming fixed preferences across the year, or to engage in a multi-season model that accounts for seasonal differences. (b) When utilizing the fitted model to predict connectivity, one can either assume a static set of environmental covariates or again attempt a seasonal take that renders how connectivity differs depending on the season. (c) Depending on these decisions, six different combinations that differ in terms of the degree of dynamism they encapsulate emerge. Our hypothesis was that increasing the degree of dynamism when predicting dispersal and connectivity would lead to improved predictions. Notably, we were particularly interested in determining at which stage the inclusion of seasonally provided the biggest benefits.

Our goal with this article is to (1) create a framework highlighting the possible avenues through which seasonality can be incorporated into connectivity analyses, (2) establish whether incorporating seasonality benefits the predictive performance of dispersal models, and (3) pinpoint at which stages the inclusion of seasonality provides the largest benefit. For this, we compare the predictive performances of six configurations that differ in terms of the dynamism they represent (Figure 4.1.1b). Specifically, we investigate if and to what degree seasonality at different stages of the connectivity modeling workflow contributes to improved predictions. We compile an extensive collection of remote sensed spatial layers that accurately render seasonality across the Okavango Delta ecosystem. We combine them with multi-year dispersal data from 30 dispersing wild dog coalitions in northern Botswana and apply k-fold cross-validation for case-control studies to compare the predictive efficacy under each configuration (Figure 4.1.1b). Finally, we employ IBMMs to simulate dispersal and estimate connectivity resulting from varying degrees of dynamism. To distinguish between different configurations, we use codes that highlight the level of dynamism represented by each configuration (e.g., SSS = Static-SingleSeason-Static and DMD = Dynamic-MultiSeason-Dynamic). We hypothesized that habitat-selection and movement behavior of dispersing wild dogs would differ significantly between seasons and that increasing the degree of dynamism would result in better agreement between observed and predicted dispersal patterns (Figure 4.1.1c).

4.2 Methods

We used the R programming language (R Core Team, 2023) for all data preparation and analyses. We performed spatial data manipulation using the `terra` (Hijmans et al., 2024) and `spatstat` (Baddeley et al., 2015) packages. We generated figures using the `ggplot2` (Wickham et al., 2024) and `ggpubr` (Kassambara, 2024) packages. To ensure reproducibility of all our analyses, we provide access to our R-scripts through an online repository upon publication of this article.

4.2.1 Study Area

The study area comprised the Okavango Delta ecosystem in northern Botswana (centered at 24°30'E 20°42'S at an elevation of approx. 950 m) and extended to parts of Namibia and Zimbabwe, encompassing an extent of 160,000 km² (Figure 4.2.1). The Okavango Delta is a flood-pulse driven mosaic of patchy woodlands, permanent swamps, and seasonally flooded grasslands that lie within the otherwise dry and sandy Kalahari Basin (Wilson & Dincer, 1976; Ramberg et al., 2006; Mendelsohn et al., 2010). Precipitation across the study area varies considerably between seasons, ranging from 0 mm during the dry season (from 15 April to 15 October) to 140 mm during the wet season (from 15 October to 15 April), totaling to 600 mm across an average year (Figure 4.2.2a). Daily maximum above-ground temper-

ature fluctuates between 7°C during the dry winter months and 38°C during the wet summer months (Figure 4.2.2b). The vegetation in the study area is mainly composed of mopane forest (*Colophospermum mopane*), mixed woodland acacia-dominated (*Acacia spp.*), and grassland. Substantial vegetation green-up (e.g., plant and shoots growth, leaf production, and grass greening) after the dry season starts with a delay of some weeks after the onset of the first rains in the wet season. The normalized difference vegetation index (NDVI) therefore depicts a smoothed and lagged response to precipitation patterns across the study area (Figure 4.2.2c). The yearly flood-cycle of the Okavango Delta is predominantly driven by rainfalls in the Angolan highlands, where water is collected and channeled through the Cubango and Cuito rivers into the Okavango Delta (McCarthy et al., 2003; Gumbrecht et al., 2004; Mendelsohn et al., 2010). Because water only slowly descends from the catchment areas in Angola into the Delta's tributaries, the flood is out of sync with local rainfalls and reaches its maximum extent during August-September, i.e. during peak dry season (Wolski et al., 2017, Figure 4.2.2d). While the extent of large-bodied rivers and floodplains is determined by precipitation in Angola, the emergence of smaller, ephemeral water-bodies (i.e., pans) is dictated by local precipitation during the wet season. 62% of the landscape in the study area form part of a protected area, such that human impact remains low and largely limited to settlements along the western part of the Okavango Delta and the city of Maun at the Delta's southern tip (Figure 4.2.1). Landscapes outside protected areas in Zimbabwe, however, are more heavily influenced by humans, mainly through agricultural fields and human settlements.

4.2.2 GPS Data

Between 2015 and 2022, we collected GPS data on 30 dispersing wild dog coalitions (15 female coalitions, 15 male coalitions; Figure 4.2.1b). We programmed GPS satellite collars to record GPS locations at 01:00, 05:00, 09:00, 17:00, and 21:00. The eight-hour window between 09:00 and 17:00 can be considered comparable to a four-hour window, as wild dogs generally rest between 11:00 and 15:00, leaving approximately four hours of activity (Hayward & Slotow, 2009). The collected GPS data were regularly transmitted to a base-station via Iridium satellite, thereby allowing dispersing individuals to be monitored, even if they ventured across national borders. In total, we obtained 5,940 locations during dispersal, with an average of 198 ± 239 locations per coalition. Occasionally, the acquisition of a GPS location failed (success rate = $93 \pm 8\%$), resulting in slight deviations from the aspired four-hourly schedule. Further details on the GPS collar fitting procedure and how we distinguished between dispersal and resident movements can be found in Cozzi et al. (2020) and Hofmann et al. (2021).

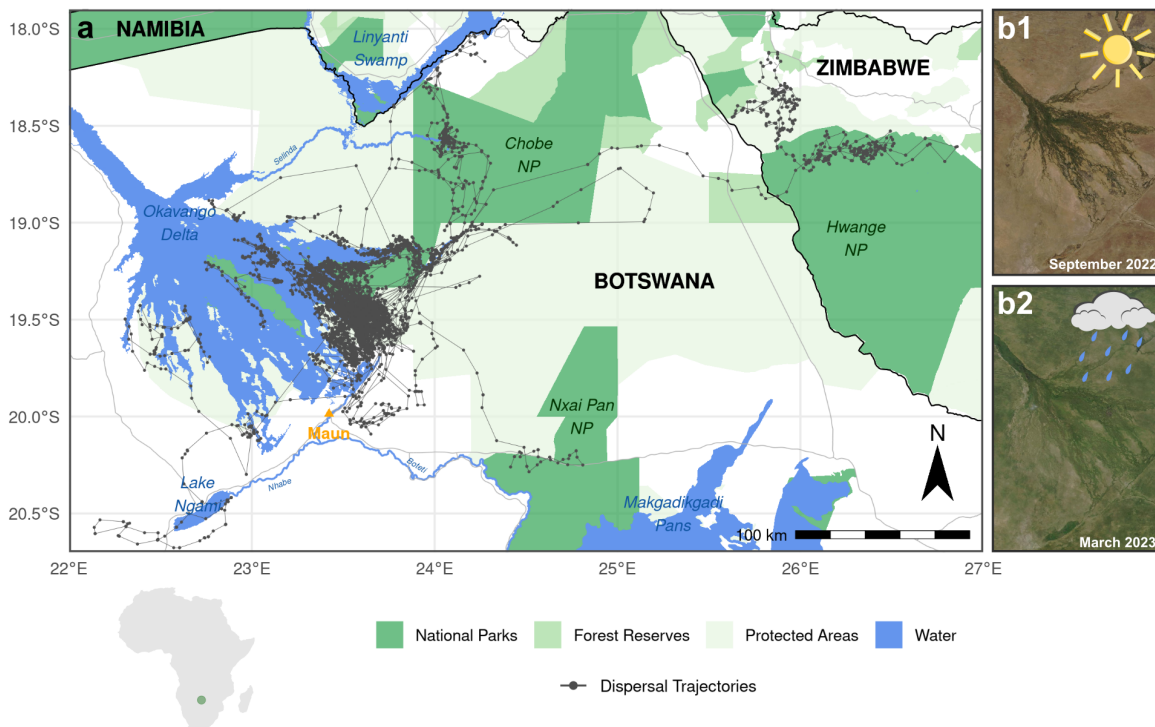


Figure 4.2.1: (a) Study area from which data on dispersing African wild dogs were collected. Dispersal trajectories are plotted in dark gray. The study area encompassed parts of the Okavango Delta in northern Botswana, a highly dynamic, flood-pulse-driven ecosystem. The entire study area undergoes substantial seasonal changes, as can be seen from two satellite images taken during peak dry season (b1) and peak rainy season (b2). Notably, the flood of the Okavango Delta reaches its maximum extent during peak dry season between August and September.

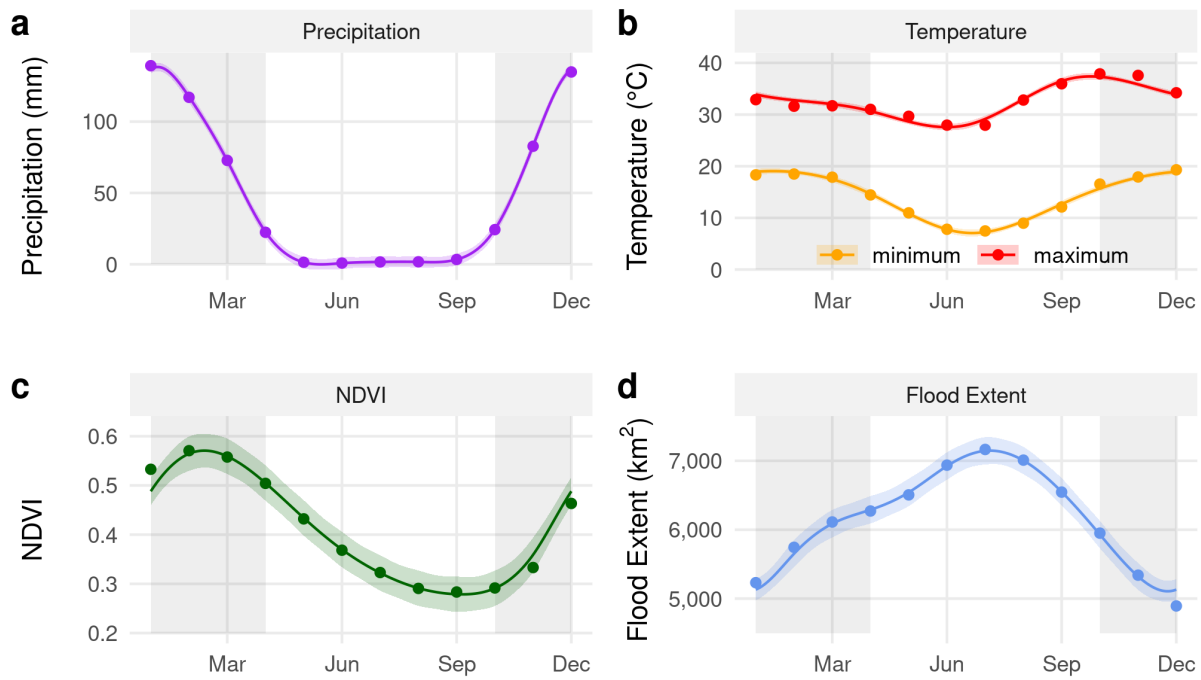


Figure 4.2.2: Illustration of how some of the covariates considered in this study vary across seasons. The wet season spans mid-October to mid-April (shaded in gray), the remainder is considered as dry season. Data for the graphs were obtained from (a) JAXA GSMP, (b) ERA5, (c) MODIS MOD13Q1, and (d) remote sensed MOD43A4 satellite images. Smoothing curves were fitted using GAMs as implemented in the `mgcv` R-package (Wood, 2011).

4.2.3 Covariates

We represented the physical landscape through which dispersers moved by a suite of spatial covariate layers known to influence wild dog movements during dispersal. We broadly categorized these spatial covariates into descriptors of (1) landscape characteristics, (2) climatic conditions, and (3) anthropogenic features (Table 4.2.1; see Hofmann et al., 2021; Hofmann, Cozzi, McNutt, et al., 2023). Besides spatial covariates, we also prepared a series of covariates relating to (4) light availability (Table 4.2.1; see Cozzi et al. 2012). To appropriately render seasonality in each of the spatial covariates (1-3), we downloaded them at the highest spatial and temporal resolutions available. That is, we obtained for each spatial covariate a stack of raster layers that spanned the entire range of dates for which we also collected GPS data on dispersing wild dogs. Depending on the covariate, this resulted in differing spatial and temporal resolutions (Table 4.2.1). Additionally, for each spatial covariate, we also generated a static layer, representing “average” conditions across the entire duration of the study. For this, we flattened each covariate stack into a single layer, thus removing seasonality from the spatial data entirely. For continuous covariates, we achieved this by averaging conditions across all collected layers, whereas for categorical (binary) layers we identified areas that were covered by the respective category in at least 50% of all layers. Using the same aggregation techniques, we computed covariate stacks representative of a typical year. That is, instead

of removing seasonality by flattening across the entire range of dates, we flattened stacks across years, thereby eliminating year-specific effects. These latter layers were later used in the dispersal simulation, where we needed spatial layers that depicted seasonal dynamism across a typical year. In summary, we prepared each covariate dynamically and statically for the entire range of dates considered, and dynamically for an average year.

Table 4.2.1: Covariates that were used in this study, including information on their temporal and spatial resolutions, as well as on the avenue through which the respective data were accessed or downloaded. Download methods printed in typewriter font indicate the use of an R-package that is available through CRAN or GitHub.

Variable	Temporal Resolution	Spatial Resolution	Source	Download Method
(1) Landscape Characteristics				
Trees	1 year	250 m	MODIS MOD44B	RGISTools
Shrubs / grassland	1 year	250 m	MODIS MOD44B	RGISTools
NDVI	16 days	250 m	MODIS MOD13Q1	rgee
Rivers	static	90 m	MERIT Hydro	website
Permanent water	static	30 m	Globeland30	website
Floodwater	8 days	500 m	MOD34A4	floodmapr
Distance to water	8 days	500 m	MOD43A4	floodmapr
Pans	5/10 days	10 m	Sentinel 2	sen2r
Distance to pans	5/10 days	10 m	Sentinel 2	sen2r
(2) Climate Descriptors				
Temperature	4 hours	10 km	ERA5	rgee
Precipitation	4 hours	10 km	JAXA GSMP	rgee
(3) Anthropogenic Features				
Human density	static	30 m	Facebook	website
Agriculture	static	30 m	Globeland30 / Cropland	website
Roads	static	vectorized	Open Street Map	website
(4) Light Availability				
Night	4 hours	-	-	moonlit
Moon illumination	4 hours	-	-	moonlit

Note: The covariates in gray were combined into proxies for water, human influence, and brightness, respectively. Detailed aggregation procedures are provided in Hofmann et al. (2021).

Landscape Characteristics

We used data from the MODIS Vegetation Continuous Fields dataset (MOD44B V061; DiMiceli et al., 2022) to represent different vegetation types across the study area. The MOD44B dataset comprises three continuous layers, depicting the percentage cover of woodland, shrubs/grassland, and bareland, respectively. The three layers added up to 100%, so we dropped bareland from further analysis, thus preventing perfect multi-collinearity. The MOD44B product is updated on day 65 of each year, so we used the R-package RGISTools (Pérez-Goya et al., 2020) to download yearly updated layers, each at a resolution of 250m x 250m. We also obtained information on the NDVI through the MODIS MOD13Q1 dataset (Didan, 2015), which also has a resolution of 250m x 250m. This product is updated every 16

days, and we accessed the respective data through Google Earth Engine (Gorelick et al., 2017) using the R-package `rgee` (Aybar et al., 2024). To depict large, permanent water-bodies, we employed the Globeland30 dataset, from which we only retained the land-cover class water, while setting all other categories to dryland. Similarly, we used the MERIT Hydro dataset to obtain information on permanent rivers (Yamazaki et al., 2019). To dynamically render large water-bodies, particularly the flood-waters of the Okavango Delta, we prepared weekly updated floodmaps using remote sensed MODIS MOD43A4 satellite images. The underlying floodmapping algorithm is described by detail by Wolski et al. (2017) and Hofmann et al. (2021) and is implemented in the `floodmapr` package (available on GitHub; <https://github.com/DavidDHofmann/floodmapr>). We combined the water (static), river (static), and flood layers (dynamic) into a single stack with a resolution of 500m x 500m (Table 4.2.1). Finally, we employed remote sensing to detect small, ephemeral water bodies (i.e., pans) using a custom random-forest classifier applied to Sentinel 2 satellite imagery (European Space Agency, 2018; details of the classifier in Section 4.A). Sentinel 2 has a resolution of 10m and is therefore particularly useful for obtaining information on small landscape features. Even though Sentinel 2 satellite imagery is updated every 5 days, cloud cover often prohibited the computation of a “pan-map”. Consequently, we settled for monthly updated composite images, which effectively alleviated problems due to cloud cover. In summary, we produced one stack of layers representing major water bodies, and another stack of layers representing ephemeral water bodies (pans). For both, we also computed corresponding distance-to stacks, indicating the distance to major and ephemeral water bodies, respectively.

Climate Descriptors

We obtained hourly updated spatial layers on 2m above-ground temperature from the ERA5-Land dataset (Muñoz-Sabater et al., 2021) and hourly updated precipitation estimates from the Global Satellite Mapping of Precipitation dataset (Kubota et al., 2020). Both datasets were accessed and downloaded through Google Earth Engine (Gorelick et al., 2017) using the `rgee` package (Aybar et al., 2024) and had a resolution of 10km x 10km. To match one-hourly temperature and precipitation estimates with the four-hourly GPS data on dispersing wild dogs, we computed average precipitation and temperature values over four hourly periods that matched the GPS collection schedule.

Anthropogenic Features

We combined information on human density, agricultural activities, and roads into a single proxy, which we generically termed human influence. We sourced information on human density from Facebook’s high resolution human density dataset (Tiecke et al., 2017), which we downloaded from the humdata website (www.data.humdata.org). We obtained information on the presence of agricultural fields from the

Globeland30 (Chen et al., 2015) and Cropland (Xiong et al., 2017) datasets. We downloaded shapefiles comprising main tar roads from OpenStreetMaps (OpenStreetMap contributors, 2017). Ultimately, we merged all anthropogenic features into a single layer that had a resolution of 250m x 250m (details are provided by Hofmann et al., 2021).

Light Availability

We computed light availability using the `suncalc` and `moonlit` R-packages (Thieurmel & Elmarhraoui, 2022; Śmielak, 2023) for the central coordinates of our study area at a 5-minute temporal resolution. The set of light statistics comprised a binary variable separating day and night (i.e., sun < -18 °below the horizon) and a continuous estimate of moonlight illumination, relative to the maximum moon illumination. Based on those covariates, we generated a binary covariate separating bright from dark conditions. Bright conditions encompassed all daytime hours and those nighttime periods during which the moon was present in the sky and illuminated by approximately one-fourth; conversely, dark conditions included nighttime periods during which the moon was absent from the sky or present and only minimally illuminated (further details in Appendices A2 and A3).

4.2.4 Step-Selection Models

We modeled dispersers' movement kernel and habitat selection using integrated step-selection functions (iSSFs, Fortin et al., 2005; Avgar et al., 2016), following the procedure described by Muff et al. (2020). For this, we identified bursts of subsequent GPS locations where the duration between two GPS locations did not exceed 4 hours (± 15 minutes) or 8 hours (± 30 minutes, for data recorded between 09:00 and 17:00). Within each burst, we converted locations into steps, where a step represented the straight line segment between two consecutive locations (Turchin, 1998). For each step, we computed the associated step length (sl, in meters) and relative turning angle (ta, in radians). After this pre-processing, a total of 26 dispersing coalitions (12 female coalitions, 14 male coalitions) remained for further analyses. 4 coalitions dropped due to temporally irregular data. The final dataset comprised 5,310 steps (204 ± 225 per coalition), which we further categorized into data collected during the wet season (15 October to 15 April) and data collected during the dry season (15 April to 15 October), yielding 3,124 steps (59%) during the dry season and 2,186 steps (41%) during the wet season.

We paired each observed step with a set of 100 random steps, generated by sampling turning angles from a uniform distribution $U(-\pi, +\pi)$ and step lengths from a gamma distribution fitted to observed steps (scale $\theta = 6341.96$ and shape $k = 0.39$). Together, an observed step and its associated random steps formed a stratum that received a unique identifier. Along each step, we extracted covariate values from the underlying spatial layers, and we assigned the appropriate light conditions (Table 4.2.1). We

opted for covariate extraction *along steps* rather than *at their endpoints*, as we believed that environmental conditions along steps were relevant in determining wild dog movement. For continuous covariates, we computed average values along each step, for categorical covariates the percentage cover of each category along the step. To model a decreasing marginal impact of “distance-to” variables, we included their square-root as predictors in the final models. To facilitate model convergence, we normalized extracted values to a range between zero and one.

To estimate movement and habitat parameters of interest, we applied the maximum likelihood procedure proposed by Muff et al. (2020), using the `glmmTMB` package (Brooks et al., 2017). To examine whether the effect of accounting for seasonality was modulated by the model structure, we employed two separate model formulas that were both generated based on knowledge about wild dog dispersal movements previous studies (Hofmann et al., 2021; Hofmann, Cozzi, McNutt, et al., 2023). In the *simple formula*, we merely included covariates relating to landscape characteristics and anthropogenic features, alongside the movement descriptors (`sl`, `log(sl)`, and `cos(ta)`) that are mandatory to fit an iSSF (Avgar et al., 2017; Fieberg et al., 2021). This formula is most akin to the type of formulas that are usually used with permeability-based approaches, which lack a mechanistic understanding of movement. In the *complex formula*, by contrast, we included several additional interactions between step-descriptors, landscape characteristics, climate descriptors and light availability, rendering that wild dog movement during dispersal may be affected by such interactions. In both formulas, we also included a stratum-specific intercept with a large fixed variance (10^6 , Muff et al., 2020), and used dispersing coalition ID to model random slopes for all main effects. To ensure comparability among each of the six configurations presented in our framework (Figure 4.1.1), we employed the same model formulas across all of them. However, we fitted models that differed in their degree of dynamism, as highlighted in Figure 4.1.1a. Models one and two were fit using static covariates, with model one being a single-season model and model two being a multi-season model (wet vs. dry). Models three and four, by contrast, were fit using dynamic covariates, with model three being a single-season model, and model four being a multi-season model (wet vs. dry). Each model was once fit using the simple formula, once using the complex formula. To quantify how many random steps were necessary before model estimates stabilized (*sensu* Fieberg et al., 2021), we fitted each model with 5, 10, 25, 50, 75, and 100 random steps.

4.2.5 Validation

We compared the predictive efficacy of each of the six configurations presented in Figure 4.1.1b using k-fold cross-validation for case-control studies (Fortin et al., 2009). For this, we split the data into training and validation sets using an 80:20 ratio and fit the four iSSF models described above. We then used the obtained β -estimates to predict the probability of each random and observed step in the validation set for

being chosen. Depending on the configuration, we predicted step-probabilities using static or dynamic covariates. Within each stratum, we assigned ranks 1-101 to each step based on predicted probabilities and recorded the number of times the observed step was assigned each rank. Finally, we computed Spearman's rank correlation between ranks and associated frequencies $r_{s,realized}$. The better a model's predictive ability, the more negative $r_{s,realized}$ should be (i.e., the less often the observed step should be assigned a low rank). For reference, we also computed Spearman's rank correlation for randomized preferences ($r_{s,random}$), which we achieved by removing the observed step from each stratum and identifying the rank of a randomly chosen step. We replicated this validation procedure 100 times and employed ANOVA to compare the predictive efficacy of different configurations.

4.2.6 Simulations

To assess differences in predicted connectivity upon increasing seasonal dynamism, we ran dispersal simulations under the two most distinct configurations, i.e. the fully static (SSS, Figure 4.1.1) and fully dynamic (DMD, Figure 4.1.1) configurations. As source areas to initiate dispersers, we defined three distinct regions known to host viable wild dog populations (Figure 4.2.1). The definition of these areas was somewhat arbitrary, albeit we deliberately selected areas in the west and east of the Okavango Delta to examine potential influences of flooding on connectivity (sensu Hofmann et al., 2024). We also selected a more independent location (Nxai Pan; Figure 4.2.1) that was not influenced directly by the Okavango Delta's flood extent. To initiate simulated dispersal trajectories, we randomly placed 1,000 start points within each of these source area, with start times that were equally distributed across the year. To simulate dispersal and obtain connectivity maps under both configurations, we applied the simulation algorithm for iSSFs described by Signer et al. (2017) and employed by Hofmann, Cozzi, McNutt, et al. (2023). A similar algorithm has recently been added to the `amt` R-package (Signer et al., 2024). We applied the simulation algorithm as follows. Originating from the start point, we generated a set of 25 random steps by sampling step lengths from the fitted gamma distribution and turning angles from a uniform distribution. Along each random step, we extracted spatial covariates, computed relevant movement metrics (sl , $\log(sl)$, and $\cos(ta)$), and assigned light conditions. We then employed the fitted iSSF model to predict the probability of each step for being chosen, thus generating a "redistribution kernel" around the current location of the simulated individual (Signer et al., 2017; Signer et al., 2024). Based on this kernel, we sampled one of the steps and updated the simulated individual's position and time. We repeated the procedure until a total of 2,000 steps were realized (~ 400 dispersal days).

Depending on the configuration, we employed different spatial covariates and preferences during the simulation. For the SSS configuration, we omitted any seasonality, using the static set of covariates and assuming dispersers to exhibit the same preferences (i.e., β -estimates) across seasons. For the DMD

configuration, on the other hand, we updated covariates and preferences dynamically as the simulated individuals moved. More specifically, we generated a new covariate stack after every simulated step, comprising spatial layers that best represented environmental conditions at that particular point in time (Figure 4.2.3). For this purpose, we employed the set of covariates representing an average year. Similarly, we predicted the redistribution kernel using β -estimates from the appropriate season. Finally, we obtained heatmaps (connectivity maps, utilization distributions) based on simulated dispersal trajectories under both configurations.

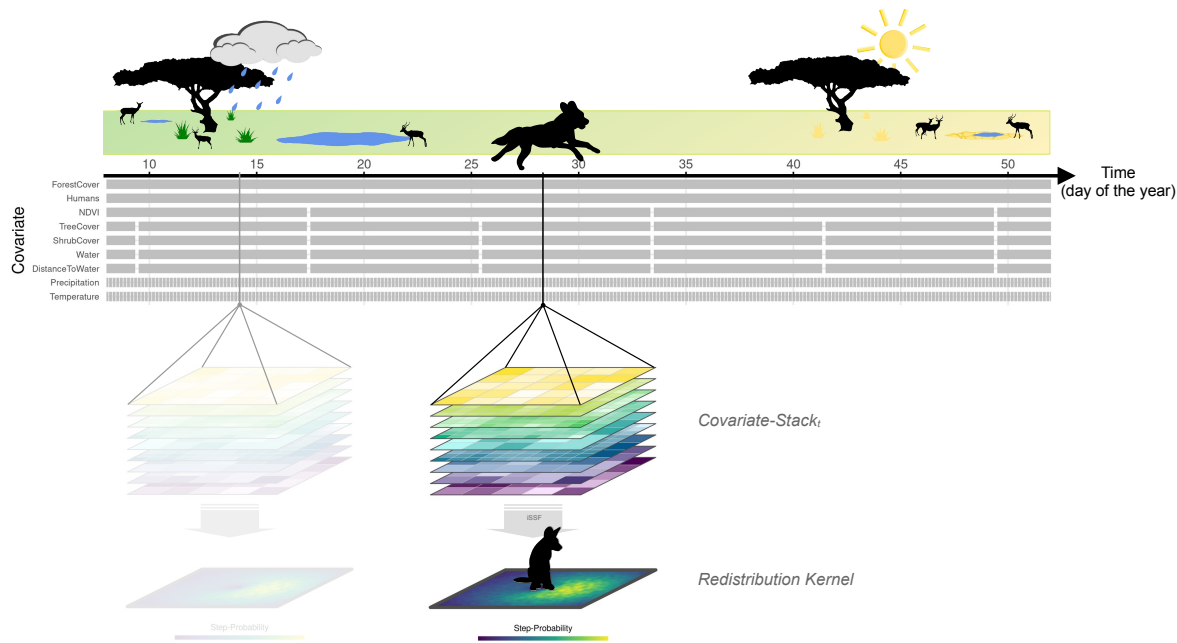


Figure 4.2.3: Schematic illustration of our dispersal simulation with dynamic covariates. As the simulation proceeded, the underlying spatial covariates (symbolized by the stack of layers) were updated. Depending on the covariate, the update frequency varied from a few hours (e.g., temperature) to multiple months (e.g., shrub cover). Each gray block represents a single layer and the duration for which it was “active”. Originating from the current position of the simulated animal, a new redistribution kernel was derived. We generated redistribution kernels by proposing a set of 25 random steps and applying the parametrized step-selection model to predict the probability of each step for being chosen. Based on this kernel, one location was randomly sampled and the animal’s position and time updated. This procedure was then repeated until 2,000 steps (~ 400 dispersal days) were simulated.

4.3 Results

Due to convergence issues, we removed the covariates NDVI, precipitation, and distance to pans from all analyses. Some minor convergence issues remained and our validation procedure failed in 59 out of 1,800 validation attempts. Since failures occurred across different configurations and were not clustered around one specific configuration, we deemed their exclusion of no concern.

4.3.1 Step-Selection Models

Patterns of habitat selection and movement behavior were qualitatively similar, irrespective of whether models were fit using static or dynamic covariates (Figure 4.3.1, Table 4.D.1, Table 4.D.2, Table 4.D.3, Table 4.D.4) and irrespective of the number of considered random steps (Figure 4.E.1). The most notable quantitative difference when using static vs. dynamic covariates was that models fitted using dynamic covariates resulted in narrower confidence intervals (Figure 4.3.1). Furthermore, effect sizes (i.e., β -estimates) of models fit using static covariates were more pronounced than effect sizes from models that were fit using dynamic covariates (Figure 4.3.1). Differences were most marked for $\beta_{DistanceToWater^{0.5}}$, which was estimated ≈ -0.8 using static covariates, but ≈ -0.3 when using dynamic covariates.

Differences in β -estimates between seasons were moderate and most pronounced when models were fit using static covariates. For instance, when models were fit using static covariates, β_{Water} was ≈ -0.9 during the dry season but ≈ 0.2 during the wet season. When dynamic covariates were used, by contrast, β_{Water} was ≈ -0.6 and ≈ -0.3 , respectively. $\beta_{sl:Dark}$ was also markedly lower during the wet season (≈ -0.9), compared to the dry season (≈ -0.1) but this was independent of the type of covariates that were used. Plots that aid with the interpretation of the models are provided in Figure 4.F.1.

4.3.2 Validation

Spearman's rank correlation coefficients (r) obtained from the validation procedure revealed that predictions using the complex formula performed markedly better than those from the simple formula ($\bar{r}_{simple} = -0.5$, $\bar{r}_{full} = -0.9$, Figure 4.3.2). Irrespective of the employed model, Spearman's rank correlation differed significantly depending on the amount of dynamism considered (simple: $F(5, 593) = 26.45$, $p < 0.001$, full: $F(5, 594) = 7.14$, $p < 0.001$), albeit with moderate effect sizes. Using the simple formula, moving from a fully static (SSS) to a fully dynamic (DMD) configuration decreased Spearmans's rank correlation (i.e., increased the predictive performance) by 0.15 from -0.41 to -0.56. Using the complex formula, conversely, moving from a fully static (SSS) to a fully dynamic (DMD) configuration even entailed a minimal increase in r (i.e., a decrease in the predictive performance) from -0.89 to -0.88. This suggests that, our hypothesis that increased dynamism results in better predictive performance only holds when using the simple formula (Figure 4.3.2a), but not when employing the complex formula (Figure 4.3.2b).

4.3.3 Simulations

Simulations under the most static (SSS) and dynamic (DMD) configurations revealed different connectivity patterns (Figure 4.3.3). In the static configuration, simulated dispersal trajectories were more concentrated, suggesting frequent movement across a few key habitats. In the dynamic configuration, by

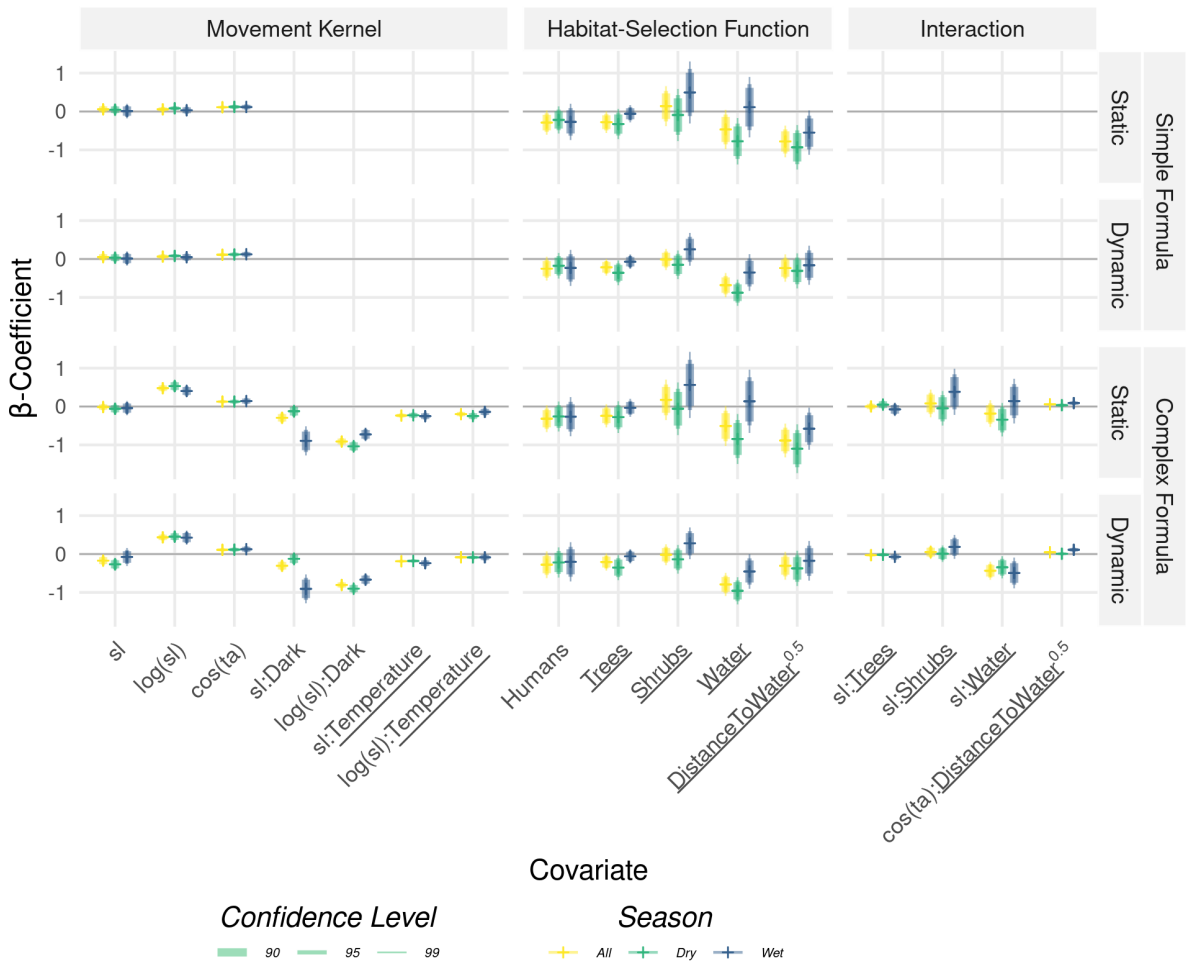


Figure 4.3.1: β -estimates from the integrated step-selection models, grouped by movement kernel, habitat-selection function, and their interaction. We either fit models using a *simple formula* (without interactions) or a *complex formula* that comprised several interaction terms that rendered how movement behavior depended on environmental conditions. Furthermore, we distinguished between models fit using *static* and *dynamic* covariates. However, only the underlined covariates differed between the static and dynamic configurations, as covariates were either represented as a single layer (static), or a stack of layers (dynamic). Furthermore, data were either pooled across seasons (yellow bars) or split into dry (green bars) and wet (blue bars) season. Results are shown for replicates that used 25 random steps, as all associated models converged. Note, however, that the number of random steps did not appear to influence model estimates (Figure 4.E.1).

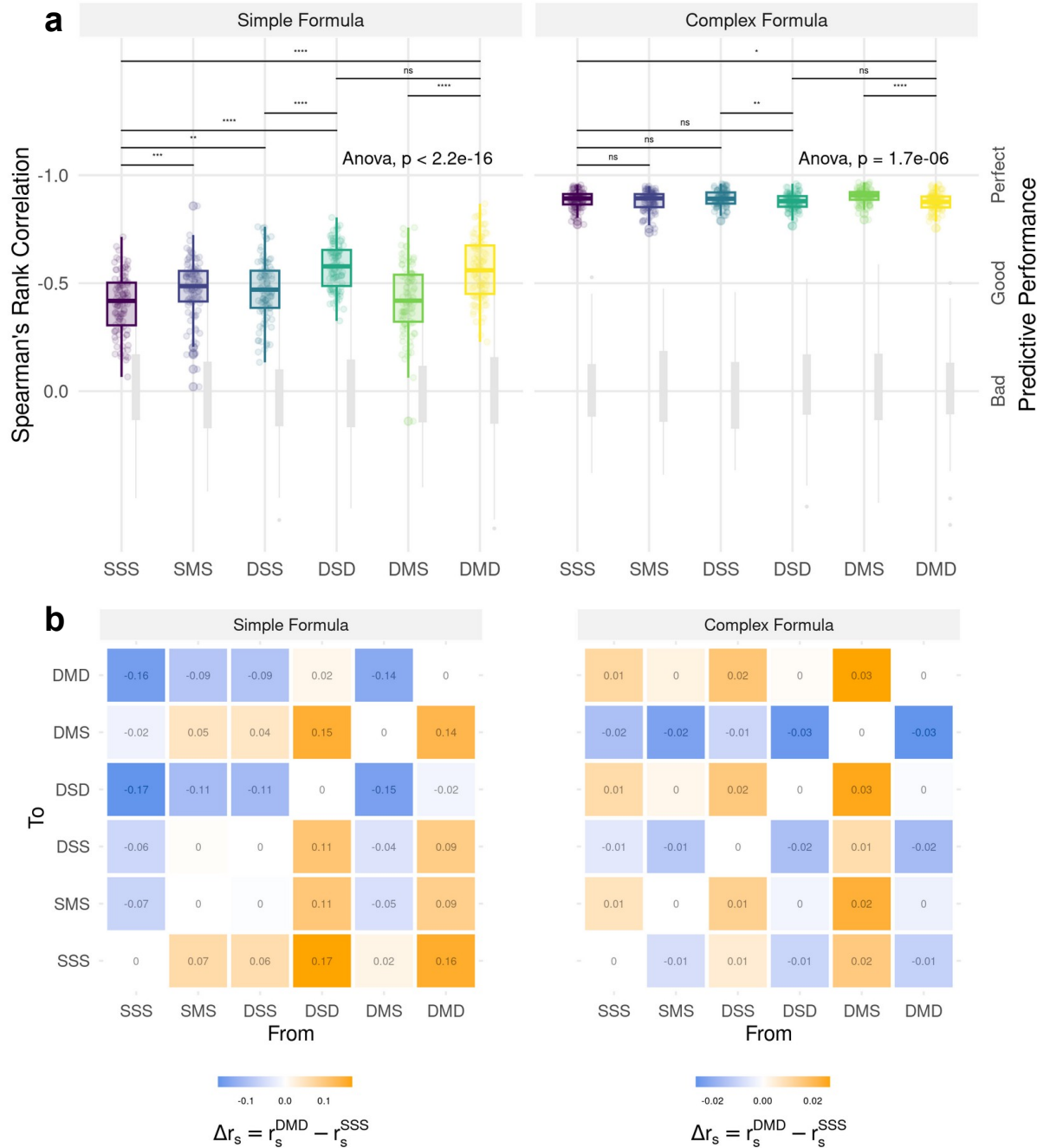


Figure 4.3.2: (a) Spearman's rank correlation across different configurations of dynamism that range from entirely static (SSS) to fully dynamic (DMD). The more negative Spearman's rank correlation, the better is the predictive performance under the respective configuration. Correlations were computed for 100 replicates. Note that the y-axis is inverted to match our expectation of increasing performance as dynamism increases. The boxplots in light gray represent Spearman's rank correlation coefficients under a null model and serve for comparison. (b) Difference in Spearman's rank correlation when moving from one configuration to another. Values < 0 (blue) indicate an increase in predictive performance, whereas values > 0 (orange) indicate a decrease in predictive performance.

contrast, simulated trajectories were more homogeneously distributed, suggesting that movement was less restricted. When qualitatively comparing the heatmaps generated under the simple and complex formulas, differences are imperceptible. Given the similarities in habitat selection emerging under the two models, this was to be expected.

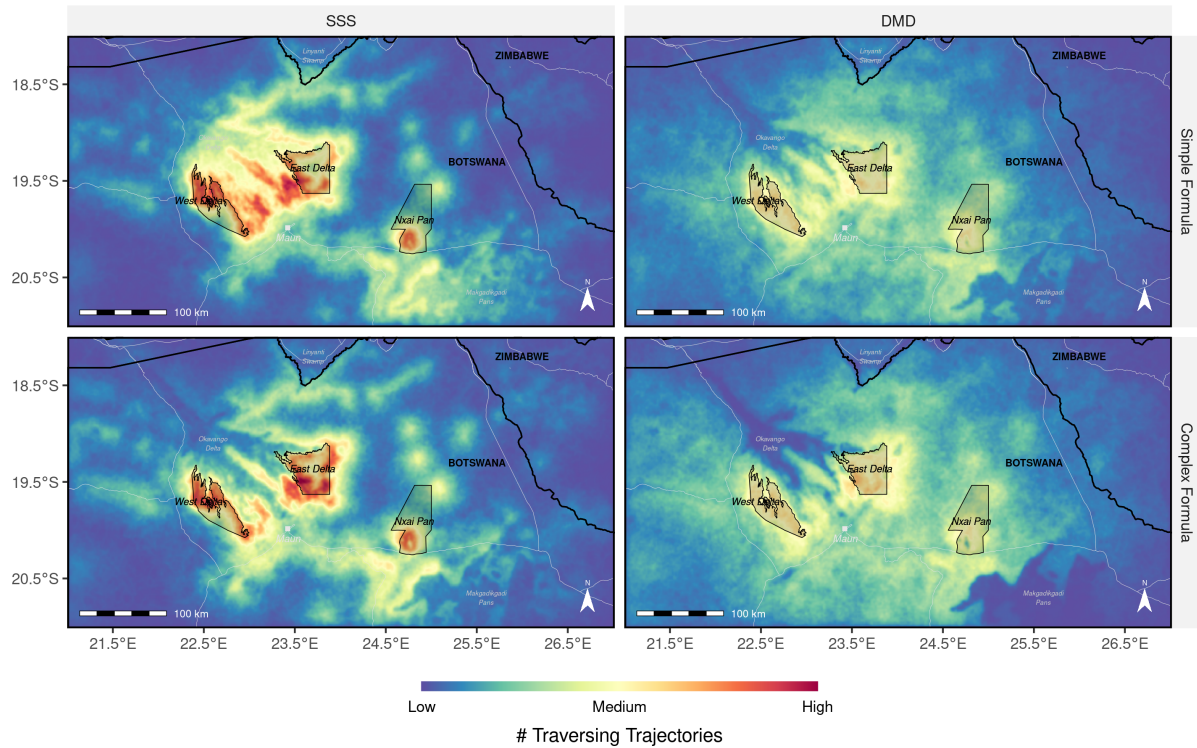


Figure 4.3.3: Heatmaps derived under the most static (SSS) and dynamic (DMD) configurations. Results are shown for simulations using the simple and complex model formulas.

4.4 Discussion

We introduced a framework to highlight that seasonality can enter a connectivity analysis at three distinct stages; (1) when extracting spatial covariates for fitting the selection model, (2) when fitting the selection model, and (3) when predicting from the fitted model. Through combination, this yields six configurations that differ in their degree of dynamism and, arguably, realism. We fit the models associated with each configuration using GPS data on dispersing wild dogs and employed a rigorous validation procedure to investigate potential gains in predictive performance that can be reaped by incorporating different levels of seasonal dynamism. Results from the fitted models showed that including seasonality only marginally affected the inferred patterns of habitat selection and movement behavior. Similarly, the validation procedure suggested only moderate improvements in predictive performance upon increasing the degree

of seasonal dynamism. Crucially, these benefits were limited to an overly simplistic model formula and vanished upon fitting a more complex one. We therefore could not pinpoint a specific stage at which including seasonality was particularly beneficial. Despite this, we found that dispersal simulations under the most static and most dynamic configurations resulted in differing connectivity patterns. Under the most static configuration, landscape connectivity was clumped around a few hot spots, whereas it was homogeneously distributed across the landscape under the most dynamic configuration. Finally, our work demonstrated that simulations from IBMMs effectively allow rendering seasonal changes in the landscape, achieving a degree of seasonal dynamism and realism that cannot be reached using permeability-based connectivity models.

Our validation procedure revealed only moderate improvements in our ability to predict dispersal movements when increasing the degree of seasonal dynamism. Given the system's extreme seasonal variability, this was somewhat surprising. We believe that the absence of a more pronounced improvement can be traced back to multiple factors. Firstly, we focused our analysis on dispersing individuals, which cover large distances in search of potential mates and a suitable territory (McNutt, 1996; Cozzi et al., 2020). In our case, the average 4-hourly step length was 2.5 km, suggesting that dispersers cross and sample numerous unfamiliar areas and potentially unsuitable habitats within short time. We thus hypothesize that the spatial scale at which seasonality affects environmental characteristics does not suffice to match the spatial scale at which our focal species perceives and moves across the landscape during dispersal. A further explanation could be that dispersing individuals prioritize finding unoccupied territories or areas with low competition, rather than focusing on specific habitat types (e.g., Creel and Creel, 1996; Creel, 2001). Dispersers' habitat selection may therefore be more strongly influenced by territorial considerations (*sensu* Cozzi et al., 2018) and only little affected by seasonally changing landscape characteristics. This would also explain the relatively weak selection or avoidance of environmental characteristics exhibited in Figure 4.3.1. Finally, the AWD is a generalist species that can occupy a broad variety of habitats (Woodroffe & Donnelly, 2011). A certain tolerance towards changing environmental conditions can therefore be expected and may explain why seasonal differences were faint. This holds particularly true for dispersers, which are usually more tolerant towards unfavorable habitat conditions as they spend little time within the same area (O'Neill et al., 2020).

In comparison to the improvements achieved by increasing dynamism, a more significant improvement in predictive ability was achieved by moving from the simple to the complex model formula. When employing the complex formula, we included several interactions that accounted for the African wild dog's biology, such as reduced movement during dark nights (Cozzi et al., 2013) or during times of high ambient temperature (Rabaiotti et al., 2021). We also allowed for potential changes in dispersers' movement behavior depending on habitat conditions, such as shorter steps in areas covered by water (Hofmann, Cozzi,

McNutt, et al., 2023). The ability of encapsulating such a detailed and mechanistic understanding of dispersal movements is unique to IBMMs and cannot be achieved using permeability-based connectivity models. Even though the additional interactions were not directly linked to connectivity, they accounted for a substantial amount of variation in observed dispersal movements and facilitated predictions from the fitted model. Notably, the inclusion of these interactions elevated the predictive ability of our dispersal model to such a high level that considering seasonal dynamism did not provide any further improvements, irrespective of the stage at which it was considered.

When comparing connectivity under the most static (SSS) and dynamic (DMD) configurations, we observed that connectivity was clumped along a few major dispersal hotspots under the static configuration, but homogeneously distributed across the entire landscape under the dynamic configuration. This corroborates previous research showing that static representations tend to result in an underestimation of connectivity because seasonal stepping stones or corridors are missed (Martensen et al., 2017). With the help of such seasonally-available dispersal habitats, areas that would otherwise be difficult to reach become accessible, even if only for a limited time. In our study, such stepping stones could arise in two ways. Firstly, the landscape changed seasonally, which caused spatial shifts in preferred and avoided habitats, leading to the emergence of alternative movement corridors. In addition, habitat or movement preferences of simulated individuals changed, which resulted in different habitat characteristics being traversed depending on the season. In combination, temporally varying landscape conditions and seasonally altered species preferences resulted in a more balanced mosaic of connectivity across the year. Importantly, the fact that connectivity was more evenly distributed across the year does not exclude the possibility that certain areas experienced lower connectivity seasonally. As already shown by Osipova et al. (2019), a static representation may result in both an over- and under-estimation of short-term connectivity, depending on the area and season. For conservation planning, this implies a need to protect landscapes at broader scales, as areas that provide little connectivity during some season may become critical during others. A dynamic take at connectivity therefore improves our understanding of ecological processes in dynamic landscapes and may help to identify otherwise overlooked dispersal hotspots.

Increasing seasonal dynamism to model dynamic connectivity comes at significant costs, both in terms of data requirements and computational challenges. To represent seasonal changes across the landscape, one needs to download and process frequently updated spatial layers for each seasonal covariate. This is time-consuming and implies a substantial increase in the data-volume that needs to be handled. Because seasonal products are comparably rare, modeling dynamic connectivity also entails a significant reduction in the number of potential covariates and may require custom remote sensing algorithms (e.g., Section 4.A). Seasonal and remote sensed layers are also more susceptible to noise and missing values, particularly during seasons when cloud cover is frequent. Extracting covariates from seasonal layers poses a further

challenge, as covariate data can no longer be extracted from single layers, but need to be extracted from exactly those layers that best represent environmental conditions at the time of the respective observed or random step. This applies to the extraction of data for model fitting, as well as when extracting data during the simulation. Finally, splitting species data by season to parametrize seasonal selection models can significantly reduce the amount of data remaining per season, potentially causing convergence issues. In our case, the moderate improvement in predictive ability did not warrant these additional efforts and complications. This conclusion is, however, likely highly specific to our study system. We therefore do not wish to discourage future studies from accounting for seasonality when assessing connectivity. Instead, we would like to view our study as an example that the benefits of increased realism do not necessarily justify the additional complexity they bring about and that the associated costs and benefits need to be carefully pondered (Puy & Saltelli, 2022).

Our validation procedure was focused on validation at the step level, but did not directly test how well predictions of functional connectivity agreed with true connectivity. This was owed to a conceptual limitation when trying to validate seasonal connectivity as predicted from an IBMM. In seasonal landscapes, connectivity not only varies spatially, but also temporally. A meaningful validation therefore requires that connectivity is predicted separately for each timestamp in the validation data. In our case, for instance, the fact that the landscape changed every four hours (i.e., with every step) entails that a new connectivity map would need to be developed around each validation step. This is equivalent to generating and validating the redistribution kernel, and therefore equivalent to validating predictions at the step level. For this reason, we deemed the application of k-fold cross-validation for case and control studies using Spearman's rank correlation as an appropriate validation technique. Note, however, that Spearman's rank correlation coefficient is heavily dependent on the number of steps per stratum and should not be used to compare predictive efficacy across studies (Figure 4.G.1). For static connectivity analyses, alternative validation techniques exist. McClure et al. (2016), for instance, proposed a suite of validation metrics (applied in Zeller et al., 2018 and Finerty et al., 2023) that largely work by comparing connectivity at random locations with connectivity at locations where the focal species was observed. Because these metrics fail to account for potential autocorrelation in the validation data (which is usually present in GPS data), Brennan et al. (2020) suggested validating connectivity by applying a path- or step-selection model to withheld data, using the connectivity map as the only spatial covariate. If the fitted model proves significant selection towards areas of high connectivity, predictions are indeed indicative of functional connectivity (*sensu* Brennan et al., 2020). Developing similar approaches for dynamic connectivity analyses remains a task for future studies.

When we fit models assuming static covariates, wild dogs displayed a preference for areas close to water, irrespective of the season. However, water itself appeared only to be avoided during the dry season.

This was likely caused by a misrepresentation of areas covered by water in the static configuration. Since rainwater collected in Angola only slowly descends through the Okavango Delta's tributaries (McCarthy et al., 1997), large portions of the Delta's floodplains remain dry during the wet season (McCarthy et al., 2003). On static covariates, which represent average conditions across both seasons, it may appear as if individuals moved through areas covered by water, albeit in reality they likely moved along them. Indeed, upon accounting for such seasonal changes by considering seasonally updated covariate layers, parameter estimates from the selection models assimilated and consistently suggested avoidance of water across both seasons. Accounting for seasonality can therefore result in vastly different biological insights. In this regard, our choice of splitting data into wet and dry season based on a fixed set of dates can be viewed as limitation, as it assumed an immediate switch from one season to another. In reality, season-transitions are not abrupt but rather gradual and their timing may vary from year to year. A more robust approach would therefore be to define the start and end of each season based on bio-climatic descriptors and to ignore data collected during transitional periods. This may imply a loss of data, but could help to detect seasonal selection patterns. In our case, retaining all data was necessary to ensure model convergence, but may have resulted in a cross-contamination between seasons and therefore reduced our ability to pick up seasonal differences estimated parameters. Indeed, other studies report that habitat selection of their focal species varied greatly between seasons (but see Squires et al., 2013). Benz et al. (2016), for instance, found that dispersing in elk (*Cervus elaphus*) exhibit vastly different habitat preferences during winter and summer. Similarly, Osipova et al. (2019) report that habitat selection of African elephants (*Loxodonta africana*) in South Africa differs between the wet and dry season. The importance of seasonality thus appears to be highly system dependent.

In conclusion, we explored the importance of incorporating different degrees of seasonal dynamism when studying dispersal and connectivity. Overall, our findings suggested only moderate improvements in predictive performance upon increasing the level of dynamism. Nevertheless, we found that connectivity patterns as inferred from simulated dispersal trajectories differed vastly, with connectivity being more evenly distributed when seasonality was accounted for. While increased realism via improved representation of seasonal dynamism may offer novel insights into ecological processes, its benefits must be carefully weighed against the added complexity introduced by seasonal data and seasonal preferences. Moving forward, our study serves as an example that while accounting for seasonality could be crucial for some study systems, it may not always justify the additional complexity, emphasizing the need for thoughtful consideration of costs and benefits in future research.

Appendices

4.A Pan Mapping

4.A.1 Satellite Product Overview

We dynamically mapped the spatial distribution of ephemeral water bodies that span only a few meters in diameter (Figure 4.A.1) using a custom remote sensing algorithm. These waterbodies are typically referred to as “pans” and mainly inundate during the rainy season, after which the cumulated water slowly evaporates. Previously, we developed an algorithm to detect large scale floodwaters across the extent of the Okavango Delta. This algorithm made use of MODIS MCD34A4 satellite imagery, which is a 8-day composite of daily updated MODIS satellite data. The benefit of MODIS’ high temporal resolution is that monthly composites are almost guaranteed to be cloud free, even during Botswana’s rainy season (mid October to mid May). However, due to its coarse spatial resolution of 250 meters, MODIS satellite data was unsuitable to detect finer-scaled waterbodies on satellite images. In an attempt to overcome this limitation, we evaluated alternative satellite products that provided better spatial resolution than MODIS, while retaining a sufficiently high temporal resolution to render seasonal patterns. Candidate products comprised Landsat 7, Landsat 8, and Sentinel 2 satellite imagery. Data associated with each of these satellites are freely accessible and provide spatial resolutions between 10 and 60 meters, depending on the respective bands. Furthermore, the satellites have revisit-times between 5 and 16 days, thus allowing to generate frequently updated composite images (Table 4.A.1).

Table 4.A.1: Overview of the spatial and temporal resolutions of the candidate satellite products.

Satellite	Availability	Spatial Resolution (m)*	Temporal Resolution (days)
Landsat 7	1999 – Present	15 – 60	16
Landsat 8	2013 – Present	15 – 100	16
Sentinel 2	2015 – Present	10 – 60	5 – 10†

* Spatial resolutions of the same product can differ depending on the band.

† Sentinel 2’s revisit duration decreased to 5 days after March 2017.

Our goal was to produce dynamically updated pan-maps that we could overlay with GPS data of dispersing African wild dogs. Since most GPS data were collected between 2015 and 2022, this implied that satellite data needed to be available for the same period. At first glance, all satellite products appeared to meet this criteria. However, Landsat 7’s scan-line detector had been failing since May 31, 2003, introducing data gaps between adjacent tiles, thus rendering the product virtually unusable for our purposes (but see Storey et al., 2005). Sentinel 2 and Landsat 8, by contrast, appeared as viable alternatives, as both of them spanned the desired period and did not exhibit any device failures.



Figure 4.A.1: A pan as it can be found in Botswana right after the rainy season. This particular pan is comparably small at around 10 meters in diameter. Some of these pans dry out quickly, whereas others provide a source of water for the entire dry-season. Here, two spotted hyenas (*Crocuta crocuta*) take a quick bath.

4.A.2 Evaluation of Landsat 8 and Sentinel 2

Training Polygons

With Landsat 8 and Sentinel 2 imagery remaining, we conducted a preliminary investigation to compare the two products and evaluate their suitability for our needs. Specifically, we investigated how well we could remote sense pans using either of the two products, utilizing supervised learning methods. For this, we prepared a set of training polygons, consisting of the land cover classes dryland, water, and wet-pans. Although our primary goal was to detect wet-pans, we included the two other classes to facilitate the categorization of reflectance values into distinct groups. Due to the large study area considered, *in situ* ground-truthing of the training polygons was impossible, and we instead opted for *on-screen selection* of training data. More specifically, we utilized Google Earth to digitize areas that were clearly identifiable as either dryland, water, or wet-pans. At the highest zoom level in Google Earth, these categories are visually easy to tell apart (Figure 4.A.2). To ensure a sharp distinction between wet-pans and dryland, we traced several dryland polygons in areas that were seasonally covered by water (Figure 4.A.2). Google Earth provides the date of any satellite map, and so we could assign a timestamp to each training-polygon. This was necessary to later match training polygons with Landsat or Sentinel data of the same date. Google Earth's ability to display imagery from different dates furthermore allowed us to generate a training dataset that comprised polygons that belonged to different classes depending on the season. For example, a dryland polygon obtained in the dry season could overlap with a wet-pan polygon obtained during the rainy season. Overall, we generated 268 polygons of varying size and shape (104 on dryland, 56 in water, and 108 in wet-pans) for 3 distinct dates (August 18, 2018, March 25, 2019, and July 24, 2021).

Satellite Data Download

We downloaded Landsat 8 imagery through Google Earth Engine using the `rgee` R-package (Aybar et al., 2024) and used the associated quality band to mask pixels classified as clouds or shadows. We also computed several normalized difference indices (NDs), as listed in Table 4.A.2. To download Sentinel 2 data, we used the `sen2r` R-package (Ranghetti et al., 2020) which provides a standardized interface to download and process Sentinel 2 imagery from the European Space Agency's data hub. Sentinel 2 data are available as either top-of-the-atmosphere (TOA, level 1C) or bottom-of-the-atmosphere (BOA, level 2A) reflectance values. In analyses where temporal trends are considered, the use of BOA reflectances is recommended, as differences in reflectance properties due to atmospheric conditions are accounted for (Gilbert et al., 1994; Vermote & Kotchenova, 2008; Chraibi et al., 2022). However, a large portion of the publicly available Sentinel 2 data has not yet been processed from level 1C to level 2A, requiring researchers to apply the corrections themselves. Fortunately, the European Space Agency provides the



Figure 4.A.2: Example of a wet pan and dryland training polygon digitized on Google Earth. The extent of water can easily be gauged at the maximum zoom level in Google Earth. While the dryland polygon in this case covered an area that is seasonally covered by water, we placed other dryland polygons in areas that were never inundated. However, to ensure reliable differentiation between wet and dry pans, we included several dryland polygons located in dry pans.

correction tool `sen2cor` for free (Main-Knorn et al., 2017), which has been integrated into the R-package `sen2r` (Ranghetti et al., 2020). We therefore applied the necessary corrections after download for any product that hadn't already been corrected. Furthermore, we used Sentinel 2's scene classification, to remove pixels classified as either clouds or shadows. Finally, we computed the same ND-indices as for Landsat 8 (Table 4.A.2).

Table 4.A.2: We computed normalized difference indices between certain bands, hoping they would improve the land-cover classifiers. Depending on the satellite, we used different bands to compute similar indices. The function to compute a normalized difference between bands b_1 and b_2 is given by $\frac{b_1 - b_2}{b_1 + b_2}$.

Index	Bands	
	Landsat 8	Sentinel 2
NDWI	B3, B5	B3, B8
NDMI	B5, B6	B8, B11
NDSI	B3, B6	B3, B11
BEST	B3, B7	B3, B12

Land Cover Classifiers

To train a land-cover classifier, we generated 3,000 random points within training polygons following a stratified equal random sampling scheme (Shetty et al., 2021). That is, we ensured that 1,000 random

points were sampled per training category. Stratified random sampling was necessary to ensure that wet-pans, our category of interest, was sampled frequently enough, as it represented a minority class, only making up of (0.27%) the total training area. Stratified equal random sampling has been shown to provide good class-level accuracy for minority classes (Shetty et al., 2021), so we deemed this approach suitable for our purposes. We also kept track of the dates of the underlying polygons from which random points were generated. At each random point, we then extracted reflectance values of Sentinel 2 and Landsat 8 data that temporally aligned with the date assigned to the random point (Figure 4.A.3a). For instance, if a random point fell into a polygon that was digitized using a Google Earth image generated on Aug 18, 2018, we extracted values from the Sentinel 2 and Landsat 8 layers that were closest to that date. Finally, we parameterized a Random Forest (RF) classifier using the R-package `randomForest` (Cutler & Wiener, 2024) and a Classification and Regression Tree (CART) classifier using the R-package `rpart` (Therneau, Atkinson, et al., 2024). In both cases, we included all bands, as well as derived ND-indices (Table 4.A.2) as explanatory covariates. We visualized the decision trees for the CART classifiers (Figure 4.A.3b) and variable importance for the RF models (Figure 4.A.3c) to investigate the importance of different bands or indices in separating the three classes. To compute variable importance we used the R-package `caret` (Kuhn, 2008).

Validation and Comparison

To validate the predictive power of the two classifiers across the two datasets, we employed 5-fold cross-validation. For this, we randomly split the data into 5 groups and repeatedly fitted both classification models using 80% of the data, to then predict land cover categories in the remaining 20%. We generated confusion matrices to contrast true and predicted labels and computed estimates of the classifier's specificity, sensitivity, and overall accuracy. The results from this validation show that both classifiers achieve $\geq 90\%$ accuracy across both satellite products (Figure 4.A.4). In fact, the RF classifier resulted in an overall accuracy of 99% on Sentinel 2 data.

4.A.3 Bulk Download

Although both Landsat 8 and Sentinel 2 provided very good results, we considered Sentinel 2 data to be marginally superior, mainly due to Sentinel's higher temporal and spatial resolution. A higher temporal resolution was key to compensate missing data from satellite mages obtained on cloudy days and therefore pivotal in achieving cloud free monthly composites. We therefore decided to download Sentinel 2 data for the period during which we also collected GPS data of dispersing individuals. Instead of downloading all Sentinel 2 tiles overlapping with our study area and matching the study-period, we created a spatio-temporal moving window (Figure 4.A.5). This window was updated each month and comprised all GPS

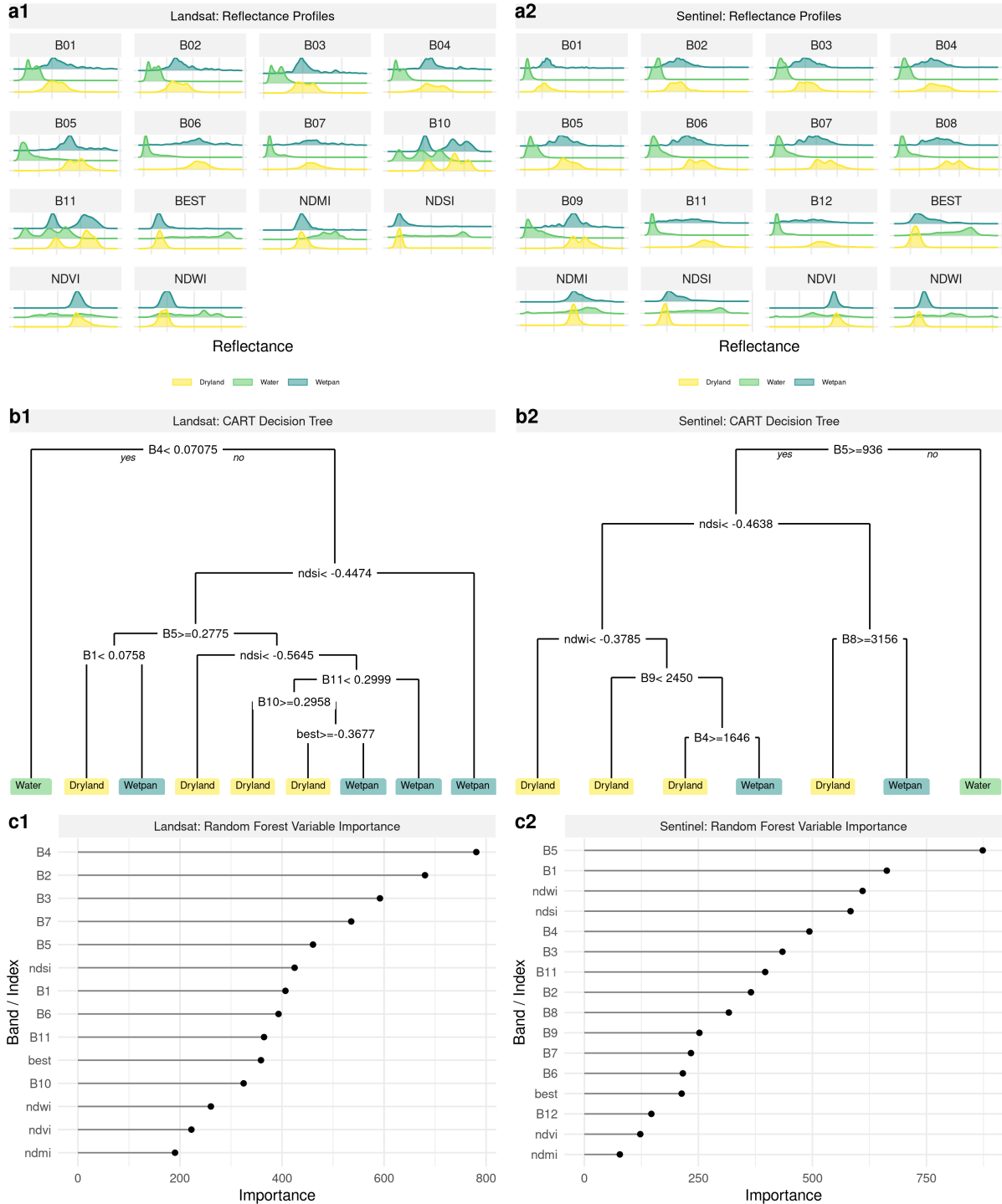


Figure 4.A.3: Reflectance properties of the Landsat 8 (a1) and Sentinel 2 (a2) bands and NDs at the extracted training points for each of the three categories (colored). Based on extracted reflectance values we parametrized Classification and Regression Tree models (b1 and b2) as well as Random Forest models (c1 and c2).

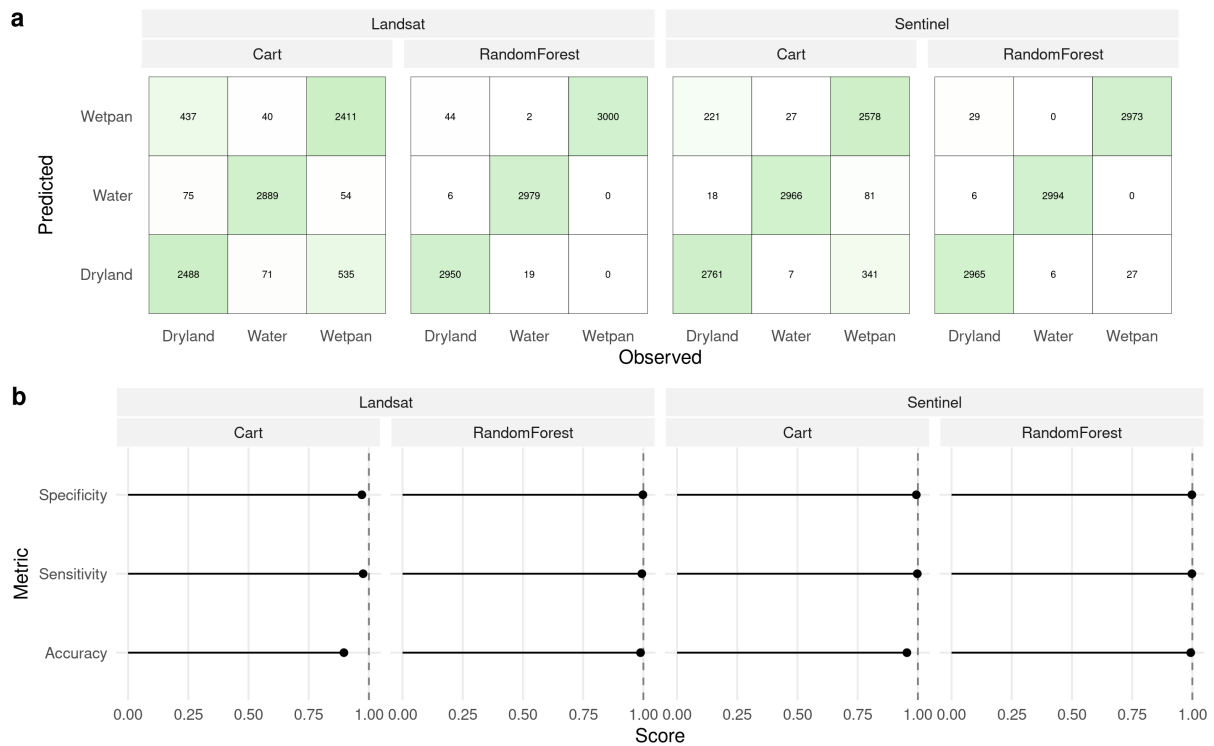


Figure 4.A.4: Confusion matrices (a) and derived performance metrics (b) for the CART and RF classifiers for both the Landsat 8 and Sentinel 2 datasets.

locations collected during that month, buffered by a 100 km radius. We then identified Sentinel 2 tiles intersecting with each of the monthly updated moving windows (Figure 4.A.6). This resulted in a list of 2,226 tiles that needed to be downloaded, 1,373 of which were already corrected to BOA reflectances, while the remaining 853 tiles still needed to be corrected. The download followed the same procedure and included the same corrections (from TOA to BOA, and cloud masking) as outlined in Section 4.A.2 using the `sen2r` package in R (Ranghetti et al., 2020). Upon completion of the download and pre-processing, we applied the trained RF classifier to obtain binary “pan-maps”, showing the spatial distribution of ephemeral water bodies. To generate monthly composites, we merged all pan-maps falling into the same month and retained pans if they were detected in at least 50% of the overlapping tiles. Finally, we generated “distance-to-pan” maps using the `distance` function from the `terra` package in R (Hijmans et al., 2024).

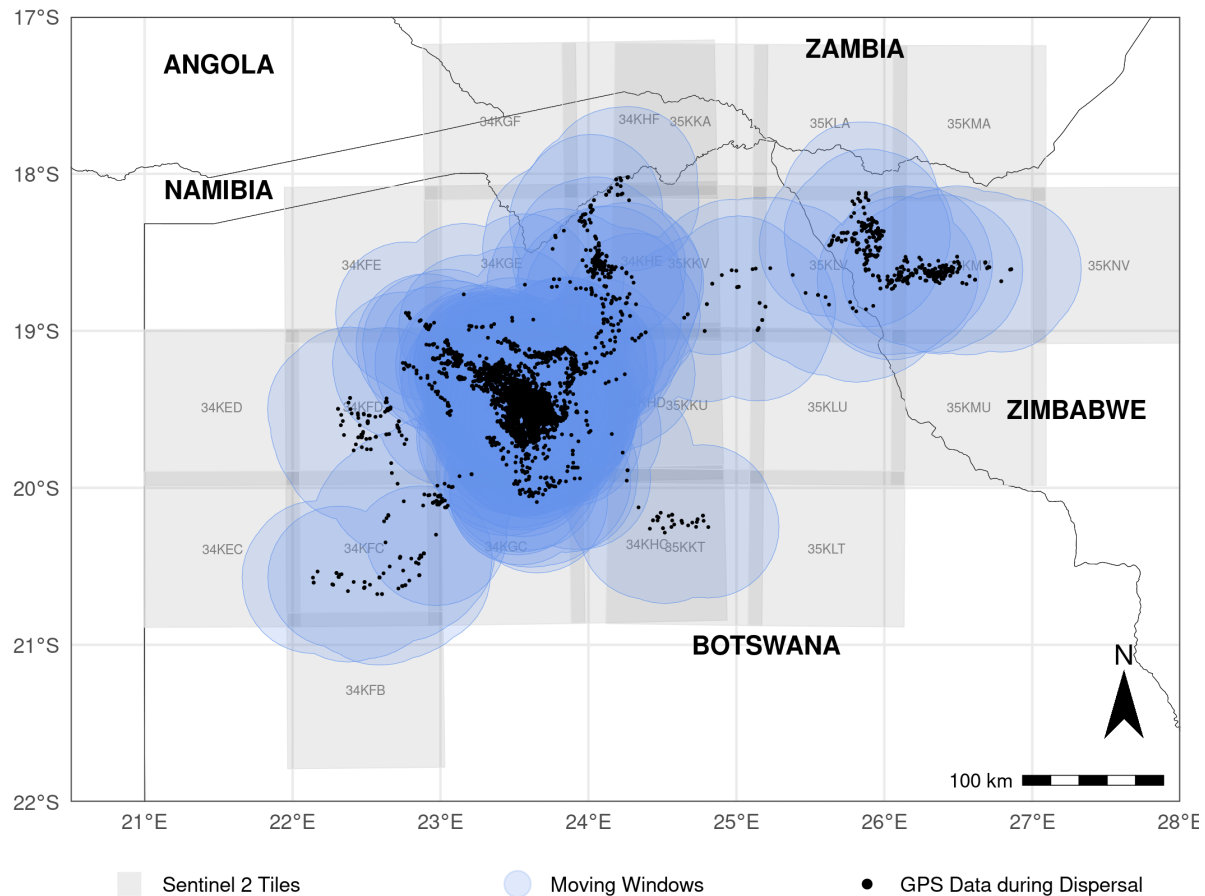


Figure 4.A.5: To reduce the number of Sentinel 2 tiles that we needed to download, we generated a monthly updated spatio-temporal moving window that comprised all GPS data of dispersing wild dogs (black dots) during the respective month, buffered by a 100 km radius. Based on the so created moving windows (in blue), we identified all overlapping Sentinel 2 tiles (tiles in gray) that we needed to download each month, which resulted in a total of 2,226 tiles.



Figure 4.A.6: This figure shows the moving windows generated for each month, as well as the underlying GPS data and overlapping Sentinel 2 tiles that we ultimately downloaded and combined into monthly composites.

4.B Moon Illumination

We used the R-package `moonlit` (Śmielak, 2023) to obtain estimates of moon illumination at 5 minute intervals at the average location of dispersal GPS data (lon = of 23.5, lat = -19.0; Figure 4.B.1). The `moonlit` package is currently not on CRAN, but can be installed from GitHub (<https://github.com/msmielak/moonlit>). Besides providing information on the moon cycle, this package also allows estimating the amount of moonlight illumination on the ground. For instance, even during full-moon nights, the moon may only appear at a low angle in the sky, thus providing minimal illumination. Estimates from the `moonlit` package can therefore be viewed as biologically more relevant. To match the temporal resolution of our GPS data during dispersal, we calculated four hourly moonlight summaries. Specifically, we computed if an interval fell into nighttime and the average amount of moon-illumination during the four hours.

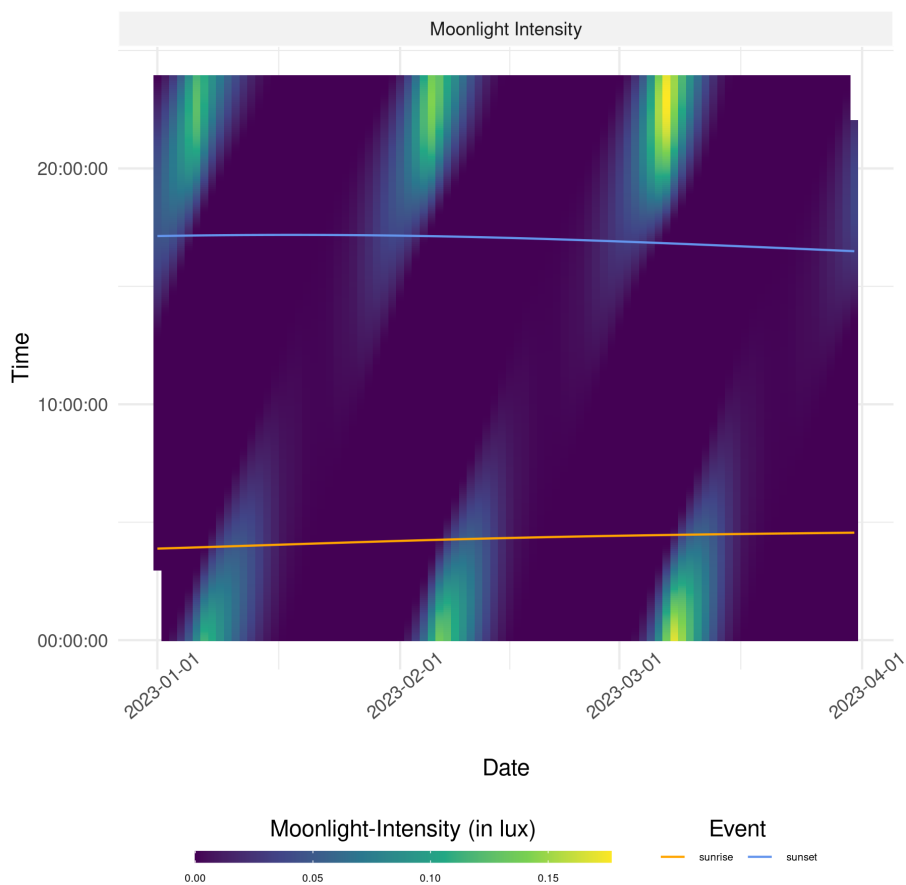


Figure 4.B.1: Moonlight intensity as estimated from the `moonlit` package (Śmielak, 2023) in R, calculated for several example timestamps in 2023.

4.C Light-Type

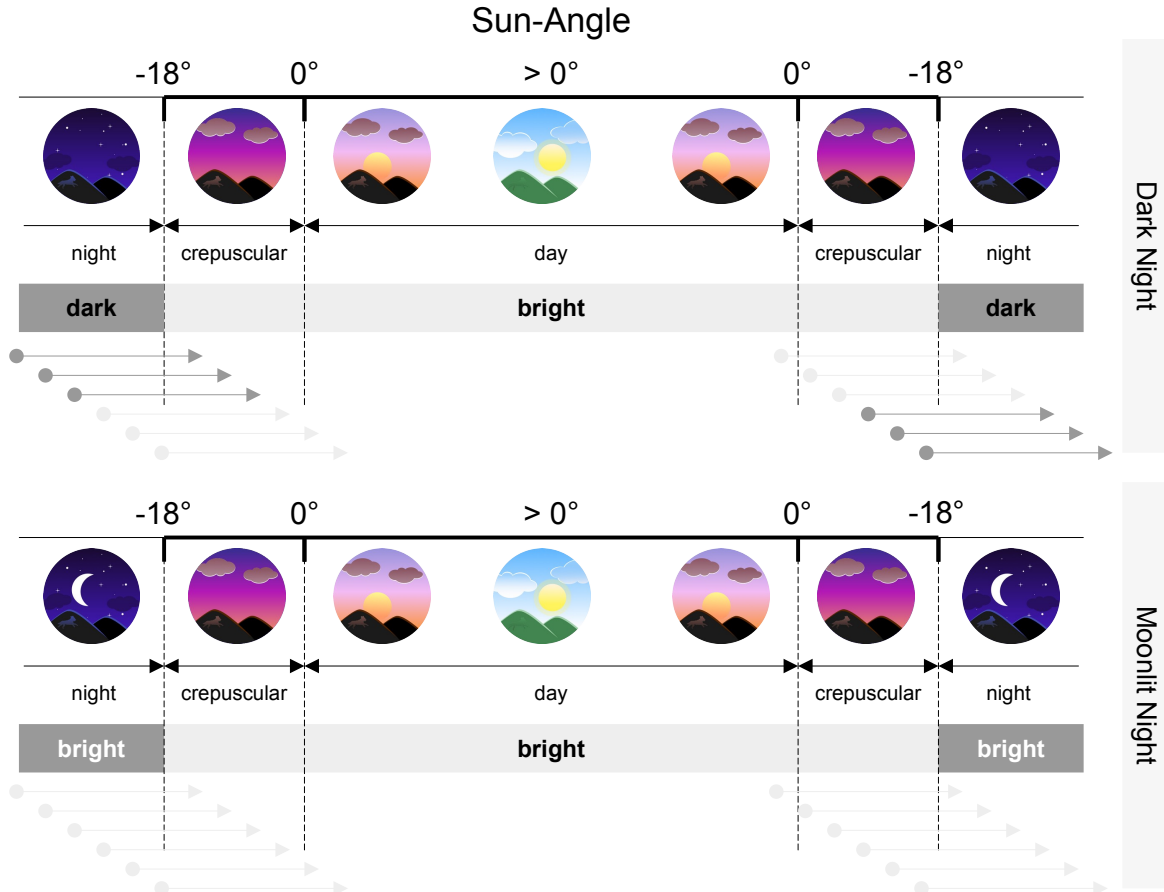


Figure 4.C.1: Schematic illustration of how we categorized steps into *dark* and *bright* steps. First, we used the `suncalc` and `moonlit` packages to obtain estimates of the sun-angle and moon illumination at 5 minute intervals for each date of interest. Whenever the sun angle was $\leq -18^\circ$, we deemed the respective period to be at night. A night was either bright (moon illumination > 0.02 of maximum illumination) or dark (moon illumination ≤ 0.02 of maximum illumination). Any other period was considered to provide enough illumination for wild dogs to move and therefore considered as bright. Since each step covered a time-span of approximately four hours, we defined a step as bright if at least 25% (i.e., one hour) of it occurred during a bright period. The gray arrows represent some example steps that are categorized as bright (light gray) or dark (dark gray).

4.D Movement Model Results

Table 4.D.1: Estimates obtained using the **simple model formula** (no interactions) and **static** covariates. GPS Data were either pooled across seasons (labeled “all”) or split into wet and dry season. Only underlined covariates differed between the static and dynamic configurations.

Season	Covariate	Fixed Effects			Random Effects
		Coefficient	p-value	Significance	
All	sl	0.058	0.214		0.203
	log(sl)	0.057	0.069	*	0.109
	cos(ta)	0.111	0.000	***	0.053
	Humans	-0.289	0.019	**	0.358
	Trees	-0.279	0.011	**	0.376
	<u>Shrubs</u>	0.139	0.492		0.170
	<u>Water</u>	-0.467	0.018	**	0.224
	<u>DistanceToWater</u> ^{0.5}	-0.780	0.000	***	0.604
Dry	sl	0.047	0.376		0.170
	log(sl)	0.083	0.004	***	0.043
	cos(ta)	0.120	0.000	***	0.060
	Humans	-0.219	0.110		0.302
	Trees	-0.327	0.031	**	0.450
	<u>Shrubs</u>	-0.091	0.730		0.321
	<u>Water</u>	-0.775	0.001	***	0.003
	<u>DistanceToWater</u> ^{0.5}	-0.932	0.000	***	0.681
Wet	sl	0.010	0.889		0.257
	log(sl)	0.032	0.497		0.128
	cos(ta)	0.116	0.001	***	0.083
	Humans	-0.271	0.140		0.366
	Trees	-0.059	0.499		0.000
	<u>Shrubs</u>	0.495	0.114		0.007
	<u>Water</u>	0.113	0.711		0.152
	<u>DistanceToWater</u> ^{0.5}	-0.550	0.014	**	0.619

Table 4.D.2: Estimates obtained using the **simple model formula** (no interactions) and **dynamic** covariates. GPS Data were either pooled across seasons (labeled “all”) or split into wet and dry season. Only underlined covariates differed between the static and dynamic configurations.

Season	Covariate	Fixed Effects			Random Effects
		Coefficient	p-value	Significance	
All	sl	0.050	0.270		0.199
	<u>log(sl)</u>	0.064	0.045	**	0.110
	cos(ta)	0.112	0.000	***	0.052
	Humans	-0.252	0.036	**	0.340
	<u>Trees</u>	-0.216	0.010	**	0.336
	<u>Shrubs</u>	-0.012	0.909		0.239
	<u>Water</u>	-0.680	0.000	***	0.252
	<u>DistanceToWater</u> ^{0.5}	-0.235	0.089	*	0.523
Dry	sl	0.035	0.506		0.175
	<u>log(sl)</u>	0.082	0.001	***	0.000
	cos(ta)	0.118	0.000	***	0.057
	Humans	-0.176	0.174		0.271
	<u>Trees</u>	-0.360	0.004	***	0.413
	<u>Shrubs</u>	-0.151	0.298		0.340
	<u>Water</u>	-0.877	0.000	***	0.000
	<u>DistanceToWater</u> ^{0.5}	-0.309	0.082	*	0.529
Wet	sl	0.012	0.864		0.251
	<u>log(sl)</u>	0.047	0.339		0.137
	cos(ta)	0.123	0.000	***	0.085
	Humans	-0.232	0.203		0.367
	<u>Trees</u>	-0.070	0.341		0.156
	<u>Shrubs</u>	0.253	0.127		0.273
	<u>Water</u>	-0.352	0.058	*	0.194
	<u>DistanceToWater</u> ^{0.5}	-0.163	0.410		0.558

Table 4.D.3: Estimates obtained using the **complex model formula** (with interactions) and **static** covariates. GPS Data were either pooled across seasons (labeled “all”) or split into wet and dry season. Only underlined covariates differed between the static and dynamic configurations.

Season	Covariate	Fixed Effects			Random Effects SD
		Coefficient	p-value	Significance	
All	sl	-0.014	0.734		0.152
	log(sl)	0.478	0.000	***	0.138
	cos(ta)	0.128	0.000	***	0.060
	sl:Dark	-0.294	0.000	***	-
	log(sl):Dark	-0.911	0.000	***	-
	sl: <u>Temperature</u>	-0.234	0.000	***	-
	log(sl): <u>Temperature</u>	-0.197	0.000	***	-
	Humans	-0.317	0.019	**	0.412
	<u>Trees</u>	-0.241	0.038	**	0.415
	Shrubs	0.173	0.397		0.128
	<u>Water</u>	-0.507	0.012	**	0.253
	<u>DistanceToWater</u> ^{0.5}	-0.885	0.000	***	0.672
	sl: <u>Trees</u>	0.001	0.974		-
	sl: <u>Shrubs</u>	0.081	0.561		-
	sl: <u>Water</u>	-0.183	0.174		-
Dry	cos(ta): <u>DistanceToWater</u> ^{0.5}	0.058	0.000	***	-
	sl	-0.057	0.311		0.163
	log(sl)	0.532	0.000	***	0.160
	cos(ta)	0.128	0.000	***	0.055
	sl:Dark	-0.122	0.070	*	-
	log(sl):Dark	-1.036	0.000	***	-
	sl: <u>Temperature</u>	-0.228	0.000	***	-
	log(sl): <u>Temperature</u>	-0.248	0.000	***	-
	Humans	-0.259	0.087	*	0.353
	<u>Trees</u>	-0.276	0.086	*	0.481
	Shrubs	-0.058	0.827		0.238
	<u>Water</u>	-0.846	0.001	***	0.209
	<u>DistanceToWater</u> ^{0.5}	-1.098	0.000	***	0.796
	sl: <u>Trees</u>	0.050	0.342		-
Wet	sl: <u>Shrubs</u>	-0.046	0.793		-
	sl: <u>Water</u>	-0.343	0.042	**	-
	cos(ta): <u>DistanceToWater</u> ^{0.5}	0.035	0.107		-
	sl	-0.041	0.568		0.217
	log(sl)	0.404	0.000	***	0.153
	cos(ta)	0.142	0.000	***	0.112
	sl:Dark	-0.894	0.000	***	-
	log(sl):Dark	-0.726	0.000	***	-
	sl: <u>Temperature</u>	-0.251	0.000	***	-
	log(sl): <u>Temperature</u>	-0.140	0.004	***	-
	Humans	-0.265	0.181		0.420
	<u>Trees</u>	-0.034	0.712		0.000
	Shrubs	0.562	0.092	*	0.141
	<u>Water</u>	0.136	0.671		0.001
	<u>DistanceToWater</u> ^{0.5}	-0.578	0.007	***	0.571
	sl: <u>Trees</u>	-0.074	0.277		-
	sl: <u>Shrubs</u>	0.383	0.101		-
	sl: <u>Water</u>	0.141	0.534		-
	cos(ta): <u>DistanceToWater</u> ^{0.5}	0.090	0.001	***	-

Table 4.D.4: Estimates obtained using the **complex model formula** (with interactions) and **dynamic covariates**. GPS Data were either pooled across seasons (labeled “all”) or split into wet and dry season. Only underlined covariates differed between the static and dynamic configurations.

Season	Covariate	Fixed Effects			Random Effects SD
		Coefficient	p-value	Significance	
All	sl	-0.172	0.002	***	0.223
	log(sl)	0.435	0.000	***	0.136
	cos(ta)	0.110	0.000	***	0.058
	sl:Dark	-0.305	0.000	***	-
	log(sl):Dark	-0.805	0.000	***	-
	sl: <u>Temperature</u>	-0.187	0.000	***	-
	log(sl): <u>Temperature</u>	-0.083	0.000	***	-
	Humans	-0.278	0.040	**	0.401
	<u>Trees</u>	-0.208	0.016	**	0.347
	Shrubs	-0.018	0.866		0.223
	<u>Water</u>	-0.791	0.000	***	0.176
	<u>DistanceToWater</u> ^{0.5}	-0.306	0.030	**	0.537
	sl: <u>Trees</u>	-0.028	0.141		-
	sl: <u>Shrubs</u>	0.051	0.462		-
Dry	sl: <u>Water</u>	-0.435	0.000	***	-
	cos(ta): <u>DistanceToWater</u> ^{0.5}	0.046	0.005	***	-
	sl	-0.267	0.000	***	0.181
	log(sl)	0.454	0.000	***	0.116
	cos(ta)	0.115	0.000	***	0.054
	sl:Dark	-0.124	0.062	*	-
	log(sl):Dark	-0.902	0.000	***	-
	sl: <u>Temperature</u>	-0.180	0.000	***	-
	log(sl): <u>Temperature</u>	-0.087	0.000	***	-
	Humans	-0.220	0.149		0.348
	<u>Trees</u>	-0.353	0.005	***	0.414
	Shrubs	-0.137	0.343		0.319
	<u>Water</u>	-0.957	0.000	***	0.001
	<u>DistanceToWater</u> ^{0.5}	-0.373	0.036	**	0.526
Wet	sl: <u>Trees</u>	-0.018	0.414		-
	sl: <u>Shrubs</u>	0.009	0.916		-
	sl: <u>Water</u>	-0.345	0.002	***	-
	cos(ta): <u>DistanceToWater</u> ^{0.5}	0.007	0.731		-
	sl	-0.077	0.401		0.284
	log(sl)	0.427	0.000	***	0.165
	cos(ta)	0.125	0.002	***	0.111
	sl:Dark	-0.907	0.000	***	-
	log(sl):Dark	-0.667	0.000	***	-
	sl: <u>Temperature</u>	-0.238	0.000	***	-
	log(sl): <u>Temperature</u>	-0.086	0.037	**	-
	Humans	-0.203	0.307		0.430
	<u>Trees</u>	-0.059	0.414		0.143
	Shrubs	0.279	0.082	*	0.217
	<u>Water</u>	-0.454	0.009	***	0.001
	<u>DistanceToWater</u> ^{0.5}	-0.177	0.378		0.571

4.E Number of Random Steps

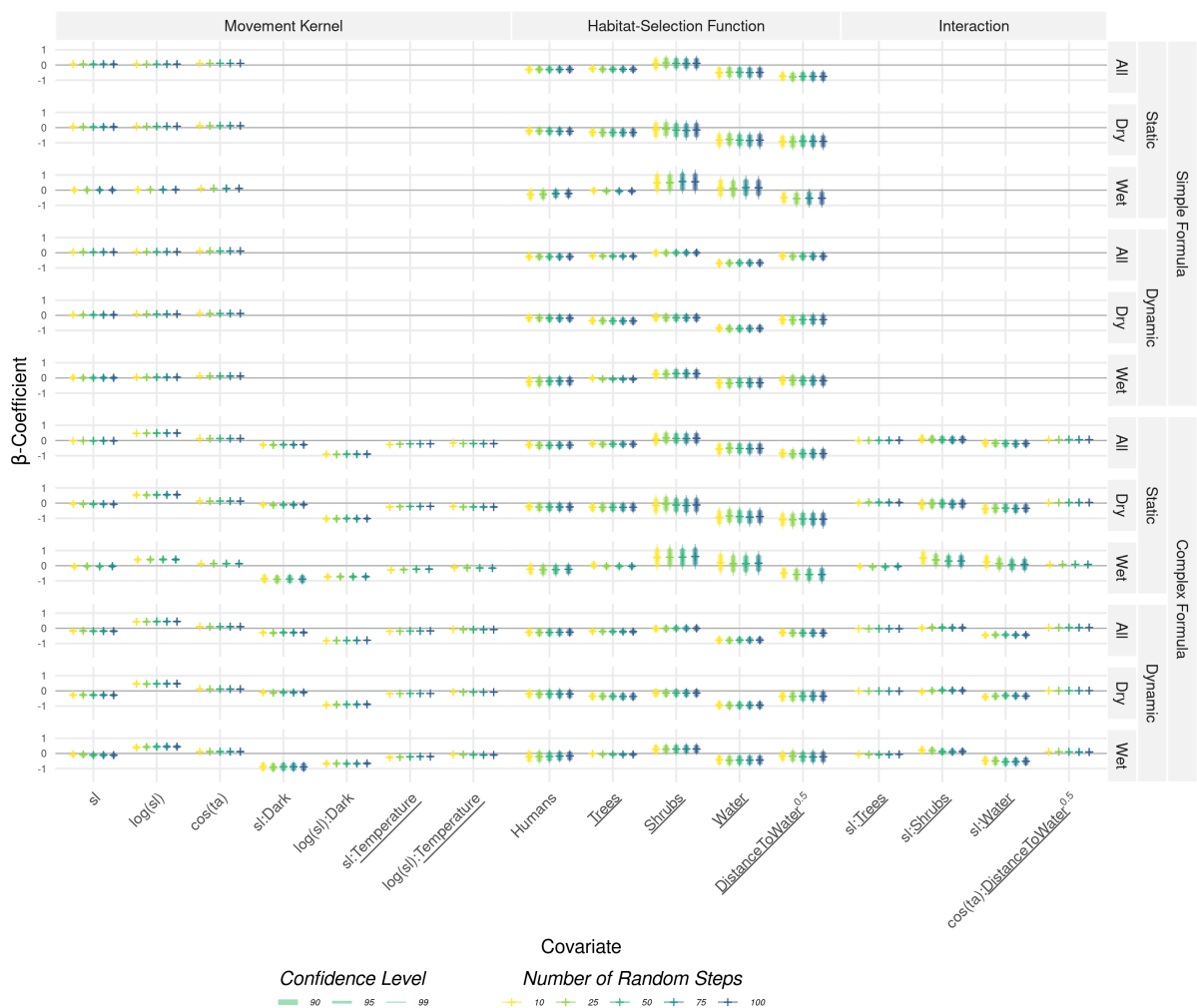


Figure 4.E.1: Results from the integrated step-selection models when considering different numbers of random steps. Results are shown for the simple and complex formulas for all configurations of fitting covariates (static vs dry) and model seasons (all vs. wet + dry). For some design combinations, models failed to converge and thus dropped from the figure.

4.F Model Interpretation

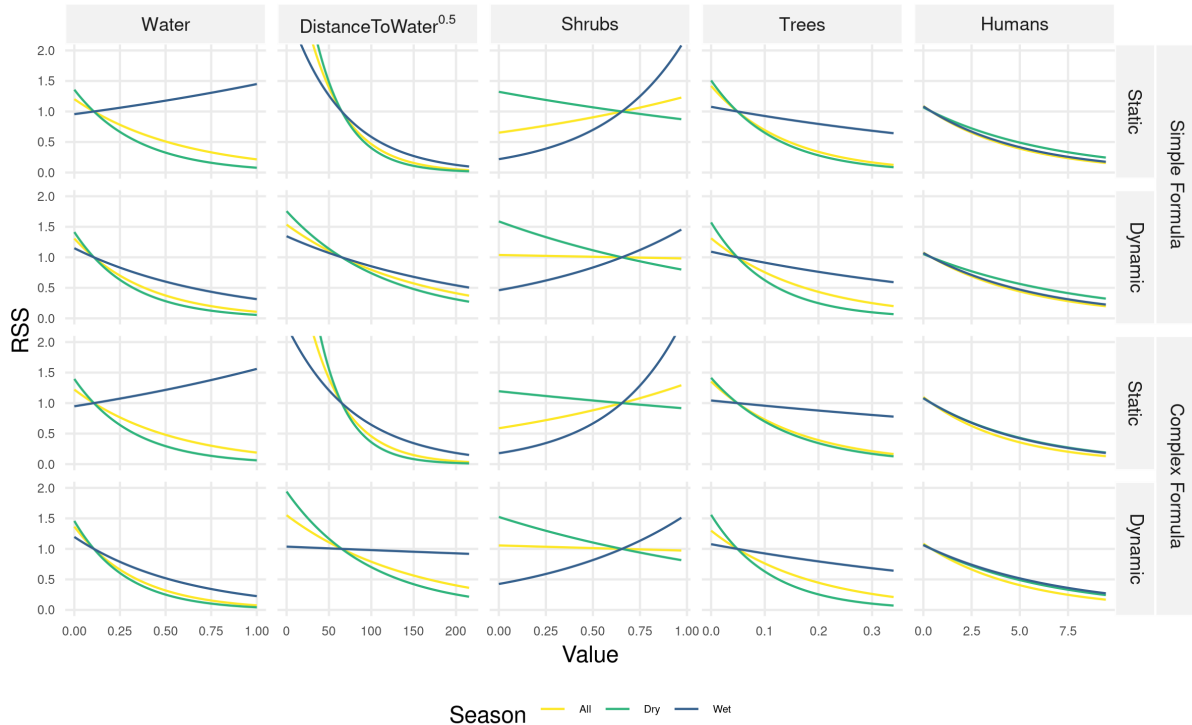


Figure 4.F.1: Relative selection scores (RSS) with respect to environmental covariates. RSS scores were computed by comparing a location x_1 with average conditions to a location x_2 with average conditions but the respective covariate varied between its minimum and maximum observed value. Confidence intervals overlapped substantially, hence we omitted them from the figure to simplify the interpretation of the differences among configurations.

4.G Spearman's Rank Correlation in Relation to the Number of Random Steps

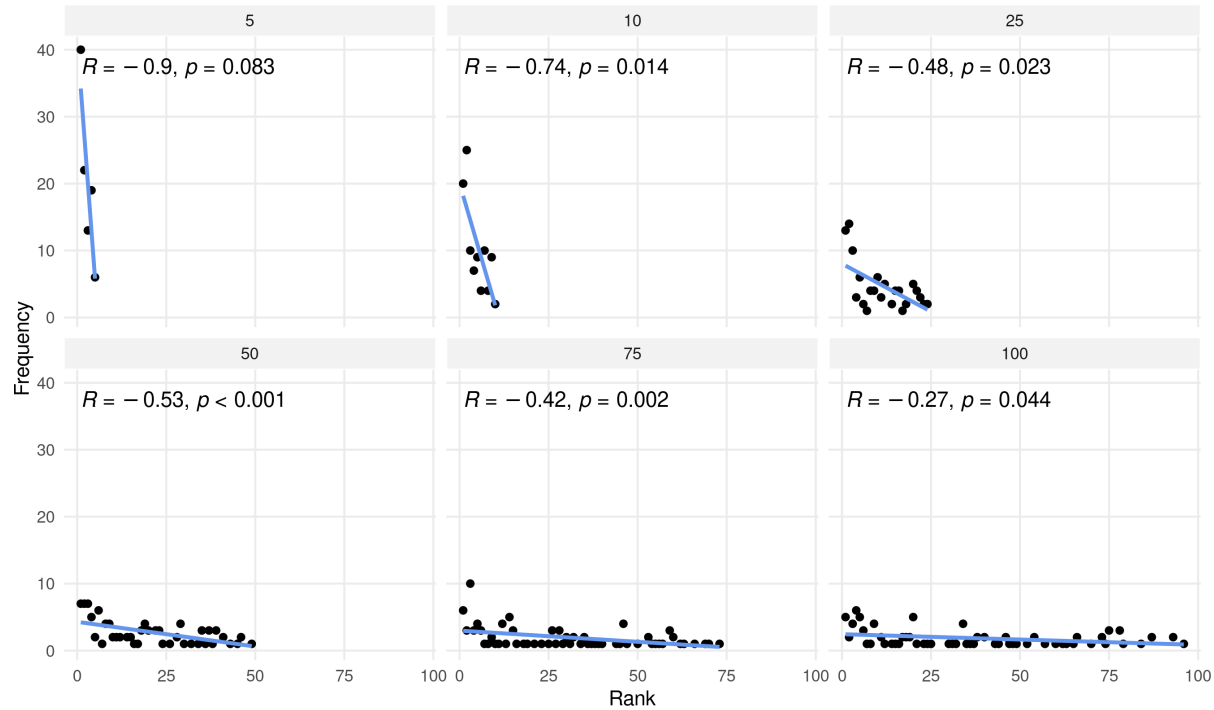


Figure 4.G.1: Illustration how the Spearman's rank correlation changes when the number of random steps per stratum is varied from 5 to 100 (facettes). The y-axis shows the frequency at which the observed step was assigned the rank indicated on the x-axis. A low rank indicates that the observed step was assigned a high probability of being chosen. The better the prediction, the more frequently the observed step should be assigned a low rank, thus resulting in negative Spearman's rank-correlation. However, it is obvious that the metric heavily depends on the number of random steps per stratum. If there are only a few random steps, the correlation is more likely to be negative. The show patterns are based on simulated data.



Chapter 5

Methods for Implementing Integrated Step-Selection Functions with Incomplete Data

David D. Hofmann , Gabriele Cozzi , and John Fieberg 

Abstract

Integrated step-selection analyses (iSSAs) are versatile and powerful frameworks for studying habitat and movement preferences of tracked animals. iSSAs utilize integrated step-selection functions (iSSFs) to model movements in discrete time, and thus, require animal location data that are regularly spaced in time. However, many real-world datasets are incomplete due to tracking devices failing to locate an individual at one or more scheduled times, leading to slight irregularities in the duration between consecutive animal locations. To address this issue, researchers typically only consider bursts of regular data (i.e., sequences of locations that are equally spaced in time), thereby reducing the number of observations used to model movement and habitat selection. We reassess this practice and explore four alternative approaches that account for temporal irregularity resulting from missing data. Using a simulation study, we compare these alternatives to a baseline approach where temporal irregularity is ignored and demonstrate the potential improvements in model performance that can be gained by leveraging these additional data. We also showcase these benefits using a case study on a spotted hyena (*Crocuta crocuta*).

5.1 Introduction

Understanding how animals move across the landscape, what habitats they prefer, and what resources they select are fundamental questions in movement ecology (Nathan, 2008). Thanks to recent advances in animal tracking (Cagnacci et al., 2010; Williams et al., 2019; Beardsworth et al., 2022) and remote sensing technologies (Toth & Józków, 2016; Rumiano et al., 2020), new opportunities and analytical tools have emerged for studying how animals move and interact with their environment (Tomkiewicz et al., 2010; Kays et al., 2015; Nathan et al., 2022). Methods commonly used to analyze animal movement data, including step-selection analyses (Fortin et al., 2005; Thurfjell et al., 2014; Fieberg et al., 2021) and hidden Markov models (Michelot et al., 2016), require **animal locations** (terms in bold at first occurrence are defined in Table 5.1.1) that are collected at a constant sampling frequency, leading to data that are equally spaced in time. Yet, it is common to encounter missing locations in most telemetry data sets (Frair et al., 2010; Hofman et al., 2019; Vales et al., 2022), which introduces unwanted irregularities in the duration between successive locations. Thus, there is a need for analytical tools that enable the analysis of such data, while mitigating potential biases arising from temporal irregularity introduced through missing animal locations.

Step-selection analyses (SSAs) are widely used to study animals' movement capacities and habitat-selection patterns (Fortin et al., 2005; Thurfjell et al., 2014). Straight-line segments connecting consecutive animal locations, referred to as **steps**, form the basic building blocks of the statistical likelihood in SSAs. Specifically, SSAs model the probability u of finding an individual at location s at time $t + 1$, given the animal's past positions at time t and $t - 1$, s_t and s_{t-1} , respectively:

$$u(s_{t+1}) = \frac{\phi(s_{t+1}, s_t, s_{t-1}; \gamma)w(x(s_{t+1}); \beta)}{\int_{s \in G} \phi(s_{t+1}, s_t, s_{t-1}; \gamma)w(x(s_{t+1}); \beta)ds} \quad (\text{Equation 5.1})$$

Here, the function ϕ represents an animal's **movement kernel** which is usually expressed in terms of **step-length** and **turning-angle** distributions, with γ representing parameters in these distributions. The function w is the **habitat-selection function** and reflects an animal's preferences β for environmental characteristics x at location s_{t+1} . In most applications, w is modeled as a log-linear function of x , taking the form $w = \exp(x^\top \beta)$. The integral in the denominator of Equation 5.1 ensures that u is a proper probability distribution (i.e., that it integrates to 1). Following Michelot et al. (2024), we call the product $\phi \times w$ the step-selection function (SSF), as it highlights that the probability of finding an animal at a certain location depends on both the animal's movement kernel and its habitat-selection function.

Given a series of **observed steps**, finding the movement and habitat-selection parameters that maximize the likelihood in Equation 5.1 requires approximating the integral in the denominator for each observed step. A variety of numerical integration techniques can be used for this purpose (Michelot et al.,

Table 5.1.1: Glossary of terms. Terms in the glossary are printed in bold at first occurrence in the main text. Definitions are always given in the context of step selection functions (SSFs).

Term	Definition
Animal locations	A series of telemetry data points that include date, time, longitude, and latitude information, describing when and where an animal was observed or recorded.
Step	A straight line connecting two consecutive locations.
Observed step	A step that connects two observed animal locations.
Random step	A step that connects an observed animal location with a random location. Random locations are typically generated by combining an observed animal location with random step lengths and turning angles.
Step length	The Euclidean distance of a step.
Turning angle	A measure of the change in direction between two consecutive steps.
Habitat-selection function	A probabilistic description of an animal's habitat preferences. It describes how an animal selects habitat when not constrained by its movement capacity. Also referred to as movement-free habitat-selection function.
Movement kernel	A probabilistic description of an animal's movement capacity. It describes how an animal would move when not constrained by habitat selection. Also referred to as selection-free movement kernel.
Trajectory	A sequence of animal locations collected on the same individual.
Step duration	The time interval associated with a particular step, i.e., the time elapsed between two consecutive animal locations.
Regular animal locations	A series of animal locations that have been obtained at regularly spaced time intervals, such as every hour.
Irregular animal locations	A series of animal locations collected at irregular time intervals.
Regular step durations	Step durations that occur when animal locations are successfully collected at regular time intervals.
Irregular step durations	Step durations that occur when animal locations are not successfully collected at regular time intervals.
Missingness	The fraction of animal locations that should have been collected but, for some reason, were not. For example, if only eight out of ten expected animal locations were successfully collected, the missingness would be 0.2 (i.e., 20%).
Forgiveness	The maximum step duration, measured in multiples of the regular step duration, a modeler is willing to include in the step-selection analysis. A modeler with a forgiveness of one, for instance, only considers regular steps, while a modeler with a forgiveness of two would consider irregular steps up to twice the regular step duration.
Burst	A sequence of consecutive animal locations equally spaced in time and with steps where the step duration does not exceed the forgiveness.
Valid step	A step for which a step length, turning angle, and step duration can be computed, and for which the step duration does not exceed the forgiveness of the modeler. These steps can be used for step-selection analysis.

2024), but a common approach is to combine observed steps with **random steps** generated by sampling step lengths and turning angles from parametric distributions informed by the data (Fortin et al., 2005; Thurfjell et al., 2014). Environmental conditions at observed steps are then contrasted with environmental conditions at random steps in a (mixed effects) conditional logistic regression framework (Fortin et al., 2005; Muff et al., 2020). To jointly estimate parameters in ϕ and w , movement descriptors (e.g., step length (sl), its natural logarithm ($\log(sl)$), and the cosine of the turning angle ($\cos(ta)$)) can be included in the conditional logistic regression model, and their estimated coefficients can be used to update the initial (tentative) step-length and turning-angle distributions (Duchesne et al., 2015; Avgar et al., 2016; Fieberg et al., 2021). The specific descriptors that need to be included depend on the assumed step-length and turning-angle distributions (for more details, see Appendix C of Fieberg et al., 2021). This approach to estimating parameters of the SSF, termed *integrated SSA* (or iSSA) by Avgar et al. (2016), is similar to using importance sampling to approximate the integral in Equation 5.1 (Michelot et al., 2024) and is readily accessible through the R-package `amt` (Signer et al., 2019).

SSAs have proven extremely effective in numerous ecological studies (Thurfjell et al., 2014), providing insights into seasonal space use (Vales et al., 2022; Enns et al., 2023), resource selection during distinct behavioral phases (Elliot et al., 2014; Abrahms et al., 2017; Cozzi et al., 2018; Broekhuis et al., 2019), and the effects of landscape familiarity or memory on animal movements (Kim et al., 2023). A model parametrized using iSSA resembles a fully mechanistic movement model that can be used to simulate space use under novel conditions (Avgar et al., 2016; Signer et al., 2017; Hofmann, Cozzi, McNutt, et al., 2023; Signer et al., 2024). This characteristic has made iSSAs a useful tool for quantifying landscape resistance and identifying movement corridors (Buchholtz et al., 2020; Zeller, Wattles, et al., 2020; Hofmann et al., 2021; Hofmann, Cozzi, McNutt, et al., 2023).

A key assumption when conducting an iSSA is that the data have been collected at a constant sampling frequency, thus producing **trajectories** with **regular step durations** (Δt ; Fortin et al., 2005; Thurfjell et al., 2014). Here, we refer to such data as **regular animal locations**, and without loss of generality, we assume the regular step duration to be one (i.e., $\Delta t = 1$). Regular step durations ensure that step lengths and turning angles are independent of the step duration, and therefore, steps can be pooled when estimating movement parameters. Since animal locations are usually obtained using automated tracking devices, such as GPS collars programmed to record data at regular intervals, satisfying this assumption seems straightforward. In reality, however, device limitations often imply that some of the aspired datapoints fail to be collected, thus introducing **missingness** and confronting researchers with **irregular animal locations** and **irregular step durations** (Frair et al., 2010). In a comprehensive study, Hofman et al. (2019) showed that across 3,000 GPS devices and 160 species, the average success rate of obtaining a scheduled animal

location was 78% (implying a missingess of 22%), thus highlighting that irregular animal locations are a frequent phenomenon in ecological studies.

It is generally recommended that, in the case of such irregular data, researchers should only retain **bursts** of steps with regular step durations (possibly with some tolerance) and discard the rest (Thurfjell et al., 2014). We will refer to this modeling approach as having a **forgiveness** level of one, indicating that only steps with step durations $\Delta t = 1$ are retained for further analysis. In R, the `amt` package provides the function `track_resample` specifically for identifying bursts of steps with regular step durations (Signer et al., 2019). The main drawback of this approach is that it may result in a substantial amount of data being discarded (Figure 5.1.1 and Figure 5.1.2). For instance, consider a hypothetical trajectory in which location 4 is missing (Figure 5.1.1a). The absence of this location prevents the computation of a step between locations 3 and 4, as well as between locations 4 and 5. Furthermore, without these steps, it becomes impossible to compute a turning angle for the step between locations 5 and 6. Consequently, the lack of a single location reduces the effective sample size, which is the number of **valid steps**, by three. Assuming that animal locations are missing at random, a missingness level of 25% causes the number of valid steps to drop by 58% (Figure 5.1.2). A modeler willing to increase their level of forgiveness to two (i.e., allowing for inclusion of steps with $\Delta t \leq 2$) would be able to increase the number of valid steps by 57% (Figure 5.1.1 and Figure 5.1.2), therefore achieving a substantial gain in effective sample size. The ability to capitalize on irregular data is likely to be particularly important for applications where data are already limited, such as, for instance, when modeling dispersing individuals (Rudnick et al., 2012; Fattebert et al., 2015; Cozzi et al., 2020). However, increasing the forgiveness also implies that step durations of the retained steps become irregular, thus necessitating appropriate tools to account for such irregularity.

Various methods have been employed in the past to address temporal irregularities in animal location data. These may serve as valuable starting points for developing approaches that enable the integration of irregular data with iSSFs.

1. *Imputation*: An intuitive solution is provided by McClintock (2017), who suggests fitting a continuous-time correlated random walk movement model (Johnson et al., 2008) to the collected data and to use the fitted model to impute missing fixes. By imputing missing locations, the analysed trajectories become entirely regular again and can be analysed using traditional techniques. This approach, which we coin the *imputation* approach, is readily available through the R-package `crawl` (Johnson et al., 2024), yet has only been tested for use with hidden Markov movement models and not with iSSFs (McClintock, 2017).
2. *Naïve*: Another approach is outlined by Munden et al. (2021), who introduced time-varying iSSFs. In this framework, a change-point detection algorithm is applied to the series of observed animal locations to identify distinct decision points where the animal turns (Potts et al., 2018; Munden et

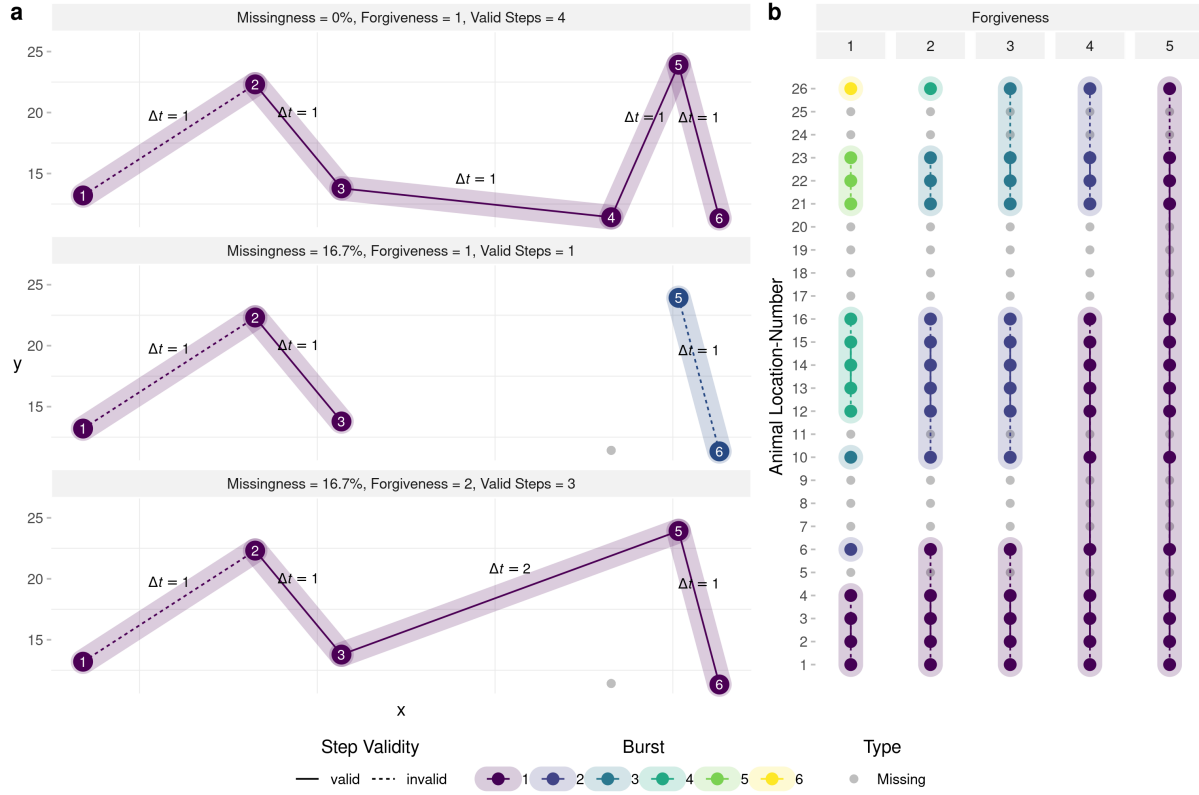


Figure 5.1.1: (a) Demonstration of how missingness affects the number of valid steps that can be used for step-selection analyses under different levels of forgiveness. The upper panel depicts a trajectory with zero missing locations. That is, all aspired locations were successfully collected on a regular interval (yielding a regular step duration of $\Delta t = 1$). This trajectory produces four valid steps that can be included in the iSSF model and one invalid step that has to be omitted because it has no turning angle associated with it. In the central panel, animal location 4 was not obtained, introducing a missingness of 16.7%. If the modeler has a forgiveness of one, only a single step can be included for further analysis, as all other steps are invalid (either because no turning angle can be computed or because step durations exceed the forgiveness). If, however, the modeler exhibited a forgiveness of two, such as in the lower panel, a total of three steps could be obtained for further analysis. (b) Conceptual illustration of how increasing the forgiveness level allows one to retain additional steps that can be used for step-selection analysis. The sequence of dots resembles the sequence of locations that were scheduled to be collected (e.g., using a GPS device), with the lines representing hypothetical steps. Because not all locations were successfully obtained (gray dots), there is missingness. Depending on the forgiveness level, already a single missing location enforces the introduction of a new burst, which leads to the loss of several steps. In addition, some of the remaining steps are invalid (dotted) because they are lacking a turning angle. By increasing the forgiveness, a modeler is willing to retain steps that exceed the regular step duration by a certain threshold, which enables them to obtain longer bursts and increase the number of steps that can be used for further analysis. In the figure, forgiveness increases from left to right.

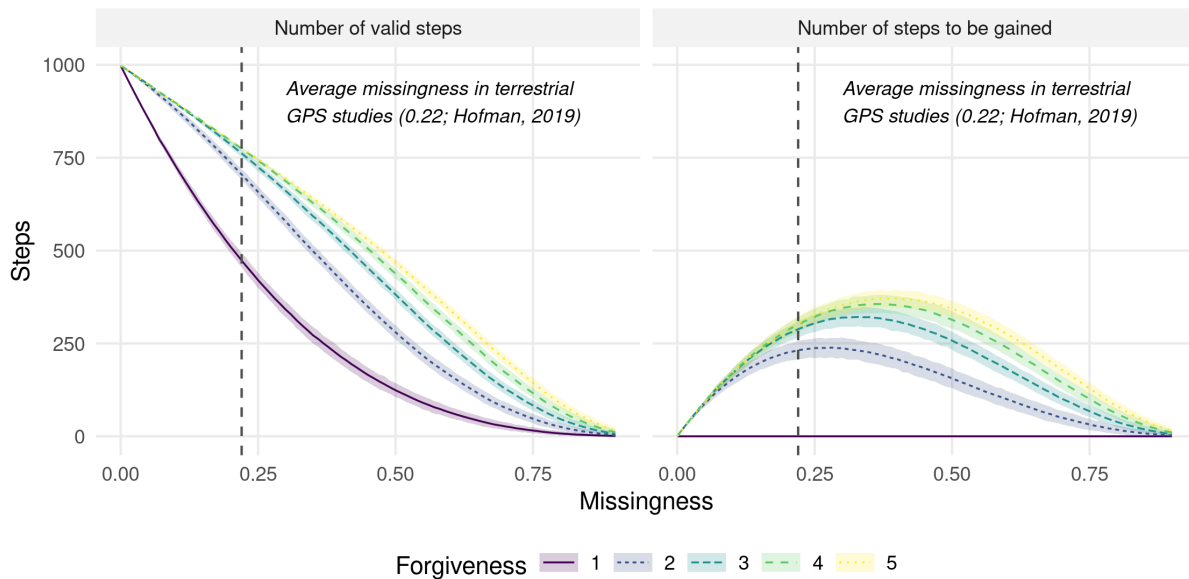


Figure 5.1.2: Illustration of how missingness in animal location data reduces the number of valid steps that can be used in step-selection analyses (left panel) and how increasing forgiveness helps to retain additional steps that are otherwise omitted (right panel). At a missingness of 0, 998 valid steps can be obtained from the total of 1,000 animal locations. At higher missingness, step durations become irregular, which means that the number of valid steps decreases substantially. However, if the modeler is willing to increase their forgiveness, additional steps can be gained. The right panel shows the number of valid steps that is gained when increasing the forgiveness from 1 to 2, 3, 4, and 5, respectively. Ribbons indicate the 95%-percentile intervals derived from 1,000 replicates.

al., 2021). Steps are then created to represent straight-line movements in-between these decision points, but because decision points are not regularly spaced in time, the resulting step durations are irregular. Thus, step durations are treated as random variables, and, instead of generating random steps by sampling step lengths and turning angles, the authors generate random steps by sampling step durations, step speeds, and turning angles. The underlying assumption is that step lengths scale linearly with step duration, and can therefore be meaningfully represented by combinations of step speeds and step durations. Although this approach was developed with ultra-high-frequency data in mind, we might *naïvely* apply it more broadly to the case of missing data if we believe the presumed linear relationship to hold true (this assumption may be reasonable when step durations are short, but it is unlikely to hold for longer step durations since an animal's path will deviate from a straight line between successive locations). Hence, we propose, with our *naïve* approach, to scale the generated random steps by the observed step duration.

3. **Dynamic+Model:** Instead of generating random steps by sampling step lengths and turning angles from distributions fitted to a single step duration, one may choose to fit separate distributions to steps of different durations, thus acknowledging potentially non-linear relationships between step duration and step lengths or turning angles. Because random steps in this approach are sampled using different tentative distributions, it is necessary to include interactions between step durations

and other step descriptors (e.g., sl, $\log(sl)$, and $\cos(ta)$) in the conditional logistic regression model to allow updating the distributions to the different step durations. We therefore refer to this approach as the *dynamic+model* approach, highlighting that step-length and turning-angle distributions are dynamically adjusted to observed step durations and that the step duration is included as a modifier of the coefficients of step descriptors in the regression model.

4. *Multistep*: Finally, we propose a *multistep* approach, where random steps of varying step durations are generated by stitching together sequences of random steps from the regular step duration. For example, one can generate a random step of duration $\Delta t = 2$ by combining two random steps of step duration $\Delta t = 1$.

Our goal with this article is to reassess the practice of discarding irregular animal locations in iSSFs and to investigate whether retaining irregular data could, in fact, serve to improve model performance. Our hypothesis is that even irregular data contains valuable information on habitat and movement preferences that could be leveraged if appropriate methods are applied. To test this notion, we conducted a comprehensive simulation study where we simulated regular animal location data with known movement and habitat parameters. We then introduced varying levels of missingness and applied iSSFs to estimate simulation parameters. Specifically, we employed the four alternative iSSF approaches outlined above and compared them to the traditional approach of including only bursts of regular data and to an uncorrected approach that simply ignored irregular step durations when using a forgiveness level > 1 . To examine the impact of different landscape configurations on derived estimates, we ran our simulations for different levels of spatial autocorrelation. The use of simulations instead of real data had the benefit that underlying parameters of the movement kernel and habitat-selection function were known, which allowed us to assess the reliability of different methods in retrieving true simulation parameters under different conditions (sensu Kéry and Royle, 2016). We then compare the traditional approach (using only bursts of steps with regular step durations) to the best-performing approach (with irregular data) using GPS locations collected on a spotted hyena (*Crocuta crocuta*).

We anticipated that increasing forgiveness without adjusting for the introduced irregularity would entail a bias-variance trade-off. Specifically, we anticipated that increasing forgiveness would allow improving estimator precision, but at the cost of introducing bias due to failing to account for irregular sampling intervals. We expected this bias to be particularly pronounced at high levels of missingness. Furthermore, we hypothesized that accounting for irregularity in the *naïve*, *dynamic+model*, and *multistep* approaches would improve model accuracy, while alleviating potential bias, thus providing an effective means of incorporating additional data. Because the *imputation* approach relied on an intermediate movement model to predict missing animal locations, we had no prior expectations for how well it would perform.

5.2 Materials and Methods

We implemented the simulation study in the programming language R version 4.3.2 (R Core Team, 2023) and achieved parallelization of simulation-runs using the R-package `pbmcapply` (Kuang, 2024). We generated figures using the `ggplot2` (Wickham et al., 2024), `ggpubr` (Kassambara, 2024), and `ggh4x` (Brand, 2024) R-packages. We manipulated raster data and computed spatial distances using the R-package `raster` (Hijmans et al., 2024). An overview of the simulation design and the different iSSF approaches is presented in Figure 5.2.1 and all codes to reproduce this study are available through an online repository (Hofmann, Cozzi, & Fieberg, 2023).

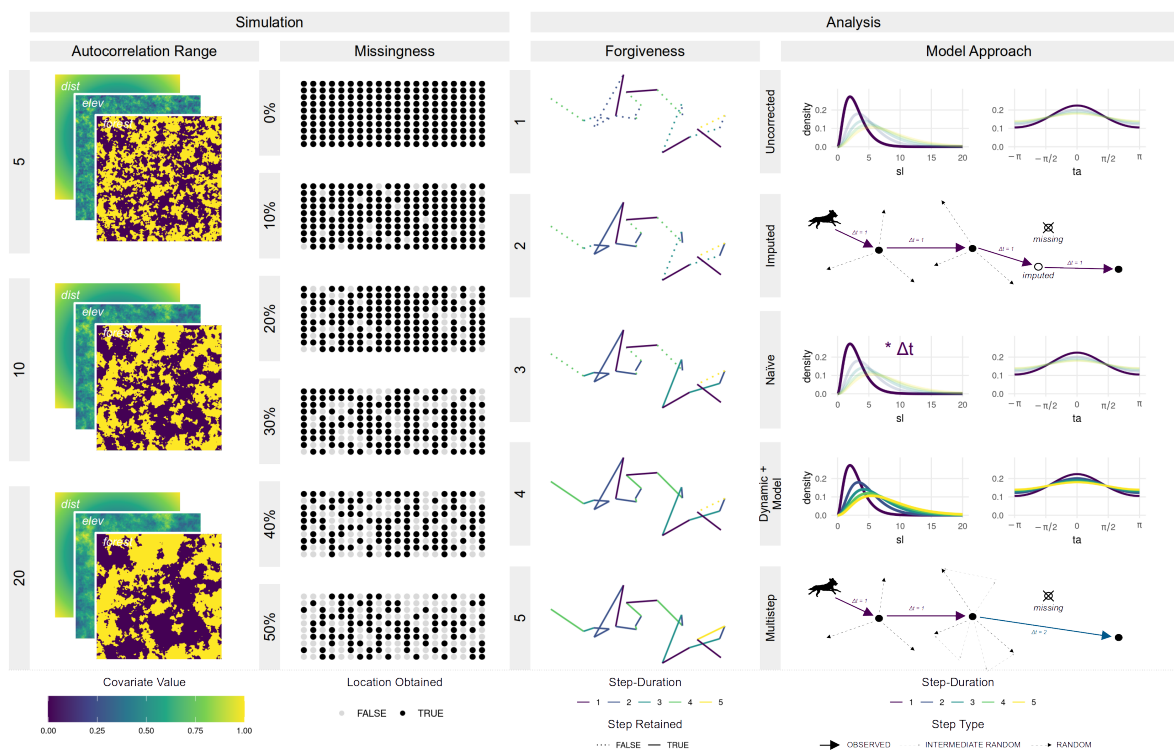


Figure 5.2.1: Illustration of the study design. We varied the autocorrelation range when simulating spatial covariates from 5 to 20 and tested for different missingness scenarios (ranging from 0% to 50% missing locations). To investigate how increasing forgiveness (i.e., the willingness to include steps with duration above the regular step duration) influenced model results, we varied its value from 1 (regular step selection) to 5 (considering steps that are five times the regular step duration). Finally, we tested five different methods to account for potential biases introduced by including irregular steps. This gave $3 \times 6 \times 5 \times 5 = 450$ combinations, each of which we replicated 100 times. We assumed step lengths (sl) to follow a gamma distribution, whereas turning angles (ta) followed a von Mises distribution.

5.2.1 Landscape Simulation

We simulated a virtual landscape comprising two continuous and one categorical (binary) spatial layers, each with a resolution of 300 x 300 pixels (Figure 5.2.2) and spanning across x- and y-coordinates from

0 to 300. The first layer, Dist (continuous), quantified the distance to the center of the virtual landscape ($x = 150, y = 150$), and can be understood as a point of attraction, such as, for instance, the center of an animal's home-range. The second layer, Elev (continuous), resembled an elevation layer and was simulated by sampling random pixel-values from a normal distribution. To achieve spatial autocorrelation, we applied a circular moving window with radius r within which we tallied pixel-values. We varied r from 5, to 10, to 20, depending on the simulated level of autocorrelation (Figure 5.A.1). The third layer, Forest (categorical), represented areas covered by woodland and was simulated similarly to the Elev layer, but we binarized the layer by setting all simulated values above the 50% quantile to forest and all other values to non-forest (our reference class). We normalized values of all simulated layers to a range between zero and one and replicated the simulation of each layer 100 times per autocorrelation scenario, thus producing 300 unique landscape configurations.

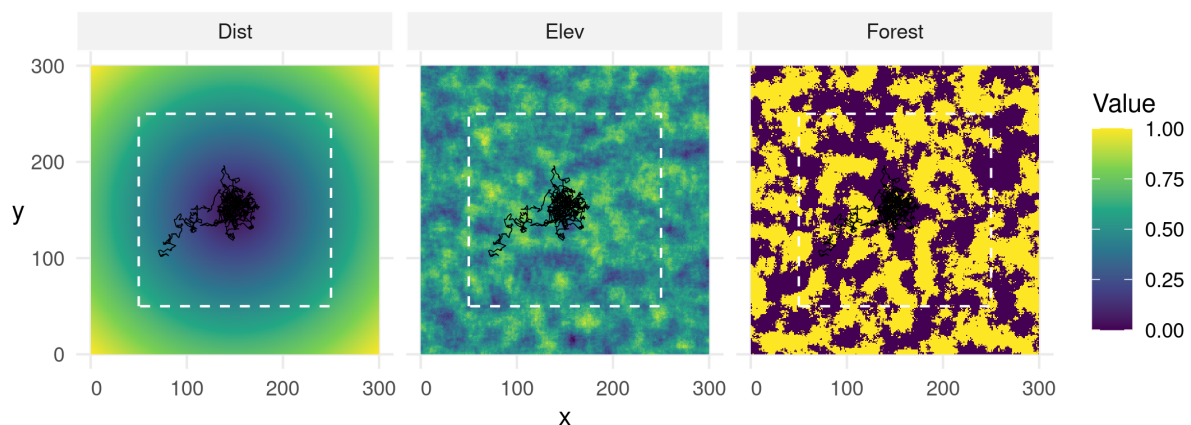


Figure 5.2.2: Example of a landscape configuration across which we simulated movement trajectories. All simulated layers had a resolution of 300 x 300 pixels. The distance layer indicated the distance to the center of the landscape and served to simulate attraction. The elevation and forest layers were simulated by sampling pixel-values from a normal distribution and applying a moving window to achieve spatial autocorrelation. Simulated individuals were initiated within the white dashed rectangle, which ensured that they would not be released directly at a map border. Simulated individuals were attracted to the landscape's center, preferred elevated areas, and avoided areas covered by forest. The black line shows the simulated trajectory associated with the visualized landscape configuration (cfr. Section 5.2.2).

5.2.2 Movement Simulation

To simulate movement across the virtual landscape, we employed the iSSF simulation algorithm developed by Signer et al. (2017) and applied in Hofmann, Cozzi, McNutt, et al. (2023). This procedure consists of a sequence of five steps that are repeated n times to generate a movement trajectory. In step one, we generated a random starting location by sampling random x- and y-coordinates on the simulated landscape. To prevent starting points near map borders, we restricted sampled locations to x- and y-coordinates be-

tween 50 and 250 (white dotted rectangle in Figure 5.2.2). In step two, we generated a set of 1,000 random steps originating from the current location, by sampling turning angles from a von Mises distribution with concentration parameter $\kappa = 0.5$ and step lengths from a gamma distribution with shape parameter $k = 3$ and scale parameter $\theta = 1$. In step three, we extracted covariate values at the end of each random step from the underlying covariate layers. In step four, we assigned to each step j a probability π_j of being selected using the equation below:

$$\pi_j = \frac{\exp(\beta^\top x_j)}{\sum_{i=1}^J \exp(\beta^\top x_i)} \quad (\text{Equation 5.2})$$

Here, β represents the vector of habitat-selection parameters and x_j the covariate value at the end of the j^{th} step. The probability of a step being selected thus depended on its associated covariate values, the covariate values of all other random steps, and the simulated preferences β . We defined the habitat-selection parameters as $\beta_{\text{dist}} = -20$, $\beta_{\text{elev}} = 0.5$, and $\beta_{\text{forest}} = -1$. That is, simulated individuals were attracted to the landscape's center, preferred elevated areas, and avoided areas covered by forest. In step five, we sampled one of the random steps based on predicted probabilities and computed the simulated individual's new position. We then repeated steps two through five until the trajectory comprised a total of 1,000 steps. Each simulated step was assumed to have a step duration of exactly $\Delta t = 1$. We repeated the simulation for each of the 300 simulated landscapes, producing 300 unique trajectories (example trajectory presented in Figure 5.2.2).

5.2.3 Data Rarefaction

To simulate missingness, we rarefied the trajectories by randomly removing a fixed fraction of animal locations. To assess the impact of different degrees of missingness, we varied the fraction of removed data from 0% (complete dataset) to 50% in increments of 10%. The random removal of animal locations introduced temporal irregularity, such that the resulting step durations differed depending on the time elapsed between remaining fixes. We replicated the rarefaction of each trajectory 100 times.

5.2.4 Computing Bursts

We used the rarefied data to compute bursts consisting of a sequence of animal locations with step durations that did not exceed the forgiveness value. To test how different levels of forgiveness impacted our results, we varied forgiveness from 1 (maximum allowed step duration was $\Delta t = 1$) to 5 (maximum allowed step duration was $\Delta t = 5$). As an example, if the forgiveness was 1, any step with step duration $\Delta t > 1$ resulted in a new burst. If the forgiveness was 2, in contrast, step durations of up to $\Delta t = 2$ were allowed before a new burst was introduced (Figure 5.1.1b). Within each burst, we calculated step

lengths and turning angles. However, due to the grouping of steps into bursts, the orientation of the first step within each burst relative to the previous step could not be determined. As a result, this step always lacked a turning angle and was considered invalid (Figure 5.1.1b).

5.2.5 Fitting Distributions

Based on the steps retained within bursts, we parametrized tentative step-length and turning-angle distributions. Specifically, we used the `fit_distr` function from the `amt` package (Signer et al., 2019), which is a wrapper function for the `fitdist` function from the `fitdistrplus` package (Delignette-Muller & Dutang, 2015), and fitted a gamma distribution to step lengths and a von Mises distribution to turning angles. Notably, we employed two different fitting procedures:

1. *Regular Distributions*: In this procedure, we fitted parametric distributions considering only step lengths and turning angles from steps that exhibited a step duration of $\Delta t = 1$ (i.e., the regular step duration). Any steps with irregular step durations ($\Delta t > 1$) were discarded and did not affect distributional parameter estimates. This represents the traditional procedure in iSSFs where only regular bursts of animal locations are considered when estimating tentative movement parameters.
2. *Dynamic Distributions*: In this procedure, we fitted separate parametric distributions to step lengths and turning angles from steps of different step durations. That is, we parametrized separate turning-angle and step-length distributions representative of steps with durations of $\Delta t = 1, 2, 3, 4$ and 5 (which corresponds to the maximum forgiveness level we tested for). Some step durations only rarely occurred at low levels of missingness, thus complicating parametrization of the associated distributions. To facilitate estimation of dynamic distribution parameters across all Δt (Figure 5.B.1), we resampled data to different step durations using the `track_resample` function from the `amt` package (Signer et al., 2019) before fitting tentative parameters. This ensured a sufficient number of steps for each step duration to estimate associated parameters. An alternative approach would be to increase missingness in the data even further, thus introducing a larger number of longer step durations.

5.2.6 Step-Selection Functions

We implemented a baseline *uncorrected* approach and four alternative iSSF approaches that mainly differed in the way in which random steps were generated, but sometimes also in the model call that was used to estimate parameters (Figure 5.2.1). In the *uncorrected* approach, we treated data as if they were regular, ignoring potential issues arising from having variable step durations. When forgiveness was one, this approach corresponded to the traditional iSSF approach. All other approaches were targeted towards

reducing potential biases arising from the inclusion of steps with irregular step durations. Irrespective of the approach employed, we paired each observed step with a total of 200 random steps:

- **Uncorrected:** In the uncorrected approach, we generated random steps by sampling step lengths and turning angles from statistical distributions fitted to steps with step durations of $\Delta t = 1$, regardless of the forgiveness value or observed step durations. Thus, this approach ignored any potential effect of step duration when generating random step lengths and turning angles.
- **Imputed:** In this approach, we sampled step lengths and turning angles from statistical distributions fitted to observed steps with a step duration of $\Delta t = 1$. However, prior to generating random steps, we imputed missing fixes using predictions from a simple movement model. Specifically, we fitted a single-state movement model (Johnson et al., 2008) to the simulated trajectories and used the parametrized model to predict coordinates for all missing animal locations. For this, we used the functions `crwFit` and `crwPredict` from the `crawl` R-package (Johnson et al., 2024). Although the `crwFit` function provides capabilities to incorporate location measurement error, we assumed animal locations were measured without error. The imputation resulted in a complete dataset without any missing animal locations, such that each trajectory consisted of a single continuous burst of locations equally spaced in time. As such, the imputation approach is not affected by the forgiveness level.
- **Naïve:** In the *naïve* approach, we again sampled step lengths and turning angles from regular distributions fitted to steps with step durations of $\Delta t = 1$. However, we linearly scaled the sampled step lengths depending on the step durations of the observed steps. For instance, we doubled the sampled step lengths for any observed step with a step duration of $\Delta t = 2$. This approach naïvely assumed that step lengths scale linearly with step durations, which is unlikely to be true, as most animals don't move in straight lines between successive observations. Furthermore, the linear approximation is likely to get worse as step duration increases (i.e., as the forgiveness value increases). Since it is not clear how turning angles should scale with step duration, we did not adjust the sampled turning angles.
- **Dynamic+Model:** In the *dynamic+model* approach, we sampled step lengths and turning angles from dynamic distributions that were fit to different step durations. That is, for observed steps with step duration of $\Delta t = 2$, we sampled step lengths and turning angles from distributions fit to observed steps with $\Delta t = 2$. We then included interactions between the step duration and other step descriptors (e.g., `sl`, `log(sl)`, `cos(ta)`), allowing us to update movement parameters for each step duration separately. To avoid numerical instabilities with the conditional logistic regression model, we only

included steps with durations $\Delta t > 1$ if the respective duration was represented at least 5 times in the rarefied dataset.

- **Multistep:** In the *multistep* approach, we sampled step lengths and turning angles from statistical distributions fitted to observed steps with step durations of $\Delta t = 1$. We then generated a sequence of random steps such that their combined step duration equaled the step duration of each observed step. For instance, for an observed step with step duration of $\Delta t = 2$, we generated sets of two random steps, which we then concatenated into a “random path”. The paths were then simplified to straight lines connecting the first and last coordinate of each path, which represented the final random step.

Together, an observed step and its 200 associated random steps formed a *stratum* that received a unique ID. At the end of each step, we extracted covariate values from the underlying covariate layers.

5.2.7 Conditional Logistic Regression Model

We estimated movement and habitat-selection parameters for the simulation scenarios presented in Figure 5.2.1 using conditional logistic regression, implemented using the `clogit` function in the R-package `survival` (Therneau, Lumley, et al., 2024). We defined a binary response variable (`observed`) indicating if a step was an observed (scored 1) or a random step (scored 0) and used the step’s ID as a stratification variable. We included habitat covariates (`dist`, `elev`, `forest`) and step descriptors (`sl`, `log(sl)`, `cos(ta)`) as predictors in the regression model. For the *dynamic+model* approach, we also included interactions between the step duration, coded as a factor, and step descriptors. To update tentative movement parameters (denoted by the subscript 0) and obtain the selection-free movement kernel (denoted by the $\hat{\cdot}$ symbol), we employed the formulas provided in (Avgar et al., 2016; Fieberg et al., 2021). Specifically, we updated the shape (\hat{k}) and scale ($\hat{\theta}$) parameters of the step-length distribution (gamma) using:

$$\hat{k} = k_0 + \beta_{log(sl)}$$

$$\hat{\theta} = \frac{1}{\frac{1}{\theta_0} - \beta_{sl}}$$

We updated the concentration parameter ($\hat{\kappa}$) of the turning-angle distribution (von Mises) using:

$$\hat{\kappa} = \kappa_0 + \beta_{cos(ta)}$$

We kept track of the estimates of the updated movement (\hat{k} , $\hat{\theta}$, and $\hat{\kappa}$) parameters and the habitat-selection ($\hat{\beta}_{dist}$, $\hat{\beta}_{elev}$, $\hat{\beta}_{forest}$) parameters, and compared them to the true simulation parameters. We also quantified model accuracy via the root-mean-square error (RMSE).

5.3 Results

Results were qualitatively similar for all three landscape autocorrelation scenarios and for different combinations of missingness and forgiveness (Figure 5.D.1). Here, we report on results for a landscape with autocorrelation of 20, while either holding constant missingness at a conservative 20% (Figure 5.3.1) or the forgiveness level at two (Figure 5.3.2) (results for all other combinations are summarized in Figure 5.D.1). The *imputation* approach resulted in biased estimators of β_{dist} and β_{forest} , whereas all other approaches were able to recover the parameters of the habitat-selection function with minimal bias (Figure 5.3.1). Note, the *imputation* approach always starts with a full trajectory and is therefore unaffected by the forgiveness level. For all other methods, increasing the forgiveness from 1 to 5 improved the precision of the estimators of habitat-selection parameters without introducing noticeable bias, with the biggest gains in precision and RMSE occurring when moving from a forgiveness of one to a forgiveness of two (Figure 5.3.1). This highlights the potential benefits of leveraging additional data compared to the traditional approach, which uses only bursts of regular data (represented by the *uncorrected* approach and forgiveness = 1).

The *uncorrected*, *naïve*, and *imputation* approaches resulted in biased estimators of the parameters in the movement kernel, particularly for high values of forgiveness (Figure 5.3.1a) and high levels of missingness (Figure 5.3.2a). The *imputation* approach appeared to perform particularly poorly at estimating the concentration parameter of the turning-angle distribution (Figure 5.3.2). The *multistep* and *dynamic+model* approaches resulted in unbiased estimators of parameters in the step-length distribution, but estimators of the concentration parameter exhibited a slight bias. This bias was, however, much smaller than we observed with the other approaches we considered. Increasing missingness negatively influenced the precision and accuracy of estimates, yet its impact could be dampened using the *dynamic+model* and *multistep* approaches (Figure 5.3.2b).

5.4 Case Study

To showcase the applicability of the *dynamic+model* approach, which appeared to perform best with simulated data, we conducted a case study with real GPS data obtained on “Apollo”, a spotted hyena (*Crocuta crocuta*) inhabiting the Okavango Delta ecosystem in northern Botswana. Apollo’s data were collected between 2007 and 2011 using GPS radio collars (*GPS Plus*; Vectronic Aerospace GmbH, Berlin, Germany)

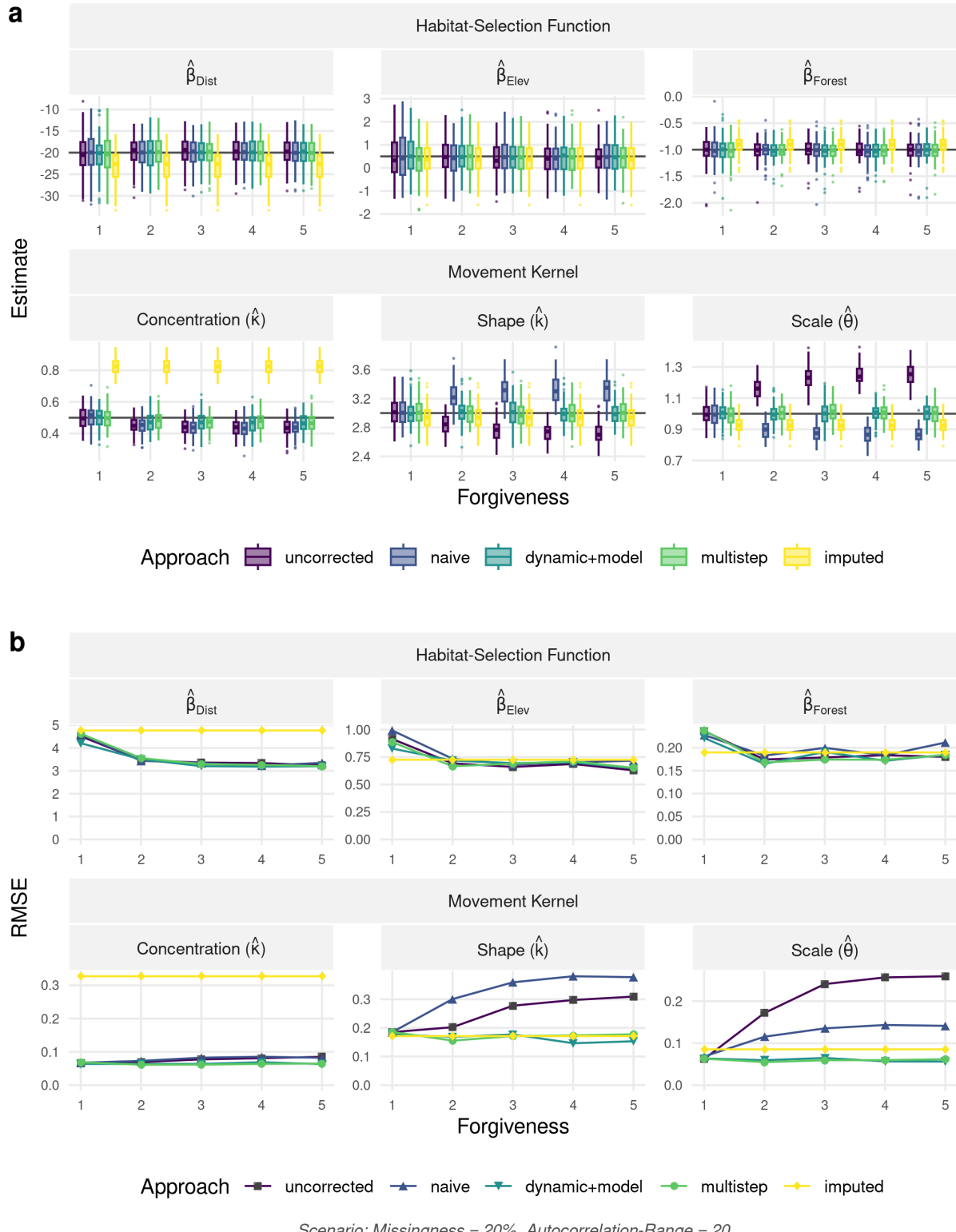


Figure 5.3.1: (a) Parameter estimates and (b) Root mean-square error (RMSE) with regard to the movement kernel and habitat-selection function as a function of forgiveness. Results are shown for the scenario with landscape autocorrelation of 20 and missingness of 20%. The movement kernel comprised of a gamma distribution with shape parameter k and scale parameter θ governing the step-length distribution and a von Mises distribution with concentration parameter κ governing the turning-angle distribution. Habitat-selection was based on three covariates, namely a Distance, Elevation, and a Forest layer. Estimates are shown for the five different approaches we tested for. The uncorrected approach ignored the fact that higher forgiveness implied temporal irregularity in the data, while all other approaches attempted to correct for the potential biases introduced by temporal irregularity. Note, the imputation approach is not affected by the forgiveness level, since it always starts with a full trajectory.

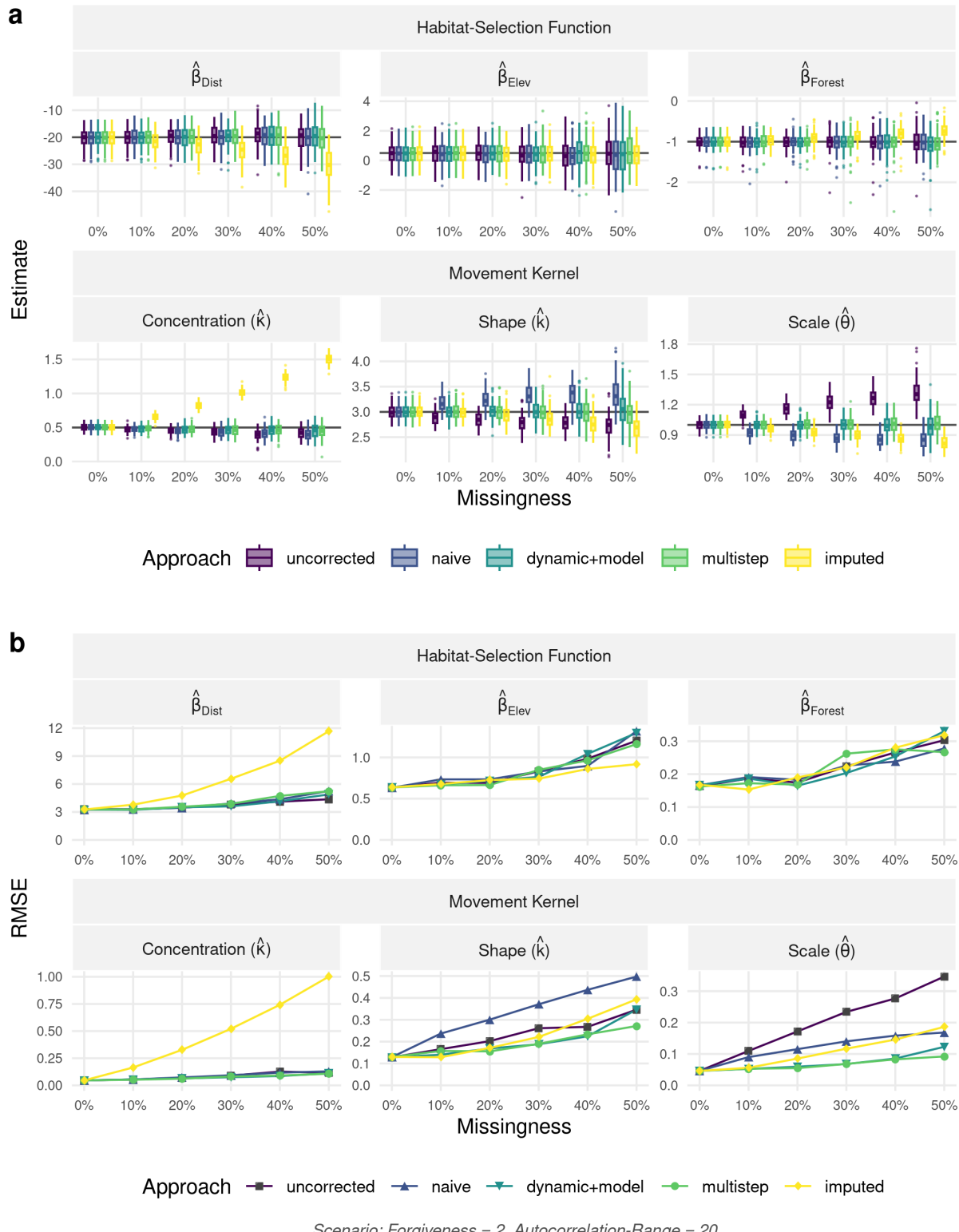


Figure 5.3.2: (a) Parameter estimates and (b) Root mean-square error (RMSE) with regard to the movement kernel and habitat-selection function as a function of missingness. Results are shown for the scenario with landscape autocorrelation of 20 and forgiveness of 2. The movement kernel comprised of a gamma distribution with shape parameter k and scale parameter θ governing the step-length distribution and a von Mises distribution with concentration parameter κ governing the turning-angle distribution. Habitat-selection was based on three covariates, namely a Distance, Elevation, and a Forest layer. Estimates are shown for the five different approaches we tested for. The uncorrected approach ignored the fact that higher forgiveness implied temporal irregularity in the data, while all other approaches attempted to correct for the potential biases introduced by temporal irregularity. Note, the imputation approach is not affected by the forgiveness level, since it always starts with a full trajectory.

and comprised 9,316 GPS locations (details in Cozzi, 2013 and Cozzi et al., 2015). Because hyenas are nocturnal (Cozzi et al., 2012), GPS collars were set to record data at two-hourly intervals between 18:00 and 06:00 o'clock, and to only record a single location at noon. For simplicity, we only considered nightly bursts and removed all locations obtained at noon. Missingness in this dataset was low (< 10 %, Cozzi et al., 2015) and to better showcase the usefulness of the *dynamic+model* approach, we thinned the data by randomly removing 25% of the obtained locations. As spatial covariate layers, we used Water, DistanceToWater and Trees (Figure 5.E.1). Water was a binary variable representing major rivers and areas inundated by floodwater, whereas DistanceToWater was a continuous variable indicating the distance (in meters) to the nearest pixel categorized as water. Trees was a continuous variable indicating the percent tree cover in each pixel. We resampled all layers to a common resolution of 250 m by 250 m and merged them into a single raster-stack (Figure 5.E.1). The derivation of each covariate layer is described in detail in Hofmann et al., 2021. We dynamically fitted step-length and turning-angle distributions to steps with step durations of 2, 4, and 6 hours, respectively, assuming a gamma distribution for step lengths and a von Mises distribution for turning angles. Instead of resampling the observed track to different step durations when fitting dynamic distributions (like we did in the simulation study), we introduced a larger amount of steps with step durations longer than two hours by thinning the data again (by another 10%). The benefit of this approach was that steps with irregular step durations occurred more randomly and were not limited to the hours specified by the resampling algorithm. Finally, we used iSSFs with the *dynamic+model* approach to estimate the habitat-selection function and movement kernel of Apollo. For this, we considered three cases:

- F1: We assumed a forgiveness of one (i.e., only steps with a regular step duration of 2 hours), which is akin to conducting a traditional iSSA.
- F3-S: We assumed a forgiveness of three (i.e., considered steps with step durations of up to three times the regular step duration) and included interactions between the step duration (Δt) and step descriptors (sl, log(sl), and cos(ta)) in the regression model.
- F3-SH: We assumed a forgiveness of three (i.e., considered steps with step durations of up to three times the regular step duration) and included interactions between the step duration (Δt) and step descriptors (sl, log(sl), and cos(ta)), as well as between the step duration and habitat covariates in the regression model.

Notably, we included F3-SH to investigate if including interactions between the step duration and habitat-covariates would provide insights into scale-dependent habitat selection. In all cases, we generated 200 random steps and extracted spatial covariates at the end of observed and random steps. We then fit the three models using the conditional logistic regression framework as implemented in the `survival`

R-package (Therneau, Lumley, et al., 2024). Lastly, we computed updated movement parameters for a regular step duration of 2 hours.

Results from the iSSF models show that increasing the level of forgiveness led to improvements in estimator precision (Figure 5.4.1). This was achieved by increasing the effective sample size from 2,179 to 4,505 valid steps (Table 5.F.1). The improvement in estimator precision was weaker for F3-SH than for F3-S, as the F3-SH model was more complex due to inclusion of additional interaction terms. Point estimates for the habitat-selection and movement parameters were similar for all 3 models, and evidence for scale dependency in habitat selection was fairly weak. F3-S and F3-SH had similar AIC scores ($\Delta AIC \leq 1$; Table 5.F.1), and the interaction terms were statistically significant only for the step duration of 6 hours and only for one of the habitat covariates (Table 5.F.1).

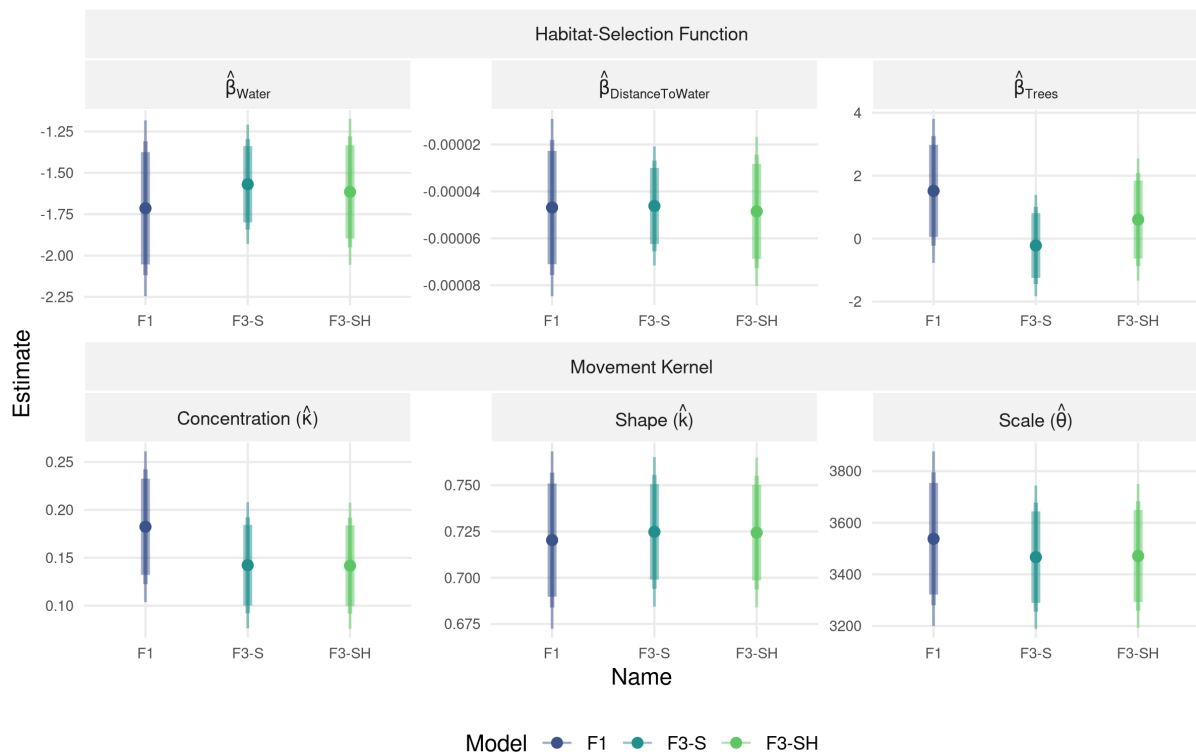


Figure 5.4.1: Model results from the case study using GPS data collected on Apollo. In F1, forgiveness was set to one (only 2-hour steps were considered), whereas in F3-S and F3-SH a forgiveness of three was employed (allowing for step durations of up to 6 hours). In model F3-S, the step duration was interacted with step descriptors. In model F3-SH, step duration was interacted with step descriptors and habitat covariates. The bars indicate the 90%, 95%, and 99% confidence intervals. Note that for simplicity, we omitted interactions with the step duration from this figure.

5.5 Discussion

We conducted a simulation study with known habitat and movement parameters to investigate if retaining irregular animal locations via increased forgiveness improves or worsens parameter estimation in iSSFs.

We also tested the performance of four different approaches that attempt to correct for potential biases introduced by using temporally irregular data, and we compared them to an uncorrected baseline approach. Our results demonstrated that retaining irregular animal locations can improve the precision of estimators of habitat-selection parameters but may lead to biased estimators of the parameters in the movement kernel. Overall, our results highlight the potential benefits of leveraging irregular animal locations, especially if an appropriate method for handling irregular data is chosen.

The *uncorrected* baseline approach ignored the fact that increasing forgiveness introduced irregularity in the data. Consequently, estimators of the parameters in the movement kernel were increasingly biased as forgiveness increased due to the inclusion of steps with varying step durations when fitting the model. Steps with longer step durations tended to have larger step lengths and less directed turning angles, which led to an overestimation of θ and underestimation of k and κ . Yet, estimators of the habitat-selection parameters remained unbiased or nearly so, even at high levels of forgiveness, and they were more precise than the standard estimator (represented by the *uncorrected* approach with forgiveness = 1). These results highlight the potential benefits that can be reaped by including additional data.

Similarly, the *naïve* approach performed well when estimating habitat-selection parameters but resulted in biased estimators of movement parameters, especially for large forgiveness values. This result was unsurprising given that our simulated trajectories were tortuous, and therefore, step lengths were not linearly related to step durations. Indeed, we found that, although there was a near linear relationship between step duration and the (tentative) scale parameter (θ_0), the relationships between step duration and the (tentative) movement parameters κ_0 and k_0 were non-linear (Figure 5.B.1). Overall, the usefulness of this approach appears highly limited, as it is often not clear by what factor distributional parameters for step lengths and turning angles should be multiplied to match the observed step duration.

The *dynamic+model* approach provided a flexible, easily implementable, and powerful framework for retrieving precise and unbiased estimators of the step-length and habitat-selection parameters, irrespective of the forgiveness level. The estimator of the concentration parameter exhibited some bias, but less than when using the *uncorrected* and *naïve* approaches. To implement the *dynamic+model* approach, we included interactions between step descriptors (sl, log(sl), and cos(ta)) and step duration in the conditional logistic regression model. This allowed the parameters of the movement kernel to depend on the step duration. A complication, however, is that turning angles are influenced by the step duration of both the current and previous step (Figure 5.C.1). The bias in the concentration parameter likely arose from only accounting for the step duration associated with the current step and not the previous one. Moreover, fitting tentative distributions for different step durations can be challenging due to some step durations occurring only rarely. However, by resampling observed animal locations to different step durations using the `track_resample` function from the `amt` R-package (Signer et al., 2019) the needed data can easily be

generated. We included step duration as a categorical covariate, yet there may be times when it would be advantageous to treat it as a continuous covariate (e.g., with its effect modeled using a low-degree polynomial or regression spline with few degrees of freedom). Treating step duration as a continuous variable may help to alleviate convergence issues in cases where some step durations are rare, and it might allow applying the *dynamic+model* approach to data that are entirely irregular.

The *multistep* approach also performed well and was relatively easy to implement. This approach is somewhat *ad hoc* in that it uses the tentative movement parameters to generate random steps to match observed steps with longer step durations (in multiples of Δt). It is similar to, but slightly less principled, than the approach developed by Vales et al. (2022), which formally constructs the likelihood for multistep durations by integrating out the missing steps. An advantage of this latter approach is that one can also attempt to account for non-random missingness by explicitly modeling factors related to the probability of obtaining a successful location (Vales et al., 2022). Nonetheless, integrating over the missing steps, as in Vales et al. (2022), can be computationally intensive and prohibitive with large data sets. Another downside of both of these approaches (the *multistep* approach and the approach of Vales et al., 2022) is that they can only be applied in cases where step durations are a fixed multiple of the regular step duration; i.e., unlike the *dynamic+model* approach, they cannot be applied when data are highly irregular.

Of the methods we considered, the *imputation* approach performed the worst. It resulted in biased estimators of parameters in both the habitat-selection function and the movement kernel. This bias likely resulted from using an overly simplistic movement model to impute missing fixes. Moreover, the imputation procedure may have led to imputed animal locations that masked important selection properties, therefore leading to inaccurate parameter estimates. While this approach appears to perform well with hidden Markov movement models (McClintock, 2017), we advise against its use with iSSFs.

For the scenarios we considered in our simulation study, the estimators of habitat-selection parameters were insensitive to the inclusion of irregular data and performed well, except for the *imputation* approach. This suggests that accounting for irregular step durations may not be particularly important if one is only interested in the habitat-selection function. When the movement kernel is also of interest, we suggest the *dynamic+model* approach, since it is flexible, easy to implement, and allows one to use more data than the traditional approach that requires bursts of regular data, leading to more precise estimators.

Several authors have emphasized that movement and habitat-selection parameters in an SSF are scale dependent and should be expected to change as the sampling frequency changes (see for example Avgar et al., 2016; Signer et al., 2017; Fieberg et al., 2021). Furthermore, Barnett and Moorcroft (2008) developed an analytical framework for investigating scale dependence and showed that habitat-selection parameters should depend on the relative width of the movement kernel in relation to habitat heterogeneity. Thus, the relative insensitivity of the habitat-selection parameters to the inclusion of steps with varying step

duration was somewhat unexpected. It would be interesting to explore the robustness of this result across a wider range of simulation scenarios in the future.

More generally, the spatial scale of a habitat-selection analysis has been recognized as an important factor, which is why Johnson (1980) proposed a hierarchical framework for examining habitat-selection across different orders (e.g., species range, individual home range, within a home range). Johnson's proposed framework acknowledges that habitat-selection may act differently at different scales, and that the interpretation of ecological processes changes depending on the spatial scale at which they are investigated (Wiens, 1989; Levin, 1992). This understanding has encouraged scientists to conduct extensive scaling analyses and to comprehensively examine habitat-selection at multiple scales (DeCesare et al., 2012; McGarigal et al., 2016; Pitman et al., 2017; Zeller et al., 2017). In studies employing SSAs, the issue of scale is often neglected, and data are most frequently analyzed at the spatio-temporal scale at which they were collected. This choice maximizes the number of locations that can be used in the analysis, yet prevents a thorough understanding of scale dependency. The use of irregular data in SSAs poses another challenge, as steps with unequal step durations may reflect selection processes occurring at different scales. The severity of this issue obviously depends on the original sampling frequency, the degree of missingness, and the scale at which animals are making decisions that are relevant in terms of their movement behavior and habitat selection. By including irregular animal locations via increased forgiveness, we may therefore average over selection processes occurring at multiple scales, which could produce estimates of habitat-selection parameters that are misleading due to contradictory effect signs at different scales. To better account for such scale-dependent processes, it may be beneficial to include interactions between step duration and habitat features (e.g., dist, elev, forest), thus allowing habitat-selection parameters to also vary as a function of step duration. We demonstrated how this could be implemented in the case study.

It is important to note that we considered a limited number of scenarios in our simulation study. For instance, we assumed that animal locations were missing at random, i.e., failure to obtain a fix was unrelated to habitat types, time of the day, etc. However, several studies have shown that missingness is often non-random and related to difficulties with satellite transmission due to topography (Lewis et al., 2007), canopy cover (Phillips et al., 1998; DeCesare et al., 2005; Hansen & Riggs, 2008), time of the day (Graves & Waller, 2006), animal behavior (Mattisson et al., 2010), or collar orientation (D'eon & Delparte, 2005). In fact, Vales et al. (2022) highlighted that missingness and the associated under-representation of certain habitat types may lead to biased estimators of parameters in iSSFs, but that accounting for the probability of obtaining a location in differing environmental conditions may alleviate this bias. Future studies should strive to further investigate these relationships and examine how our proposed approaches perform when missingness is habitat-dependent.

A major benefit of using iSSFs is the ability to allow an individual's movement kernel to depend on local habitat features (Avgar et al., 2016). In our simulation study, we considered simplified scenarios where the movement kernel was unchanging, which simplified the simulation and inference. Nevertheless, such interactions often play a crucial role in real ecosystems. For instance, Dickie et al. (2020) employed iSSFs and revealed that several large mammal species moved faster while on linear features. Similarly, Hofmann, Cozzi, McNutt, et al. (2023) found that African wild dogs moved significantly slower and less directed in areas that were covered by floodwater. Future studies could investigate simulation scenarios in which individuals alter their movement tendencies in response to local environmental features (i.e., models with habitat dependent movement kernels) and examine how this influences the robustness of our proposed approaches.

While our results suggest that irregularity due to missing animal locations can effectively be accounted for in iSSFs and that increasing the forgiveness, thus allowing for inclusion of irregular data, improves estimator precision, we also found a decreasing marginal benefit of increased forgiveness. In fact, increasing the forgiveness beyond a value of two (i.e., allowing for steps of twice the regular step duration) only marginally improved model performance in our case. This can also be seen in Figure 5.1.2, which shows that the largest number of steps that can be gained is when increasing the forgiveness level from one to two. Having a higher forgiveness beyond two may thus not even be necessary, therefore limiting the need to correct biases emerging from the inclusion of irregular data.

Although we focused on the case of missing location data, the proposed approaches may also prove useful for situations where sampling is irregular for other reasons. For example, it is not uncommon to adjust sampling regimes after a preliminary phase, following improvements to collar-battery-lifetime, or for sampling rates to vary depending on type and manufacturer of the collar (Brown et al., 2023). Similarly, it is common practice to adjust the GPS regime to the biology of the focal species and only record data during a specific time of the day (e.g., Broekhuis et al., 2013; Cozzi et al., 2013; Elliot et al., 2014). These irregularities might be addressed using the *dynamic+model* approach, with interactions between step duration and movement descriptors. Interactions between step duration and habitat-selection covariates should also be considered, particularly if the sampling regime is adjusted to coincide with changes in animal behavior. We expect this approach will work fairly well in many cases, but we might expect a slight bias in the estimated concentration parameters, as observed in our simulation study.

Our study contributes to the growing body of literature that extends iSSFs and improves the method's robustness under various conditions. This includes approaches for modeling irregular data (Munden et al., 2021; Eisaguirre et al., 2024), accounting for spatial dependence among residuals (Arce Guillen et al., 2023), methodological frameworks for fitting iSSFs with random slopes (Muff et al., 2020) and random smooths (Klappstein et al., 2024), incorporating the probability of successfully obtaining an animal location

in different habitat conditions (Vales et al., 2022), and considering the behavioral states of the tracked animals (Klappstein et al., 2023; Pohle et al., 2023).

In conclusion, our study shows that inclusion of irregular animal locations can improve model performance, yet only when an appropriate approach to account for irregularity is selected. Here, the *dynamic+model* and *multistep* approaches performed well and resulted in improved estimators of habitat-selection and movement parameters, even at elevated levels of missingness and forgiveness. Both methods are easy to implement, and the associated models can readily be fitted using the R-packages `amt` (Signer et al., 2019), `survival` (Therneau, Lumley, et al., 2024), `coxme` (Therneau, 2024), and `mgcv` (Wood, 2011; 2017; Klappstein et al., 2024). To facilitate uptake and encourage use of the proposed approaches among practitioners, we provide all of our codes through an online repository, which includes an example application of the *dynamic+model* approach. With this, we hope practitioners will rethink the common use of discarding large portions of data and instead use methods that can accommodate irregular data.

Appendices

5.A Landscape Simulation: Different Autocorrelation Scenarios

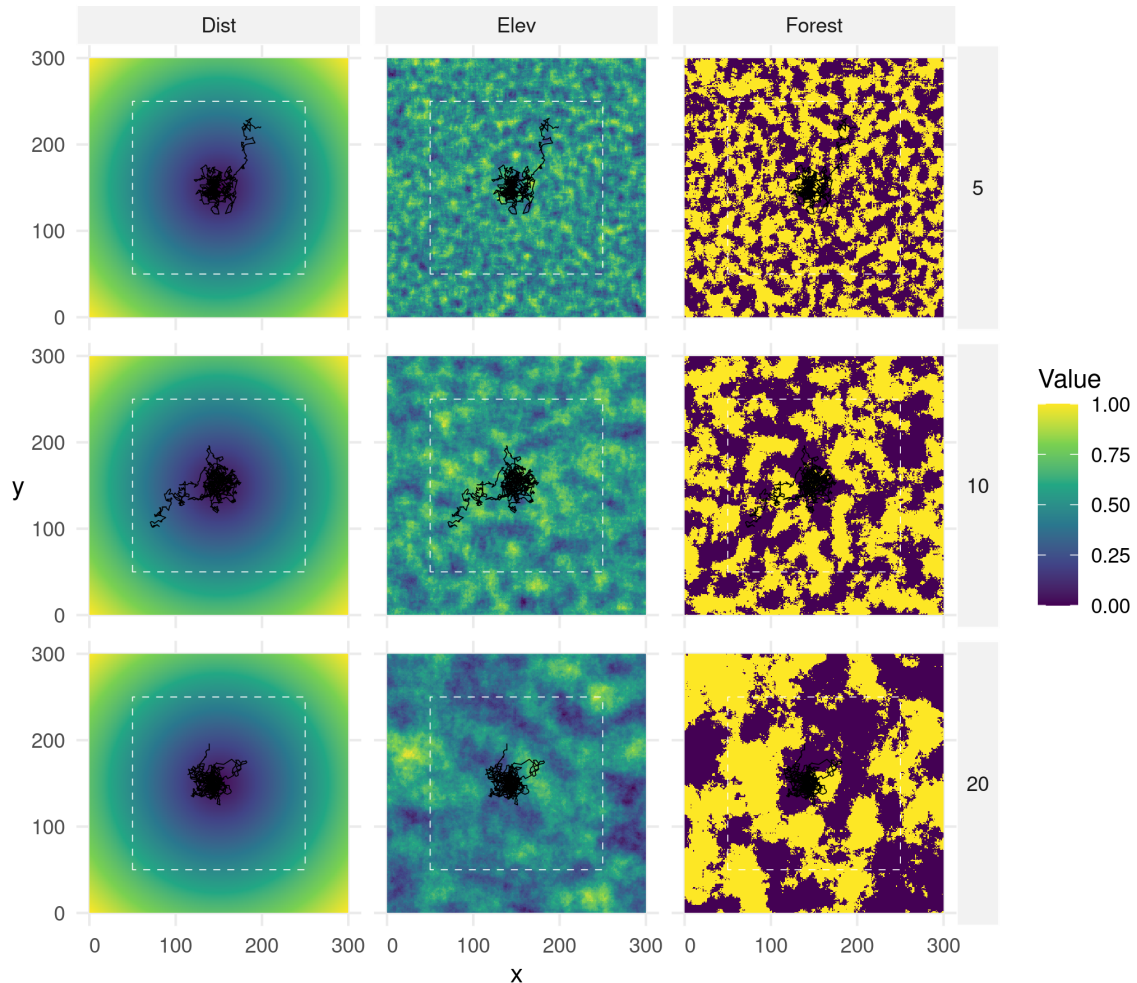


Figure 5.A.1: Simulated landscapes under different levels of autocorrelation (5, 10, 20; from top to bottom). Autocorrelation only affected the layers elev and forest, which were both simulated using a Gaussian random field neutral landscape model (Schlather et al., 2015) using the R-package NLMR (Scaini et al., 2018). Simulations were repeated 100 times for each autocorrelation scenario, thus resulting in 300 unique landscape configurations.

5.B Dynamic Tentative Distribution Parameters

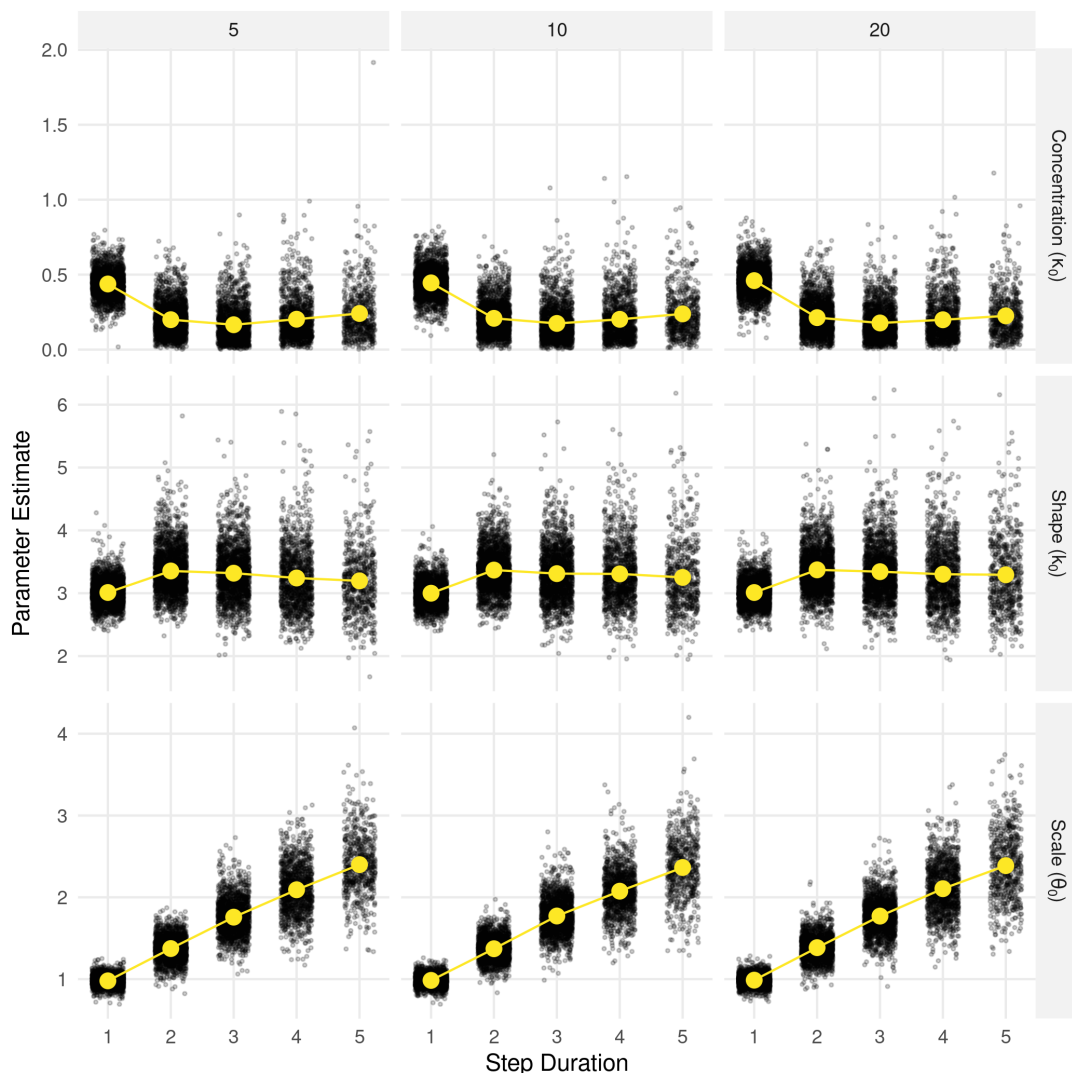


Figure 5.B.1: Tentative parameter estimates for the von Mises distribution (top row) and gamma distribution (bottom row) fitted to steps with different durations. The von Mises distribution requires one parameter, namely a concentration parameter (κ). The gamma distribution requires a shape parameter (k) and a scale parameter (θ). The subscript $_0$ is used to indicate that these are tentative distribution parameters (sensu Avgar et al., 2016 and Fieberg et al., 2021).

5.C Distribution of Relative Turning Angles following Different Step Durations

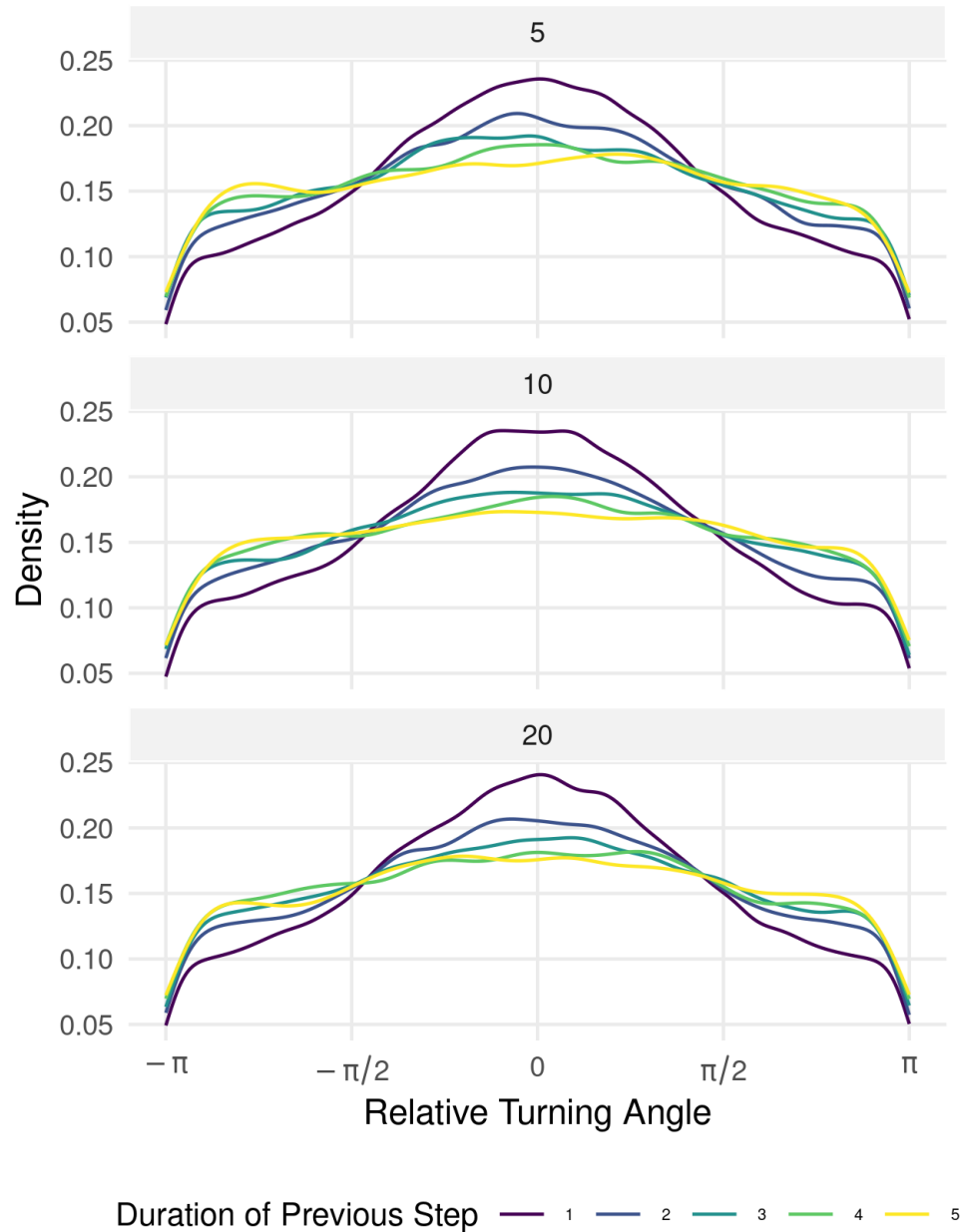


Figure 5.C.1: Density of relative turning angles associated with steps of $\Delta t = 1$ following steps with different durations for all three autocorrelation scenarios (5, 10, and 20). To generate this figure, we assumed a missingness of 0.5 and forgiveness of 5.

5.D Model Estimates across all Scenarios

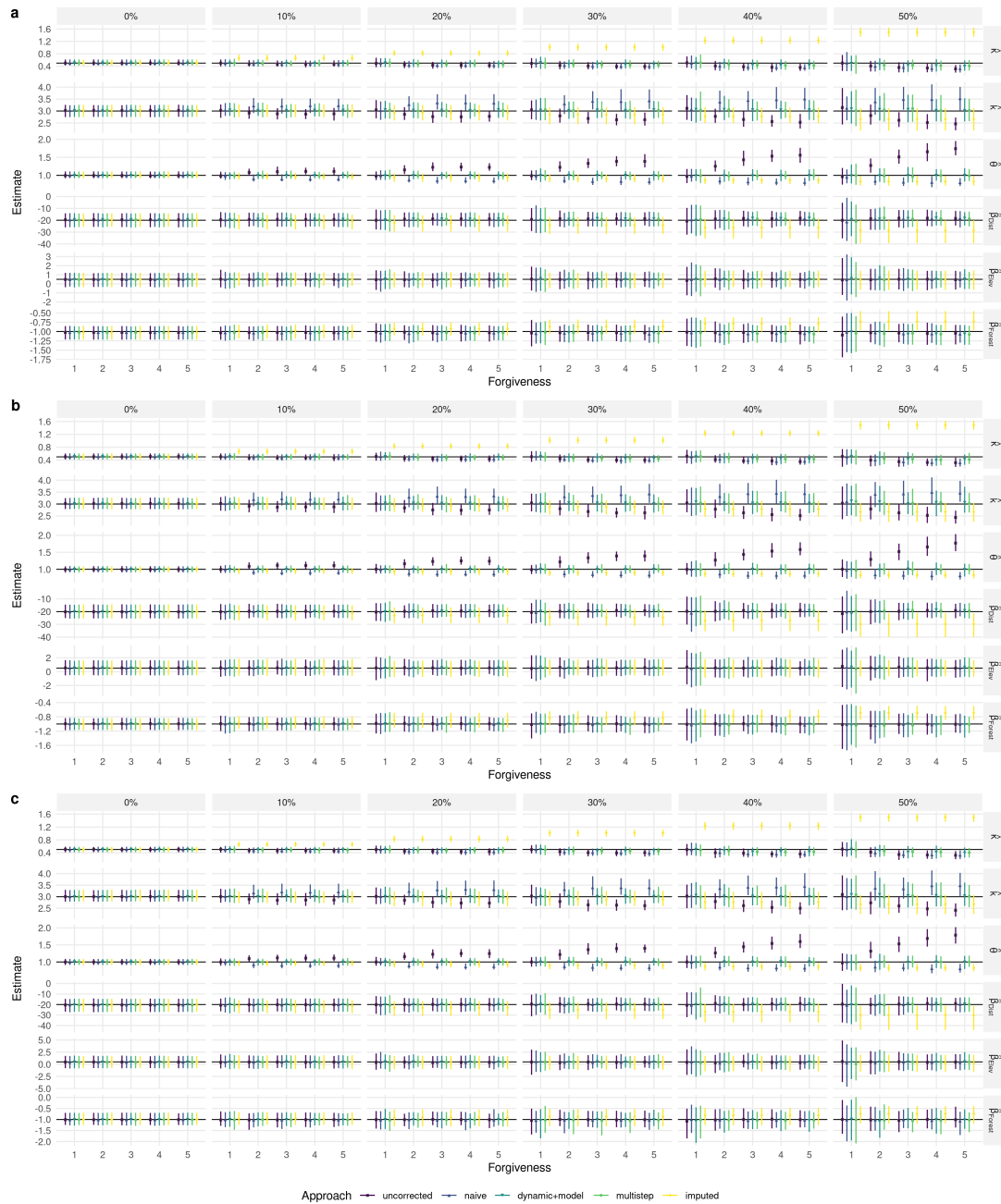


Figure 5.D.1: Parameter estimates across different autocorrelation scenarios (5, 10, 20; panels a, b, and c) and missingness levels (0% - 50%; from left to right). True simulation parameters are indicated by the solid black lines. Parameter estimates from the different approaches are given by the colored symbols, and their bootstrap 95% CIs across 100 replicates by the colored lines.

5.E Case Study Covariates

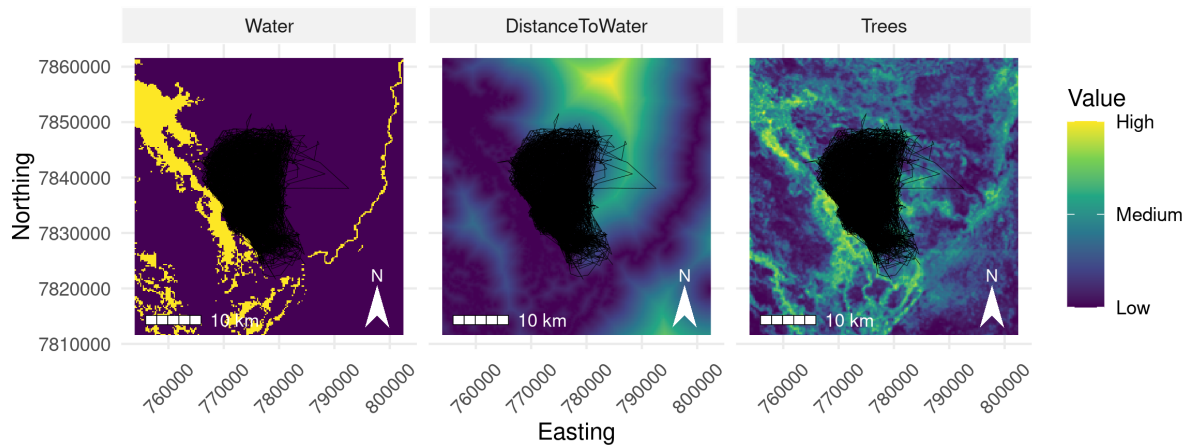


Figure 5.E.1: Covariates used for the case study, overlaid with the GPS data of a spotted hyena called “Apollo” (lines in black). Apollo was originally collared in 2007 in northern Botswana and monitored until 2011. The depicted area is part of the Okavango Delta, which is a massive wetland area. Data was projected to a local projection (EPSG:32734).

5.F Case Study Model Output

Table 5.F.1: Model results from the case study using GPS data collected on Apollo. In F1, forgiveness was set to one (only 2-hour steps were considered), whereas in F3-S and F3-SH a forgiveness of three was employed (allowing for step durations of up to 6 hours). In model F3-S, the step duration was interacted with step descriptors. In model F3-SH, step duration was interacted with step descriptors and habitat covariates.

Coefficient	F1	F3-S	F3-SH
sl	0.00002 (0.00001)	0.00001 (0.00001)	0.00001 (0.00001)
log_sl	-0.02251 (0.01862)	-0.01805 (0.0157)	-0.01846 (0.0157)
cos_ta	0.03166 (0.03055)	-0.0085 (0.02557)	-0.009 (0.02558)
Water	-1.71418*** (0.20628)	-1.56915*** (0.13995)	-1.61501*** (0.17121)
DistanceToWater	-0.00005*** (0.00001)	-0.00005*** (0.00001)	-0.00005*** (0.00001)
Trees	1.51764* (0.88816)	-0.2178 (0.62517)	0.60764 (0.75259)
sl:duration4		-0.00001 (0.00002)	-0.00001 (0.00002)
sl:duration6		-0.00004** (0.00002)	-0.00004** (0.00002)
log_sl:duration4		0.08122 (0.05075)	0.07978 (0.0508)
log_sl:duration6		0.02867 (0.02471)	0.03058 (0.02474)
cos_ta:duration4		-0.07526 (0.05784)	-0.07635 (0.05788)
cos_ta:duration6		-0.16358*** (0.06055)	-0.16105*** (0.06059)
Water:duration4			0.08548 (0.34111)
Water:duration6			0.20782 (0.46194)
DistanceToWater:duration4			0.00002 (0.00002)
DistanceToWater:duration6			-0.00001 (0.00003)
Trees:duration4			-0.04696 (1.61148)
Trees:duration6			-6.73474*** (1.97442)
Steps	2,179	4,505	4,505
AIC	-	47,565	47,564

Significance codes: * $p < 0.10$ ** $p < 0.05$ *** $p < 0.01$



Chapter 6

General Discussion

6.1 A Fresh Take on Connectivity

In this thesis, I explored several critical factors linked to various aspects of dispersal and landscape connectivity. In Chapter 2, I introduced a novel approach to assess functional landscape connectivity via simulated dispersal from iSSFs and demonstrated its application using GPS data from dispersing AWDs. In Chapter 3, I used the newly developed approach to reveal potential differences in connectivity for dispersing AWDs under varying environmental conditions in the context of ongoing climate change. In Chapter 4, I examined the importance of seasonal dynamism and investigated how the inclusion of seasonality affects dispersal simulations and inferred patterns of connectivity. Lastly, in Chapter 5, I revisited the iSSF framework employed throughout Chapters 2 to 4, and proposed various methods to generalize the framework for application in scenarios where GPS data exhibit temporal irregularities.

Probably the most pressing question with regard to the investigated factors is whether they actually matter for our understanding of connectivity, and whether their consideration alters our insights into conservation. If we qualitatively compare the connectivity maps generated from my master's thesis (Hofmann et al., 2021) and the various chapters of this doctoral thesis (Figure 6.1.1), the sobering answer would probably be a simple no. While the maps may not be entirely identical, they appear qualitatively similar. This is insofar surprising, as the maps were generated using rather different approaches and simulation parameters. One may conclude that these differences do not warrant the additional efforts of parameterizing a mechanistic IBMM and addressing several typically overlooked limitations, thus resolving to traditional, presumably simpler, methods to model connectivity. However, such a view would overlook various improvements that are achieved "under the hood" and I will argue that it is precisely these improvements that increase our ability to simulate dispersal and quantify connectivity to a new level.

A major benefit of using iSSF-based IBMMs over traditional connectivity modeling methods is that they bypass the necessity for a permeability surface (Diniz et al., 2019; Unnithan Kumar, Kaszta, et al., 2022). Permeability surfaces are often based on arbitrary conversions from habitat suitability to habitat permeability (Zeller et al., 2018), yielding unconditional predictions of a species' ability to move and disperse (Signer et al., 2017). Essentially, this implies that the permeability of an area (i.e. of a single grid-cell) is solely determined by the area's characteristics, without consideration of possible alternatives. This is in direct contradiction to the conditional logistic regression models that are normally utilized to parameterize such permeability surfaces (Zeller et al., 2012); these are inherently based on the principle of conditional probabilities (Avgar et al., 2017). In reality, it can also be assumed that an animal's willingness to traverse a specific area is contingent on what is available elsewhere. For instance, an animal encountering a densely populated human area may find the alternative of moving into a forest more appealing than if it were

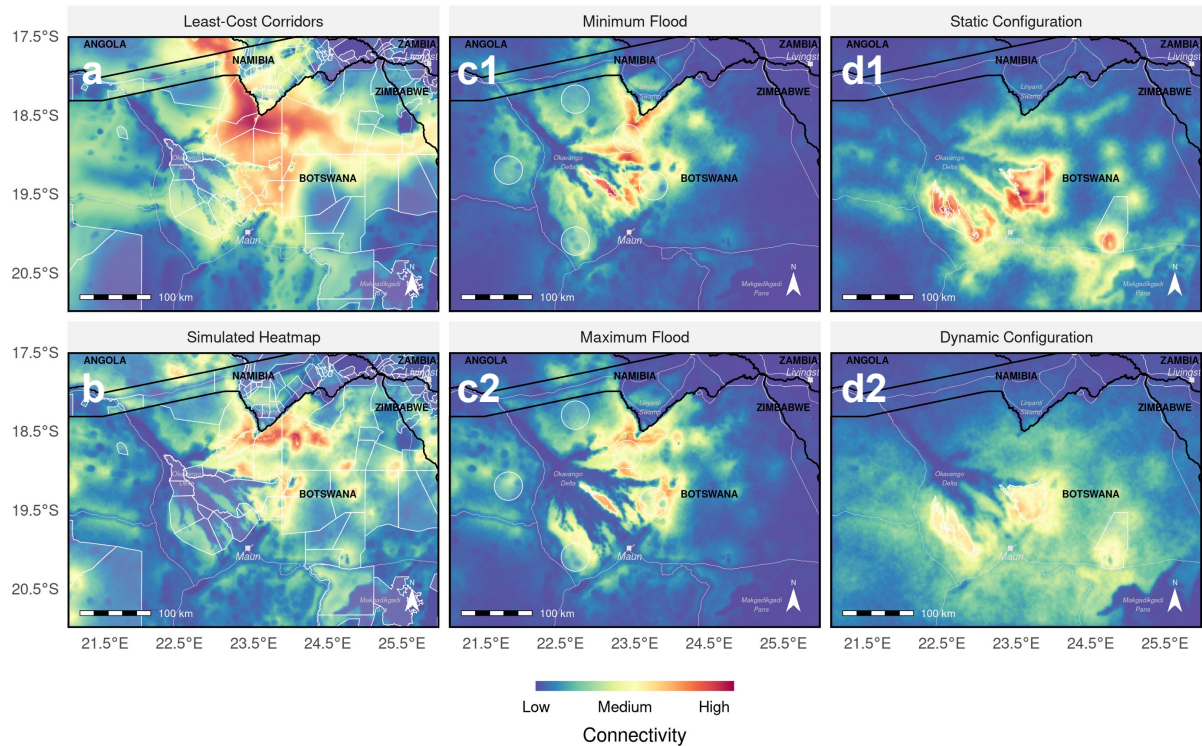


Figure 6.1.1: Comparison of the connectivity maps resulting from my master's thesis and throughout the chapters of this PhD thesis. Since methodology, data, covariates, and source areas (semi-transparent white polygons) differed from chapter to chapter, this should be considered a qualitative comparison. (a) Least-cost corridors computed between national parks and protected areas, computed as part of my master's thesis (Hofmann, Cozzi, McNutt, et al., 2023). (b) Heatmap emerging after simulating dispersal trajectories using the three-step approach introduced in Chapter 2. (c1, c2) Heatmaps produced from simulated dispersal trajectories under the minimum flood extent and maximum flood extent in Chapter 3. (d1, d2) Heatmaps produced from simulated dispersal trajectories in a fully static and dynamic configuration in Chapter 4.

currently situated in open Savannah habitat. A conditional prediction therefore seems more appropriate, and is precisely what is achieved through iSSF-based IBMMs (Signer et al., 2017).

Utilizing a mechanistic movement model to simulate dispersal also opens up new avenues for incorporating factors that play an important role in reality. In Chapter 2, for instance, I accounted for the fact that movement behavior depended on habitat characteristics by including interactions between step-descriptors and habitat covariates. In Chapter 3, I further modeled that dispersal movements depend on temperature and light availability. Incorporating such intricacies using permeability-based connectivity models is simply not feasible, as they lack a mechanistic understanding of movement (Zeller et al., 2012). Instead, permeability-based models adopt a series of simplistic grid-based movement rules that govern how individuals move from one grid-cell into a neighboring one. This also implies that the resolution of spatial covariates determines the presumed perception radius the focal species, as well as the temporal scale at which it moves across the landscape (Diniz et al., 2019). iSSF-based IBMMs overcome this limitation and instead permit to create models that allow animals to traverse multiple grid-cells in a single go, thus extending their landscape perception to a more meaningful distance. By simulating dispersal trajectories in space and time, the output of an iSSF-based IBMM is not limited to a single map, but allows preparing a suite of complementary connectivity metrics that provide a more nuanced and comprehensive view on a system's landscape connectivity (Diniz et al., 2019). In Chapter 2, I suggested preparing the metrics inter-patch connectivity, betweenness, and traversal frequency (heatmap), as each of those focuses on a different aspect of connectivity.

The realization that connectivity need not be confined to a single metric alludes to another problem in current connectivity studies, namely that they all exhibit a slightly different understanding of what connectivity actually entails. While many studies readily cite Taylor et al. (1993)'s definition of connectivity, they typically employ very different methods and metrics to quantify it. Some studies gauge connectivity through the strength of association between different habitats as measured based on observed or simulated movements (e.g., Revilla and Wiegand, 2008; Kanagaraj et al., 2013; Dilts et al., 2016), while others assess it by focusing on the matrix between such habitats (Etherington, 2016; Diniz et al., 2019). The latter group can again be separated into studies that estimate permeability within their study area (e.g. Martin et al., 2018), studies that estimate the intensity of use of different areas (e.g. Zeller, Wattles, et al., 2020), and studies that attempt to identify distinct movement corridors (e.g., Elliot et al., 2014; Benz et al., 2016; Brennan et al., 2020). Undoubtedly, each of these approaches is valid for capturing some aspect of connectivity, albeit they all focus on a slightly different one. Therefore, I propose to reconsider the term "connectivity" by viewing it as an overarching concept that can be further subdivided into the dimensions of connectedness, conductance and betweenness. I would define these terms as follows:

- **Connectedness:** Connectedness refers to the degree to which different patches or habitats within a landscape are functionally connected. It measures the ease and frequency with which organisms can move between different areas of the landscape. I have previously investigated this aspect of connectivity via *Inter-Patch Connectivity Maps*.
- **Conductance:** Conductance describes the degree to which the landscape allows movement or flow of organisms across it. It considers factors such as habitat structure, land use, and barriers that affect the ability of organisms to move through the landscape. I have previously investigated this aspect of connectivity via *Heatmaps*.
- **Betweenness:** Betweenness quantifies the importance of different elements of the matrix in facilitating connectivity between other patches or habitats within the landscape. It identifies key corridors or bottlenecks that serve as critical links for maintaining overall connectivity in the landscape. I have previously investigated this aspect of connectivity via *Betweenness Maps*.

Adopting this terminology and acknowledging that connectivity can be multidimensional would greatly facilitate navigating the confusing diversity of connectivity literature and connectivity modeling approaches, and help to clarify what dimension of connectivity they measure. A major benefit of using iSSF-based IB-MMs over permeability-based approaches is that they permit statements about all three dimensions, thus offering a holistic view on connectivity patterns.

6.2 Conservation Insights

Even though my chapters were primarily focused on methodological aspects, their results permit several conclusions on the conservation of AWDs, as well as on some ecological principles. Probably the most important result is that the AWD population studied in this thesis appears to benefit from a comparably high degree of connectivity. This is a testimony to the area's pristine condition and relatively low human disturbance, which permit dispersing coalitions to roam relatively unhindered in their pursuit to find potential mates and a new territory. Moreover, the planned KAZA-TFCA initiative appears to align well with many of the critical dispersal routes between existing national parks and wildlife management areas, thereby providing an effective means to safeguard the species' ability to disperse. I arrived at this conclusion already in my master's thesis (Hofmann et al., 2021), but the results of this PhD thesis further corroborate this notion. Notably, GPS data collected on dispersing coalitions revealed several successful dispersal events from BPC's study area into surrounding, less pristine habitats. The study population, which is currently considered a stronghold population, may thus considerably contribute to the recolonization of surrounding habitat patches and reinforcement of weakened subpopulations. Besides this, my

dispersal simulations from Chapter 2 revealed that the study area in northern Botswana likely acts as a major dispersal hub where several dispersal routes that run across the KAZA-TFCA ecosystem are funneled due to natural and human impediments. The protection of this area therefore plays a crucial role in conserving AWDs, particularly in light of ongoing climate change. As demonstrated in Chapter 3, climate change holds the potential to disrupt and rearrange preferred movement corridors, thus leading to the emergence of novel hotspots for human-wildlife conflict. Initiatives aimed at raising awareness and educating affected communities, as well as the implementation of appropriate prevention and compensation systems, will help ensure greater acceptance by the local population. Finally, I motivated in Chapter 4 that connectivity should not be viewed as a static property but rather as a dynamic and multidimensional concept. Although I found that the incorporation of seasonality only marginally improved the predictive power of dispersal models, inferred connectivity patterns differed significantly. In particular, a seasonal take at connectivity appeared to result in connectivity being more homogeneously distributed than what was suggested by a static analysis. This was likely due to seasonally available dispersal habitats. A more holistic perspective must be adopted for the successful conservation of dispersing species, as conservation measures cannot be limited to preserving highway-like corridors, but should be broadened to encompass the diversity of dispersal routes emerging under dynamic environmental conditions.

6.3 Methodological Considerations and Limitations

The additional realism and flexibility gained by moving from permeability-based connectivity assessments to an iSSF-based IBMM, and the novel insights gained from studying the impacts of climate change and seasonality come at considerable costs, both in terms of data and computational requirements. For example, parameterizing an IBMM via iSSFs necessitates GPS data on the study species (Fortin et al., 2005; Thurfjell et al., 2014; Avgar et al., 2016), preferably collected during dispersal (Elliot et al., 2014). In many instances, GPS data or data during dispersal are unavailable (e.g. Jackson et al., 2016; Day et al., 2019; Day et al., 2020). In this case fitting an iSSF is simply not possible, and the modeler needs to revert to a traditional connectivity model. Similarly, data on on-the-ground conditions under climate change or seasonality can be challenging to collect. Seasonal data can sometimes be obtained via remote sensing, which has become vastly facilitated thanks to centralized data hubs (e.g., Google Earth Engine). Nevertheless, the incorporation of seasonality necessitates handling large data-volumes and dealing with noise due to missing values or cloud cover. A seasonal take at connectivity also requires splitting the input data by season, which can substantially reduce the amount of data remaining to inform habitat-selection and movement behavior in distinct seasons. Similarly, obtaining information on environmental conditions under climate change remains difficult (Littlefield et al., 2019). Spatial data on atmospheric conditions may be readily available (e.g., Copernicus Climate Change Service, 2021), yet these are rarely translated

into on-the-ground information on land-cover and land-use, thus limiting their usefulness for connectivity studies (but see Sleeter et al., 2018). In Chapter 3, I proposed exploiting seasonal extremes to gauge the likely impacts of climate change on environmental conditions, yet this remains a poor proxy for long-term shifts in the biosphere. Either way, the benefits gained by increasing realism need to be carefully balanced against the potential costs of doing so (Puy & Saltelli, 2022).

In Chapter 2, I highlighted that connectivity studies entail numerous non-trivial modeling decisions (Beier et al., 2008). These encompass the selection of suitable species data and covariate layers (Elliot et al., 2014; Fattebert et al., 2015; Finerty et al., 2023), as well as the choice of an adequate spatial and temporal scale (Zeller et al., 2014; Zeller et al., 2017; Ciudad et al., 2021). For iSSF-based IBMMs, additional modeling decisions emerge (Figure 6.3.1), including how to deal with individual variability, the number and placement of starting points, and the behavior of simulated individuals at map boundaries (Diniz et al., 2019).

For permeability-based connectivity studies, several useful reference works and overviews that help with the application of established approaches and the associated decision-making processes exist (Beier et al., 2008; Beier et al., 2011; Zeller et al., 2012; Etherington, 2016; Zeller et al., 2018; Diniz et al., 2019; Hilty et al., 2020). It is imperative that analogous reference material is developed for iSSF-based IBMMs, both to facilitate the uptake and application of new methods, as well as to maintain comparability of studies from different species and systems. As already motivated by Finerty et al. (2023), maintaining comparability between connectivity studies is of central importance to distinguish biological differences from methodological artifacts. This holds particularly true for methods that exhibit greater flexibility and thus higher variability in outputted results. In this context, comprehensive sensitivity analyses will become of great importance, as they serve to pinpoint simulation parameters that require particular attention due to their disproportionate impact on the resultant connectivity patterns (Kanagaraj et al., 2013). Quantifying the sensitivity of non-spatial metrics to simulation parameters is straightforward. However, extending a sensitivity analysis to spatial metrics, such as betweenness or conductance, seems more involved. In simple cases, connectivity maps emerging under different scenarios can simply be contrasted using difference maps (e.g., Day et al., 2020). I have applied the same technique in Chapter 3 to highlight differences in connectivity between the maximum and minimum flood scenario. An alternative approach is provided by Marrec et al. (2020), who assess the sensitivity of their connectivity outputs by comparing connectivity values via violin-plots and map-correlations. Unfortunately, this approach fails to provide a spatial depiction of sensitivities. I therefore propose yet another solution, which is to simulate connectivity under varying parameters and generate the spatial metrics of interest (e.g., heatmap, betweenness map, etc.). Then, one can apply grid-cell-wise linear regression to quantify how strongly the value of each grid-cell

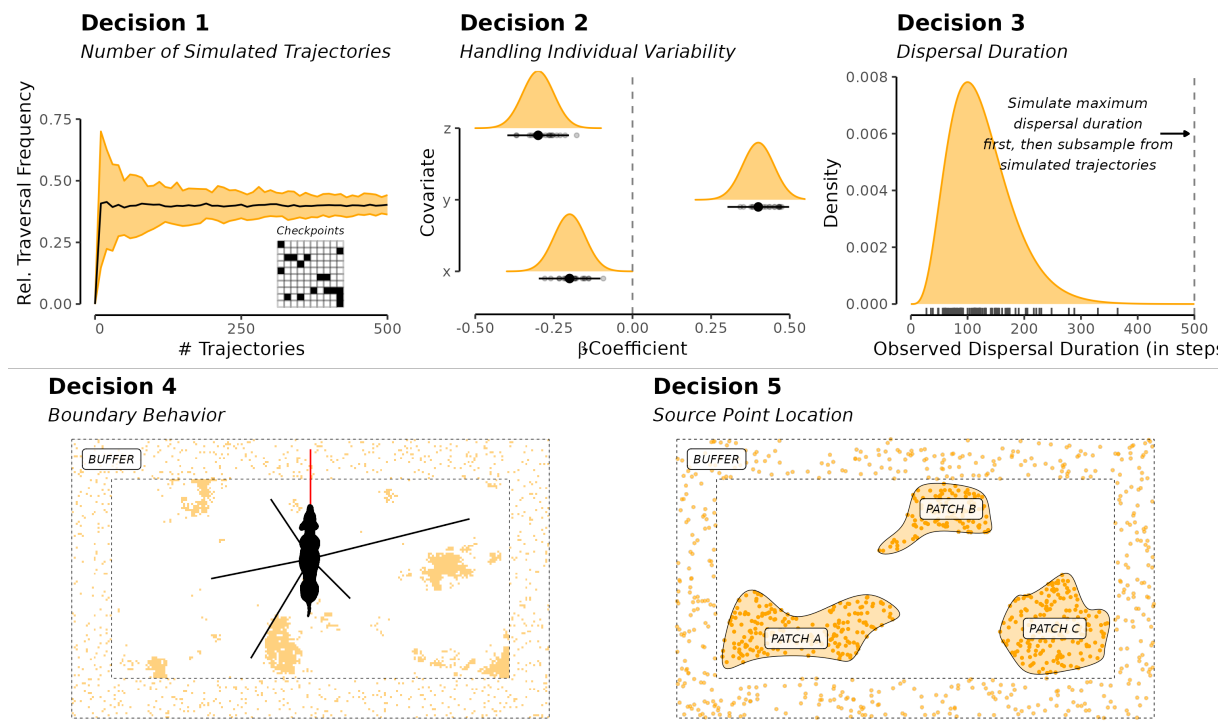


Figure 6.3.1: When simulating dispersal trajectories using IBMMs, a modeler needs to consider several design choices. This includes the choice of the number of simulated trajectories (Decision 1), how to handle individual variability in habitat and movement preferences (Decision 2), as well as the selection of a dispersal duration (Decision 3). Finally, the modeler needs to define how individuals behave at map borders (Decision 4), and the location of source points from which dispersal is simulated (Decision 5).

responds to changes in simulation parameters. The benefit of this approach is that it allows visualizing sensitivity spatially, thus highlighting areas that require particular attention.

While many studies focus on documenting the current state of connectivity for their study system, only few dare to pose the question: “what could be?” By this, I don’t simply mean how connectivity might evolve in response to anticipated conditions under climate change, but rather how conditions could be actively manipulated to enhance connectivity. This is insofar interesting in that connectivity modeling is usually viewed as a means to help decision makers improve, rather than simply preserve, connectivity (Heller & Zavaleta, 2009; Rudnick et al., 2012). As such, connectivity models could serve to inform the creation of new corridors that facilitate dispersal between existing but isolated areas. A focus on potential connectivity is particularly relevant in light of the realization that many historically relevant movement routes have been disrupted and vanished due to human activity. In northern Botswana, for instance, the erection of various veterinary cordon fences in the 1960s led to a stop in wildebeest (*Conochetes taurinus*) and zebra (*Equus quagga*) migrations, which only resumed upon destruction of the fences in 2004 (Bartlam-Brooks et al., 2011; Bartlam-Brooks et al., 2013). While this case is well-documented and the underlying causes of reduced connectivity were known, there are many instances where the loss of crucial corridors remained unnoticed, resulting in an overall reduction of terrestrial animal movements across the globe

(Tucker et al., 2018). Using appropriate methods, connectivity studies could help to reveal areas where the negative consequences of habitat fragmentation could be reversed via restoration measures, allowing to re-establish previously existing connectivity. Along this vein, Cushman et al. (2010) predict movement corridors for African elephants in the absence of humans, thereby attempting to reveal historically relevant dispersal routes. For the same species, Bastille-Rousseau et al. (2018) employ an algorithmic approach to pinpoint areas that appear particularly well-suited to construct wildlife crossing features to help mitigate the detrimental impacts of roads on connectivity. Future studies could develop similar approaches that allow randomizing or permuting current landscapes to identify regions where enhanced connectivity could be achieved with minimal efforts.

6.4 Ecological Considerations and Limitations

While working on the various chapters, I repeatedly had the impression that the movement behavior of dispersing AWDs was only marginally driven by environmental factors. This was insofar frustrating, as environmental data constituted the only covariate data available to me at meaningful spatial scales. Although significant selection or avoidance patterns towards certain features were evident (e.g., water, human influence) they were generally weak. This became particularly evident in Chapter 4, where any benefits gained from moving from a static to a dynamic representation of the landscape were strongly diminished by the inclusion of additional interactions that predominantly accounted for AWDs' circadian cycle and their tendency to move less during hot periods. As alluded to in Chapter 4, I suspect that a combination of three factors explains the relatively weak association between AWDs and their environment. Firstly, I kept my representation of land cover rather basic. This was primarily due to the fact that I had to use categories that were consistent across countries, which meant that I needed to limit myself to relatively simple categories. For example, my representation of vegetation comprised only three continuous covariates, including the percentage cover of forest, shrubs/grassland and bare-land. In reality, the Okavango Delta ecosystem hosts a much broader variety of vegetation patterns. Unfortunately, these remain extremely challenging to remote sense at the required spatial scales. Secondly, the AWD can be considered as a generalist species, currently occurring across wide range of habitat types (Woodroffe & Sillero-Zubiri, 2020). The species thus seems little limited by environmental factors. This particularly applies to dispersing individuals, which only remain in a specific area for a short time, thus exhibiting a higher tolerance towards unsuitable conditions (O'Neill et al., 2020). This brings me to the third point; throughout the chapters, I have exclusively utilised data collected on dispersing AWDs. As dispersers are in search of a suitable territory and possible mates, intra- and inter-specific factors likely play a significant role, potentially outweighing the influence of the landscape. AWDs are weaker competitors, finding it difficult to prevail against lions and hyenas (Creel & Creel, 1996; 2002; Dröge et al., 2017; Marneweck

et al., 2022). Therefore, it can be expected that the presence of competitors deters dispersers that are in seek of a vacant territory. Similarly, dispersers will likely avoid areas already occupied by established packs because dispersal coalitions are easily outnumbered by resident groups. Besides this, dispersing coalitions are in search of potential mates, suggesting that their movement is also driven by the availability of other-sex individuals. Considering the low density at which the species occurs, locating mates must represent a tremendous challenge (Masenga et al., 2016; Woodroffe & Sillero-Zubiri, 2020). The mechanisms that facilitate mate-finding are presently unknown, but shared marking sites are believed to play a pivotal role (Apps et al., 2022; Claase et al., 2022). The notion that dispersal is influenced not only by biophysical factors but also by “social cues” is generally referred to as the “social resistance hypothesis”, which presumes that species are embedded into an intra- and inter-specific landscape (Armansin et al., 2020). Corresponding scientific evidence that supports this hypothesis was provided by Cozzi et al. (2018), who concluded that social factors may exert an even greater influence on dispersal movements than landscape characteristics. A better understanding of the importance of such “social cues” could improve our ability to more reliably predict dispersal movements, yet necessitates appropriate data on the presence or absence of other animals. In Section A.1 of the Appendix, I will outline the implementation of a cameratrap project that aims to fill this gap by collecting novel information on large mammals across BPC’s historic study area. In a future analysis, the so collected data could be used to generate additional spatial layers that allow modeling the influence of other species on AWD dispersal movements.

A concept closely related to the notion of “social resistance” is that of “anthropogenic resistance” (Ghoddousi et al., 2021). It coins the idea that anthropogenic factors can majorly alter landscape connectivity and should be considered when studying dispersal. In Chapter 3, I have encapsulated anthropogenic resistance in two ways. First, I modeled that dispersers avoid areas influenced by humans, thus highlighting that the mere presence of humans can hamper connectivity. Furthermore, I overlaid predicted dispersal movements with a human influence map, thereby disclosing potential hotspots of human-wildlife conflict. Similar approaches were previously employed by Cushman et al. (2018) and Buchholtz et al. (2020) to uncover human-wildlife interaction hotspots for lions and African elephants, respectively. However, as noted by Ghoddousi et al. (2021), an important aspect of anthropogenic resistance is that its influence depends on human attitude. Notably, a similar degree of human influence can result in vastly different consequences for connectivity (Ghoddousi et al., 2021). Using questionnaires, valuable insights into human attitudes can be gained, enabling more informed predictions about the spatial distribution of areas with an elevated potential for human-wildlife conflict (Feldmeier et al., 2024). Behr et al. (2017), for instance, conducted questionnaires to develop a socio-ecological model, highlighting areas where both environmental and anthropogenic factors favored the re-establishment of wolves (*Canis lupus*) in Switzerland.

Along a similar vein, socio-ecological connectivity models could serve to map dispersal routes accepted by humans.

Throughout all chapters, I simulated individuals for predefined dispersal durations, thus ignoring mortality. However, several studies have shown that this can lead to an overestimation of dispersal success and therefore an overestimation of connectivity (Kramer-Schadt et al., 2004; Fletcher Jr. et al., 2019; Day et al., 2020). There are two ways in which mortality could enter my simulation framework. First, it could be modeled as a binomial draw with constant probability that determines whether an animal survives or dies at each simulated step. This would merely shorten simulated dispersal paths, thus affecting inferred connectivity patterns in relative terms. In fact, the same effect could be achieved by simulating dispersal for a shorter duration, although this does not capture the same level of stochasticity that would result from using a “coin flip” approach. Alternatively, mortality could enter the framework spatially explicitly, reflecting the fact that mortality likely varies between areas. Kramer-Schadt et al. (2004), for instance, used an IBMM where lynx (*Lynx lynx*) mortality was assumed to be higher in areas with dense road networks. Fletcher Jr. et al. (2019) and Day et al. (2020) followed a similar approach and incorporated mortality via spatially explicit “mortality layers”, which consolidate various sources of mortality, such as predation, starvation and human-wildlife conflict. However, spatially mapping the mortality risk requires adequate data, which were lacking for my study system. Additionally, mortality may further vary with individual (e.g., sex, age), social (e.g., dispersal coalition size), and environmental (e.g., temperature) factors (Behr et al., 2023). Ultimately, the impact of mortality on dispersing AWDs may be buffered, given that AWDs disperse in coalitions; a single individual perishing therefore does not imply a failure of the coalition’s dispersal attempt. It is also worth noting that mortality cannot be incorporated into traditional connectivity models, because these do not simulate movement explicitly. The ability to account for mortality should therefore be viewed as another major benefit of using IBMMs over traditional models (Diniz et al., 2019).

In this thesis, I focused on the influence of various factors on the movement behavior of dispersing individuals, but have ignored any demographic consequences of dispersal for metapopulation viability. Yet, such demographic considerations are of vital importance to design more effective conservation networks. After all, the protection of movement corridors is only meaningful if these significantly contribute to metapopulation persistence. The movement model parameterized in this thesis therefore serves an important component to an individual-based population viability analysis, in which dispersal is reproduced mechanistically and spatially realistically. Such a model could, for example, be used to explore the demographic consequences of land protection and conversion through hypothetical scenarios. A suitable demographic model for my study system was parametrized by Dominik Behr as part of his PhD thesis (Behr, 2021). In order to combine the two models, we currently lack information on two processes: settlement and home ranging behavior. A better representation of these two processes is necessary to delineate

possible home ranges and determine under which conditions a dispersal coalition settles. Once these processes are better understood, the combined models can be used to simulate how dispersing animals move between subpopulations, allowing to estimate their impact on different demographic components.

6.5 Conclusion

In conclusion, this thesis provided comprehensive exploration into the assessment of functional landscape connectivity via individual-based dispersal simulations, using dispersing AWDs as an example system. Through the development and application of new methodologies, as well as by incorporating multiple previously disregarded factors, several key insights have been gained:

- **Integration of Novel Approaches:** I introduced a novel method to assess functional landscape connectivity via simulated dispersal from an IBMM parameterized via iSSFs. This approach offers a more mechanistic understanding of connectivity compared to traditional methods, overcoming the limiting need for a permeability surface and enabling the preparation of a complementary suite of connectivity metrics that provide a more nuanced view of functional connectivity.
- **Comprehensive Understanding of Connectivity:** By examining factors such as flooding conditions and seasonality, I have comparatively investigated how changes in landscape conditions can alter connectivity patterns for dispersing animals, thus highlighting the need for adopting a more dynamic view on landscape characteristics. Importantly, I suggested to not limit functional connectivity to a single dimension, but to distinguish between connectedness, conductance, and betweenness, thereby allowing for a more holistic assessment of connectivity.
- **Challenges and Future Directions:** Despite the many benefits they bring about, I have also acknowledged challenges and limitations associated with IBMM-based connectivity studies. This included substantial data requirements, computational demands, and the need for well-informed modeling decisions. Moving forward, I emphasized the importance of incorporating mortality into the simulation-process and to utilize iSSF-based IBMMs to gauge the demographic consequences of dispersal and connectivity. I also called for the inclusion of intra- and inter-specific factors into connectivity models, as well as a more detailed representation of anthropogenic resistance that acknowledges the importance of human attitude towards wildlife.

Overall, this thesis contributes significantly to the fields of movement and landscape ecology, as well as to conservation science in general, by advancing methodologies, providing insights into the movement behavior of dispersing individuals, and offering recommendations for future research and conservation.



Acknowledgements

This work would not have been possible without help and support from countless people and organizations. I'd like to start by thanking the Ministry of Environment and Tourism of Botswana for generously granting permission to conduct research for this project. Financial support for this thesis was provided by Albert-Heim Foundation, Basler Stiftung für Biologische Forschung, Claraz Foundation, Idea Wild, Jacot Foundation, National Geographic Society, Parrotia Stiftung, Stiftung Temperatio, Wilderness Wildlife Trust, Forschungskredit of the University of Zürich (no. FK-21-091), a Swiss National Science Foundation grant (no. 31003A_182286) awarded to Arpat Ozgul, and a Swiss National Science Foundation grant (no. 310030_204478) awarded to Gabriele Cozzi.

I am particularly grateful to my supervisor, Gabriele Cozzi, who has initiated and managed the African wild dog dispersal project over the past decade and has been an outstanding mentor. His leadership and dedication to research and conservation were absolutely instrumental to this work. He provided unstinting support for my doctoral thesis and has significantly contributed to the success of each chapter. Gabriele played a pivotal role in securing both material and salary funds for my research, and eventually included me under his own research grant. Moreover, he introduced me to the challenges and rewards of fieldwork in one of this planet's most pristine environments. Through his training, I acquired a diverse set of skills, from tracking and monitoring large carnivores, navigating and driving in the African Savannah, sedating and equipping animals with GPS satellite collars, to fixing Land Rovers. Gabriele's constant supervision ensured my scientific progress, and he continuously provided timely guidance whenever I veered off course. His unwavering motivation and belief in my abilities kept me energized, especially during moments of self-doubt. Even beyond academic support, Gabriele spared no expense and happily assisted Manuela and me in our endeavor of finding a Land Rover for our upcoming adventures in Africa. Besides our working relationship, Gabriele and I have developed an integral friendship, which hopefully continues to grow in the future. Thanks for the countless BBQs, beers, and Italian fine dines. I don't think anybody can wish for a better PhD supervisor.

I extend my gratitude to Arpat Ozgul, whose belief in my scientific abilities and provision of funds enabled me to embark on my PhD as part of his research group. Arpat was an excellent supervisor, and his scientific rigor significantly advanced my understanding of ecology and propelled my academic growth. It was a privilege to be part of his research group and I found tremendous pleasure in participating in the various group-retreats, potlucks, and other social gatherings.

I am immensely grateful to Dominik Behr, who has accompanied my academic career from the very beginning. Dominik demonstrated to me that transitioning into the field of ecology was not only feasible, but also highlighted the personal fulfillment this pursuit may bring about. Under his mentorship, I conducted my master's thesis on dispersing AWDs, which ultimately laid the foundation for this PhD. He also infected me with the African virus, giving me an unhealthy passion for African wild dogs and African

wildlife in general. Beyond academic mentorship, Dominik has continuously inspired me to embrace creativity when crafting PowerPoint presentations, scientific figures, or when taking photos of wildlife. It's been an incredible journey, and I've enjoyed each and every of our many fruitful discussions.

I am deeply thankful to have had an opportunity to collaborate with John Fieberg, whose expertise was invaluable to my academic journey. John is among the most humble yet inspiring people I have ever met. His ability to return any email with an in-depth response within less than 24 hours is one in a kind and makes collaborating with him an absolute blast. If one imagines a statistics professor as being an uncoordinated nerd, beware of John's ability to throw a Frisbee at the speed of light; it will prove you wrong. It was a pleasure organizing and teaching a movement ecology workshop with John in Faido, and I am looking forward to organizing another one in the future.

I extend my sincere appreciation to thank all my committee members, namely Lukas Keller, Arpat Ozgul, Juan Manuel Morales, John "Tico" McNutt, and Gabriele Cozzi for their valuable insights and stimulating discussions during our committee meetings. Their collective expertise and guidance tremendously facilitated a series of focused and coherent research chapters. I'd particularly like to thank Lukas for adopting me in his research group without hesitation.

I would like to express special thanks to Florian Hodel for his contagious ingenuity and infectious humor, which never failed to brighten even the dullest moments. Florian's creativity has sparked an incredible amount of interesting ideas and his friendship has been invaluable to me. It was a shame we only overlapped for such a short time at the University, although I have a notion that it was for the better of my productivity. Maybe π -ranha will provide further opportunities for collaborations in the future. I also want to thank his wife, Rahel, who was a source of strength and probably provided more life-advice than she is aware of. The joy shared with you both has been unparalleled; I even suffer from soar jaw-muscles from all the laughter whenever we spend time together.

I am also grateful to all current and former Popecol members, including Benedetta, Che, Daniela, Dechen, Dilsad, Esin, Eva, Lorena, Lukas, Lorena, Louis, Monica, Omar, Patrick, Philip, Rasmithah, Tis, and Vera-Lu for an unforgettable time and many exciting moments. I'd like to especially thank two master students that I co-supervised, Megan Robinson and Raphaël Destriau, for their effort and motivation which have laid the foundation for future works. It's rare to supervise students with such drive and dedication, and it's been a pleasure being part of their exciting works.

Further gratitude is due to the University's secretaries and technical support, who ensured that all organizational tasks were taken care off; something I'm terribly bad at. Many thanks to Jacqui, Judith, Ursina, Debra, Susanne, Isabel, Michel, and Tina.

Thanks also to Johannes Signer and Theo Michelot for sharing their insights on how to simulate movement from fitted step-selection functions, and to Guillaume Bastille-Rousseau for helping me with computing network metrics from GPS data.

Furthermore, I want to extend my gratitude to Glauco Camenisch, who assisted at countless wild dog immobilizations and has always provided an ear when I needed one. Experiencing the bush together with you and Gabs was a unique privilege and among the most fun I've had in Africa thus far.

In Botswana, a heartfelt "Thank You" goes to Tico and Lesley for establishing Dog Camp and for the passion and love that they keep pouring into this amazing research project. Through Wild Entrust, you have created something truly extraordinary that holds the promise of providing a future where humans and wildlife can coexist. It is an honor to be part of this endeavor, and one can only aspire to contribute to its success in the future.

Special thanks to Peter Brack for showing me how to cross water with a Land Rover (a proper lake, in fact), how to hot-wire a Land Rover, for organizing a walking safari (let's do another one!), and for the countless inspiring discussions we had in camp. Similarly, I'd like to thank his wife, Nicola Hawes, for accommodating me on various occasions in their wonderful "termite mound" house in town. Further thanks go to Megan Claase, for exemplifying true dedication and passion for conservation and for serving as a fieldwork role model. Our expedition to David's Kingdom marks one of my favorite trips in Africa to date. Further thanks go to Whitney Hansen, for bringing me on some incredible wild dog follows and for introducing me to the imperial system ("come within a whale of me and say that again"). Thanks to Emily Bennett, Mark and Caroll Swaffield for providing me with shelter and food in Maun, to Rob Jackson for providing veterinary services, and to Mary Hastag from Abercrombie & Kent for organizing several trips into the Okavango Delta and for initiating an exciting collaboration that hopefully continues into the future. Gratitude is also due to all research assistants in Botswana, including Rio Dipuo, John Neelo, Megan Robinson, Alex Dibnah, and Mara Zali, for relentlessly collecting data in the field, as well as to all staff members in camp, including Allen, for providing mechanical support and fixing our Land-Rovers and for his musical irradiation in the shower, to Fine and Tea for preparing the most elaborate meals with the least elaborate items, to Borden, Opi, and Obie for keeping camp clean and tidy, and to Last, for tirelessly fixing our continuously punctured tires.

Special thanks go to our former research assistant Aobakwe Sengate (a.k.a. AB), for being an incredible field-mentor and for filling my knowledge gaps with regard to the African wildlife. Though our time in the field was short, every trip with AB was exciting, even if it only was to check cameratraps. AB's abilities to read the environment and track animals are second-to-none, and his never-ending curiosity and willingness to investigate even the faintest evidence of large predators were inspiring and informative. He taught me some of the most useful skills, and I've enjoyed some of the most memorable sightings with

him. I'll never forget the look on his face when he realized a lioness stole a leopard's kill just behind his tent in camp.

My deepest gratitude goes to my family, including my parents, Rahel and Denis, and my grandparents Elizabeth, Hans-Peter, and Josephine. They have always been there for me and provided me with all the psychological and financial stability that I needed throughout this journey. Similarly, I'd like to thank my girlfriend's family, namely her parents Yvonne and Max, as well as her grandparents Willy and Annula. I also want to thank her grandfather Ernst, who sadly passed away recently. Being embraced by such a wonderful social environment is a gift beyond measure, and I am incredibly grateful for the love and support I have received from both families.

Finally, I want to thank my girlfriend Manuela, who supported me through all of my undertakings, no matter how devious some of them must have sounded to her. Despite her own demanding schedule, Manuela consistently found the time and energy to uplift and motivate me when I needed it most. Manuela was not only at peace with my passion for Africa, but got infected with an unhealthy enthusiasm herself. Please excuse that I have spent several months in the field, leaving you and our cat Nala behind, and thank you for crunching through the countless cameratrap images (there will be more...). It is not a given to find a partner that can cope with a scientist's lifestyle, and I appreciate your unconditional support. I can't wait to explore the African wilderness further with you in our Landy!



Appendix

Additional Works

A.1 Cameratrap Survey

Our current understanding of AWD dispersal movements is primarily based on models that consider landscape-scale information and environmental features (e.g., water cover, vegetation cover, human influence) but are completely uninformed with respect to the effect that intra- and inter-specific factors may have. Recent studies have indicated that these factors may play a crucial role in shaping dispersal movements, potentially even outweighing the role of environmental factors, particularly in social species (Cozzi et al., 2018; Armansin et al., 2020). To fill this data gap, I initiated a large-scale cameratrap survey across BPC's historic study area (Figure A.1.1a). The goal of this ongoing project is to obtain data on the distribution and abundance of AWDs' main prey and competitor species, while also providing a non-invasive, long-term monitoring system for the local fauna. Starting in November 2021, I deployed 60 cameras at as many stations on a 4x4 km raster grid, stratified by the three predominant habitat types; grassland/floodplain (Figure A.1.1c), mixed woodland acacia dominated (Figure A.1.1e), and mopane woodland (Figure A.1.1d). To maximize the probability of detecting animals while reducing our influence on the landscape, I placed cameras on trees (Figure A.1.1b) facing dirt roads and programmed them to record bursts of four images whenever an animal passed by.

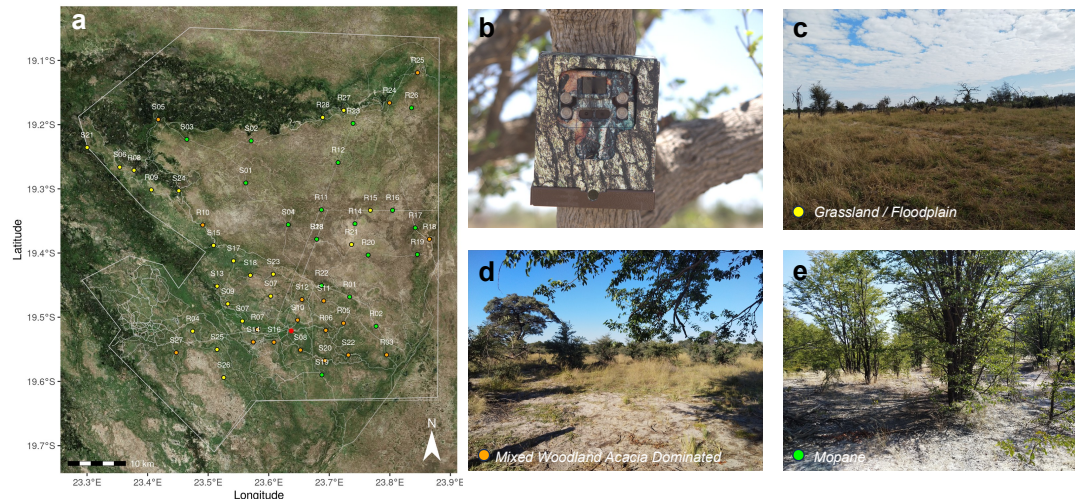


Figure A.1.1: (a) Cameratraps deployed in BPC's historic study area. (b) Cameras were deployed on trees facing dirt roads and stratified across three major habitat types: (c) grassland / floodplain, (d) mixed woodland acacia dominated, and (e) mopane.

To cope with the large amount of incoming data, I developed a processing pipeline that streamlines and automates numerous processing steps, thereby reducing the need for manual labor (Figure A.1.2). Notably, I programmed a series of R-functions that allow pre-processing the collected data using an object-oriented approach. Besides trivial tasks, such as equalizing image dimensions or extracting EXIF-metadata,

the functions also allow feeding images into Microsoft's MegaDetector (<https://github.com/microsoft/CameraTraps>). The MegaDetector utilizes an AI model to separate images containing animals from those that are empty or contain people and vehicles. This is particularly useful considering that cameratraps are often triggered by moving vegetation, leading to false positives. Finally, the data are automatically prepared for upload to Wildeye's TrapTagger (www.wildeyeconservation.org) software for species classification. In collaboration with Raphaël Destriau (see Section A.2), this allowed me to classify animals on all 3.5 Mio. collected images. As a follow-up from my doctoral thesis, I plan to use the so collected and processed data to model the distribution of relevant species, and to include the resulting layers as additional covariates in the dispersal models that I developed and used thus far.

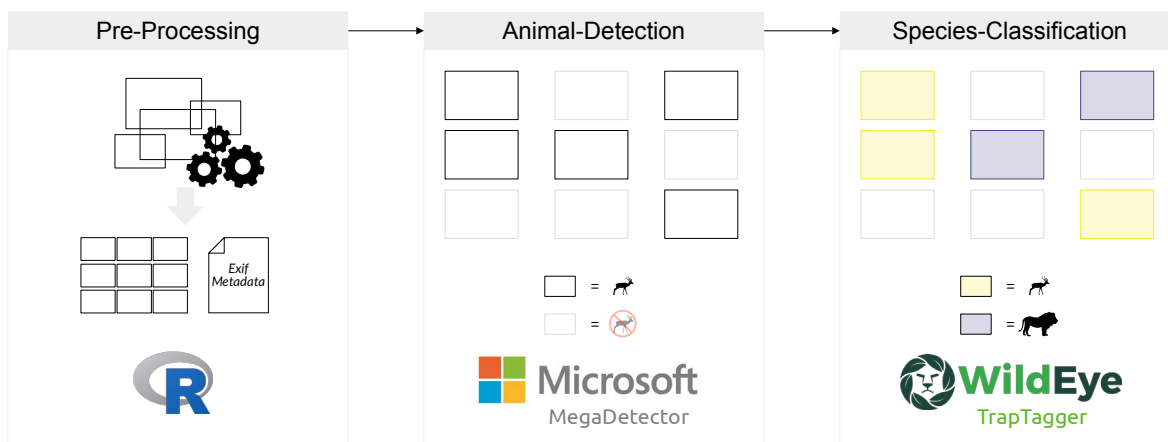


Figure A.1.2: Automated processing pipeline for the cameratrap data. In a first step, cameratrap images are preprocessed. This includes the equalization of image dimensions, extraction of EXIF-metadata, as well as the assignment of a spatial location to each image. In a second step, the pre-processed data is fed into Microsoft's MegaDetector, which allows separating empty images from images that contain animals. Images with animals are finally processed through TrapTagger, which facilitates an AI-aided classification of animals to the species level.

A.2 Supervised Theses

During the course of my PhD, I had the opportunity to co-supervise two master students together with my main supervisor, Dr. Gabriele Cozzi. Here, I'd like to briefly summarize the two students' theses and explain how they embed into my own work and potentially the work I will conduct during my PostDoc.

- **Factors Influencing Phase-Specific Movement and Activity Patterns of African Wild Dogs (by Megan Robinson):**

The first thesis was conducted by Megan Robinson, who joined our research group in June 2022. Megan previously worked as a research assistant for BPC and later embarked as a master student in the program for quantitative environmental sciences at the University of Zurich. Megan's primary research objective was to quantify differences in movement behavior and activity patterns

of AWDs during residence and dispersal. For this, Megan used GPS and Activity data obtained on 33 resident and 19 dispersing AWDs, which she linked to observations recorded by staff members in the field to segment the collected data into four behavioral movement modes. Specifically, she differentiated between the resident phase, when individuals are with the natal pack; the exploratory phase, when prospecting individuals may leave the pack for short exploratory forays but eventually return to the pack; the transient dispersal phase, when dispersing individuals leave their natal pack forever, and the settlement phase, during which a newly formed group establishes a new territory. She then applied generalized linear mixed-effects models to compare step-lengths, turning-angles, and average activity between phases, while holding constant for several other factors, including habitat cover, group-size, and moon-illumination. Her results revealed that individuals in the exploratory, transience, and settlement phase covered significantly larger daily distances and exhibited higher average activity than residents (Figure A.2.1a). These differences were particularly pronounced during transience, when dispersers cover long distances in a short amount of time. Megan also found that AWD activity was positively correlated with moon illumination at night, irrespective of the animals' behavioral movement mode. During my PostDoc, I envision to build on these insights and further investigate differences between resident and dispersing wild dogs via iSSFs. My goal is to further assess if observed differences are limited to differences in animals' movement behavior (i.e. their movement kernel) or if there are equally relevant differences in their habitat-selection function (habitat preferences).

- **Spatial Analysis of Wild Animal Populations in Northern Botswana Using Camera Traps Data (by Raphaël Destriau):** The second co-supervised thesis was conducted by Raphaël Destriau, who joined our research group as an external student from the Ecole Polytechnique Federale in Lausanne. Raphaël's background was in engineering, yet he was dedicated to expand his expertise in ecology. To accommodate both his expertise and interest, we developed a two-stage master thesis, which started with an engineering component and later culminated in an ecological analysis. The goal of this thesis was to expand on my previously developed processing pipeline to process cameratrap data and to conduct a preliminary occupancy analysis on several key species. In the first stage, Raph expanded the pipeline and implemented a semi-automated workflow to annotate cameratrap images and classify species using artificial intelligence. For this, Raph employed an already-existing open-source software called TrapTagger (www.wildeyeconservation.org) which provided several pre-trained neural networks to detect and classify large mammal species from cameratrap images. To benchmark the performances of the available models, Raph manually compiled a large validation-dataset that allowed him to compute confusion matrices for each available model. Based on these results, Raph developed a "best-practices" guide that facilitates minimizing potential errors due to

misclassifications (Figure A.2.1b), while maximizing the efficiency at which data can be processed. In a second stage, Raph utilized the automatically processed cameratrap data and applied occupancy models to derive species-habitat associations for several species that we believed could influence AWDs. The list of modeled species included main AWD prey species such as impala (*Aepyceros melampus*), lechwe (*Kobus leche*), kudu (*Tragelaphus strepsiceros*), and main AWD competitors such as lions (*Panthera leo*), and hyenas (*Crocuta crocuta*). His findings suggested significant associations between occupancy and environmental factors (e.g. distance to permanent water, vegetation cover, proximity to human activity) during the dry season, yet only weak associations during the wet season, suggesting either complex ecological dynamics during this period or a lack of appropriate spatial information that results in stronger species-habitat associations. Raph's thesis laid the foundation for an effective pipeline to process additional cameratrap data obtained in Botswana, as well as to prepare spatially explicit raster layers that represent the distribution of several species that are likely to affect wild dog dispersal. During my PostDoc, I plan to rerun Raph's occupancy models using updated cameratrap data and to predict spatial layers that can then be used as additional covariates in the AWD dispersal model to render the influence of competitors and prey on the dispersal behavior of AWDs.

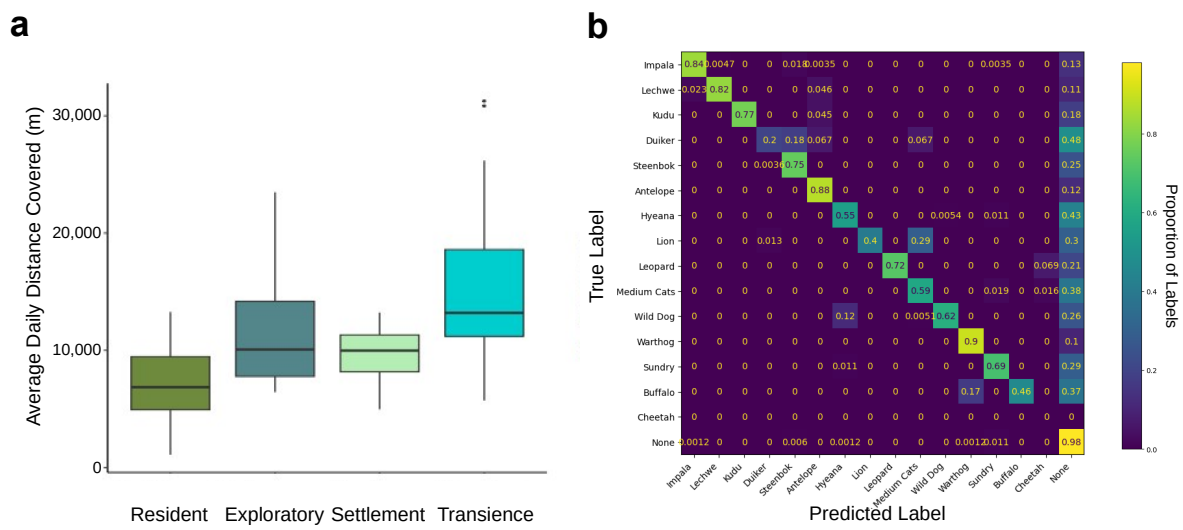


Figure A.2.1: (a) Results from Megan Robinson's master thesis on differences in movement behavior of AWDs depending on their behavioral mode / phase. (b) Confusion matrix of predicted vs. true labels as obtained from Raphaël Destriau's thesis, in which he assessed the reliability of TrapTagger to correctly assign species labels to cameratrap images.

A.3 R-Packages

During the course of my PhD, I developed four small R-packages that provided useful functionalities for my own work. The packages are available on GitHub (<https://github.com/DavidDHofmann>) and can be installed via the `devtools` package. I will here briefly summarize each package's functionality:

- `video2pic`: `video2pic` is an R-package that allows extracting still frames from a video. In contrast to existing packages, the frame-extraction algorithm is implemented in Python, which improves efficiency. The ability to extract still images from videos is particularly useful in cameratrapping studies, where videos of animals need to be converted into still images for classification.
- `floodmapr`: `floodmapr` is an R-package that allows downloading and classifying MODIS MCD43A4 satellite imagery into binary maps of dryland and water cover. The classification algorithm is based on Wolski et al. (2017) and currently only applicable for the extent of the Okavango Delta. The package handles all data download, as well as the necessary processing steps to obtain a “floodmap” of the Okavango Delta for any desired date.
- `rainmapr`: `rainmapr` is an R-package that allows downloading spatially mapped precipitation estimates from the CHIRPS database (Funk et al., 2015). CHIRPS provides precipitation data dating back to 1981 at daily or monthly temporal resolutions and spatial resolutions of up to 0.05° .
- `riversim`: `riversim` is an R-package that provides functionalities to simulate river networks. Comparable algorithms to simulate land-cover or land-use patterns already exist (e.g., `NLMR`, Sciaiani et al., 2018 or `gstat`, Pebesma, 2004), yet none of them achieves realistic looking river systems. The ability to simulate river networks is useful for ecological simulation studies, where rivers are assumed to play an important role. The original simulation algorithm was developed by a reddit user (“TalksInMaths”), yet I translated it into R.

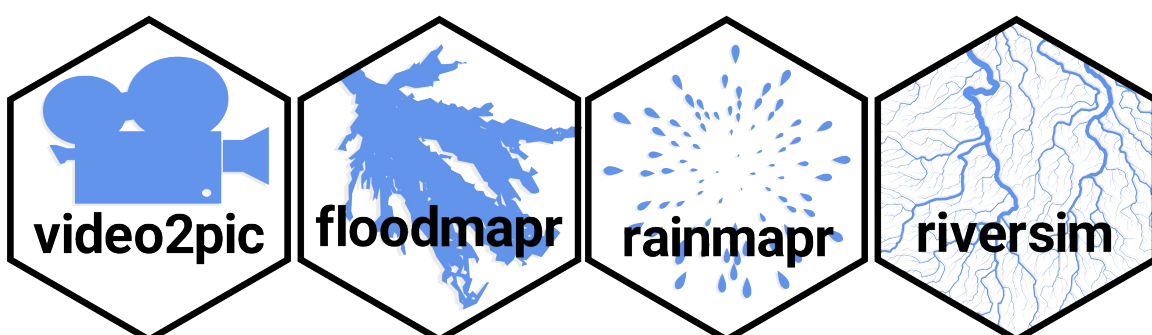


Figure A.3.1: Logos of the R-packages that I developed during the course of my PhD.



References

- Abrahms, B., Carter, N. H., Clark-Wolf, T. J., Gaynor, K. M., Johansson, E., McInturff, A., Nisi, A. C., Rafiq, K., & West, L. (2023). Climate Change as a Global Amplifier of Human–Wildlife Conflict. *Nature Climate Change*, 13(3), 224–234. <https://doi.org/10.1038/s41558-023-01608-5>
- Abrahms, B., Jordan, N. R., Golabek, K. A., McNutt, J. W., Wilson, A. M., & Brashares, J. S. (2016). Lessons from Integrating Behaviour and Resource Selection: Activity-Specific Responses of African Wild Dogs to Roads. *Animal Conservation*, 19(3), 247–255. <https://doi.org/10.1111/acv.12235>
- Abrahms, B., Rafiq, K., Jordan, N. R., & McNutt, J. W. (2022). Long-Term, Climate-Driven Phenological Shift in a Tropical Large Carnivore. *Proceedings of the National Academy of Sciences*, 119(27), e2121667119. <https://doi.org/10.1073/pnas.2121667119>
- Abrahms, B., Sawyer, S. C., Jordan, N. R., McNutt, J. W., Wilson, A. M., & Brashares, J. S. (2017). Does Wildlife Resource Selection Accurately Inform Corridor Conservation? *Journal of Applied Ecology*, 54(2), 412–422. <https://doi.org/10.1111/1365-2664.12714>
- Adriaensen, F., Chardon, J., De Blust, G., Swinnen, E., Villalba, S., Gulinck, H., & Matthysen, E. (2003). The Application of ‘Least-Cost’ Modelling as a Functional Landscape Model. *Landscape and Urban Planning*, 64(4), 233–247. [https://doi.org/10.1016/S0169-2046\(02\)00242-6](https://doi.org/10.1016/S0169-2046(02)00242-6)
- Akinyemi, F. O., & Abiodun, B. J. (2019). Potential Impacts of Global Warming Levels 1.5 °C and Above on Climate Extremes in Botswana. *Climatic Change*, 154, 387–400. <https://doi.org/10.1007/s10584-019-02446-1>
- Alberts, S. C., & Altmann, J. (1995). Balancing Costs and Opportunities: Dispersal in Male Baboons. *The American Naturalist*, 145(2), 279–306. <https://doi.org/10.1086/285740>
- Alerstam, T. (1993). *Bird Migration*. Cambridge University Press.
- Allen, C. H., Parrott, L., & Kyle, C. (2016). An Individual-Based Modelling Approach to Estimate Landscape Connectivity for Bighorn Sheep (*Ovis canadensis*). *PeerJ*, 4, e2001. <https://doi.org/10.7717/peerj.2001>
- Almond, R., Grooten, M., Juffe Bignoli, D., & Petersen, T. (2022). Living Planet Report 2022 - Building a Nature Positive Society. WWF: Gland, Switzerland.
- Alting, B. F., Bennett, E., Golabek, K. A., Pitcher, B. J., McNutt, J. W., Wilson, A. M., Bates, H., & Jordan, N. R. (2021). The Characteristics and Consequences of African Wild Dog (*Lycaon pictus*) Den Site Selection. *Behavioral Ecology and Sociobiology*, 75(7), 109. <https://doi.org/10.1007/s00265-021-03047-8>
- Apps, P. J., Claase, M. J., van Mourik, E., Lostrom, S., Yexley, B., Webster, H., & McNutt, J. W. (2022). A Description of a New Discovery: African Wild Dog Packs Communicate with Other Packs by Posting Scent-Mark Messages at a Shared Marking Site. *Behavioral Ecology and Sociobiology*, 76(3), 37. <https://doi.org/10.1007/s00265-022-03148-y>
- Arce Guillen, R., Lindgren, F., Muff, S., Glass, T. W., Breed, G. A., & Schlägel, U. E. (2023). Accounting for Unobserved Spatial Variation in Step Selection Analyses of Animal Movement Via Spatial Random Effects. *Methods in Ecology and Evolution*, 2041–210X.14208. <https://doi.org/10.1111/2041-210X.14208>
- Armansin, N. C., Stow, A. J., Cantor, M., Leu, S. T., Klarevas-Irby, J. A., Chariton, A. A., & Farine, D. R. (2020). Social Barriers in Ecological Landscapes: The Social Resistance Hypothesis. *Trends in Ecology & Evolution*, 35(2), 137–148. <https://doi.org/10.1016/j.tree.2019.10.001>
- Ashrafzadeh, M. R., Naghipour, A. A., Haidarian, M., Kusza, S., & Pilliod, D. S. (2019). Effects of Climate Change on Habitat and Connectivity for Populations of a Vulnerable, Endemic Salamander in Iran. *Global Ecology and Conservation*, 19, e00637. <https://doi.org/10.1016/j.gecco.2019.e00637>
- Avgar, T., Lele, S. R., Keim, J. L., & Boyce, M. S. (2017). Relative Selection Strength: Quantifying Effect Size in Habitat- and Step-Selection Inference. *Ecology and Evolution*, 7(14), 5322–5330. <https://doi.org/10.1002/ece3.3122>

- Avgar, T., Potts, J. R., Lewis, M. A., & Boyce, M. S. (2016). Integrated Step Selection Analysis: Bridging the Gap Between Resource Selection and Animal Movement. *Methods in Ecology and Evolution*, 7(5), 619–630. <https://doi.org/10.1111/2041-210X.12528>
- Aybar, C., Qiusheng, W., Bautista, L., Yali, R., Barja, A., Ushey, K., Ooms, J., Appelhans, T., Allaire, J. J., Tang, Y., Roy, S., Adauto, M., Carrasco, G., Bengtsson, H., Hollister, J., Donchyts, G., & JOSS, M. (2024). *Rgee: R Bindings for Calling the 'Earth Engine' API* (Version 1.1.7). Retrieved April 28, 2024, from <https://cran.r-project.org/web/packages/rgee/index.html>
- Baddeley, A., Rubak, E., & Turner, R. (2015). *Spatial Point Patterns: Methodology and Applications with R*. Chapman and Hall/CRC Press.
- Baguette, M., Blanchet, S., Legrand, D., Stevens, V. M., & Turlure, C. (2013). Individual Dispersal, Landscape Connectivity and Ecological Networks. *Biological Reviews*, 88(2), 310–326. <https://doi.org/10.1111/brv.12000>
- Baldwin, R. F., Calhoun, A. J. K., & deMaynadier, P. G. (2006). Conservation Planning for Amphibian Species with Complex Habitat Requirements: A Case Study Using Movements and Habitat Selection of the Wood Frog *Rana Sylvatica*. *Journal of Herpetology*, 40(4), 442–453. [https://doi.org/10.1670/0022-1511\(2006\)40\[442:CPFASW\]2.0.CO;2](https://doi.org/10.1670/0022-1511(2006)40[442:CPFASW]2.0.CO;2)
- Barnett, A. H., & Moorcroft, P. R. (2008). Analytic Steady-State Space Use Patterns and Rapid Computations in Mechanistic Home Range Analysis. *Journal of Mathematical Biology*, 57(1), 139–159. <https://doi.org/10.1007/s00285-007-0149-8>
- Barnosky, A. D., Matzke, N., Tomiya, S., Wogan, G. O. U., Swartz, B., Quental, T. B., Marshall, C., McGuire, J. L., Lindsey, E. L., Maguire, K. C., Mersey, B., & Ferrer, E. A. (2011). Has the Earth's Sixth Mass Extinction Already Arrived? *Nature*, 471(7336), 51–57. <https://doi.org/10.1038/nature09678>
- Bartlam-Brooks, H. L. A., Beck, P. S. A., Bohrer, G., & Harris, S. (2013). In search of greener pastures: Using satellite images to predict the effects of environmental change on zebra migration. *Journal of Geophysical Research: Biogeosciences*, 118(4), 1427–1437. <https://doi.org/10.1002/jgrg.20096>
- Bartlam-Brooks, H., Bonyongo, M., & Harris, S. (2011). Will Reconnecting Ecosystems Allow Long-Distance Mammal Migrations to Resume? A Case Study of a Zebra *Equus Burchelli* Migration in Botswana. *Oryx*, 45(2), 210–216. <https://doi.org/10.1017/S0030605310000414>
- Bastille-Rousseau, G., Douglas-Hamilton, I., Blake, S., Northrup, J. M., & Wittemyer, G. (2018). Applying Network Theory to Animal Movements to Identify Properties of Landscape Space Use. *Ecological Applications*, 28(3), 854–864. <https://doi.org/10.1002/eap.1697>
- Bastille-Rousseau, G., Wall, J., Douglas-Hamilton, I., & Wittemyer, G. (2018). Optimizing the Positioning of Wildlife Crossing Structures Using GPS Telemetry. *Journal of Applied Ecology*, 55(4), 2055–2063. <https://doi.org/10.1111/1365-2664.13117>
- Bastille-Rousseau, G., & Wittemyer, G. (2020). Characterizing the Landscape of Movement to Identify Critical Wildlife Habitat and Corridors. *Conservation Biology*, 35(1), 346–359. <https://doi.org/10.1111/cobi.13519>
- Beardsworth, C. E., Gobbens, E., van Maarseveen, F., Denissen, B., Dekkinga, A., Nathan, R., Toledo, S., & Bileveld, A. I. (2022). Validating Atlas: A Regional-Scale High-Throughput Tracking System. *Methods in Ecology and Evolution*, 13(9), 1990–2004. <https://doi.org/10.1111/2041-210X.13913>
- Behr, D. M. (2021). *Dispersal and Demography in the Endangered African Wild Dog (*Lycaon pictus*)*. University of Zurich.
- Behr, D. M., Hodel, F. H., Cozzi, G., McNutt, J. W., & Ozgul, A. (2023). Higher Mortality Is Not a Universal Cost of Dispersal: A Case Study in African Wild Dogs. *The American Naturalist*, 202(5), 616–629. <https://doi.org/10.1086/726220>
- Behr, D. M., McNutt, J. W., Ozgul, A., & Cozzi, G. (2020). When to Stay and When to Leave? Proximate Causes of Dispersal in an Endangered Social Carnivore. *Journal of Animal Ecology*, 89(10), 2356–2366. <https://doi.org/10.1111/1365-2656.13300>
- Behr, D. M., Ozgul, A., & Cozzi, G. (2017). Combining Human Acceptance and Habitat Suitability in a Unified Socio-Ecological Suitability Model: A Case Study of the Wolf in Switzerland. *Journal of Applied Ecology*, 54(6), 1919–1929. <https://doi.org/10.1111/1365-2664.12880>
- Beier, P., Majka, D. R., & Spencer, W. D. (2008). Forks in the Road: Choices in Procedures for Designing Wildland Linkages. *Conservation Biology*, 22(4), 836–851. <https://doi.org/10.1111/j.1523-1739.2008.00942.x>
- Beier, P., Spencer, W., Baldwin, R. F., & McRAE, B. H. (2011). Toward Best Practices for Developing Regional Connectivity Maps. *Conservation Biology*, 25(5), 879–892. <https://doi.org/10.1111/j.1523-1739.2011.01716.x>

- Bennitt, E., Bonyongo, M. C., & Harris, S. (2014). Habitat Selection by African Buffalo (*Syncerus caffer*) in Response to Landscape-Level Fluctuations in Water Availability on Two Temporal Scales. *PLoS ONE*, 9(7), e101346. <https://doi.org/10.1371/journal.pone.0101346>
- Benz, R. A., Boyce, M. S., Thurfjell, H., Paton, D. G., Musiani, M., Dormann, C. F., & Ciuti, S. (2016). Dispersal Ecology Informs Design of Large-Scale Wildlife Corridors. *PLoS ONE*, 11(9), e0162989. <https://doi.org/10.1371/journal.pone.0162989>
- Beyer, H. L., Haydon, D. T., Morales, J. M., Frair, J. L., Hebblewhite, M., Mitchell, M., & Matthiopoulos, J. (2010). The Interpretation of Habitat Preference Metrics Under Use–Availability Designs. *Philosophical Transactions of the Royal Society B: Biological Sciences*, 365(1550), 2245–2254. <https://doi.org/10.1098/rstb.2010.0083>
- Bingham, H., Lewis, E., Tayleur, J., Cunningham, C., Kingston, N., Burgess, N., Ash, N., Sandwith, T., & MacKinnon, K. (2021). *Protected Planet Report 2020*.
- Bishop-Taylor, R., Tulbure, M. G., & Broich, M. (2018). Evaluating Static and Dynamic Landscape Connectivity Modelling Using a 25-Year Remote Sensing Time Series. *Landscape Ecology*, 33(4), 625–640. <https://doi.org/10.1007/s10980-018-0624-1>
- Bonte, D., Van Dyck, H., Bullock, J. M., Coulon, A., Delgado, M., Gibbs, M., Lehouck, V., Matthysen, E., Mustin, K., Saastamoinen, M., Schtickzelle, N., Stevens, V. M., Vandewoestijne, S., Baguette, M., Barton, K., Benton, T. G., Chaput-Bardy, A., Cloët, J., Dytham, C., ... Travis, J. M. J. (2012). Costs of Dispersal. *Biological Reviews*, 87(2), 290–312. <https://doi.org/10.1111/j.1469-185X.2011.00201.x>
- Bonyongo, C. M. (2005). Habitat Utilization by Impala (*Aepyceros memppus*) in the Okavango Delta. *Botswana Notes & Records*, 37(1), 227–235.
- Börger, L., & Fryxell, J. (2012). Quantifying Individual Differences in Dispersal Using Net Squared Displacement. In *Dispersal Ecology and Evolution* (pp. 222–230). Oxford University Press.
- Bowler, D. E., & Benton, T. G. (2005). Causes and Consequences of Animal Dispersal Strategies: Relating Individual Behaviour to Spatial Dynamics. *Biological Reviews*, 80(2), 205–225. <https://doi.org/10.1017/S1464793104006645>
- Boyce, M. S., Vernier, P. R., Nielsen, S. E., & Schmiegelow, F. K. (2002). Evaluating Resource Selection Functions. *Ecological Modelling*, 157(2-3), 281–300. [https://doi.org/10.1016/S0304-3800\(02\)00200-4](https://doi.org/10.1016/S0304-3800(02)00200-4)
- Brachet, S., Olivier, I., Godelle, B., Klein, E., Frascaria-Lacoste, N., & Gouyon, P.-H. (1999). Dispersal and Metapopulation Viability in a Heterogeneous Landscape. *Journal of Theoretical Biology*, 198(4), 479–495. <https://doi.org/10.1006/jtbi.1999.0926>
- Brand, T. van den. (2024). *Ggh4x: Hacks for 'ggplot2'* (Version 0.2.6). <https://cran.rstudio.com/web/packages/ggh4x/index.html>
- Brennan, A., Beytell, P., Aschenborn, O., Du Preez, P., Funston, P., Hanssen, L., Kilian, J., Stuart-Hill, G., Taylor, R., & Naidoo, R. (2020). Characterizing Multispecies Connectivity Across a Transfrontier Conservation Landscape. *Journal of Applied Ecology*, 57(9), 1700–1710. <https://doi.org/10.1111/1365-2664.13716>
- Briatte, F., Bojanowski, M., Canoui, M., Charlop-Powers, Z., Fisher, J. C., Johnson, K., & Rinker, T. (2024). *Ggnetwork: Geometries to Plot Networks with 'ggplot2'* (Version 0.5.12). <https://cran.r-project.org/web/packages/ggnetwork/index.html>
- Broekhuis, F., Madsen, E. K., & Klaassen, B. (2019). Predators and Pastoralists: How Anthropogenic Pressures Inside Wildlife Areas Influence Carnivore Space Use and Movement Behaviour. *Animal Conservation*, 22(4), 404–416. <https://doi.org/10.1111/acv.12483>
- Broekhuis, F., Cozzi, G., Valeix, M., McNutt, J. W., & Macdonald, D. W. (2013). Risk Avoidance in Sympatric Large Carnivores: Reactive or Predictive? *Journal of Animal Ecology*, 82(5), 1098–1105. <https://doi.org/10.1111/1365-2656.12077>
- Brooks, M. E., Kristensen, K., van Benthem, K. J., Magnusson, A., Berg, C. W., Nielsen, A., Skaug, H. J., Maechler, M., & Bolker, B. M. (2017). glmmTMB Balances Speed and Flexibility Among Packages for Zero-Inflated Generalized Linear Mixed Modeling. *The R Journal*, 9(2), 378–400. <https://doi.org/10.32614/RJ-2017-066>
- Brown, J. H., & Kodric-Brown, A. (1977). Turnover Rates in Insular Biogeography: Effect of Immigration on Extinction. *Ecology*, 58(2), 445–449. <https://doi.org/10.2307/1935620>
- Brown, M. B., Fennessy, J. T., Crego, R. D., Fleming, C. H., Alves, J., Brandlová, K., Fennessy, S., Ferguson, S., Hauptfleisch, M., Hejcmanova, P., Hoffman, R., Leimgruber, P., Maslaine, S., McQualter, K., Mueller, T., Muller, B., Muneza, A., O'Connor, D., Olivier, A. J., ... Stabach, J. (2023). Ranging Be-

- haviours Across Ecological and Anthropogenic Disturbance Gradients: A Pan-African Perspective of Giraffe (*Giraffa spp.*) Space Use. *Proceedings of the Royal Society B: Biological Sciences*, 290(2001), 20230912. <https://doi.org/10.1098/rspb.2023.0912>
- Buchholtz, E. K., Stronza, A., Songhurst, A., McCulloch, G., & Fitzgerald, L. A. (2020). Using Landscape Connectivity to Predict Human-Wildlife Conflict. *Biological Conservation*, 248, 108677. <https://doi.org/10.1016/j.biocon.2020.108677>
- Burnham, K. P., & Anderson, D. R. (2002). *Model Selection and Multimodel Inference: A Practical Information-Theoretic Approach*. Springer Science & Business Media.
- Cagnacci, F., Boitani, L., Powell, R. A., & Boyce, M. S. (2010). Animal Ecology Meets GPS-Based Radiotelemetry: A Perfect Storm of Opportunities and Challenges. *Philosophical Transactions of the Royal Society B: Biological Sciences*, 365(1550), 2157–2162. <https://doi.org/10.1098/rstb.2010.0107>
- Ceballos, G., Ehrlich, P. R., Barnosky, A. D., García, A., Pringle, R. M., & Palmer, T. M. (2015). Accelerated Modern Human-Induced Species Losses: Entering the Sixth Mass Extinction. *Science Advances*, 1(5), e1400253. <https://doi.org/10.1126/sciadv.1400253>
- Ceballos, G., Ehrlich, P. R., & Dirzo, R. (2017). Biological Annihilation Via the Ongoing Sixth Mass Extinction Signaled by Vertebrate Population Losses and Declines. *Proceedings of the National Academy of Sciences*, 114(30), E6089–E6096. <https://doi.org/10.1073/pnas.1704949114>
- Chapman, B. K., & McPhee, D. (2016). Global Shark Attack Hotspots: Identifying Underlying Factors Behind Increased Unprovoked Shark Bite Incidence. *Ocean & Coastal Management*, 133, 72–84. <https://doi.org/10.1016/j.ocecoaman.2016.09.010>
- Chen, I.-C., Hill, J. K., Ohlemüller, R., Roy, D. B., & Thomas, C. D. (2011). Rapid Range Shifts of Species Associated with High Levels of Climate Warming. *Science*, 333(6045), 1024–1026. <https://doi.org/10.1126/science.1206432>
- Chen, J., Chen, J., Liao, A., Cao, X., Chen, L., Chen, X., He, C., Han, G., Peng, S., & Lu, M. (2015). Global Land Cover Mapping at 30 m Resolution: A POK-Based Operational Approach. *ISPRS Journal of Photogrammetry and Remote Sensing*, 103, 7–27. <https://doi.org/10.1016/j.isprsjprs.2014.09.002>
- Chetkiewicz, C.-L. B., & Boyce, M. S. (2009). Use of Resource Selection Functions to Identify Conservation Corridors. *Journal of Applied Ecology*, 46(5), 1036–1047. <https://doi.org/10.1111/j.1365-2664.2009.01686.x>
- Chraibi, E., de Boissieu, F., Barbier, N., Luque, S., & Féret, J.-B. (2022). Stability in Time and Consistency Between Atmospheric Corrections: Assessing the Reliability of Sentinel-2 Products for Biodiversity Monitoring in Tropical Forests. *International Journal of Applied Earth Observation and Geoinformation*, 112, 102884. <https://doi.org/10.1016/j.jag.2022.102884>
- Ciudad, C., Mateo-Sánchez, M. C., Gastón, A., Blazquez-Cabrera, S., & Saura, S. (2021). Landscape Connectivity Estimates Are Affected by Spatial Resolution, Habitat Seasonality and Population Trends. *Biodiversity and Conservation*, 30(5), 1395–1413. <https://doi.org/10.1007/s10531-021-02148-0>
- Claase, M. J., Cherry, M. I., Apps, P. J., McNutt, J. W., Hansen, W. K., & Jordan, N. R. (2022). Interpack Communication in African Wild Dogs at Long-Term Shared Marking Sites. *Animal Behaviour*, 192, 27–38. <https://doi.org/10.1016/j.anbehav.2022.07.006>
- Clark, J. D., Laufenberg, J. S., Davidson, M., & Murrow, J. L. (2015). Connectivity Among Subpopulations of Louisiana Black Bears as Estimated by a Step Selection Function. *The Journal of Wildlife Management*, 79(8), 1347–1360. <https://doi.org/10.1002/jwmg.955>
- Cleaveland, S., Appel, M., Chalmers, W., Chillingworth, C., Kaare, M., & Dye, C. (2000). Serological and Demographic Evidence for Domestic Dogs as a Source of Canine Distemper Virus Infection for Serengeti Wildlife. *Veterinary Microbiology*, 72(3-4), 217–227. [https://doi.org/10.1016/S0378-1135\(99\)00207-2](https://doi.org/10.1016/S0378-1135(99)00207-2)
- Clevenger, A. P., Wierzchowski, J., Chruszcz, B., & Gunson, K. (2002). GIS-Generated, Expert-Based Models for Identifying Wildlife Habitat Linkages and Planning Mitigation Passages. *Conservation Biology*, 16(2), 503–514. <https://doi.org/10.1046/j.1523-1739.2002.00328.x>
- Clobert, J., Baguette, M., Benton, T. G., & Bullock, J. M. (2012). *Dispersal Ecology and Evolution*. Oxford University Press. <https://doi.org/10.1093/acprof:oso>
- Collins, M., Chandler, R. E., Cox, P. M., Huthnance, J. M., Rougier, J., & Stephenson, D. B. (2012). Quantifying Future Climate Change. *Nature Climate Change*, 2(6), 403–409. <https://doi.org/10.1038/nclimate1414>
- Copernicus Climate Change Service. (2021). CMIP6 predictions underpinning the C3S decadal prediction prototypes. <https://doi.org/10.24381/CDS.C866074C>

- Cozzi, G. (2013). *Patterns of Habitat Use and Segregation Among African Large Carnivores*. University of Zurich. <https://doi.org/10.5167/UZH-93646>
- Cozzi, G., Behr, D. M., Webster, H. S., Claase, M., Bryce, C. M., Modise, B., McNutt, J. W., & Ozgul, A. (2020). African Wild Dog Dispersal and Implications for Management. *The Journal of Wildlife Management*, 84(4), 614–621. <https://doi.org/10.1002/jwmg.21841>
- Cozzi, G., Börger, L., Hutter, P., Abegg, D., Beran, C., McNutt, J. W., & Ozgul, A. (2015). Effects of Trophy Hunting Leftovers on the Ranging Behaviour of Large Carnivores: A Case Study on Spotted Hyenas. *PLoS ONE*, 10(3), e0121471. <https://doi.org/10.1371/journal.pone.0121471>
- Cozzi, G., Broekhuis, F., McNutt, J. W., & Schmid, B. (2013). Comparison of the Effects of Artificial and Natural Barriers on Large African Carnivores: Implications for Interspecific Relationships and Connectivity. *Journal of Animal Ecology*, 82(3), 707–715. <https://doi.org/10.1111/1365-2656.12039>
- Cozzi, G., Broekhuis, F., McNutt, J. W., Turnbull, L. A., Macdonald, D. W., & Schmid, B. (2012). Fear of the Dark or Dinner by Moonlight? Reduced Temporal Partitioning Among Africa's Large Carnivores. *Ecology*, 93(12), 2590–2599. <https://doi.org/10.1890/12-0017.1>
- Cozzi, G., Maag, N., Börger, L., Clutton-Brock, T. H., & Ozgul, A. (2018). Socially Informed Dispersal in a Territorial Cooperative Breeder. *Journal of Animal Ecology*, 87(3), 838–849. <https://doi.org/10.1111/1365-2656.12795>
- Cozzi, G., Reilly, M., Abegg, D., Behr, D. M., Brack, P., Claase, M. J., Holmberg, J., Hofmann, D. D., Kalil, P., Ndlovu, S., Neelo, J., & McNutt, J. W. (2023). An AI-Based Platform to Investigate African Large Carnivore Dispersal and Demography Across Broad Landscapes: A Case Study and Future Directions Using African Wild Dogs. *African Journal of Ecology*, 62(1), e13227. <https://doi.org/10.1111/aje.13227>
- Creel, S. (2001). Four Factors Modifying the Effect of Competition on Carnivore Population Dynamics as Illustrated by African Wild Dogs. *Conservation Biology*, 15(1), 271–274. <https://doi.org/10.1111/j.1523-1739.2001.99534.x>
- Creel, S., Becker, M. S., De Merkle, J. R., & Goodheart, B. (2023). Hot or Hungry? A Tipping Point in the Effect of Prey Depletion on African Wild Dogs. *Biological Conservation*, 282, 110043. <https://doi.org/10.1016/j.biocon.2023.110043>
- Creel, S., & Creel, N. M. (1995). Communal Hunting and Pack Size in African Wild Dogs, *Lycaon pictus*. *Animal Behaviour*, 50(5), 1325–1339. [https://doi.org/10.1016/0003-3472\(95\)80048-4](https://doi.org/10.1016/0003-3472(95)80048-4)
- Creel, S., & Creel, N. M. (1996). Limitation of African Wild Dogs by Competition with Larger Carnivores. *Conservation Biology*, 10(2), 526–538. <https://doi.org/10.1046/j.1523-1739.1996.10020526.x>
- Creel, S., & Creel, N. M. (2002). *The African Wild Dog: Behavior, Ecology, and Conservation*. Princeton University Press.
- Creel, S., Merkle, J., Mweetwa, T., Becker, M. S., Mwape, H., Simpamba, T., & Simukonda, C. (2020). Hidden Markov Models Reveal a Clear Human Footprint on the Movements of Highly Mobile African Wild Dogs. *Scientific Reports*, 10(1), 1–11. <https://doi.org/10.1038/s41598-020-74329-w>
- Crutzen, P. J. (2006). The "Anthropocene". In *Earth System Science in the Anthropocene* (pp. 13–18). Springer. https://doi.org/10.1007/3-540-26590-2_3
- Csardi, G., & Nepusz, T. (2006). The igraph Software Package for Complex Network Research. *InterJournal, Complex Systems*, 1695. <https://igraph.org>
- Cushman, S. A., Chase, M., & Griffin, C. (2010). Mapping Landscape Resistance to Identify Corridors and Barriers for Elephant Movement in Southern Africa. In *Spatial Complexity, Informatics, and Wildlife Conservation* (pp. 349–367). Springer Japan. https://doi.org/10.1007/978-4-431-87771-4_19
- Cushman, S. A., Elliot, N. B., Bauer, D., Kesch, K., Bahaa-el-din, L., Bothwell, H., Flyman, M., Mtare, G., Macdonald, D. W., & Loveridge, A. J. (2018). Prioritizing Core Areas, Corridors and Conflict Hotspots for Lion Conservation in Southern Africa. *PLoS ONE*, 13(7), e0196213. <https://doi.org/10.1371/journal.pone.0196213>
- Cushman, S. A., & Lewis, J. S. (2010). Movement Behavior Explains Genetic Differentiation in American Black Bears. *Landscape Ecology*, 25(10), 1613–1625. <https://doi.org/10.1007/s10980-010-9534-6>
- Cutler, F. o. b. L. B. a. A., & Wiener, R. p. b. A. L. a. M. (2024). *randomForest: Breiman and Cutler's Random Forests for Classification and Regression* (Version 4.7-1.1). <https://cran.r-project.org/web/packages/randomForest/index.html>
- Dalerum, F., Somers, M. J., Kunkel, K. E., & Cameron, E. Z. (2008). The Potential for Large Carnivores to Act as Biodiversity Surrogates in Southern Africa. *Biodiversity and Conservation*, 17(12), 2939–2949. <https://doi.org/10.1007/s10531-008-9406-4>

- Davies, A. B., Marneweck, D. G., Druce, D. J., & Asner, G. P. (2016). Den Site Selection, Pack Composition, and Reproductive Success in Endangered African Wild Dogs. *Behavioral Ecology*, 27(6), 1869–1879. <https://doi.org/10.1093/beheco/arw124>
- Davies-Mostert, H. T., Kamler, J. F., Mills, M. G. L., Jackson, C. R., Rasmussen, G. S. A., Groom, R. J., & Macdonald, D. W. (2012). Long-Distance Transboundary Dispersal of African Wild Dogs Among Protected Areas in Southern Africa. *African Journal of Ecology*, 50(4), 500–506. <https://doi.org/10.1111/j.1365-2028.2012.01335.x>
- Day, C. C., McCann, N. P., Zollner, P. A., Gilbert, J. H., & MacFarland, D. M. (2019). Temporal Plasticity in Habitat Selection Criteria Explains Patterns of Animal Dispersal. *Behavioral Ecology*, 30(2), 528–540. <https://doi.org/10.1093/beheco/ary193>
- Day, C. C., Zollner, P. A., Gilbert, J. H., & McCann, N. P. (2020). Individual-Based Modeling Highlights the Importance of Mortality and Landscape Structure in Measures of Functional Connectivity. *Landscape Ecology*, 35(10), 2191–2208. <https://doi.org/10.1007/s10980-020-01095-5>
- DeCesare, N. J., Hebblewhite, M., Schmiegelow, F., Hervieux, D., McDermid, G. J., Neufeld, L., Bradley, M., Whittington, J., Smith, K. G., Morgantini, L. E., Wheatley, M., & Musiani, M. (2012). Transcending Scale Dependence in Identifying Habitat with Resource Selection Functions. *Ecological Applications*, 22(4), 1068–1083. <https://doi.org/10.1890/11-1610.1>
- DeCesare, N. J., Squires, J. R., & Kolbe, J. A. (2005). Effect of Forest Canopy on GPS-Based Movement Data. *Wildlife Society Bulletin*, 33(3), 935–941. [https://doi.org/10.2193/0091-7648\(2005\)33\[935:EOFCOG\]2.0.CO;2](https://doi.org/10.2193/0091-7648(2005)33[935:EOFCOG]2.0.CO;2)
- Delignette-Muller, M. L., & Dutang, C. (2015). fitdistrplus: An R package for fitting distributions. *Journal of Statistical Software*, 64(4), 1–34. <https://doi.org/10.18637/jss.v064.i04>
- D'eon, R. G., & Delparte, D. (2005). Effects of Radio-Collar Position and Orientation on GPS Radio-Collar Performance, and the Implications of PDOP in Data Screening. *Journal of Applied Ecology*, 42(2), 383–388. <https://doi.org/10.1111/j.1365-2664.2005.01010.x>
- Dickie, M., McNay, S. R., Sutherland, G. D., Cody, M., & Avgar, T. (2020). Corridors or Risk? Movement Along, and Use of, Linear Features Varies Predictably Among Large Mammal Predator and Prey Species. *Journal of Animal Ecology*, 89(2), 623–634. <https://doi.org/10.1111/1365-2656.13130>
- Didan, K. (2015). MOD13Q1 Modis/Terra Vegetation Indices 16-Day L3 Global 250m Sin Grid V006. NASA EOSDIS Land Processes Distributed Active Archive Center. <https://doi.org/10.5067/MODIS/MOD13Q1.006>
- Dilts, T. E., Weisberg, P. J., Leitner, P., Matocq, M. D., Inman, R. D., Nussear, K. E., & Esque, T. C. (2016). Multiscale connectivity and graph theory highlight critical areas for conservation under climate change. *Ecological Applications*, 26(4), 1223–1237. <https://doi.org/10.1890/15-0925>
- DiMiceli, C., Sohlberg, R., & Townshend, J. (2022). MODIS/Terra Vegetation Continuous Fields Yearly L3 Global 250m SIN Grid V061. NASA EOSDIS Land Processes Distributed Active Archive Center. <https://doi.org/10.5067/MODIS/MOD44B.061>
- Diniz, M. F., Cushman, S. A., Machado, R. B., & De Marco Júnior, P. (2019). Landscape Connectivity Modeling from the Perspective of Animal Dispersal. *Landscape Ecology*, 35, 41–58. <https://doi.org/10.1007/s10980-019-00935-3>
- Doerr, V. A. J., Barrett, T., & Doerr, E. D. (2011). Connectivity, Dispersal Behaviour and Conservation Under Climate Change: A Response to Hodgson et al.: Connectivity and Dispersal Behaviour. *Journal of Applied Ecology*, 48(1), 143–147. <https://doi.org/10.1111/j.1365-2664.2010.01899.x>
- Dray, S., Royer-Carenzi, M., & Calenge, C. (2010). The Exploratory Analysis of Autocorrelation in Animal-Movement Studies. *Ecological Research*, 25(3), 673–681. <https://doi.org/10.1007/s11284-010-0701-7>
- Dröge, E., Creel, S., Becker, M. S., & M'soka, J. (2017). Spatial and Temporal Avoidance of Risk Within a Large Carnivore Guild. *Ecology and Evolution*, 7(1), 189–199. <https://doi.org/10.1002/ece3.2616>
- Duchesne, T., Fortin, D., & Rivest, L.-P. (2015). Equivalence between Step Selection Functions and Biased Correlated Random Walks for Statistical Inference on Animal Movement. *PLoS ONE*, 10(4), e0122947. <https://doi.org/10.1371/journal.pone.0122947>
- Durant, J., Hjermann, D., Ottersen, G., & Stenseth, N. (2007). Climate and the Match or Mismatch Between Predator Requirements and Resource Availability. *Climate Research*, 33, 271–283. <https://doi.org/10.3354/cr033271>
- Eddelbuettel, D. (2013). *Seamless R and C++ Integration with Rcpp*. Springer New York. <https://doi.org/10.1007/978-1-4614-6868-4>

- Eddelbuettel, D., & Balamuta, J. J. (2018). Extending R with C++: A Brief Introduction to Rcpp. *The American Statistician*, 72(1), 28–36. <https://doi.org/10.1080/00031305.2017.1375990>
- Eddelbuettel, D., & François, R. (2011). Rcpp: Seamless R and C++ integration. *Journal of Statistical Software*, 40(8), 1–18. <https://doi.org/10.18637/jss.v040.i08>
- Eisaguirre, J. M., Williams, P. J., & Hooten, M. B. (2024). Rayleigh Step-Selection Functions and Connections to Continuous-Time Mechanistic Movement Models. *Movement Ecology*, 12(1), 14. <https://doi.org/10.1186/s40462-023-00442-w>
- Elliot, N. B., Cushman, S. A., Macdonald, D. W., & Loveridge, A. J. (2014). The Devil Is in the Dispersers: Predictions of Landscape Connectivity Change with Demography. *Journal of Applied Ecology*, 51(5), 1169–1178. <https://doi.org/10.1111/1365-2664.12282>
- Engelbrecht, F., Adegoke, J., Bopape, M.-J., Naidoo, M., Garland, R., Thatcher, M., McGregor, J., Katzfey, J., Werner, M., Ichoku, C., & Gatebe, C. (2015). Projections of Rapidly Rising Surface Temperatures Over Africa Under Low Mitigation. *Environmental Research Letters*, 10(8), 085004. <https://doi.org/10.1088/1748-9326/10/8/085004>
- Enns, G. E., Jex, B., & Boyce, M. S. (2023). Diverse Migration Patterns and Seasonal Habitat Use of Stone's Sheep (*Ovis dalli stonei*). *PeerJ*, 11, e15215. <https://doi.org/10.7717/peerj.15215>
- Estes, R. D., & Goddard, J. (1967). Prey Selection and Hunting Behavior of the African Wild Dog. *The Journal of Wildlife Management*, 31(1), 52–70. <https://doi.org/10.2307/3798360>
- Etherington, T. R. (2016). Least-Cost Modelling and Landscape Ecology: Concepts, Applications, and Opportunities. *Current Landscape Ecology Reports*, 1(1), 40–53. <https://doi.org/10.1007/s40823-016-0006-9>
- European Space Agency. (2018). Sentinel-2 MSI Level-2A BOA Reflectance. https://doi.org/10.5270/S2_6eb6imz
- Fahrig, L. (2003). Effects of Habitat Fragmentation on Biodiversity. *Annual Review of Ecology, Evolution, and Systematics*, 34(1), 487–515. <https://doi.org/10.1146/annurev.ecolsys.34.011802.132419>
- Fahrig, L. (2007). Non-Optimal Animal Movement in Human-Altered Landscapes. *Functional Ecology*, 21(6), 1003–1015. <https://doi.org/10.1111/j.1365-2435.2007.01326.x>
- Fanshawe, J. H., Frame, L. H., & Ginsberg, J. R. (1991). The Wild Dog - Africa's Vanishing Carnivore. *Oryx*, 25(3), 137–146. <https://doi.org/10.1017/S0030605300034165>
- Fattebert, J., Robinson, H. S., Balme, G., Slotow, R., & Hunter, L. (2015). Structural Habitat Predicts Functional Dispersal Habitat of a Large Carnivore: How Leopards Change Spots. *Ecological Applications*, 25(7), 1911–1921. <https://doi.org/10.1890/14-1631.1>
- Feldmeier, D. E., Schmitz, O. J., Carter, N. H., Masunga, G. S., & Orrick, K. D. (2024). Predictions & Perceptions: A Social-Ecological Analysis of Human-Carnivore Conflict in Botswana. *Biological Conservation*, 294, 110615. <https://doi.org/10.1016/j.biocon.2024.110615>
- Fieberg, J., Matthiopoulos, J., Hebblewhite, M., Boyce, M. S., & Frair, J. L. (2010). Correlation and Studies of Habitat Selection: Problem, Red Herring or Opportunity? *Philosophical Transactions of the Royal Society B: Biological Sciences*, 365(1550), 2233–2244. <https://doi.org/10.1098/rstb.2010.0079>
- Fieberg, J., Signer, J., Smith, B., & Avgar, T. (2021). A 'How to' Guide for Interpreting Parameters in Habitat-Selection Analyses. *Journal of Animal Ecology*, 90(5), 1027–1043. <https://doi.org/10.1111/1365-2656.13441>
- Finerty, G. E., Cushman, S. A., Bauer, D. T., Elliot, N. B., Kesch, M. K., Macdonald, D. W., & Loveridge, A. J. (2023). Evaluating Connectivity Models for Conservation: Insights from African Lion Dispersal Patterns. *Landscape Ecology*, 38(12), 3205–3219. <https://doi.org/10.1007/s10980-023-01782-z>
- Fletcher Jr., R. J., Iezzi, M. E., Guralnick, R., Marx, A. J., Ryan, S. J., & Valle, D. (2023). A Framework for Linking Dispersal Biology to Connectivity Across Landscapes. *Landscape Ecology*, 38(10), 1–14. <https://doi.org/10.1007/s10980-023-01741-8>
- Fletcher Jr., R. J., Sefair, J. A., Wang, C., Poli, C. L., Smith, T. A. H., Bruna, E. M., Holt, R. D., Barfield, M., Marx, A. J., & Acevedo, M. A. (2019). Towards a Unified Framework for Connectivity That Disentangles Movement and Mortality in Space and Time. *Ecology Letters*, 22(10), 1680–1689. <https://doi.org/10.1111/ele.13333>
- Forester, J. D., Im, H. K., & Rathouz, P. J. (2009). Accounting for Animal Movement in Estimation of Resource Selection Functions: Sampling and Data Analysis. *Ecology*, 90(12), 3554–3565. <https://doi.org/10.1890/08-0874.1>
- Forrest, S. W., Pagendam, D., Bode, M., Drovandi, C., Potts, J. R., Perry, J., Vanderduys, E., & Hoskins, A. J. (2024). Simulating Animal Movement Trajectories from Temporally Dynamic Step Selection Functions. <https://doi.org/10.1101/2024.03.19.585696>

- Fortin, D., Beyer, H. L., Boyce, M. S., Smith, D. W., Duchesne, T., & Mao, J. S. (2005). Wolves Influence Elk Movements: Behavior Shapes a Trophic Cascade in Yellowstone National Park. *Ecology*, 86(5), 1320–1330. <https://doi.org/10.1890/04-0953>
- Fortin, D., Fortin, M.-E., Beyer, H. L., Duchesne, T., Courant, S., & Dancose, K. (2009). Group-Size-Mediated Habitat Selection and Group Fusion–Fission Dynamics of Bison Under Predation Risk. *Ecology*, 90(9), 2480–2490. <https://doi.org/10.1890/08-0345.1>
- Fair, J. L., Fieberg, J., Hebblewhite, M., Cagnacci, F., DeCesare, N. J., & Pedrotti, L. (2010). Resolving Issues of Imprecise and Habitat-Biased Locations in Ecological Analyses Using GPS Telemetry Data. *Philosophical Transactions of the Royal Society B: Biological Sciences*, 365(1550), 2187–2200. <https://doi.org/10.1098/rstb.2010.0084>
- Frame, L. H., Malcolm, J. R., Frame, G. W., & Van Lawick, H. (1979). Social Organization of African Wild Dogs (*Lycaon pictus*) on the Serengeti Plains, Tanzania 1967–1978 1. *Zeitschrift für Tierpsychologie*, 50(3), 225–249. <https://doi.org/10.1111/j.1439-0310.1979.tb01030.x>
- Frankham, R., Ballou, J. D., Briscoe, D. A., & McInnes, K. H. (2002). *Introduction to Conservation Genetics*. Cambridge University Press. <https://doi.org/10.1017/CBO9780511808999>
- Fuller, A., Mitchell, D., Maloney, S. K., & Hetem, R. S. (2016). Towards a Mechanistic Understanding of the Responses of Large Terrestrial Mammals to Heat and Aridity Associated with Climate Change. *Climate Change Responses*, 3(1), 10. <https://doi.org/10.1186/s40665-016-0024-1>
- Fuller, T. K., Kat, P. W., Bulger, J. B., Maddock, A. H., Ginsberg, J. R., Burrows, R., McNutt, J. W., & Mills, M. G. L. (1992). Population Dynamics of African Wild Dogs. In *Wildlife 2001: Populations* (pp. 1125–1139). Springer.
- Funk, C., Peterson, P., Landsfeld, M., Pedreros, D., Verdin, J., Shukla, S., Husak, G., Rowland, J., Harrison, L., Hoell, A., & Michaelsen, J. (2015). The Climate Hazards Infrared Precipitation with Station - A New Environmental Record for Monitoring Extremes. *Scientific Data*, 2(1), 150066. <https://doi.org/10.1038/sdata.2015.66>
- Gastón, A., Blázquez-Cabrera, S., Garrote, G., Mateo-Sánchez, M. C., Beier, P., Simón, M. A., & Saura, S. (2016). Response to Agriculture by a Woodland Species Depends on Cover Type and Behavioural State: Insights from Resident and Dispersing Iberian Lynx. *Journal of Applied Ecology*, 53(3), 814–824. <https://doi.org/10.1111/1365-2664.12629>
- Ghoddousi, A., Buchholtz, E. K., Dietsch, A. M., Williamson, M. A., Sharma, S., Balkenhol, N., Kuemmerle, T., & Dutta, T. (2021). Anthropogenic Resistance: Accounting for Human Behavior in Wildlife Connectivity Planning. *One Earth*, 4(1), 39–48. <https://doi.org/10.1016/j.oneear.2020.12.003>
- Gilabert, M. A., Conese, C., & Maselli, F. (1994). An Atmospheric Correction Method for the Automatic Retrieval of Surface Reflectances from TM Images. *International Journal of Remote Sensing*, 15(10), 2065–2086. <https://doi.org/10.1080/01431169408954228>
- Gorelick, N., Hancher, M., Dixon, M., Ilyushchenko, S., Thau, D., & Moore, R. (2017). Google Earth Engine: Planetary-Scale Geospatial Analysis for Everyone. *Remote Sensing of Environment*. <https://doi.org/10.1016/j.rse.2017.06.031>
- Graves, T. A., Chandler, R. B., Royle, J. A., Beier, P., & Kendall, K. C. (2014). Estimating Landscape Resistance to Dispersal. *Landscape Ecology*, 29(7), 1201–1211. <https://doi.org/10.1007/s10980-014-0056-5>
- Graves, T. A., & Waller, J. S. (2006). Understanding the Causes of Missed Global Positioning System Telemetry Fixes. *Journal of Wildlife Management*, 70(3), 844–851. [https://doi.org/10.2193/0022-541X\(2006\)70\[844:UTCOMG\]2.0.CO;2](https://doi.org/10.2193/0022-541X(2006)70[844:UTCOMG]2.0.CO;2)
- Gumbrecht, T., Wolski, P., Frost, P., & McCarthy, T. (2004). Forecasting the Spatial Extent of the Annual Flood in the Okavango Delta, Botswana. *Journal of Hydrology*, 290(3-4), 178–191. <https://doi.org/10.1016/j.jhydrol.2003.11.010>
- Gusset, M., Swarner, M., Mponwane, L., Keletile, K., & McNutt, J. (2009). Human–Wildlife Conflict in Northern Botswana: Livestock Predation by Endangered African Wild Dog *Lycaon pictus* and Other Carnivores. *Oryx*, 43(1), 67–72. <https://doi.org/10.1017/S0030605308990475>
- Gustafson, E. J., & Gardner, R. H. (1996). The Effect of Landscape Heterogeneity on the Probability of Patch Colonization. *Ecology*, 77(1), 94–107. <https://doi.org/10.2307/2265659>
- Haddad, N. M., Brudvig, L. A., Clobert, J., Davies, K. F., Gonzalez, A., Holt, R. D., Lovejoy, T. E., Sexton, J. O., Austin, M. P., Collins, C. D., Cook, W. M., Damschen, E. I., Ewers, R. M., Foster, B. L., Jenkins, C. N., King, A. J., Laurance, W. F., Levey, D. J., Margules, C. R., ... Townshend, J. R. (2015). Habitat Fragmentation and Its Lasting Impact on Earth's Ecosystems. *Science Advances*, 1(2), e1500052. <https://doi.org/10.1126/sciadv.1500052>

- Hansen, M. C., & Riggs, R. A. (2008). Accuracy, Precision, and Observation Rates of Global Positioning System Telemetry Collars. *The Journal of Wildlife Management*, 72(2), 518–526. <https://doi.org/10.2193/2006-493>
- Hanski, I. (1999a). Habitat Connectivity, Habitat Continuity, and Metapopulations in Dynamic Landscapes. *Oikos*, 87(2), 209–219. <https://doi.org/10.2307/3546736>
- Hanski, I. (1999b). *Metapopulation Ecology*. Oxford University Press.
- Hauenstein, S., Fattebert, J., Grüebler, M. U., Naef-Daenzer, B., Pe'er, G., & Hartig, F. (2019). Calibrating an Individual-Based Movement Model to Predict Functional Connectivity for Little Owls. *Ecological Applications*, 29(4), e01873. <https://doi.org/10.1002/eap.1873>
- Hayward, M. W., O'Brien, J., Hofmeyr, M., & Kerley, G. I. H. (2006). Prey Preferences of the African Wild Dog Lycaon Pictus (Canidae: Carnivora): Ecological Requirements for Conservation. *Journal of Mammalogy*, 87(6), 1122–1131. <https://doi.org/10.1644/05-MAMM-A-304R2.1>
- Hayward, M. W., & Slotow, R. (2009). Temporal Partitioning of Activity in Large African Carnivores: Tests of Multiple Hypotheses. *South African Journal of Wildlife Research*, 39(2), 109–125. <https://doi.org/10.3957/056.039.0207>
- Heinz, S. K., Wissel, C., & Frank, K. (2006). The Viability of Metapopulations: Individual Dispersal Behaviour Matters. *Landscape Ecology*, 21(1), 77–89. <https://doi.org/10.1007/s10980-005-0148-3>
- Heller, N. E., & Zavaleta, E. S. (2009). Biodiversity Management in the Face of Climate Change: A Review of 22 Years of Recommendations. *Biological Conservation*, 142(1), 14–32. <https://doi.org/10.1016/j.biocon.2008.10.006>
- Hijmans, R. J., Bivand, R., Pebesma, E., & Sumner, M. D. (2024). *Terra: Spatial Data Analysis* (Version 1.7-38). <https://cran.r-project.org/web/packages/terra/index.html>
- Hilty, J., Worboys, G. L., Keeley, A., Woodley, S., Lausche, B. J., Locke, H., Carr, M., Pulsford, I., Pittcock, J., White, J. W., Theobald, D. M., Levine, J., Reuling, M., Watson, J. E., Ament, R., & Tabor, G. M. (2020). *Guidelines for Conserving Connectivity Through Ecological Networks and Corridors* (C. Groves, Ed.). IUCN, International Union for Conservation of Nature. <https://doi.org/10.2305/IUCN.CH.2020.PAG.30.en>
- Hodel, F. H., & Fieberg, J. R. (2022). Circular–Linear Copulae for Animal Movement Data. *Methods in Ecology and Evolution*, 13(5), 1001–1013. <https://doi.org/10.1111/2041-210X.13821>
- Hodgson, J. A., Thomas, C. D., Dytham, C., Travis, J. M. J., & Cornell, S. J. (2012). The Speed of Range Shifts in Fragmented Landscapes. *PLoS ONE*, 7(10), e47141. <https://doi.org/10.1371/journal.pone.0047141>
- Hodgson, J. A., Wallis, D. W., Krishna, R., & Cornell, S. J. (2016). How to Manipulate Landscapes to Improve the Potential for Range Expansion. *Methods in Ecology and Evolution*, 7(12), 1558–1566. <https://doi.org/10.1111/2041-210X.12614>
- Hofman, M. P. G., Hayward, M. W., Heim, M., Marchand, P., Rolandsen, C. M., Mattisson, J., Urbano, F., Heurich, M., Mysterud, A., Melzheimer, J., Morellet, N., Voigt, U., Allen, B. L., Gehr, B., Rouco, C., Ullmann, W., Holand, Ø., Jørgensen, N. H., Steinheim, G., ... Balkenhol, N. (2019). Right on Track? Performance of Satellite Telemetry in Terrestrial Wildlife Research. *PLoS ONE*, 14(5), e0216223. <https://doi.org/10.1371/journal.pone.0216223>
- Hofmann, D. D., Behr, D. M., McNutt, J. W., Ozgul, A., & Cozzi, G. (2021). Bound Within Boundaries: Do Protected Areas Cover Movement Corridors of Their Most Mobile, Protected Species? *Journal of Applied Ecology*, 58(6), 1133–1144. <https://doi.org/10.1111/1365-2664.13868>
- Hofmann, D. D., Behr, D. M., McNutt, J. W., Ozgul, A., & Cozzi, G. (2024). Dispersal and Connectivity in Increasingly Extreme Climatic Conditions. *Global Change Biology*.
- Hofmann, D. D., Cozzi, G., & Fieberg, J. R. (2023). *R Code Associated with Methods for Implementing Integrated Step-Selection Functions with Incomplete Data*. Data Repository for the University of Minnesota (DRUM). <https://doi.org/10.13020/6WCD-6S43>
- Hofmann, D. D., Cozzi, G., McNutt, J. W., Ozgul, A., & Behr, D. M. (2023). A Three-Step Approach for Assessing Landscape Connectivity Via Simulated Dispersal: African Wild Dog Case Study. *Landscape Ecology*, 38(4), 981–998. <https://doi.org/10.1007/s10980-023-01602-4>
- Howard, W. E. (1960). Innate and Environmental Dispersal of Individual Vertebrates. *American Midland Naturalist*, 63(1), 152–161. <https://doi.org/10.2307/2422936>
- Hubel, T. Y., Myatt, J. P., Jordan, N. R., Dewhirst, O. P., McNutt, J. W., & Wilson, A. M. (2016). Additive Opportunistic Capture Explains Group Hunting Benefits in African Wild Dogs. *Nature Communications*, 7(1), 11033. <https://doi.org/10.1038/ncomms11033>

- Hughes, D. A., Kingston, D. G., & Todd, M. C. (2011). Uncertainty in Water Resources Availability in the Okavango River Basin as a Result of Climate Change. *Hydrology and Earth System Sciences*, 15(3), 931–941. <https://doi.org/10.5194/hess-15-931-2011>
- Hundertmark, K. J. (2007). Home Range, Dispersal and Migration. *Ecology and Management of the North American Moose*, 303–335. <https://doi.org/10.13140/2.1.4757.9843>
- IPBES. (2019, May 4). *Global Assessment Report on Biodiversity and Ecosystem Services of the Intergovernmental Science-Policy Platform on Biodiversity and Ecosystem Services*. [object Object]. <https://doi.org/10.5281/ZENODO.3831673>
- IPCC. (2022). *Summary for Policymakers*. Cambridge University Press. Cambridge, UK, New York, NY, USA. <https://doi.org/10.1017/9781009157926.001>
- Jackson, C. R., Marnewick, K., Lindsey, P. A., Røskart, E., & Robertson, M. P. (2016). Evaluating Habitat Connectivity Methodologies: A Case Study with Endangered African Wild Dogs in South Africa. *Landscape Ecology*, 31(7), 1433–1447. <https://doi.org/10.1007/s10980-016-0342-5>
- Jackson, C. R., Power, R. J., Groom, R. J., Masenga, E. H., Mjingo, E. E., Fyumagwa, R. D., Røskart, E., & Davies-Mostert, H. (2014). Heading for the Hills: Risk Avoidance Drives Den Site Selection in African Wild Dogs. *PLoS ONE*, 9(6), e99686. <https://doi.org/10.1371/journal.pone.0099686>
- Johns, D., Crist, E., & Sahgal, B. (2022). Ending the Domination of Nature. *Biological Conservation*, 273, 109703. <https://doi.org/10.1016/j.biocon.2022.109703>
- Johnson, D. S., London, J. M., & McClintock, B. (2024). NMML/crawl: Last CRAN release (Version v2.3.0-1). <https://doi.org/10.5281/ZENODO.596464>
- Johnson, D. S., London, J. M., Lea, M.-A., & Durban, J. W. (2008). Continuous-Time Correlated Random Walk Model for Animal Telemetry Data. *Ecology*, 89(5), 1208–1215. <https://doi.org/10.1890/07-1032.1>
- Johnson, D. H. (1980). The Comparison of Usage and Availability Measurements for Evaluating Resource Preference. *Ecology*, 61(1), 65–71. <https://doi.org/10.2307/1937156>
- Jønsson, K. A., Tøttrup, A. P., Borregaard, M. K., Keith, S. A., Rahbek, C., & Thorup, K. (2016). Tracking Animal Dispersal: From Individual Movement to Community Assembly and Global Range Dynamics. *Trends in Ecology & Evolution*, 31(3), 204–214. <https://doi.org/10.1016/j.tree.2016.01.003>
- Jordan, N. R., Golabek, K. A., Behr, D. M., Walker, R. H., Plimpton, L., Lostrom, S., Claase, M., Van der Weyde, L. K., & McNutt, J. W. (2022). Priority of Access to Food and Its Influence on Social Dynamics of an Endangered Carnivore. *Behavioral Ecology and Sociobiology*, 76(1), 13. <https://doi.org/10.1007/s00265-021-03115-z>
- Kanagaraj, R., Wiegand, T., Kramer-Schadt, S., & Goyal, S. P. (2013). Using Individual-Based Movement Models to Assess Inter-Patch Connectivity for Large Carnivores in Fragmented Landscapes. *Biological Conservation*, 167, 298–309. <https://doi.org/10.1016/j.biocon.2013.08.030>
- Kareiva, P., Watts, S., McDonald, R., & Boucher, T. (2007). Domesticated Nature: Shaping Landscapes and Ecosystems for Human Welfare. *Science*, 316(5833), 1866–1869. <https://doi.org/10.1126/science.1140170>
- Kassambara, A. (2024). Ggpubr: 'ggplot2' Based Publication Ready Plots (Version 0.6.0). <https://cran.r-project.org/web/packages/ggpubr/index.html>
- Kaszta, Ź., Cushman, S. A., & Slotow, R. (2021). Temporal Non-Stationarity of Path-Selection Movement Models and Connectivity: An Example of African Elephants in Kruger National Park. *Frontiers in Ecology and Evolution*, 9, 553263. <https://doi.org/10.3389/fevo.2021.553263>
- Kays, R., Crofoot, M. C., Jetz, W., & Wikelski, M. (2015). Terrestrial Animal Tracking as an Eye on Life and Planet. *Science*, 348(6240), aaa2478–aaa2478. <https://doi.org/10.1126/science.aaa2478>
- Keeley, A. T. H., Beier, P., Creech, T., Jones, K., Jongman, R. H., Stonecipher, G., & Tabor, G. M. (2019). Thirty Years of Connectivity Conservation Planning: An Assessment of Factors Influencing Plan Implementation. *Environmental Research Letters*, 14(10), 103001. <https://doi.org/10.1088/1748-9326/ab3234>
- Keeley, A. T., Beier, P., Keeley, B. W., & Fagan, M. E. (2017). Habitat Suitability Is a Poor Proxy for Landscape Connectivity During Dispersal and Mating Movements. *Landscape and Urban Planning*, 161, 90–102. <https://doi.org/10.1016/j.landurbplan.2017.01.007>
- Kelly, M. J. (2001). Computer-Aided Photograph Matching in Studies Using Individual Identification: An Example from Serengeti Cheetahs. *Journal of Mammalogy*, 82(2), 440–449. [https://doi.org/10.1644/1545-1542\(2001\)082<0440:CAPMIS>2.0.CO;2](https://doi.org/10.1644/1545-1542(2001)082<0440:CAPMIS>2.0.CO;2)
- Kéry, M., & Royle, J. A. (2016). Introduction to Data Simulation. In *Applied Hierarchical Modeling in Ecology* (pp. 123–143). Elsevier. <https://doi.org/10.1016/B978-0-12-801378-6.00004-7>

- Kgathi, D., Kniveton, D., Ringrose, S., Turton, A., Vanderpost, C., Lundqvist, J., & Seely, M. (2006). The Okavango; a River Supporting Its People, Environment and Economic Development. *Journal of Hydrology*, 331(1-2), 3–17. <https://doi.org/10.1016/j.jhydrol.2006.04.048>
- Kim, D., Thompson, P. R., Wolfson, D., Merkle, J., Oliveira-Santos, L. G. R., Forester, J. D., Avgar, T., Lewis, M. A., & Fieberg, J. (2023, August 17). *Identifying Signals of Memory from Observations of Animal Movements in Plato's Cave* (preprint). <https://doi.org/10.1101/2023.08.15.553411>
- Kingdon, J. (2015). *The Kingdon Field Guide to African Mammals*. Bloomsbury.
- Klappstein, N. J., Thomas, L., & Michelot, T. (2023). Flexible Hidden Markov Models for Behaviour-Dependent Habitat Selection. *Movement Ecology*, 11(1), 30. <https://doi.org/10.1186/s40462-023-00392-3>
- Klappstein, N., Michelot, T., Fieberg, J., Pedersen, E., Field, C., & Flemming, J. M. (2024). Step Selection Analysis with Non-Linear and Random Effects in mgcv. <https://doi.org/10.1101/2024.01.05.574363>
- Koen, E. L., Bowman, J., Sadowski, C., & Walpole, A. A. (2014). Landscape Connectivity for Wildlife: Development and Validation of Multispecies Linkage Maps. *Methods in Ecology and Evolution*, 5(7), 626–633. <https://doi.org/10.1111/2041-210X.12197>
- Koen, E. L., Garraway, C. J., Wilson, P. J., & Bowman, J. (2010). The Effect of Map Boundary on Estimates of Landscape Resistance to Animal Movement. *PLoS ONE*, 5(7), e11785. <https://doi.org/10.1371/journal.pone.0011785>
- Kokko, H. (2006). From Individual Dispersal to Species Ranges: Perspectives for a Changing World. *Science*, 313(5788), 789–791. <https://doi.org/10.1126/science.1128566>
- Koshy, R., Alwiel, R., Adrian, B., Grossman, A., & Smith, H. F. (2020). Adaptations to Cursoriality and Digit Reduction in the Forelimb of the African Wild Dog (*Lycaon pictus*). *The FASEB Journal*, 34(S1), 1. <https://doi.org/10.1096/fasebj.2020.34.s1.01994>
- Kramer-Schadt, S., Revilla, E., Wiegand, T., & Breitenmoser, U. (2004). Fragmented Landscapes, Road Mortality and Patch Connectivity: Modelling Influences on the Dispersal of Eurasian Lynx: Lynx Dispersal in Fragmented Landscapes. *Journal of Applied Ecology*, 41(4), 711–723. <https://doi.org/10.1111/j.0021-8901.2004.00933.x>
- Kuang, K. (2024). *Pbmapply: Tracking the Progress of Mc*pply with Progress Bar* (Version 1.5.1). <https://cran.r-project.org/web/packages/pbmapply/index.html>
- Kubota, T., Aonashi, K., Ushio, T., Shige, S., Takayabu, Y. N., Kachi, M., Arai, Y., Tashima, T., Masaki, T., Kawamoto, N., Mega, T., Yamamoto, M. K., Hamada, A., Yamaji, M., Liu, G., & Oki, R. (2020). Global Satellite Mapping of Precipitation (GSMP) Products in the GPM Era. In *Satellite Precipitation Measurement: Volume 1* (pp. 355–373). Springer International Publishing. https://doi.org/10.1007/978-3-030-24568-9_20
- Kühme, W. (1965). Freilandstudien zur Soziologie des Hyänenhundes (*Lycaon pictus lupinus*, Thomas 1902) 2. *Zeitschrift für Tierpsychologie*, 22(5), 495–541.
- Kuhn, M. (2008). Building Predictive Models in R Using the caret Package. *Journal of Statistical Software*, 28(5). <https://doi.org/10.18637/jss.v028.i05>
- Landguth, E. L., Hand, B. K., Glassy, J., Cushman, S. A., & Sawaya, M. A. (2012). UNICOR: A Species Connectivity and Corridor Network Simulator. *Ecography*, 35(1), 9–14. <https://doi.org/10.1111/j.1600-0587.2011.07149.x>
- LaPoint, S., Gallery, P., Wikelski, M., & Kays, R. (2013). Animal Behavior, Cost-Based Corridor Models, and Real Corridors. *Landscape Ecology*, 28(8), 1615–1630. <https://doi.org/10.1007/s10980-013-9910-0>
- Latham, A. D. M., Latham, M. C., Boyce, M. S., & Boutin, S. (2011). Movement Responses by Wolves to Industrial Linear Features and Their Effect on Woodland Caribou in Northeastern Alberta. *Ecological Applications*, 21(8), 2854–2865. <https://doi.org/10.1890/11-0666.1>
- Leigh, K. A., Zenger, K. R., Tammen, I., & Raadsma, H. W. (2012). Loss of Genetic Diversity in an Outbreeding Species: Small Population Effects in the African Wild Dog (*Lycaon pictus*). *Conservation Genetics*, 13(3), 767–777. <https://doi.org/10.1007/s10592-012-0325-2>
- Levin, S. A. (1992). The Problem of Pattern and Scale in Ecology: The Robert H. MacArthur Award Lecture. *Ecology*, 73(6), 1943–1967. <https://doi.org/10.2307/1941447>
- Lewis, J. S., Rachlow, J. L., Garton, E. O., & Vierling, L. A. (2007). Effects of Habitat on GPS Collar Performance: Using Data Screening to Reduce Location Error: GPS Collar Performance. *Journal of Applied Ecology*, 44(3), 663–671. <https://doi.org/10.1111/j.1365-2664.2007.01286.x>
- Lines, R., Bompoudakis, D., Xofis, P., & Tzanopoulos, J. (2021). Modelling Multi-Species Connectivity at the Kafue-Zambezi Interface: Implications for Transboundary Carnivore Conservation. *Sustainability*, 13(22), 12886. <https://doi.org/10.3390/su132212886>

- Littlefield, C. E., Crosby, M., Michalak, J. L., & Lawler, J. J. (2019). Connectivity for Species on the Move: Supporting Climate-Driven Range Shifts. *Frontiers in Ecology and the Environment*, 17(5), 270–278. <https://doi.org/10.1002/fee.2043>
- Locke, H., Ellis, E. C., Venter, O., Schuster, R., Ma, K., Shen, X., Woodley, S., Kingston, N., Bhola, N., Strassburg, B. B. N., Paulsch, A., Williams, B., & Watson, J. E. M. (2019). Three Global Conditions for Biodiversity Conservation and Sustainable Use: An Implementation Framework. *National Science Review*, 6(6), 1080–1082. <https://doi.org/10.1093/nsr/nwz136>
- Luo, Z., Wang, X., Yang, S., Cheng, X., Liu, Y., & Hu, J. (2021). Combining the Responses of Habitat Suitability and Connectivity to Climate Change for an East Asian Endemic Frog. *Frontiers in Zoology*, 18(1), 14. <https://doi.org/10.1186/s12983-021-00398-w>
- MacArthur, R. H., & Wilson, E. O. (2001). *The Theory of Island Biogeography*. Princeton University Press. <https://doi.org/10.1515/9781400881376>
- Main-Knorn, M., Pflug, B., Louis, J., Debaecker, V., Müller-Wilm, U., & Gascon, F. (2017, October 4). Sen2Cor for Sentinel-2. In *Image and Signal Processing for Remote Sensing XXIII* (p. 3). SPIE. <https://doi.org/10.1117/12.2278218>
- Mallory, C. D., & Boyce, M. S. (2019). Prioritization of Landscape Connectivity for the Conservation of Peary Caribou. *Ecology and Evolution*, 9(4), 2189–2205. <https://doi.org/10.1002/ece3.4915>
- Manly, B. F., McDonald, L., Thomas, D. L., McDonald, T. L., & Erickson, W. P. (2007). *Resource Selection by Animals: Statistical Design and Analysis for Field Studies*. Springer Science & Business Media.
- Marneweck, D. G., Druce, D. J., Cromsigt, J. P. G. M., le Roux, E., & Somers, M. J. (2022). The Relative Role of Intrinsic and Extrinsic Drivers in Regulating Population Change and Survival of African Wild Dogs (*Lycaon pictus*). *Mammalian Biology*. <https://doi.org/10.1007/s42991-022-00281-z>
- Marnewick, K., Ferreira, S. M., Grange, S., Watermeyer, J., Maputla, N., & Davies-Mostert, H. T. (2014). Evaluating the Status of African Wild Dogs *Lycaon pictus* and Cheetahs *Acinonyx jubatus* through Tourist-based Photographic Surveys in the Kruger National Park. *PLoS ONE*, 9(1), e86265. <https://doi.org/10.1371/journal.pone.0086265>
- Marrec, R., Abdel Moniem, H. E., Iravani, M., Hricko, B., Kariyeva, J., & Wagner, H. H. (2020). Conceptual framework and uncertainty analysis for large-scale, species-agnostic modelling of landscape connectivity across Alberta, Canada. *Scientific Reports*, 10(1), 6798. <https://doi.org/10.1038/s41598-020-63545-z>
- Marsh, D. M., Thakur, K. A., Bulka, K. C., & Clarke, L. B. (2004). Dispersal and Colonization Through Open Fields by a Terrestrial, Woodland Salamander. *Ecology*, 85(12), 3396–3405. <https://doi.org/10.1890/03-0713>
- Martensen, A. C., Saura, S., & Fortin, M.-J. (2017). Spatio-Temporal Connectivity: Assessing the Amount of Reachable Habitat in Dynamic Landscapes. *Methods in Ecology and Evolution*, 8(10), 1253–1264. <https://doi.org/10.1111/2041-210X.12799>
- Martin, J., Vourc'h, G., Bonnot, N., Cargnelutti, B., Chaval, Y., Lourtet, B., Goulard, M., Hoch, T., Plantard, O., Hewison, A. J. M., & Morellet, N. (2018). Temporal Shifts in Landscape Connectivity for an Ecosystem Engineer, the Roe Deer, Across a Multiple-Use Landscape. *Landscape Ecology*, 33(6), 937–954. <https://doi.org/10.1007/s10980-018-0641-0>
- Masenga, E. H., Jackson, C. R., Mjingo, E. E., Jacobson, A., Riggio, J., Lyamuya, R. D., Fyumagwa, R. D., Borner, M., & Røskaft, E. (2016). Insights into Long-Distance Dispersal by African Wild Dogs in East Africa. *African Journal of Ecology*, 54(1), 95–98. <https://doi.org/10.1111/aje.12244>
- Mattisson, J., Andrén, H., Persson, J., & Segerström, P. (2010). Effects of Species Behavior on Global Positioning System Collar Fix Rates. *Journal of Wildlife Management*, 74(3), 557–563. <https://doi.org/10.2193/2009-157>
- Mbizah, M. M., Joubert, C. J., Joubert, L., & Groom, R. J. (2014). Implications of African Wild Dog (*Lycaon pictus*) Denning on the Density and Distribution of a Key Prey Species: Addressing Myths and Misperceptions. *Biodiversity and Conservation*, 23(6), 1441–1451. <https://doi.org/10.1007/s10531-014-0675-9>
- McCarthy, J. M., Gumbrecht, T., McCarthy, T., Frost, P., Wessels, K., & Seidel, F. (2003). Flooding Patterns of the Okavango Wetland in Botswana between 1972 and 2000. *AMBIO: A Journal of the Human Environment*, 32(7), 453–457. <https://doi.org/10.1579/0044-7447-32.7.453>
- McCarthy, T. S. (2006). Groundwater in the Wetlands of the Okavango Delta, Botswana, and Its Contribution to the Structure and Function of the Ecosystem. *Journal of Hydrology*, 320(3), 264–282. <https://doi.org/10.1016/j.jhydrol.2005.07.045>

- McCarthy, T., Barry, M., Bloem, A., Ellery, W., Heister, H., Merry, C., Röther, H., & Sternberg, H. (1997). The Gradient of the Okavango Fan, Botswana, and Its Sedimentological and Tectonic Implications. *Journal of African Earth Sciences*, 24(1-2), 65–78. [https://doi.org/10.1016/S0899-5362\(97\)00027-4](https://doi.org/10.1016/S0899-5362(97)00027-4)
- McClintock, B. T. (2017). Incorporating Telemetry Error into Hidden Markov Models of Animal Movement Using Multiple Imputation. *Journal of Agricultural, Biological and Environmental Statistics*, 22(3), 249–269. <https://doi.org/10.1007/s13253-017-0285-6>
- McClintock, B. T., King, R., Thomas, L., Matthiopoulos, J., McConnell, B. J., & Morales, J. M. (2012). A General Discrete-Time Modeling Framework for Animal Movement Using Multistate Random Walks. *Ecological Monographs*, 82(3), 335–349. <https://doi.org/10.1890/11-0326.1>
- McClure, M. L., Hansen, A. J., & Inman, R. M. (2016). Connecting Models to Movements: Testing Connectivity Model Predictions Against Empirical Migration and Dispersal Data. *Landscape Ecology*, 31(7), 1419–1432. <https://doi.org/10.1007/s10980-016-0347-0>
- McGarigal, K., Wan, H. Y., Zeller, K. A., Timm, B. C., & Cushman, S. A. (2016). Multi-Scale Habitat Selection Modeling: A Review and Outlook. *Landscape Ecology*, 31(6), 1161–1175. <https://doi.org/10.1007/s10980-016-0374-x>
- McNutt, J. W. (1996). Sex-Biased Dispersal in African Wild Dogs, *Lycaon pictus*. *Animal Behaviour*, 52(6), 1067–1077. <https://doi.org/10.1006/anbe.1996.0254>
- McNutt, J. W., Stein, A. B., McNutt, L. B., & Jordan, N. R. (2017). Living on the Edge: Characteristics of Human-Wildlife Conflict in a Traditional Livestock Community in Botswana. *Wildlife Research*, 44(7), 546–557. <https://doi.org/10.1071/WR16160>
- McRae, B. H. (2006). Isolation by Resistance. *Evolution*, 60(8), 1551–1561. <https://doi.org/10.1111/j.0014-3820.2006.tb00500.x>
- McRae, B. H., Dickson, B. G., Keitt, T. H., & Shah, V. B. (2008). Using Circuit Theory to Model Connectivity in Ecology, Evolution, and Conservation. *Ecology*, 89(10), 2712–2724. <https://doi.org/10.1890/07-1861.1>
- Melbourne, B. A., & Hastings, A. (2008). Extinction Risk Depends Strongly on Factors Contributing to Stochasticity. *Nature*, 454(7200), 100–103. <https://doi.org/10.1038/nature06922>
- Mendelsohn, J. M., & El Obeid, S. (2004). *Okavango River: The Flow of a Lifeline*. Struik.
- Mendelsohn, J. M., Vander Post, C., Ramberg, L., Murray-Hudson, M., Wolski, P., & Mosepele, K. (2010). *Okavango Delta: Floods of Life*. RAISON.
- Merkle, J. A., Monteith, K. L., Aikens, E. O., Hayes, M. M., Hersey, K. R., Middleton, A. D., Oates, B. A., Sawyer, H., Scurlock, B. M., & Kauffman, M. J. (2016). Large Herbivores Surf Waves of Green-up During Spring. *Proceedings of the Royal Society B: Biological Sciences*, 283(1833), 20160456. <https://doi.org/10.1098/rspb.2016.0456>
- Michalski, F., Boulhosa, R. L. P., Faria, A., & Peres, C. A. (2006). Human-Wildlife Conflicts in a Fragmented Amazonian Forest Landscape: Determinants of Large Felid Depredation on Livestock. *Animal Conservation*, 9(2), 179–188. <https://doi.org/10.1111/j.1469-1795.2006.00025.x>
- Michelot, T., Klappstein, N. J., Potts, J. R., & Fieberg, J. (2024). Understanding Step Selection Analysis Through Numerical Integration. *Methods in Ecology and Evolution*, 15(1), 24–35. <https://doi.org/10.1111/2041-210X.14248>
- Michelot, T., Langrock, R., & Patterson, T. A. (2016). moveHMM: An R Package for the Statistical Modelling of Animal Movement Data Using Hidden Markov Models. *Methods in Ecology and Evolution*, 7(11), 1308–1315. <https://doi.org/10.1111/2041-210X.12578>
- Mills, M. G. L., & Gorman, M. L. (1997). Factors Affecting the Density and Distribution of Wild Dogs in the Kruger National Park. *Conservation Biology*, 11(6), 1397–1406. <https://doi.org/10.1046/j.1523-1739.1997.96252.x>
- Moses, O., & Hambira, W. L. (2018). Effects of Climate Change on Evapotranspiration Over the Okavango Delta Water Resources. *Physics and Chemistry of the Earth, Parts A/B/C*, 105, 98–103. <https://doi.org/10.1016/j.pce.2018.03.011>
- Muff, S., Signer, J., & Fieberg, J. (2020). Accounting for Individual-Specific Variation in Habitat-Selection Studies: Efficient Estimation of Mixed-Effects Models Using Bayesian or Frequentist Computation. *Journal of Animal Ecology*, 89(1), 80–92. <https://doi.org/10.1111/1365-2656.13087>
- Mui, A. B., Caverhill, B., Johnson, B., Fortin, M.-J., & He, Y. (2017). Using Multiple Metrics to Estimate Seasonal Landscape Connectivity for Blanding's Turtles (*Emydoidea blandingii*) in a Fragmented Landscape. *Landscape Ecology*, 32(3), 531–546. <https://doi.org/10.1007/s10980-016-0456-9>

- Munden, R., Börger, L., Wilson, R. P., Redcliffe, J., Brown, R., Garel, M., & Potts, J. R. (2021). Why Did the Animal Turn? Time-Varying Step Selection Analysis for Inference Between Observed Turning-Points in High Frequency Data. *Methods in Ecology and Evolution*, 12(5), 921–932. <https://doi.org/10.1111/2041-210X.13574>
- Muñoz-Sabater, J., Dutra, E., Agustí-Panareda, A., Albergel, C., Arduini, G., Balsamo, G., Boussetta, S., Choulga, M., Harrigan, S., & Hersbach, H. (2021). ERA5-Land: A state-of-the-art global reanalysis dataset for land applications. *Earth System Science Data*, 13(9), 4349–4383.
- Murray-Hudson, M., Wolski, P., & Ringrose, S. (2006). Scenarios of the Impact of Local and Upstream Changes in Climate and Water Use on Hydro-Ecology in the Okavango Delta, Botswana. *Journal of Hydrology*, 331(1), 73–84. <https://doi.org/10.1016/j.jhydrol.2006.04.041>
- Naidoo, R., Chase, M. J., Beytell, P., Du Preez, P., Landen, K., Stuart-Hill, G., & Taylor, R. (2016). A Newly Discovered Wildlife Migration in Namibia and Botswana Is the Longest in Africa. *Oryx*, 50(1), 138–146. <https://doi.org/10.1017/S0030605314000222>
- Nathan, R. (2008). An Emerging Movement Ecology Paradigm. *Proceedings of the National Academy of Sciences*, 105(49), 19050–19051. <https://doi.org/10.1073/pnas.0808918105>
- Nathan, R. (2001). The Challenges of Studying Dispersal. *Trends in Ecology & Evolution*, 16(9), 481–483.
- Nathan, R., Monk, C. T., Arlinghaus, R., Adam, T., Alós, J., Assaf, M., Baktoft, H., Beardsworth, C. E., Bertram, M. G., Bijleveld, A. I., Brodin, T., Brooks, J. L., Campos-Candela, A., Cooke, S. J., Gjelland, K. Ø., Gupte, P. R., Harel, R., Hellström, G., Jeltsch, F., ... Jarić, I. (2022). Big-Data Approaches Lead to an Increased Understanding of the Ecology of Animal Movement. *Science*, 375(6582), eabg1780. <https://doi.org/10.1126/science.abg1780>
- O'Neill, H. M. K., Durant, S. M., & Woodroffe, R. (2020). What Wild Dogs Want: Habitat Selection Differs Across Life Stages and Orders of Selection in a Wide-Ranging Carnivore. *BMC Zoology*, 5(1). <https://doi.org/10.1186/s40850-019-0050-0>
- OpenStreetMap contributors. (2017). Planet dump retrieved from <https://planet.osm.org>. Retrieved July 12, 2023, from <https://www.openstreetmap.org>
- Osipova, L., Okello, M. M., Njumbi, S. J., Ngene, S., Western, D., Hayward, M. W., & Balkenhol, N. (2019). Using Step-Selection Functions to Model Landscape Connectivity for African Elephants: Accounting for Variability Across Individuals and Seasons. *Animal Conservation*, 22(1), 35–48. <https://doi.org/10.1111/acv.12432>
- Osofsky, S. A., McNutt, J. W., & Hirsch, K. J. (1996). Immobilization of Free-Ranging African Wild Dogs (*Lycaon pictus*) Using a Ketamine/Xylazine/Atropine Combination. *Journal of Zoo and Wildlife Medicine*, 27(4), 528–532. <https://doi.org/10.2307/20095618>
- Ozgul, A., Fichtel, C., Paniw, M., & Kappeler, P. M. (2023). Destabilizing Effect of Climate Change on the Persistence of a Short-Lived Primate. *Proceedings of the National Academy of Sciences*, 120(14), e2214244120. <https://doi.org/10.1073/pnas.2214244120>
- Paniw, M., James, T. D., Ruth Archer, C., Römer, G., Levin, S., Compagnoni, A., Che-Castaldo, J., Bennett, J. M., Mooney, A., Childs, D. Z., Ozgul, A., Jones, O. R., Burns, J. H., Beckerman, A. P., Patwary, A., Sanchez-Gassen, N., Knight, T. M., & Salguero-Gómez, R. (2021). The Myriad of Complex Demographic Responses of Terrestrial Mammals to Climate Change and Gaps of Knowledge: A Global Analysis. *Journal of Animal Ecology*, 90(6), 1398–1407. <https://doi.org/10.1111/1365-2656.13467>
- Paniw, M., Maag, N., Cozzi, G., Clutton-Brock, T., & Ozgul, A. (2019). Life History Responses of Meerkats to Seasonal Changes in Extreme Environments. *Science*, 363(6427), 631–635. <https://doi.org/10.1126/science.aau5905>
- Panzacchi, M., Van Moorter, B., Strand, O., Saerens, M., Kivimäki, I., St. Clair, C. C., Herfindal, I., & Boitani, L. (2016). Predicting the Continuum Between Corridors and Barriers to Animal Movements Using Step Selection Functions and Randomized Shortest Paths. *Journal of Animal Ecology*, 85(1), 32–42. <https://doi.org/10.1111/1365-2656.12386>
- Pebesma, E. J. (2004). Multivariable Geostatistics in S: The gstat Package. *Computers & Geosciences*, 30(7), 683–691. <https://doi.org/10.1016/j.cageo.2004.03.012>
- Pennycuick, C. J., & Rudnai, J. (1970). A Method of Identifying Individual Lions *Panthera leo* with an Analysis of the Reliability of Identification. *Journal of Zoology*, 160(4), 497–508. <https://doi.org/10.1111/j.1469-7998.1970.tb03093.x>
- Pérez-Goya, U., Montesino-SanMartin, M., Militino, A. F., & Ugarte, M. D. (2020). RGISTools: Downloading, Customizing, and Processing Time Series of Remote Sensing Data in R (1). <https://doi.org/10.48550/ARXIV.2002.01859>

- Perrin, N., & Mazalov, V. (2000). Local Competition, Inbreeding, and the Evolution of Sex-Biased Dispersal. *The American Naturalist*, 155(1), 116–127. <https://doi.org/10.1086/303296>
- Phillips, K. A., Elvey, C. R., & Abercrombie, C. L. (1998). Applying GPS to the Study of Primate Ecology: A Useful Tool? *American Journal of Primatology*, 46(2), 167–172. [https://doi.org/10.1002/\(SICI\)1098-2345\(1998\)46:2<167::AID-AJP6>3.0.CO;2-U](https://doi.org/10.1002/(SICI)1098-2345(1998)46:2<167::AID-AJP6>3.0.CO;2-U)
- Pinto, N., & Keitt, T. H. (2009). Beyond the Least-Cost Path: Evaluating Corridor Redundancy Using a Graph-Theoretic Approach. *Landscape Ecology*, 24(2), 253–266. <https://doi.org/10.1007/s10980-008-9303-y>
- Pitman, R. T., Fattebert, J., Williams, S. T., Williams, K. S., Hill, R. A., Hunter, L. T. B., Robinson, H., Power, J., Swanepoel, L., Slotow, R., & Balme, G. A. (2017). Cats, Connectivity and Conservation: Incorporating Data Sets and Integrating Scales for Wildlife Management. *Journal of Applied Ecology*, 54(6), 1687–1698. <https://doi.org/10.1111/1365-2664.12851>
- Pohle, J., Signer, J., Eccard, J. A., Dammhahn, M., & Schlägel, U. E. (2023). How to Account for Behavioural States in Step-Selection Analysis: A Model Comparison (1). <https://doi.org/10.48550/ARXIV.2304.12964>
- Pomilia, M. A., McNutt, J. W., & Jordan, N. R. (2015). Ecological Predictors of African Wild Dog Ranging Patterns in Northern Botswana. *Journal of Mammalogy*, 96(6), 1214–1223. <https://doi.org/10.1093/jmammal/gyv130>
- Potts, J. R., Bastille-Rousseau, G., Murray, D. L., Schaefer, J. A., & Lewis, M. A. (2013). Predicting Local and Non-Local Effects of Resources on Animal Space Use Using a Mechanistic Step Selection Model. *Methods in Ecology and Evolution*, 5(3), 253–262. <https://doi.org/10.1111/2041-210X.12150>
- Potts, J. R., & Börger, L. (2023). How to Scale up from Animal Movement Decisions to Spatiotemporal Patterns: An Approach Via Step Selection. *Journal of Animal Ecology*, 92(1), 16–29. <https://doi.org/10.1111/1365-2656.13832>
- Potts, J. R., Börger, L., Scantlebury, D. M., Bennett, N. C., Alagaili, A., & Wilson, R. P. (2018). Finding Turning-Points in Ultra-High-Resolution Animal Movement Data. *Methods in Ecology and Evolution*, 9(10), 2091–2101. <https://doi.org/10.1111/2041-210X.13056>
- Puy, A., & Saltelli, A. (2022). *Mind the Hubris: Complexity Can Misfire*. arXiv: 2207.12230 [cs, math]. Retrieved January 9, 2024, from <http://arxiv.org/abs/2207.12230>
- R Core Team. (2023). *R: A Language and Environment for Statistical Computing*. manual. R Foundation for Statistical Computing. Vienna, Austria. <https://www.R-project.org/>
- Rabaiotti, D., & Woodroffe, R. (2019). Coping with Climate Change: Limited Behavioral Responses to Hot Weather in a Tropical Carnivore. *Oecologia*, 189(3), 587–599. <https://doi.org/10.1007/s00442-018-04329-1>
- Rabaiotti, D., Coulson, T., & Woodroffe, R. (2023). Climate Change Is Predicted to Cause Population Collapse in a Cooperative Breeder. *Global Change Biology*, 29(21), 6002–6017. <https://doi.org/10.1111/gcb.16890>
- Rabaiotti, D., Groom, R., McNutt, J. W., Watermeyer, J., O'Neill, H. M. K., & Woodroffe, R. (2021). High Temperatures and Human Pressures Interact to Influence Mortality in an African Carnivore. *Ecology and Evolution*, 11(13), 8495–8506. <https://doi.org/10.1002/ece3.7601>
- Radchuk, V., Reed, T., Teplitsky, C., van de Pol, M., Charmantier, A., Hassall, C., Adamík, P., Adriaensen, F., Ahola, M. P., Arcese, P., Miguel Avilés, J., Balbontin, J., Berg, K. S., Borras, A., Burthe, S., Clober, J., Dehnhard, N., de Lope, F., Dhondt, A. A., ... Kramer-Schadt, S. (2019). Adaptive Responses of Animals to Climate Change Are Most Likely Insufficient. *Nature Communications*, 10(1), 3109. <https://doi.org/10.1038/s41467-019-10924-4>
- Ramberg, L., Hancock, P., Lindholm, M., Meyer, T., Ringrose, S., Sliva, J., Van As, J., & Vander Post, C. (2006). Species Diversity of the Okavango Delta, Botswana. *Aquatic Sciences*, 68(3), 310–337. <https://doi.org/10.1007/s00027-006-0857-y>
- Ranghetti, L., Boschetti, M., Nutini, F., & Busetto, L. (2020). “sen2r”: An R Toolbox for Automatically Downloading and Preprocessing Sentinel-2 Satellite Data. *Computers & Geosciences*, 139, 104473. <https://doi.org/10.1016/j.cageo.2020.104473>
- Rasmussen, G. S. A., & Macdonald, D. W. (2012). Masking of the Zeitgeber: African Wild Dogs Mitigate Persecution by Balancing Time. *Journal of Zoology*, 286(3), 232–242. <https://doi.org/10.1111/j.1469-7998.2011.00874.x>
- Rasmussen, K., Palacios, D. M., Calambokidis, J., Saborío, M. T., Dalla Rosa, L., Secchi, E. R., Steiger, G. H., Allen, J. M., & Stone, G. S. (2007). Southern Hemisphere Humpback Whales Wintering Off Central

- America: Insights from Water Temperature into the Longest Mammalian Migration. *Biology Letters*, 3(3), 302–305. <https://doi.org/10.1098/rsbl.2007.0067>
- Reppert, S. M., & De Roode, J. C. (2018). Demystifying Monarch Butterfly Migration. *Current Biology*, 28(17), R1009–R1022. <https://doi.org/10.1016/j.cub.2018.02.067>
- Revilla, E., & Wiegand, T. (2008). Individual Movement Behavior, Matrix Heterogeneity, and the Dynamics of Spatially Structured Populations. *Proceedings of the National Academy of Sciences*, 105(49), 19120–19125. <https://doi.org/10.1073/pnas.0801725105>
- Rhodes, R., & Rhodes, G. (2004). Prey Selection and Use of Natural and Man-Made Barriers by African Wild Dogs While Hunting. *South African Journal of Wildlife Research*, 34(2).
- Rudnick, D. A., Ryan, S. J., Beier, P., Cushman, S. A., Dieffenbach, F., Epps, C. W., Gerber, L. R., Hartter, J., Jenness, J. S., Kintsch, J., Merenlender, A. M., Perkl, R. M., Preziosi, D. V., & Trombulak, S. C. (2012). The Role of Landscape Connectivity in Planning and Implementing Conservation and Restoration Priorities. *Issues in Ecology*, (16), 1–23.
- Rumiano, F., Wielgus, E., Miguel, E., Chamaillé-Jammes, S., Valls-Fox, H., Cornélis, D., Garine-Wichatitsky, M. D., Fritz, H., Caron, A., & Tran, A. (2020). Remote Sensing of Environmental Drivers Influencing the Movement Ecology of Sympatric Wild and Domestic Ungulates in Semi-Arid Savannas, a Review. *Remote Sensing*, 12(19), 3218. <https://doi.org/10.3390/rs12193218>
- Saleni, P., Gusset, M., Graf, J. A., Szykman, M., Walters, M., & Somers, M. J. (2007). Refuges in Time: Temporal Avoidance of Interference Competition in Endangered Wild Dogs *Lycaon pictus*. *Canid News*, 10(2), 1–5.
- Sandoval-Seres, E., Moyo, W., Madhlamoto, D., Madzikanda, H., Blinston, P., Kotze, R., Van Der Meer, E., & Loveridge, A. (2022). Long-Distance African Wild Dog Dispersal Within the Kavango-Zambezi Transfrontier Conservation Area. *African Journal of Ecology*, 60(4), 1262–1266. <https://doi.org/10.1111/aje.13065>
- Sawyer, S. C., Epps, C. W., & Brashares, J. S. (2011). Placing Linkages Among Fragmented Habitats: Do Least-Cost Models Reflect How Animals Use Landscapes? *Journal of Applied Ecology*, 48(3), 668–678. <https://doi.org/10.1111/j.1365-2664.2011.01970.x>
- Scheiter, S., & Higgins, S. I. (2009). Impacts of Climate Change on the Vegetation of Africa: An Adaptive Dynamic Vegetation Modelling Approach. *Global Change Biology*, 15(9), 2224–2246. <https://doi.org/10.1111/j.1365-2486.2008.01838.x>
- Schlather, M., Malinowski, A., Menck, P. J., Oesting, M., & Strokorb, K. (2015). Analysis, Simulation and Prediction of Multivariate Random Fields with Package RandomFields. *Journal of Statistical Software*, 63, 1–25. <https://doi.org/10.18637/jss.v063.i08>
- Sciaini, M., Fritsch, M., Scherer, C., & Simpkins, C. E. (2018). NLMR and landscapetools: An Integrated Environment for Simulating and Modifying Neutral Landscape Models in R. *Methods in Ecology and Evolution*, 9(11), 2240–2248. <https://doi.org/10.1111/2041-210X.13076>
- Serneels, S., & Lambin, E. F. (2001). Impact of Land-Use Changes on the Wildebeest Migration in the Northern Part of the Serengeti–Mara Ecosystem. *Journal of Biogeography*, 28(3), 391–407. <https://doi.org/10.1046/j.1365-2699.2001.00557.x>
- Shaffer, M. L., & Samson, F. B. (1985). Population Size and Extinction: A Note on Determining Critical Population Sizes. *The American Naturalist*, 125(1), 144–152. <https://doi.org/10.1086/284332>
- Shetty, S., Gupta, P. K., Belgui, M., & Srivastav, S. K. (2021). Assessing the Effect of Training Sampling Design on the Performance of Machine Learning Classifiers for Land Cover Mapping Using Multi-Temporal Remote Sensing Data and Google Earth Engine. *Remote Sensing*, 13(8), 1433. <https://doi.org/10.3390/rs13081433>
- Signer, J., Fieberg, J., & Avgar, T. (2017). Estimating Utilization Distributions from Fitted Step-Selection Functions. *Ecosphere*, 8(4), e01771. <https://doi.org/10.1002/ecs2.1771>
- Signer, J., Fieberg, J., & Avgar, T. (2019). Animal movement tools (amt): R package for managing tracking data and conducting habitat selection analyses. *Ecology and Evolution*, 9(2), 880–890. <https://doi.org/10.1002/ece3.4823>
- Signer, J., Fieberg, J., Reineking, B., Schlägel, U. E., Smith, B. J., Balkenhol, N., & Avgar, T. (2024). Simulating Animal Space Use from Fitted Integrated Step-Selection Functions. *Methods in Ecology and Evolution*, 15(1), 43–50. <https://doi.org/10.1111/2041-210X.14263>
- Simpkins, C. E., Dennis, T. E., Etherington, T. R., & Perry, G. L. W. (2017). Effects of Uncertain Cost-Surface Specification on Landscape Connectivity Measures. *Ecological Informatics*, 38, 1–11. <https://doi.org/10.1016/j.ecoinf.2016.12.005>

- Simpkins, C. E., & Perry, G. L. (2017). Understanding the Impacts of Temporal Variability on Estimates of Landscape Connectivity. *Ecological Indicators*, 83, 243–248. <https://doi.org/10.1016/j.ecolind.2017.08.008>
- Sleeter, B., Loveland, T. R., Domke, G. M., Herold, N., Wickham, J., & Wood, N. J. (2018). Chapter 5 : Land Cover and Land Use Change. *Impacts, Risks, and Adaptation in the United States: The Fourth National Climate Assessment, Volume II*. U.S. Global Change Research Program. <https://doi.org/10.7930/NCA4.2018.CH5>
- Śmielak, M. K. (2023). Biologically Meaningful Moonlight Measures and Their Application in Ecological Research. *Behavioral Ecology and Sociobiology*, 77(2), 21. <https://doi.org/10.1007/s00265-022-03287-2>
- Smith, H. F., Adrian, B., Koshy, R., Alwiel, R., & Grossman, A. (2020). Adaptations to Cursoriality and Digit Reduction in the Forelimb of the African Wild Dog (*Lycaon pictus*). *PeerJ*, 8, e9866. <https://doi.org/10.7717/peerj.9866>
- Spear, S. F., Balkenhol, N., Fortin, M.-J., Mcrae, B. H., & Scribner, K. (2010). Use of Resistance Surfaces for Landscape Genetic Studies: Considerations for Parameterization and Analysis: Resistance Surfaces in Landscape Genetics. *Molecular Ecology*, 19(17), 3576–3591. <https://doi.org/10.1111/j.1365-294X.2010.04657.x>
- Squires, J. R., DeCesare, N. J., Olson, L. E., Kolbe, J. A., Hebblewhite, M., & Parks, S. A. (2013). Combining Resource Selection and Movement Behavior to Predict Corridors for Canada Lynx at Their Southern Range Periphery. *Biological Conservation*, 157, 187–195. <https://doi.org/10.1016/j.biocon.2012.07.018>
- Stamps, J. A., Krishnan, V. V., & Reid, M. L. (2005). Search Costs and Habitat Selection by Dispersers. *Ecology*, 86(2), 510–518. <https://doi.org/10.1890/04-0516>
- Storey, J., Scaramuzza, P., Schmidt, G., & Barsi, J. (2005). Landsat 7 Scan Line Corrector-Off Gap-Filled Product Development.
- Stott, P. (2016). How Climate Change Affects Extreme Weather Events. *Science*, 352(6293), 1517–1518. <https://doi.org/10.1126/science.aaf7271>
- Taylor, C., Schmidt-Nielsen, K., Dmi'el, R., & Fedak, M. (1971). Effect of Hyperthermia on Heat Balance During Running in the African Hunting Dog. *American Journal of Physiology-Legacy Content*, 220(3), 823–827. <https://doi.org/10.1152/ajplegacy.1971.220.3.823>
- Taylor, P. D., Fahrig, L., Henein, K., & Merriam, G. (1993). Connectivity Is a Vital Element of Landscape Structure. *Oikos*, 68(3), 571–573. <https://doi.org/10.2307/3544927>
- Tensen, L., Jansen van Vuuren, B., Groom, R., Bertola, L. D., de longh, H., Rasmussen, G., Du Plessis, C., Davies-Mostert, H., van der Merwe, D., Fabiano, E., Lages, F., Rocha, F., Monterroso, P., & Godinho, R. (2022). Spatial Genetic Patterns in African Wild Dogs Reveal Signs of Effective Dispersal Across Southern Africa. *Frontiers in Ecology and Evolution*, 10, 992389. <https://doi.org/10.3389/fevo.2022.992389>
- Therneau, T., Atkinson, B., & Ripley, B. (2024). *Rpart: Recursive Partitioning and Regression Trees* (Version 4.1.21). <https://cran.r-project.org/web/packages/rpart/index.html>
- Therneau, T. M. (2024). *Coxme: Mixed Effects Cox Models* (Version 2.2-18.1). <https://cran.r-project.org/web/packages/coxme/index.html>
- Therneau, T. M., Lumley, T., Elizabeth, A., & Cynthia, C. (2024). *Survival: Survival Analysis* (Version 3.5-7). <https://cran.r-project.org/web/packages/survival/index.html>
- Thieurmel, B., & Elmarhraoui, A. (2022). *Suncalc: Compute Sun Position, Sunlight Phases, Moon Position and Lunar Phase*. manual. <https://CRAN.R-project.org/package=suncalc>
- Thomas, C. D., Cameron, A., Green, R. E., Bakkenes, M., Beaumont, L. J., Collingham, Y. C., Erasmus, B. F. N., De Siqueira, M. F., Grainger, A., Hannah, L., Hughes, L., Huntley, B., Van Jaarsveld, A. S., Midgley, G. F., Miles, L., Ortega-Huerta, M. A., Townsend Peterson, A., Phillips, O. L., & Williams, S. E. (2004). Extinction Risk from Climate Change. *Nature*, 427(6970), 145–148. <https://doi.org/10.1038/nature02121>
- Thuiller, W., Broennimann, O., Hughes, G., Alkemade, J. R. M., Midgley, Guy. F., & Corsi, F. (2006). Vulnerability of African Mammals to Anthropogenic Climate Change Under Conservative Land Transformation Assumptions. *Global Change Biology*, 12(3), 424–440. <https://doi.org/10.1111/j.1365-2486.2006.01115.x>
- Thurfjell, H., Ciuti, S., & Boyce, M. S. (2014). Applications of Step-Selection Functions in Ecology and Conservation. *Movement Ecology*, 2(1), 4. <https://doi.org/10.1186/2051-3933-2-4>

- Tiecke, T. G., Liu, X., Zhang, A., Gros, A., Li, N., Yetman, G., Kilic, T., Murray, S., Blakespoor, B., Prydz, E. B., & Dang, H.-A. H. (2017). *Mapping the World Population One Building at a Time*. arXiv: 1712.05839 [cs]. Retrieved June 19, 2023, from <http://arxiv.org/abs/1712.05839>
- Tischendorf, L., & Fahrig, L. (2000). On the Usage and Measurement of Landscape Connectivity. *Oikos*, 90(1), 7–19. <https://doi.org/10.1034/j.1600-0706.2000.900102.x>
- Tomkiewicz, S. M., Fuller, M. R., Kie, J. G., & Bates, K. K. (2010). Global Positioning System and Associated Technologies in Animal Behaviour and Ecological Research. *Philosophical Transactions of the Royal Society B: Biological Sciences*, 365(1550), 2163–2176. <https://doi.org/10.1098/rstb.2010.0090>
- Toth, C., & Józków, G. (2016). Remote Sensing Platforms and Sensors: A Survey. *ISPRS Journal of Photogrammetry and Remote Sensing*, 115, 22–36. <https://doi.org/10.1016/j.isprsjprs.2015.10.004>
- Treves, A., Martin, K. A., Wydeven, A. P., & Wiedenhoeft, J. E. (2011). Forecasting Environmental Hazards and the Application of Risk Maps to Predator Attacks on Livestock. *BioScience*, 61(6), 451–458. <https://doi.org/10.1525/bio.2011.61.6.7>
- Tshimologo, B. T., Reading, R. P., Mills, M. G., Bonyongo, M. C., Rutina, L., Collins, K., & Maude, G. (2021). Prey Selection by African Wild Dogs (*Lycaon pictus*) in Northern Botswana. *African Journal of Wildlife Research*, 51(1). <https://doi.org/10.3957/056.051.0001>
- Tucker, M. A., Böhning-Gaese, K., Fagan, W. F., Fryxell, J. M., Van Moorter, B., Alberts, S. C., Ali, A. H., Allen, A. M., Attias, N., Avgar, T., Bartlam-Brooks, H., Bayarbaatar, B., Belant, J. L., Bertassoni, A., Beyer, D., Bidner, L., van Beest, F. M., Blake, S., Blaum, N., ... Mueller, T. (2018). Moving in the Anthropocene: Global Reductions in Terrestrial Mammalian Movements. *Science*, 359(6374), 466–469. <https://doi.org/10.1126/science.aam9712>
- Turchin, P. (1998). *Quantitative Analysis of Movement: Measuring and Modeling Population Redistribution in Animals and Plants*. Sinauer Associates.
- Ummenhofer, C. C., & Meehl, G. A. (2017). Extreme Weather and Climate Events with Ecological Relevance: A Review. *Philosophical Transactions of the Royal Society B: Biological Sciences*, 372(1723), 20160135. <https://doi.org/10.1098/rstb.2016.0135>
- Unnithan Kumar, S., Kaszta, Ž., & Cushman, S. A. (2022). Pathwalker: A New Individual-Based Movement Model for Conservation Science and Connectivity Modelling. *ISPRS International Journal of Geo-Information*, 11(6), 329. <https://doi.org/10.3390/ijgi11060329>
- Unnithan Kumar, S., Turnbull, J., Hartman Davies, O., Hodgetts, T., & Cushman, S. A. (2022). Moving Beyond Landscape Resistance: Considerations for the Future of Connectivity Modelling and Conservation Science. *Landscape Ecology*, 37(10), 2465–2480. <https://doi.org/10.1007/s10980-022-01504-x>
- Vales, D. J., Nielson, R. M., & Middleton, M. P. (2022). Black-Tailed Deer Seasonal Habitat Selection: Accounting for Missing Global Positioning System Fixes. *The Journal of Wildlife Management*, 86(8). <https://doi.org/10.1002/jwmg.22305>
- Van De Bildt, M. W. (2002). Distemper Outbreak and Its Effect on African Wild Dog Conservation. *Emerging Infectious Diseases*, 8(2), 212–213. <https://doi.org/10.3201/eid0802.010314>
- Van Der Meer, E., Fritz, H., Blinston, P., & Rasmussen, G. S. (2014). Ecological Trap in the Buffer Zone of a Protected Area: Effects of Indirect Anthropogenic Mortality on the African Wild Dog *Lycaon pictus*. *Oryx*, 48(2), 285–293. <https://doi.org/10.1017/S0030605312001366>
- Van Der Meer, E., Mpofu, J., Rasmussen, G. S., & Fritz, H. (2013). Characteristics of African Wild Dog Natal Dens Selected Under Different Interspecific Predation Pressures. *Mammalian Biology*, 78(5), 336–343. <https://doi.org/10.1016/j.mambio.2013.04.006>
- Vasudev, D., Fletcher, R. J., Goswami, V. R., & Krishnadas, M. (2015). From Dispersal Constraints to Landscape Connectivity: Lessons from Species Distribution Modeling. *Ecography*, 38(10), 967–978. <https://doi.org/10.1111/ecog.01306>
- Vasudev, D., Fletcher, R. J., Srinivas, N., Marx, A. J., & Goswami, V. R. (2023). Mapping the Connectivity-Conflict Interface to Inform Conservation. *Proceedings of the National Academy of Sciences*, 120(1), e2211482119. <https://doi.org/10.1073/pnas.2211482119>
- Venter, O., Sanderson, E. W., Magrach, A., Allan, J. R., Beher, J., Jones, K. R., Possingham, H. P., Laurance, W. F., Wood, P., Fekete, B. M., Levy, M. A., & Watson, J. E. M. (2016). Sixteen Years of Change in the Global Terrestrial Human Footprint and Implications for Biodiversity Conservation. *Nature Communications*, 7(1), 12558. <https://doi.org/10.1038/ncomms12558>
- Vermote, E. F., & Kotchenova, S. (2008). Atmospheric Correction for the Monitoring of Land Surfaces. *Journal of Geophysical Research: Atmospheres*, 113(D23). <https://doi.org/10.1029/2007JD009662>

- Vial, F., Cleaveland, S., Rasmussen, G., & Haydon, D. (2006). Development of Vaccination Strategies for the Management of Rabies in African Wild Dogs. *Biological Conservation*, 131(2), 180–192. <https://doi.org/10.1016/j.biocon.2006.04.005>
- Vogel, J. T., Somers, M. J., & Venter, J. A. (2019). Niche Overlap and Dietary Resource Partitioning in an African Large Carnivore Guild. *Journal of Zoology*, 309(3), 212–223. <https://doi.org/10.1111/jzo.12706>
- Wasserman, T. N., Cushman, S. A., Shirk, A. S., Landguth, E. L., & Littell, J. S. (2012). Simulating the Effects of Climate Change on Population Connectivity of American Marten (*martes Americana*) in the Northern Rocky Mountains, Usa. *Landscape Ecology*, 27(2), 211–225. <https://doi.org/10.1007/s10980-011-9653-8>
- Whittingham, M. J., Stephens, P. A., Bradbury, R. B., & Freckleton, R. P. (2006). Why Do We Still Use Stepwise Modelling in Ecology and Behaviour? *Journal of Animal Ecology*, 75(5), 1182–1189. <https://doi.org/10.1111/j.1365-2656.2006.01141.x>
- Wickham, H., Chang, W., Henry, L., Pedersen, T. L., Takahashi, K., Wilke, C., Woo, K., Yutani, H., Dunnigton, D., Posit, & PBC. (2024). *Ggplot2: Create Elegant Data Visualisations Using the Grammar of Graphics* (Version 3.4.3). <https://cran.r-project.org/web/packages/ggplot2/index.html>
- Wiens, J. A. (1989). Spatial Scaling in Ecology. *Functional Ecology*, 3(4), 385. <https://doi.org/10.2307/2389612>
- Williams, H. J., Taylor, L. A., Benhamou, S., Bijleveld, A. I., Clay, T. A., Grissac, S., Demšar, U., English, H. M., Franconi, N., Gómez-Laich, A., Griffiths, R. C., Kay, W. P., Morales, J. M., Potts, J. R., Rogerson, K. F., Rutz, C., Spelt, A., Trevail, A. M., Wilson, R. P., & Börger, L. (2019). Optimizing the Use of Biologgers for Movement Ecology Research. *Journal of Animal Ecology*, 89(1), 186–206. <https://doi.org/10.1111/1365-2656.13094>
- Wilson, B. H., & Dincer, T. (1976). An Introduction to the Hydrology and Hydrography of the Okavango Delta. Presented at the Symposium on the Okavango Delta and Its Future Utilization; Gaborone (Botswana); 30 Aug 1976. *Proceedings of the Symposium on the Okavango Delta and Its Future Utilization, Barone, Botswana*.
- Wolski, P., & Murray-Hudson, M. (2008). Alternative Futures' of the Okavango Delta Simulated by a Suite of Global Climate and Hydro-Ecological Models. *Water SA*, 34(5), 605. <https://doi.org/10.4314/wsa.v34i5.180658>
- Wolski, P., Todd, M., Murray-Hudson, M., & Tadross, M. (2012). Multi-Decadal Oscillations in the Hydro-Climate of the Okavango River System During the Past and Under a Changing Climate. *Journal of Hydrology*, 475, 294–305. <https://doi.org/10.1016/j.jhydrol.2012.10.018>
- Wolski, P., Murray-Hudson, M., Thito, K., & Cassidy, L. (2017). Keeping It Simple: Monitoring Flood Extent in Large Data-Poor Wetlands Using MODIS SWIR Data. *International Journal of Applied Earth Observation and Geoinformation*, 57, 224–234. <https://doi.org/10.1016/j.jag.2017.01.005>
- Wood, S. N. (2011). Fast Stable Restricted Maximum Likelihood and Marginal Likelihood Estimation of Semiparametric Generalized Linear Models. *Journal of the Royal Statistical Society Series B: Statistical Methodology*, 73(1), 3–36. <https://doi.org/10.1111/j.1467-9868.2010.00749.x>
- Wood, S. N. (2017). *Generalized Additive Models: An Introduction with R*. CRC Press/Taylor & Francis Group.
- Woodroffe, R., & Sillero-Zubiri, C. (2012). *Lycaon pictus*. *The IUCN Red List of Threatened Species*, 2012, e. T12436A16711116.
- Woodroffe, R., & Sillero-Zubiri, C. (2020). *Lycaon pictus* (amended version of 2012 assessment). *The IUCN Red List of Threatened Species*, 2020. <https://doi.org/https://dx.doi.org/10.2305/IUCN.UK.2020-1.RLTS.T12436A166502262.en>
- Woodroffe, R., Cleaveland, S., Courtenay, O., Laurenson, M. K., Artois, M., MacDonald, D. W., & Sillero-Zubiri, C. (2004). Infectious Disease in the Management and Conservation of Wild Canids. In *The Biology and Conservation of Wild Canids*. Oxford University Press. <https://doi.org/10.1093/acprof:oso/9780198515562.003.0006>
- Woodroffe, R., & Donnelly, C. A. (2011). Risk of Contact Between Endangered African Wild Dogs *Lycaon Pictus* and Domestic Dogs: Opportunities for Pathogen Transmission. *Journal of Applied Ecology*, 48(6), 1345–1354. <https://doi.org/10.1111/j.1365-2664.2011.02059.x>
- Woodroffe, R., Groom, R., & McNutt, J. W. (2017). Hot Dogs: High Ambient Temperatures Impact Reproductive Success in a Tropical Carnivore. *Journal of Animal Ecology*, 86(6), 1329–1338. <https://doi.org/10.1111/1365-2656.12719>

- Woodroffe, R., Rabaiotti, D., Ngatia, D. K., Smallwood, T. R. C., Strelbel, S., & O'Neill, H. M. K. (2020). Dispersal Behaviour of African Wild Dogs in Kenya. *African Journal of Ecology*, 58(1), 46–57. <https://doi.org/10.1111/aje.12689>
- Xiong, J., Thenkabail, P., Tilton, J., Gumma, M., Teluguntla, P., Oliphant, A., Congalton, R., Yadav, K., & Gorelick, N. (2017). Nominal 30-m Cropland Extent Map of Continental Africa by Integrating Pixel-Based and Object-Based Algorithms Using Sentinel-2 and Landsat-8 Data on Google Earth Engine. *Remote Sensing*, 9(10), 1065. <https://doi.org/10.3390/rs9101065>
- Yamazaki, D., Ikeshima, D., Sosa, J., Bates, P. D., Allen, G., & Pavelsky, T. (2019). MERIT HYDRO: A High-Resolution Global Hydrography Map Based on Latest Topography Datasets. *Water Resources Research*. <https://doi.org/10.1029/2019WR024873>
- Yoder, J. M. (2004). The Cost of Dispersal: Predation as a Function of Movement and Site Familiarity in Ruffed Grouse. *Behavioral Ecology*, 15(3), 469–476. <https://doi.org/10.1093/beheco/arh037>
- Zeller, K., Lewison, R., Fletcher, R., Tulbure, M., & Jennings, M. (2020). Understanding the Importance of Dynamic Landscape Connectivity. *Land*, 9(9), 303. <https://doi.org/10.3390/land9090303>
- Zeller, K. A., Jennings, M. K., Vickers, T. W., Ernest, H. B., Cushman, S. A., & Boyce, W. M. (2018). Are All Data Types and Connectivity Models Created Equal? Validating Common Connectivity Approaches with Dispersal Data. *Diversity and Distributions*, 24(7), 868–879. <https://doi.org/10.1111/ddi.12742>
- Zeller, K. A., McGarigal, K., Beier, P., Cushman, S. A., Vickers, T. W., & Boyce, W. M. (2014). Sensitivity of Landscape Resistance Estimates Based on Point Selection Functions to Scale and Behavioral State: Pumas as a Case Study. *Landscape Ecology*, 29(3), 541–557. <https://doi.org/10.1007/s10980-014-9991-4>
- Zeller, K. A., McGarigal, K., Cushman, S. A., Beier, P., Vickers, T. W., & Boyce, W. M. (2016). Using Step and Path Selection Functions for Estimating Resistance to Movement: Pumas as a Case Study. *Landscape Ecology*, 31(6), 1319–1335. <https://doi.org/10.1007/s10980-015-0301-6>
- Zeller, K. A., McGarigal, K., & Whiteley, A. R. (2012). Estimating Landscape Resistance to Movement: A Review. *Landscape Ecology*, 27(6), 777–797. <https://doi.org/10.1007/s10980-012-9737-0>
- Zeller, K. A., Vickers, T. W., Ernest, H. B., & Boyce, W. M. (2017). Multi-Level, Multi-Scale Resource Selection Functions and Resistance Surfaces for Conservation Planning: Pumas as a Case Study. *PLoS ONE*, 12(6), e0179570.
- Zeller, K. A., Wattles, D. W., Bauder, J. M., & DeStefano, S. (2020). Forecasting Seasonal Habitat Connectivity in a Developing Landscape. *Land*, 9(7), 233. <https://doi.org/10.3390/land9070233>